SYNTHESIS AND CHARACTERIZATION OF

NOVEL CELLULOSICS

A Dissertation
Presented to
The Academic Faculty

by

Rajalaxmi Dash

In Partial Fulfillment
of the Requirements for the Degree
Doctor of Philosophy in the
School of Chemistry and Biochemistry

Georgia Institute of Technology
December 2012

SYNTHESIS AND CHARACTERIZATION OF

NOVEL CELLULOSICS

Approved by:

Dr. Arthur J. Ragauskas, Advisor
School of Chemistry and Biochemistry
Georgia Institute of Technology

Dr. Stefan France
School of Chemistry and Biochemistry
Georgia Institute of Technology

Dr. Charles L. Liotta
School of Chemistry and Biochemistry
Georgia Institute of Technology

Dr. Preet Singh
School of Materials Science and Engineering
Georgia Institute of Technology

Dr. Laren Tolbert
School of Chemistry and Biochemistry
Georgia Institute of Technology

Date Approved: 08/27/2012

ACKNOWLEDGEMENTS

My wonderful journey of PhD and dissertation writing would not have been possible without the guidance, support and love of several individuals, who in one way or another contributed and extended their valuable assistance in the preparation and completion of this study. This is a precious opportunity and it gives me immense pleasure to say "Thank you" to all of them.

First and foremost, my utmost gratitude to my advisor Dr. Arthur Ragauskas for his kind guidance, constant encouragement, and advice to fulfill my goal. I would also like to thank him for letting me face many challenges, which made me stronger and independent during my doctoral research.

I owe my sincere and earnest thankfulness to all my committee members, Dr. Charles L. Liotta, Dr. Stefan France, Dr. Laren M. Tolbert and Dr. Preet Singh for listening to my work and also for their valuable suggestions, feedbacks, and support during every stage of my PhD, which helped me to become more and more perfect.

I am grateful to Dr. Gelbaum Leslie from School of Chemistry and Biochemistry at Georgia Institute of Technology for his assistance during my NMR experiments. I would like to thank Thomas Elder from USDA-Forest Service, Pineville, LA for helping me with AFM experiments.

I would like to thank my co-workers at Georgia Tech., Dr. Nan Jiang, Dr. Yunqiao Pu, Dr. Fang Huang, Dr. Reichel Samuel, Matyas Kosa, Dr. Yang Li, Mikhail Levit, Fan Hu, Quining Sun, Haoxi Ben. I am truly thankful to my friends at Georgia Tech. Swagat

Mohapatra, Jangyaseni Tripathy, Dushmanta Mohapatra, Ellina Acharya, Rakesh Behera, Shantivadra Das, Rudra Choudhury, and Durba Chakrabarty for their kind help and wonderful time.

A special thanks to Shaobo Pan, Dr. Poulomi Sannigrahi, Dr. Carolina Cateto, Seokown Jung, Dadasaheb Vilas Patil, Swati Mohite, Sonal Patel and Saroja Nayak for their support, help, encouragement and guidance both in academically and in personal life.

I am most grateful to Charles Brookshire and Bob Davis for helping me with my computer whenever I needed.

Above all, I owe my deepest gratitude to my parents, and sisters, who have given me their unequivocal support throughout, as always, for which my mere expression of thanks likewise does not suffice.

Finally, I would like to acknowledge the financial support from National Science of Foundation (NSF), Department of Energy (DOE) and Graduate Teaching Assistantship from Georgia Institute of Technology.

TABLE OF CONTENTS

LIST OF TABLES

Page

LIST OF FIGURES

Page

LIST OF SYMBOLS AND ABBREVIATIONS

AC	Algal cellulose
AFM	Atomic force microscopy
AGU	Anhydroglucose unit
ASA	Alkenyl succinic anhydride
BC	Bacterial cellulose
CN	Cellulose nanoparticles
CNC	Cellulose nanocrystals
conc.	Concentration
CP/MAS	Cross polarization/magnetic angle spinning
CCOA	carbazole-9-carboxylic acid [2-(2 aminooxyethoxy)ethoxy]amide
CNWs	Cellulose nanowhiskers
CrI	Crystallinity index
D_2O	Deuterium oxide
DAC	Dialdehyde cellulose
DCC	Dicarboxyl cellulose
DDLS	Depolarized dynamic light scattering
DEPT	Distortionless enhancement by polarization transfer
DEAE	Diethylaminoethyl
DI	Deionized water
DMSO-d_6	Deuterated dimethyl sulfoxide
DMAc	Dimethyl acetamide

DMAP	4-(Dimethylamino) pyridine
DOSY	Diffusion ordered NMR spectroscopy
DP	Degree of polymerization
DPw	Weight-average degree of polymerization
DR	Disperse Red S-R
DS	Degree of substitution
EDC	1-Ethyl-3-(3-dimethylaminopropyl) carbodiimide
FT-IR	Fourier transform infrared
G’	Storage modulus
G”	Loss modulus
GABA	Gamma aminobutyric acid
GPC	Gel permeation chromatography
HCl	Hydrochloric acid
H_2SO_4	Sulfuric acid
HW	Hardwood
HPLC	High pressure liquid chromatography
HSQC	Heteronuclear single quantum coherence
MCC	Microcrystalline cellulose
mL	Milliliter
M_n	Number-average molecular weight
M_w	Weight-average molecular weight
MWCO	Molecular weight cut off
N	Normality

$NaBH_4$	Sodium borohydride
$NaCNBH_3$	Sodium cyanoborohydride
NFC	Nanofibrillated cellulose
$NaIO_4$	Sodium periodate
NHS	Sulfo-N-hydroxysuccinimide
NMR	Nuclear magnetic resonance
NMMO	N-methylmorpholine oxide
o.d.	Oven dry
ODA	Octadecylamine
P_2O_5	Phosphorous pentoxide
PCL	Polycaprolactone
PEG	Polyethylene glycol
PF	Pulp fiber
Poly-DADMAC	Polydiallyldimethylammonium chloride
ppm	Parts per million
PVSK	Potassium polyvinyl sulfate
R_g	Radius of gyration
SA	Syringyl alcohol
SEC	Size exclusion chromatography
MALLS	Multi-angle laser light scattering detection
SANS	Small angle neutron scattering
SC	Sulfonated cellulose
SEM	Scanning electron microscopy

SW	Softwood
TAPPI	Technical association of the pulp and paper industry
TEMPO	2,2,6,6-tetramethylpiperidine-1-oxyl radical
THF	Tetrahydrofuran
TEM	Transmission electron microscopy
UV	Ultraviolet
WAXS	Wide-angle X-ray scattering
WF	Wood fiber
XPS	X-ray photoelectron spectroscopy
XRD	X-ray diffraction

SUMMARY

The search for alternatives to the fossil-based products has dramatically surged during the past few decades primarily due to the problems associated with the scarcity of these sources and global environmental concerns. The steadily growing number of publications, patents and scientific meetings, coupled with the increasing commitments and investments by the public and private sectors to sustain the R&D initiatives are the best indicators of this reality. Among those many alternatives, exploitation of cellulose, as a raw material to develop novel products has been a constant attempt since it has never lost its both economic and industrial impact. Not only is cellulose known for its significant contribution as a raw material to many industries, but it's also as a fascinating sustainable macromolecule, which exhibits wide availability and versatile chemical reactivity to discover novel derivatives for broad range of applications.

Cellulose is found in nature as a condensation polymer of D-anhydroglucopyranose monomers, which are connected through β-1,4 glycosidic linkages. The chemical versatility of cellulose is provided by three units of reactive hydroxyl groups present on each monomer. A wide range of cellulose derivatives has been prepared and studied in the literature in consequence of the chemical functionalization of these three hydroxyl units including esterification, etherification and oxidation. Conversion of cellulose C_2/C_3 secondary hydroxyl groups to dialdehyde groups in the presence of periodate is an extremely useful method for regioselective oxidation of cellulose and to activate the polymer for further derivatization. Therefore,

research is primarily focused on synthesis and characterization of wide range of cellulose derivatives exploiting periodate oxidation methodology.

The first study investigated the use of periodate oxidation as a potential method to synthesize a novel water soluble derivative of cellulose from bleached hardwood Kraft pulp. The work focused on the effect of increase in periodate charge followed by the sulfonation reaction on water solubility, morphology and structure of cellulose fibers. Increased periodate resulted in an increase in carbonyl content (0.12-0.28 mmol/g) as well as the sulfonic acid content. Periodate oxidation and sulfonation completely changed the surface morphology of cellulose fibers as observed by SEM and water solubility was significantly increased (2.85 -28.57 g/L) due to the introduction of sulfonic acid groups.

In order to further explore the application of the periodate oxidation and sulfonation scheme, this method was employed on bead cellulose to prepare anionic 2,3-disulfonated beads in the second study. The study was carried out at low levels of oxidation and sulfonation and it was concluded that slow stirring is required to retain the spherical shape of bead cellulose. Due to the presence of negatively charged sulfonic acid groups the beads were found to be agglomerated in presence of cationic starch, exhibiting their future application in chromatographic separation.

The next study applied the periodate oxidation fragmentation reaction to synthesize novel derivatives from cellulose nanowhiskers considering their increasing demand in various structural and biological applications. First of all, model primary amine compounds such as methyl and butyl amines were grafted to nanowhisker surfaces following periodate oxidation and reductive amination. It was determined that for complete conversion of the carbonyl groups to their corresponding amines an excess of

amines (1:20 eq) is required. It was also reported that the nanowhisker surfaces became partially hydrophobic due to the incorporation of non-polar alkyl chains. Furthermore, the introduction of primary amines did not affect the morphology and crystallinity of the nanowhiskers as examined by AFM and CP MAS NMR spectroscopy respectively.

Based on the previous study a novel drug delivery system was synthesized through chemical modification of cellulose nanowhiskers in the next study. Periodate oxidation and reductive amination was followed to graft gamma aminobutyric acid (GABA) to cellulose nanowhisker as a spacer molecule followed by attachment to syringyl alcohol as a linker molecule. Syringyl alcohol was chosen to control the release of the drug or biomolecule following a classic 1,6-benzyl elimination release mechanism. All the products were identified and well characterized using various techniques such as FT-IR, NMR, XPS and TEM.

The final study employed periodate oxidized nanowhiskers as cross-linkers to stabilize gelatin gels. Results showed an increase in the degree of chemical cross-linking (0.14-17%) between gelatin and nanowhiskers with increased amount of aldehyde content (0.062-0.230 mmol/g). It was concluded that the chemical cross-linking has a significant effect on relative increase in percentage of rigid protons, reduced water uptake ability and reduced pore size of the gels. Not only did chemical cross-linking improve the storage modulus of the gels (150%) and but it also increased the thermal resistance until 50 ^{o}C as obtained by rheological measurements.

CHAPTER 1

INTRODUCTION

Due to the growing concern of limited existing fossil supplies, escalating cost and environmental issues regarding the non-biodegradation of petroleum based products, recent research is focused towards the development of bio-based eco-friendly products. In other words, there is a global level of commitment to make "renewable", "recyclable", "sustainable" or "triggered biodegradable" materials.[1] In this regard, polymeric raw materials from natural resources have been gaining considerable attention because of their renewable, environment-friendly, biocompatible and biodegradable nature along with their properties comparable to petroleum based polymers. Additionally, they contain a number of reactive functional groups, which can be chemically modified using cost effective technologies for their extensive utilization. According to the technology road map for plant/crop based renewable resources 2020, the U.S. Department of Energy (DOE), has targeted to achieve 10% of basic chemical building blocks from plant derived renewable sources by 2020, with development concepts in place by then to achieve a further increase to 50% by 2050. The U.S. agricultural, forestry, life sciences, and chemical communities have developed a strategic vision for using crops, trees, and agricultural residues to manufacture industrial products and have identified major barriers to its implementation.[2]

Being the most abundant polymer on earth with an annual production of 10^{11}–10^{12} tons, cellulose remains as an excellent natural raw material with fascinating structure and properties. As one of the most inexhaustible resources of raw materials, cellulose and its

derivatives have been widely used in textiles (cotton, linen, viscose, and acetate), plastics (cellophane and celluloid), paper, food (thickener agent, enhancer of organoleptic properties, texture modifier, etc) and as a pharmaceutical additive (filler, binder, disintegrant, film maker adhesive).[3] Cellulose is a homopolymer of β-1,4-D-anhydroglucose units, and each unit consists of three hydroxyl groups, providing a reactive backbone to synthesize versatile derivatives of cellulose. Chemical functionalization of cellulose includes various reactions at these hydroxyl groups such as esterification, etherification, intermolecular crosslinking reactions, substitution, oxidation and macrocellulosic free radical reactions. Using oxidizing agents to modify cellulose structure and properties is one of the frequently used approaches and among these, oxidation of cellulose at the C_2/C_3 hydroxyl groups in the presence of sodium periodate is an example to obtain a regioselective dialdehyde cellulose product. Besides its high selectivity, this reaction is well known for its mild reaction conditions, absence of any side reactions and, finally, the formation of a useful and reactive dialdehyde product for further derivatization of cellulose, a promising path to broaden the application of cellulose.

The primary goal of this thesis is to utilize periodate oxidative fragmentation methodology to modify cellulose structure for various applications. We used three different types of cellulose particles such as cellulose fibers, bead cellulose and cellulose nanowhiskers, which have significant importance in many conventional as well as advanced applications. Water soluble forms of cellulose have been the most commonly and widely studied cellulose derivative due to their many valuable properties such as thickener, thermal gelation, surfactant, film formation, and adhesive. However, there has

been no report on the employment of periodate oxidation to prepare a water soluble cellulose derivative. Chapter 4 of the thesis deals with the chemical modification of cellulose fibers to obtain novel water soluble cellulose following periodate oxidation and sulfonation reaction. Bead cellulose, also referred as cellulose microspheres is a special kind of regenerated cellulose, characterized by specific characteristics; such as well-defined particle size and distribution; a both highly porous and rigid structure; a large specific surface area; high chemical reactivity; and mechanical and thermal stability. Due to these properties bead cellulose represents an excellent raw material for chromatographic applications. Chapter 5 hence, describes the introduction of negatively charged sulfonate groups to bead cellulose surface using the same periodate oxidation and sulfonation scheme to prepare 2,3-disulfonated beads.

The second part of the thesis involves the chemical modification of cellulose nanowhiskers through the periodate oxidation approach. Cellulose nanowhiskers are defined as unique rod-like nanoparticles with distinctive properties including their nano dimension, high aspect ratio, high surface area, high mechanical property and chemical modification of nanowhisker is still in the early stage in terms of their broad potential areas of application. Chapter 6 studies the periodate oxidation and reductive amination reaction on cellulose nanowhisker to incorporate model primary amine compounds on to its surface. Based on this study, Chapter 7 investigates the synthesis of a novel cellulose nanowhisker based drug delivery system through a series of oxidation, reductive amination and esterification reactions. Due to their renewable, biocompatible and non-toxic nature, periodate-oxidized cellulose nanowhiskers were further utilized as a chemical cross-linker to establish cross-linking between the protein chains of gelatin

molecules in Chapter 8. In addition, this study investigates the effect of cross-linking on mechanical and thermal stability of gelatin gels in detail.

CHAPTER 2

LITERATURE REVIEW

2.1 Introduction

Formed by the condensation of monosaccharides and derived from a wide range of natural resources such as algal origin (e.g. alginate), plant origin (e.g. pectin, guar gum), microbial origin (e.g. dextran, xanthan gum), and animal origin (chitosan, chondroitin), polysaccharides have attracted considerable attention in recent research. They exist as short oligosaccharide sequences or polymeric repeat units linked to other biopolymers, as in glycoproteins and glycolipids. Due to the presence of large numbers of reactive groups, wide range of molecular weights and varying amount of chemical compositions, polysaccharides are known as versatile raw materials with varied structure and properties. Further, depending on the type of applications, various derivable groups on molecular chains of polysaccharides can be easily modified chemically and biochemically, resulting into many kinds of polysaccharide derivatives. Particularly, most natural polysaccharides have hydrophilic groups such as hydroxyl, carboxyl and amino groups, which can form both covalent and non-covalent bonds, playing an important role in various structural and biomedical applications. Additionally, polysaccharides are highly stable, safe, non-toxic, hydrophilic, renewable and they have abundant resources in nature. Among all the polysaccharides, cellulose is known as the most abundant polymer in nature and is well known for its historical utilizations in textiles, paper and cardboard, packaging, and as a reinforcing element in composite materials with macromolecular matrices along with a number of advanced applications.[4]

2.2 Cellulose

Cellulose is the most abundant, renewable and high molecular weight linear polysaccharide in nature. Approximately, 10^{10}-10^{12} tons of cellulose are produced annually in pure form as well as lignocellulosic materials.[5-6] It is the most common component of all the plants and to lesser extent in some fungi, bacteria, algae and tunicates. About 150 years ago, Anselme Payen[7] first discovered and isolated cellulose and since then it has been extensively studied both in academia and industry for various applications. Commercial cellulose production, however, concentrates only on some easily harvested sources such as wood or naturally occurring highly pure source as cotton. Other cellulose containing materials include agricultural residues, water plants, grasses and other plant sources. Table 2.1 shows some examples of commercially produced cellulose containing materials and their compositions.[8]

Table 2.1 Composition of commercially produced cellulose containing materials.[8]

Sources	Compositions (%)			
	Cellulose	Hemicellulose	Lignin	Extract
Hardwood	43-47	25-35	16-24	2-8
Softwood	40-44	25-29	25-35	1-5
Cotton	95	2	1	0.4
Bagasse	40	30	20	10
Flax	71	21	2	6
Hemp	70	22	6	2
Jute	71	14	13	2
Ramie	76	17	1	6
Sisal	73	14	11	2

Located primarily in the secondary cell wall, cellulose is a homopolymer of anhydroglucopyranose units (AGU, $C_6H_{11}O_5$), where the monomers are linked by β-1,4 glycosidic linkages and every unit is twined by 180^o with respect to each other. So the repeat unit is generally considered as a dimer of glucose, known as cellobiose.[9] Each cellulose chain has a reducing end (hemiacetal unit) and a non-reducing end, which gives it directionality. The reducing end ring can be opened and reduced to an aldehyde group at the C-1 position. As shown in Fig. 2.1, the β-D-glucopyranose unit adopts the $^4C_1$ chain conformation resulting in the hydroxyl groups at the equatorial and hydrogen atoms at the axial positions. There are three hydroxyl groups present at C-2, C-3, and C-6 positions, and they show a strong tendency to form inter-and intra-molecular hydrogen bonds rendering cellulose its unique mechanical strength and chemical stability.[10-11]

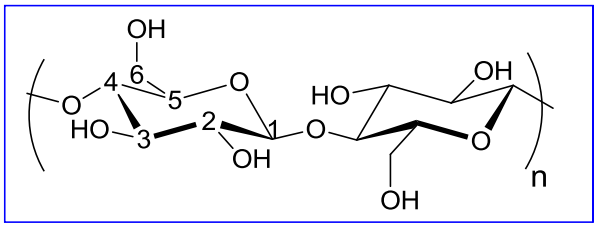

Fig. 2.1 Structure of cellulose showing one cellobiose unit.

The weight average molecular weight (M_w) of cellulose was found to be approximately in the range of 7×10^5 - 3.2×10^6 g/mol.[12] However, the size of the cellulose molecule is typically defined by the average number of monomer units i.e. degree of polymerization (DP). The DP of cellulose can be determined by various physical methods such as gel permeation chromatography (GPC), light scattering intrinsic viscosity measurements and viscometric methods. Depending on its origin as well as on the

pretreatment of the sample, cellulose shows a wide range of degree of polymerization varying from 300 to 30,000 (Table 2.2). The DP or molecular weight distribution in many cases profoundly influences the mechanical, solution, biological, and physiological properties of cellulose and has given very useful clues for designing effective cellulose derivatives.[13]

Table 2.2 Weight average degree of polymerization (DP_w) of cellulose obtained from various sources.[14]

Cellulose source	DPw
Cotton	8000-15000
Wood	8000-9000
Pulp	500-2100
Valonia	25000-27000
Rayon	300
Bagasse	700-900
Acetobacter xylinum	2000-6000

DP_w was obtained by viscometric methods

The crystalline structure of cellulose has been the focus of many studies since Mayer et al.[15] first investigated the packing of native cellulose. The abundance of hydroxyl groups form hydrogen bonding networks, resulting in various molecular orientatiosn of cellulose chains giving rise to different polymorphs of cellulose. So far, all investigations revealed that cellulose exists in four major different forms, depending on native origin and treatment, i. e. cellulose I (α and β), II, III, and IV.[16-17] Among the different polymorphs, cellulose I and II are the most predominant; cellulose I is the main

polymorph found in native form and it contains parallel cellulose chains (i.e. the reducing ends are aligned in same direction while for cellulose II chains they are anti-parallel).[18] Nuclear magnetic resonance (NMR), Infrared (IR), and X-ray diffraction studies have confirmed that two intra-chain hydrogen bonds exist between O3-H and O5 and between O2-H and O6, along with one inter-chain hydrogen bond between O6-H and O3 and these are responsible for the structure of cellulose I.[19] Further, it was shown by a high resolution solid state ^{13}C NMR study that native cellulose or cellulose I exists in two different crystal structures, I_α and I_β.[20] For example, algae and bacterial cellulose contains primarily $I_{\alpha,}$ while ramie, cotton, and wood fibers have primarily the I_β form. The differences between these two polymorphs lie in their hydrogen bonding pattern resulting in different crystal structures, although both have cellulose chains aligned in parallel. I_α has a triclinic one-chain unit cell, whereas I_β has a monoclinic two-chain unit cell and is actually more stable between the two forms. I_α is a metastable phase and can be transformed into I_β phase by annealing at 260-280 ^oC.[21-23]

Cellulose II is the second most extensively studied crystalline form of cellulose and has a monoclinic unit cell. Cellulose II can be derived from cellulose I by mercerization in alkali or through regenerating cellulose I in a suitable solvent such as heavy metal-amine complex solutions, copper with ammonia in water, some inorganic salts above 100°C, thiocyanate/amine, LiCl/DMAc mixtures, and NMMO/water systems, among others.[24] Transformation of cellulose I to cellulose II is generally considered to be irreversible.[25-26]

The nature of hydrogen bonding in cellulose II chains was confirmed by neutron diffraction, which suggests that the outer chains contain intermolecular hydrogen bonding

between O2-H and O-6 and intramolecular hydrogen bonding between O3-H and both O5 and O6. The center chains contain intermolecular hydrogen bonding between O6-H and O2 and intramolecular hydrogen bonding is similar to the outer chains. Between outer and center chains, intermolecular hydrogen bonding occurs between O2-H and O2 and between O6-H and O6.[27] Fig. 2.2 shows the inter- and intra-molecular hydrogen bonds present in cellulose I and II.

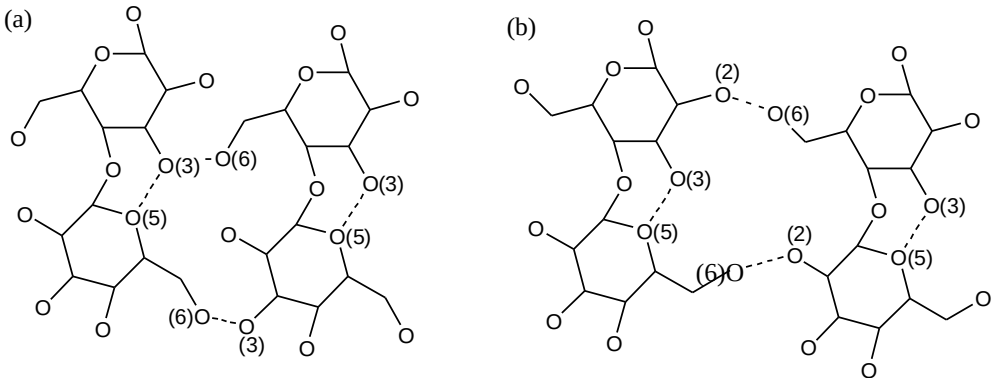

Fig. 2.2 Illustrating inter- and intra-molecular hydrogen bonds in (a) cellulose I and (b) cellulose II.

Cellulose III is usually obtained from cellulose I and II by treating with liquid ammonia at low temperatures or in ethylene diamine followed by washing with alcohol. Cellulose IV is formed from cellulose II and III upon treatment in a suitable liquid at high temperatures. Fig. 2.3 shows a schematic of the transformation of cellulose into various polymorphs.

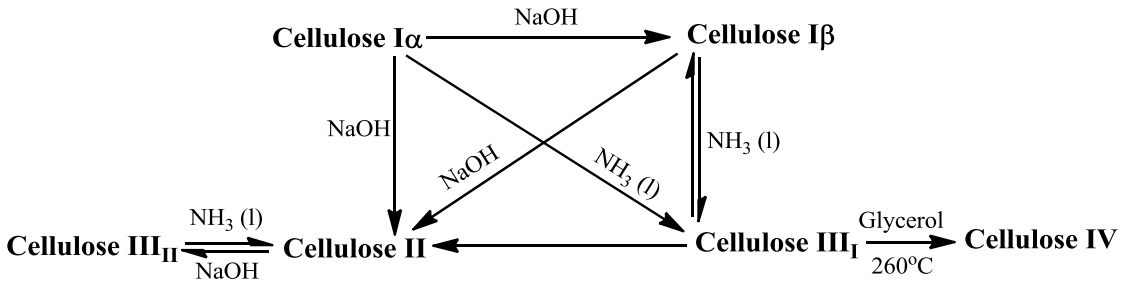

Fig. 2.3 Schematic diagram of cellulose transformation into various polymorphs.[14]

2.3 Cellulose I and cellulose II particle types

An overview of cellulose morphology represents a well-organized architecture of fibrillar elements and various methods have been used to convert the fibrils of plant cell wall to cellulose particles of different size and shape. There have been no explicit studies on the standardization of cellulose particle nomenclature yet. Therefore, there is an inconsistent use of terms in the literature to describe a given set of cellulose particles. However, based on the cellulose source materials and the particle extraction method, cellulose can be differentiated into nine different particle types to distinguish cellulose particles of different length scale that have been studied and well characterized in literature (Table 2.3). It has been found that each particle type is distinct, with a characteristic size, aspect ratio, morphology, crystallinity, crystal structure, and properties. The term cellulose nanoparticles (CN) used to broadly refer to several of the particle types that have at least one dimension in the nanoscale; MFC (microfibrillated cellulose), NFC (nanofibrillated cellulose), CNC (cellulose nanocrystals), t-CNC (tunicate cellulose nanocrystals), AC (algal cellulose) and BC (bacterial cellulose). For comparison purposes micron and macrosized scaled particles (wood fiber (WF), plant fiber (PF), and microcrystalline cellulose (MCC)) are also defined. It should be noted that

within each particle type there is a distribution of length, width, and percent crystallinity. This is likely a result of several factors, some of which are, (i) the inherent variability of biological processes resulting in statistical variability in the formation of the crystals, (ii) the type and severity of the given particle extraction process, and (iii) the differences in measurement techniques used and the quality of the data analysis. Fig. 2.4 shows characteristic micrographs of each particle type. A brief description of extraction method and characteristic physical properties of few particle types are discussed in the following section.[29]

Table 2.3 Dimensions and crystallinity of different cellulose particles.[29]

	Particle size		
Particle Type	Length (μm)	Width(nm)	Crystallinity (%)
Wood fiber & Plant fiber	> 2000	20-50(μm)	43-65[5]
Microcrystalline cellulose	10-50	10-50(μm)	80-85[30-31]
Microfibrillated	0.5-10's	10-100	51-69[32-38]
Nanofibrillated cellulose	0.5-2	4-20	54-88[32, 39-43]
Cellulose nanocrystals	0.05-0.5	3-8	>80 [5, 44-46]
Algae cellulose	>1	20-30	65-79[5, 47-49]
Bacterial cellulose	>1	6-50	60-80[47]
Cellulose II			27-43[5]

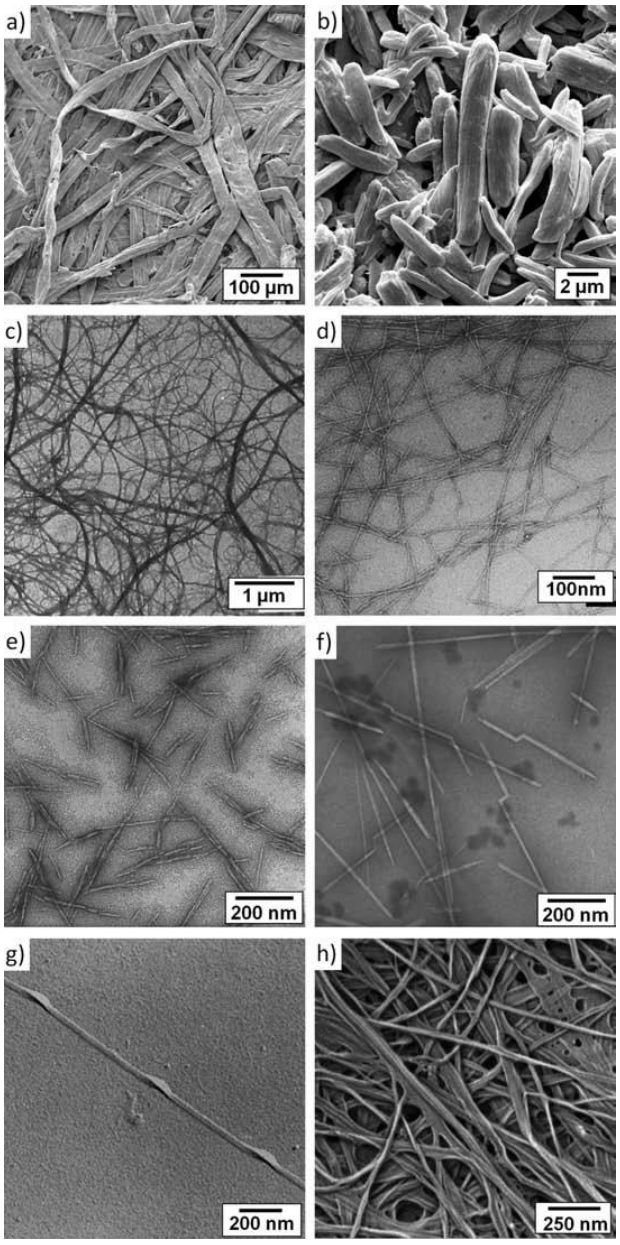

Fig. 2.4 Characteristic morphologies of various cellulose particles cellulose particle types, (a) SEM image of WF, (b) SEM image of MCC that has been deagglomerated, (c) Transmission electron microscope (TEM) image of MFC, (d) TEM image of 2,2,6,6-tetramethylpiperidine-1-oxyl radical (TEMPO) TEMPO-NFC, (e) TEM image of wood CNCs, (f) TEM image of t-CNC, (g) TEM of AC (h) SEM image of BC.[29] (Reproduced by permission of The Royal Society of Chemistry)

2.3.1 Wood fiber

Wood fibers are the largest of all the cellulose particle types, and have dominated the paper, textile and biocomposites industries for centuries.[50] They are commonly classified into two types; softwood and hardwood. The chemical composition of softwood is different from hardwood with different amount of lignin, hemicelluloses and wood extractives, but they contain approximately equal amount of cellulose (Table 2.4). About 80% of the cellulose fibers used in industry is in the purified form called pulp because the pulping process is used to convert the WF into fibrous mass.

Kraft pulping is one of the chemical pulping processes that accounts for the 95% of North American annual pulp production. The Kraft pulping process involves cooking the wood chips in a solution of sodium hydroxide and sodium sulfide, where the swollen lignin in the wood chips is chemically fragmented by the hydroxyl (OH^-) and hydrosulfide (SH^-) present in the pulping liquor. The lignin fragments are then dissolved as phenolate or carboxylate ions and the remaining residue is called pulp. Carbohydrates are also chemically attacked and dissolved to some extent in this process. During a typical Kraft cook, approximately 80% of the lignin, 50% of the hemicelluloses and 10% of the cellulose are dissolved. The use of sodium hydroxide and sulfide brings a number of advantages compared to other processes especially in terms of fiber strength. One of the major disadvantages of this process is the loss of the pulp due to the degradation of the carbohydrates under the alkaline conditions. Therefore, it is always important to understand the processing conditions, raw material, and the interaction between them, leading to carbohydrate preservation and pulp yield. Further, easier lignin breakdown during pulping may permit the use of less drastic processing conditions, leading to more carbohydrate preservation. It has been observed that softwood species are harder to pulp in comparison to hardwood because softwood lignin

varies little between species but hardwood lignin varies greatly between species and allows more opportunities to improve the process conditions.[51] The typical pulps produced by Kraft pulping process usually consist of individual fibers that are 10's of microns in diameter, millimeters in length, with a high percent cellulose, and a relatively low crystallinity (43–65%).[29]

Table 2.4 Compositions of hardwood vs. softwood.[52]

Composition	Hardwood	Softwood
Cellulose	45±2%	42±3%
Hemicellulose	19±2%	8±5%
Lignin	20±3%	28±2%
Extractives	3±2%	5±3%

2.3.2 Bead cellulose

Bead cellulose or cellulose microspheres represent a unique cellulose particle. They are spherical in shape and obtained by regeneration of cellulose with a distribution of size from 1 to a few hundred microns. During early days, microcrystalline cellulose fibers or granules were used as chromatographic material, but they exhibited poor mechanical stability and flow characteristic. Considering the increasing requirements including specificity, good chemical and mechanical stability, good recoverability and binding capacity as well as low cost for ideal chromatographic packing materials, in 1951, O'Neill and Reichardt first proposed and developed a method to manufacture cellulose based beads.[53] This method relies on a jet injection process of cellulose xanthate

viscose, which was used for a few decades until 1979, when Stamberg et al. proposed a simple and reproducible process for preparing spherical cellulose.[54] According to them, spherical bead cellulose has been prepared by different processes but all of the processes follow the steps: (1) dissolution of cellulosics; (2) formation of spherical droplets from these solution; (3) stabilization of the droplets; (4) phase inversion of the droplets so as to produce a gel; and (5) washing. Due to the lack of a neutral cellulose solvent, initially beads were prepared from cellulose derivatives such as cellulose acetate or xanthate. However, the development of new cellulose solvents, such as ionic liquids, LiCl/Dimethyl acetamide (DMAc), N-methylmorpholine-N-oxide, NaOH/Urea allowed the synthesis of beads from unsubstituted cellulose.[55-57] Nowadays, both porous and solid forms of substituted and unsubstitued cellulose microspheres are commercially available.

In the regenerated form of cellulose, the elementary microfibrils are not arranged into layers, rather they are randomly distributed making the cellulose structure more amorphous. They have also the cellulose II crystal structure. Cellulose microspheres possess large surface area, high chemical and mechanical stability, porosity, hydrophilicity and a reactive surface with an abundance of –OH groups as a potential anchor for many chemical reactions. In fact, bead cellulosics have been successfully developed both in unmodified and surface modified form and potentially employed in various fields.[57] Especially they have great demand in the fields of chromatography, separation technology, and sorbent. Moreover, due to their biocompatibility, microspheres with reactive carbonyl, hydroxyl, carboxyl or amino groups can be used as a support for immobilization of antibodies, proteins, and enzymes through covalent bonding.

For instance, Yu et al.[58] prepared a novel lipoprotein adsorbent by directly phosphonating porous bead cellulose, and these adsorbent demonstrated quite good adsorption performance for selective removal of low-density lipoprotein from human plasma. Bead cellulose, a potential scavenger resin in the field of combinatorial chemistry, was rapidly and easily derivatized to convert into a high- loading amine resin and they were successfully employed to remove excess electrophiles from solution.[59] Fan et al. prepared cellulose triacetate beads by reacting a mixture of acetic anhydride and acetic acid containing sulfuric acid as catalyst with ramie fiber followed by the formation of honeycomb-like cellulose triacetate microspheres with an average diameter of 14 μm. The cellulose triacetate microspheres exhibited a 16.5 mg/g capability to remove DR **(**Disperse Red S-R**)** dye from water at 50 °C and pH 7.[60] Table 2.5 shows a list of several applications of bead cellulose and its various derivatives as reported in literature. A schematic diagram of few functionalized bead cellulose is illustrated in Fig. 2.5.

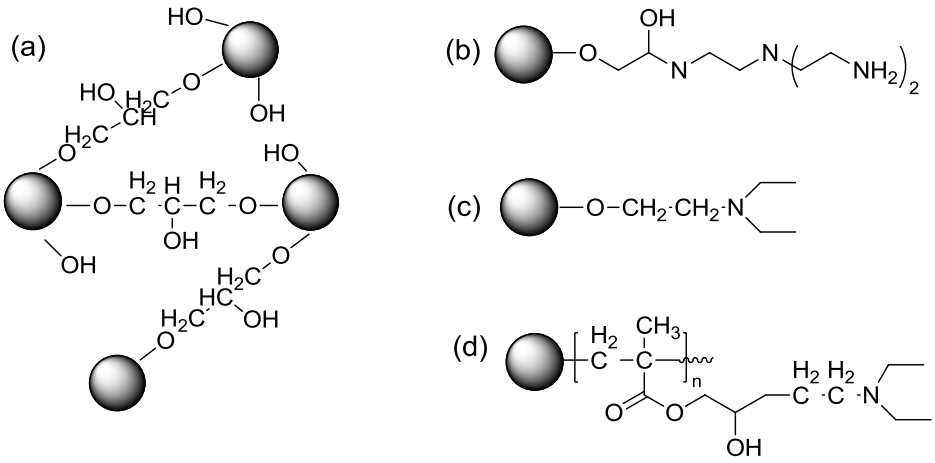

Fig. 2.5 Schematic diagram of some functionalized bead cellulose (a) cross-linked (b) amine derivative (c) diethylaminoethyl derivative (d) glycidyl methacrylate grafted.[59, 61-63]

Table 2.5 List of various applications of bead cellulose.

Applications	Derivatives of bead cellulose
Immobilization support	Aldehyde derivative[64] Unmodified bead cellulose [65] 2,4,6-trichloro-1,3,5-triazine activated bead cellulose[66] Concanavalin A-triazine bead celluloses[67] Unmodified bead cellulose[68]
Drug delivery	Unmodified bead cellulose[69] Dihydrogenphosphate and carboxymethyl bead cellulose[70] Bead cellulose and bead cellulose derivatives[71]
Protein separation	Diethylaminoethyl DEAE and carboxymethyl bead cellulose[72] DEAE bead cellulose[73]
Ion exchanger and metal adsorption	Cellulose-tungsten carbide composite beads[62] DEAE bead cellulose,[74] cellulose/chitin beads,[75] monoclonal antibody attached to dialdehyde cellulose microspheres[76] Chitosan-cellulose hydrogel beads[77] Iron oxyhydroxide loaded on bead cellulose[78] Cellulose/chitin beads[75] Iron oxyhydroxide loaded on bead cellulose[79] Porous bead cellulose[80]

2.3.3 Cellulose nanowhiskers (CNWs)

Cellulose nanowhiskers are defined as rod-like nanoparticles obtained by controlled acid hydrolysis of native cellulose. In the 1950'S, Ranby[81] first reported that a colloidal suspension can be obtained by harsh acid hydrolysis of cellulose fibers. Using XRD and TEM, Mukherjee and Woods[82] studied the lateral dimension and crystal

structure of the dried suspension confirming their needle shape and similar crystal structure as the original fibers. Later they named the particles as cellulose nanowhiskers or nanocrystals. Since then cellulose nanowhiskers were produced and studied from a range of cellulosics including tunicate cellulose, bacterial cellulose, Kraft pulp, MCC, sugar beet pulp, softwood pulp, ramie, sisal, straw, and cotton. Cellulose nanowhiskers are addressed by various names in the literature, such as "cellulose nanocrystals", "cellulose nanofibers", "cellulose nanowhiskers", "cellulose microcrystals", "microcrystalline cellulose" etc. However, according to the definition, cellulose nanowhiskers should be defined in terms of their method of preparation and their lateral dimension and should not be confused with "microcrystalline cellulose", "nanofibrillar cellulose" or "microfibrillar cellulose. Although microcrystalline cellulose is produced by the acid hydrolysis of plant cellulose, a much wider reaction window is followed and its dimensions are much larger than cellulose nanowhiskers. On the other hand, "nanofibrillar cellulose" or "microfibrillar cellulose" is generated by mechanical/chemical or only by chemical methods producing long nanosized individual fibrils.[83]

2.3.3.1 Preparation of cellulose nanowhiskers

Cellulose nanowhiskers are generally extracted from native cellulose by an acid hydrolysis process using sulfuric and hydrochloric acid followed by ultra-sonication. Native cellulose is a semicrystalline polymer consisting of both ordered (crystalline) and disordered (amorphous) packing of cellulose chains. Due to their low packing density, amorphous regions are preferentially more susceptible to acid attack than the crystalline

regions. Thus, during the acid treatment, the hydronium ion selectively hydrolyses the amorphous region promoting the cleavage of glycosidic bonds and releases the rod like nanocrystals called nanowhiskers (Fig. 2.6).

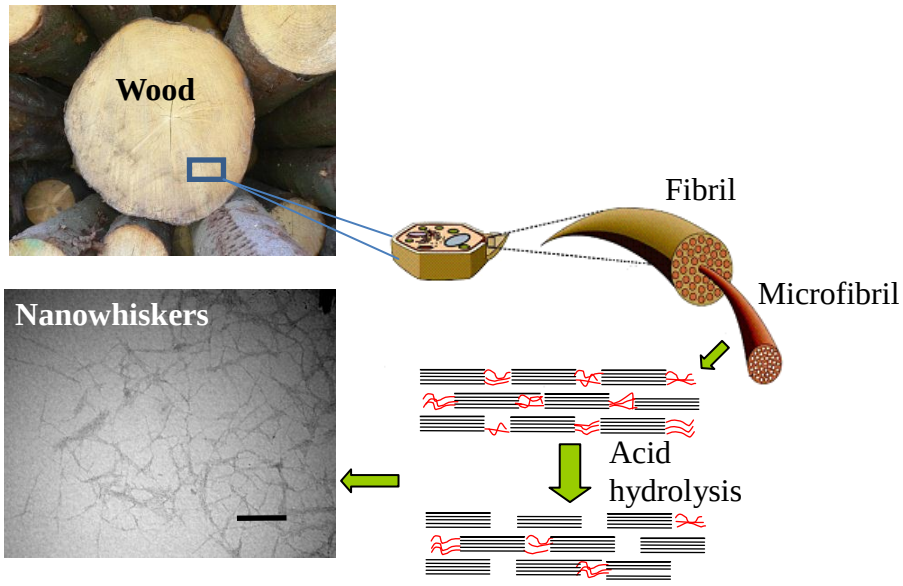

Fig. 2.6 Schematic representation of nanowhiskers formation from wood fibers.

Apart from the origin of cellulose, the properties of cellulose nanowhiskers for a given raw material, depend on the processing conditions such as acid concentration, acid to pulp ratio, hydrolysis time and temperature. Although a range of sulfuric acid concentration (60-70 %, w/w) was used for the hydrolysis, 64 wt. % was concluded to be the optimal acid concentration and hence it was the most preferred.[84] Further, Kontturi and Vuorinen[85] investigated that sulfuric acid hydrolysis is more efficient on the dried fibers since a higher amount of very short CNCs and a lower amount of long CNCs were obtained from dried pulps. On the other hand, a higher number of longer crystals and lower number of shorter crystals were obtained from acid hydrolysis of never dried pulps.

The effect of hydrolysis temperature, time and ultrasonic treatment on the whisker properties from cotton cellulose was first studied by Dong et al.[86] in order to optimize the hydrolysis conditions in terms of surface charge, dimensions, yield and birefringence. It was observed that at low hydrolysis temperature (26 ^{o}C), longer reaction time (18 h) was required to produce the cellulose microcrystallites and at high temperature (65 ^{o}C), the hydrolysis was not controlled easily. However, at 45 ^{o}C, the hydrolysis reaction proceeded smoothly. Table 2.6 shows the effect of hydrolysis conditions on the properties of cellulose suspension.

Table 2.6 Effect of hydrolysis condition on the properties of cellulose suspension.[86]

Hydrolysis temperature ^{o}C	Hydrolysis time (h)	Appearance of product	Yield (% w/v)
26	1	White, with some pulp particles	89.9
26	18	Ivory white, viscous suspension	34.4
45	1	Ivory white, viscous suspension	43.5
65	0.25	Yellow, very viscous suspension	48.1
65	1	Black	N/A

After investigating a set of experiments with varying hydrolysis time, temperature and ultrasonic duration, the suitable preparation condition was found to be sulfuric acid concentration, 64% (w/v); acid to pulp ratio, 1:8.75; reaction temperature 45^{o}C; reaction time 1 h; and ultrasonic treatment time about 5 min. Beck-Candanedo et al.[41] investigated the effect of hydrolysis time and acid to pulp ratio on the behavior of cellulose nanowhiskers obtained by 64% sulfuric acid hydrolysis of black spruce

(softwood) and eucalyptus (hardwood) pulp at a constant temperature of 45 ^{o}C. They reported that nanowhisker suspensions from both the pulp exhibited similar dimensions, surface charge, and critical concentration required to form anisotropic phases. However, by increasing the hydrolysis time and acid to fiber ratio for a particular fiber, a reduction in the length of the nanowhiskers was observed. Table 2.7 summarizes the dimension and properties of cellulose nanowhiskers obtained from black spruce with varying reaction conditions.

Table 2.7 Effect of reaction condition on the properties of cellulose nanowhisker obtained from black spruce.[41]

Reaction conditions (reaction time (min), acid/pulp)	Length (nm)	Aspect ratio	Sulfur content (%)	Surface charge density (e/nm^2)
25, 8.75	141±6	28.2	0.89±0.06	0.33±0.02
45, 8.75	120±5	24.5	1.06±0.02	0.38±0.01
45, 17.5	105±4	23.3	1.26±0.01	__

Bondeson et al.[31] optimized the reaction conditions for sulfuric acid hydrolysis of Norway spruce using a surface response methodology and concluded that temperature, acid concentration, and time of hydrolysis are the important factors to obtain a suspension of negatively charged isolated cellulose whiskers. With a sulfuric acid concentration of 63.55% (w/w) they were able to produce cellulose whiskers of length 200-400 nm and width less than 10 nm in approximately 2 h with a yield of 30%. Degradation of amorphous region is the most possible explanation for the typical low yield of cellulose nanowhiskers. In order to improve the yield of cellulose nanowhiskers from chemical

pulp, recently, Hamad and Hu[87] examined the effect of hydrolysis conditions on degree of polymerization, the extent of sulfation, morphology, and solid-state characteristics of the extracted nanowhiskers as shown in Table 2.8. It was demonstrated that the hydrolysis process is highly reproducible and a 64 wt. % sulfuric acid at 45-65 ^{o}C could yield a maximum of 21-38% nanowhiskers from fully bleached, commercial softwood Kraft pulp. However, they also observed that sulfation has a significant role in determining the yield and the solid state characteristics of the extracted materials.

Table 2.8 Effect of hydrolysis condition on sulfur content, DP and yield of nanowhisker.[87]

Acid (wt. %)	Temperature (^{o}C)	S(%) (elemental analysis)	DP (intrinsic viscosity)	Yield (%)
-	-	<0.3	1179	100
16	45	<0.3	678	93.7
16	65	-	426	90.2
16	85	-	180	91.4
40	45	<0.3	280	89.6
40	65	<0.3	121	87.4
40	85	<0.3	90	69.2
64	45	0.92	92	22.4
64	65	1.03	96	32.9
64	85	1.29	90	20.9

2.3.3.2 Mechanisms of acid hydrolysis of cellulose

Figure 2.7 (a) shows the reaction mechanisms involved during the acid hydrolysis of cellulose to obtain cellulose nanowhiskers. In general the reaction occurs in three steps: rapid protonation of glucosidic oxygen or cyclic oxygen by acidic proton, followed by the cleavage of ether linkage and finally hydration induced by water.[88-89] Since amorphous regions are most susceptible to acid attack, mostly crystalline regions known as nanowhiskers are left behind in the solution. Due to the cleavage of glycosidic linkages, this process yields different fragments of cellulose leading to a decrease in DP of native cellulose. Besides sulfuric acid, hydrochloric acid, phosphoric acid and hydrobromic acid has also been reported for hydrolysis of cellulose.

In the case of hydrochloric acid hydrolysis, a similar procedure was followed as sulfuric acid hydrolysis but the yield was lower in HCl-whiskers.[90] To produce nanowhiskers with similar dimension, H_2SO_4-hydrolysis needs lower reaction temperature, acid to pulp ratio and less time than that of HCl-hydrolysis,[90] however, the dispersibility of nanowhiskers obtained from these two kinds of acids is different. This is mainly due to the difference in surface charge of the whiskers. During H_2SO_4-hydrolysis, the acid reacts with the surface hydroxyl groups to form charged sulfate esters as shown in Fig. 2.7 (b) leading to the formation of a negatively charged surface. Repulsion between the charges causes electrostatic stabilization of the suspension, which lacks in HCl-hydrolysis resulting into a suspension that tends to flocculate.[87] Table 2.9 shows the effect of hydrolysis time on sulfur content of sulfuric acid hydrolyzed nanowhiskers. In addition, it was shown that the presence of sulfate ester compromises the thermal stability of nanowhiskers and influences its rheological property. Sulfuric acid treated suspension

has shown time independent viscosity whereas, the hydrochloric acid treated suspension has shown thixotropic behavior above 0.5% (w/v) and anti-thixotropic behavior below 0.3%.[91] Due to the above properties, the ultrasonic treatment of cellulose nanowhiskers is generally carried out in an ice bath to avoid the desulfation.

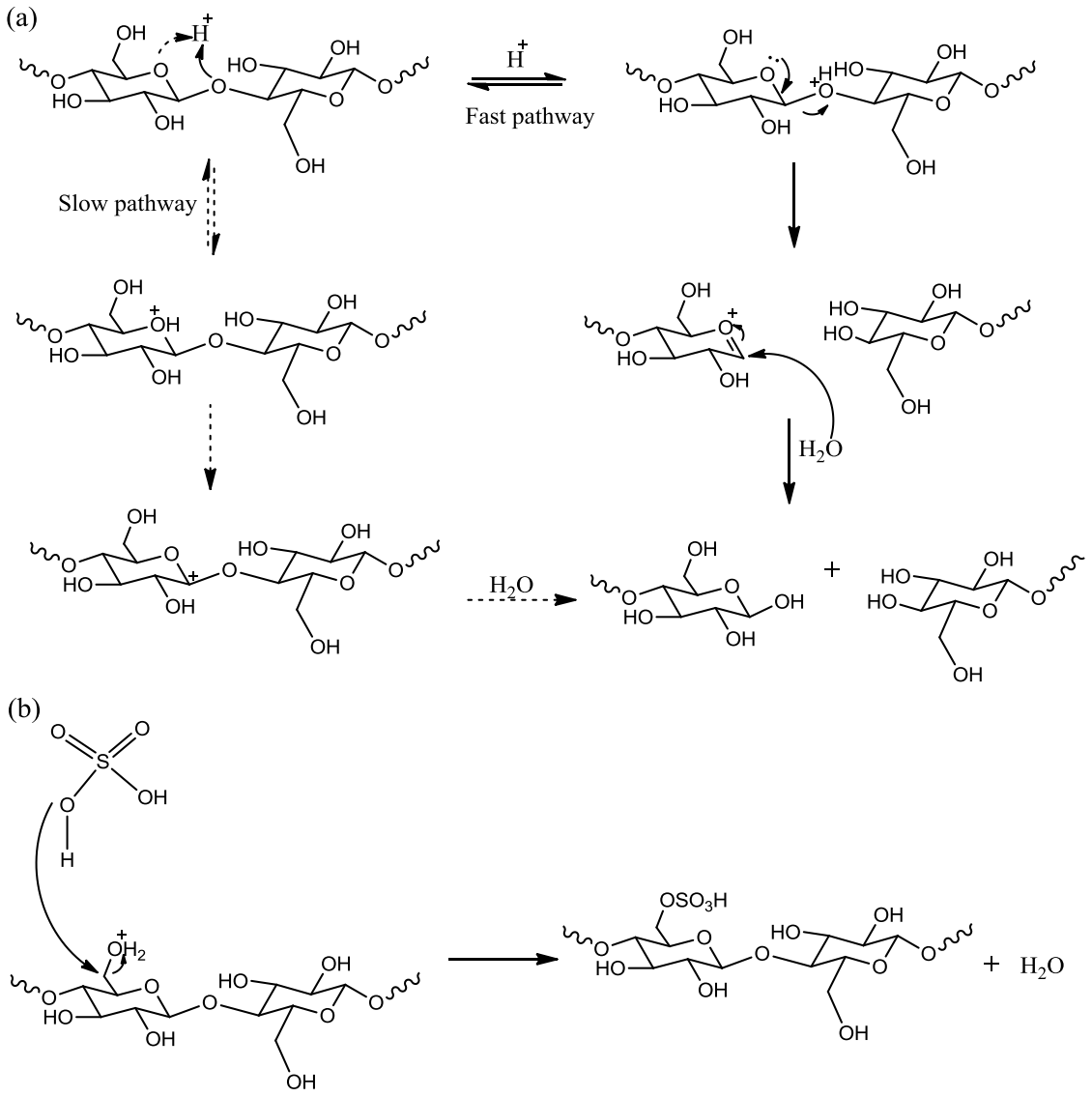

Fig. 2.7 (a) Acid hydrolysis mechanism of cellulose fibers (b) sulfation mechanism of cellulose surface during H_2SO_4 hydrolysis.[88-89]

Table 2.9 Effect of H_2SO_4 hydrolysis time on the sulfur content of cellulose nanowhiskers.[86]

Hydrolysis time at 45 ^oC (min)	Total sulfur content (%)[a]	Surface charge (OSO_3^-) (S%)[b]
10	0.53	0.30
20	0.50	0.33
30	0.58	0.50
45	0.62	0.64
60	0.69	0.68
120	0.74	0.68
240	0.75	0.62

a: elemental analysis, b: conductometric titration

2.3.3.3 Characterization and properties of cellulose nanowhiskers

The dimensions of the nanowhiskers obtained by hydrolysis depend on the degree of crystallinity and the dimensions of the native fiber, which varies with the source of cellulose. For highly crystalline algal and tunicate cellulose, the nanowhisker dimensions are up to several micrometers in length whereas, wood fibrils with lower crystallinity yields nanowhiskers of shorter length. Average dimensions of cellulose nanowhiskers obtained from various sources are shown in Table 2.10. TEM micrographs of nanowhiskers obtained from various sources are shown in Fig. 2.8.

Table 2.10 Typical average dimensions of cellulose nanowhiskers hydrolyzed from different sources.

Source	Length (nm)	Width (nm)	Technique
Bacterial	100-1000	10-50	TEM[92]
Cotton	100-150	5-10	TEM[92]
	150-210	5-11	E-SEM[93]
MCC	~500	10	AFM[94]
Ramie	50-150	5-10	TEM[95]
Sisal	100-500	3-5	TEM[40]
Tunicate	1160	16	DDLS[96]
	100-several 1000	15-30	TEM[97]
Valonia	>1000	10-20	TEM[98]
wood	100-300	3-5	AFM[41]

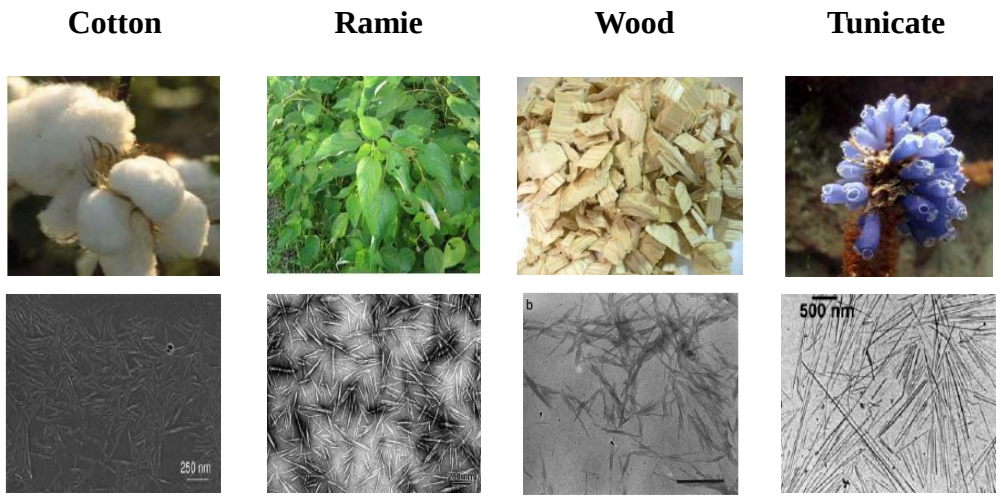

Fig. 2.8 TEM micrographs of cellulose nanowhiskers and their corresponding sources.[90, 99-101102]

A number of techniques have been utilized to characterize the morphology of cellulose nanowhiskers. TEM is the most common and conventional technique to obtain

high resolution images of cellulose nanowhiskers. Other instruments including atomic force microscopy (AFM), and high resolution scanning electron microscopy, small angle neutron scattering (SANS)[103] and polarized and depolarized dynamic light scattering (DLS, DDLS)[104,96] were also used to measure the lateral dimension of cellulose nanowhiskers. TEM images are generally obtained after drying a very dilute (0.02 wt. %) suspension followed by a negative staining with uranyl acetate solution (2 wt. %), which results in aggregation of particles. In order to prevent the aggregation of particles, Elazzouzi-Hafraoui et al.[39] reported cellulose nanowhisker micrographs using cryogenic TEM.

AFM is another powerful tool and has been widely used to obtain surface topography, dimensions of nanowhiskers and mechanical properties including stiffness and adhesion and pull-off forces.[105] This technique provides an overestimation of CNWs dimensions due to the artifacts induced by AFM tip and tip-broadening effects. Typical geometries of CNWs extracted from various sources and measured by different techniques are summarized in the Table 2.10. Shape of cellulose nanowhiskers was determined by Terech et al.[103] using neutron and XRD technique showing that these rigid nanowhiskers have a rectangular 8.8 nm × 18.2 nm cross-section.

Onsager[106] was the first to observe and study the spontaneous ordering or nematic phase transition occurring with rod-like particles. The self-assembly of chiral nematic phases was also observed by cellulose nanowhisker suspension, which depends on the mineral acid chosen for hydrolysis.[107] H_2SO_4-hydrolyzed whiskers yield a chiral nematic phase but the HCl- hydrolysis does not due to the absence of surface ester groups to promote a perfectly uniform dispersion. Moreover, the phase formation ability is

concentration driven. In dilute suspension, cellulose nanowhiskers are randomly oriented forming an isotropic phase, which appears as spheroids or ovaloids in polarized optical microscope. However, with the increase in concentration they adopt a nematic liquid crystalline alignment due to the formation of anisotropic phase, generally characterized by unidirectional self-orientation of CNWs rods. When the concentration reaches a critical value, they change into a chiral nematic ordered phase, a characteristic liquid crystalline fingerprint.

Above critical concentration, the CNWs suspensions show a shear birefringence phenomenon, which can spontaneously separate into an upper isotropic and a lower anisotropic phase on standing.[43] A shear birefringence behavior is shown in Fig. 2.9 as observed through a cross polarized films. For sulfated CNWs the critical concentration ranges from 1-10 % (w/w), which is also a function of aspect ratio, charge density and osmolarity. Stroobants et al.[108] have studied in detail the theories behind the parameters influencing this phenomenon. The self-induced ordered nematic phenomenon of cellulose nanowhiskers was typically explained as an entropically driven self-orientation behavior of rod-like species, originated favorably from excluded volume interactions leading to higher packing entropy of the ordered phase at higher densities of nano rods. Interestingly, the chiral nematic structure can be preserved even after the complete evaporation of water to form nanowhisker iridescent films, exhibiting a unique characteristic and opening a door towards numerous potential optical applications of nanowhiskers.

Fig. 2.9 Aqueous sulfated cellulose nanowhisker suspension (1 wt. %) as observed through cross polarized films.

2.4 Chemical modification of cellulose

Each repeating unit of cellulose contains three reactive hydroxyl groups which can be chemically modified to the desired functionalities. The accessibility of the hydroxyl groups and their ease of reactivity facilitate the preparation of specific molecular structures for a broad range of applications. As a result, chemical modifications continue to play a dominant role in improving the overall utilization of cellulosic polymers. The typical modifications of cellulose are etherifications, esterifications, and oxidation at the hydroxyl groups of cellulose. Most water-soluble and organic solvent-soluble cellulose derivatives are prepared by the substitution reactions, and drastic changes in the original properties of cellulose can usually be achieved by these chemical modifications. Other reactions include ionic and radical grafting, acetylation, deoxyhalogenation. Fig. 2.10 shows schematic representation of the positions in cellulose structure for chemical modifications.

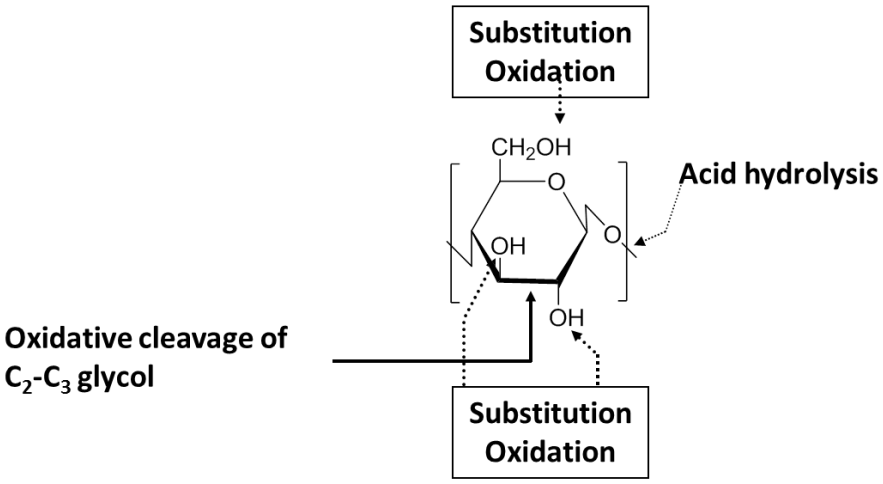

Fig. 2.10 Schematic representation of typical chemical modification reaction of cellulose.[14]

2.4.1 Substitution reaction

2.4.1.1 Etherification

Cellulose ethers are the most common derivatives of cellulose that has been applied in many industrial sectors. Reaction of alkyl halides, alkyl sulfates and alkene oxides with cellulose in presence of alkali followed by purification process, which is generally accomplished by washing the reaction product with hot water results cellulose ethers. A typical etherification reaction of cellulose is shown below (Fig 2.11), where R is any alkyl group such as the methyl (CH_3–), ethyl (C_2H_5–), or a more complex structure, which will react with three OH groups in an AGU.

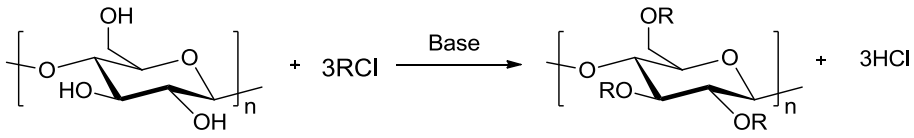

Fig. 2.11 Etherification reaction of cellulose.[14]

Examples of cellulose ethers include methyl cellulose, ethyl cellulose, carboxymethyl cellulose, hydroxyethyl and hydroxypropyl cellulose. The degree of etherification can be controlled by the molar ratio of the reagent to yield products with varying viscosities in solution. Sometimes mixed cellulose ethers for example ethylpropyl cellulose ethers are prepared by adding both ethyl chloride and propyl chloride consecutively or as a mixture and the degree of substitution (DS) depends on the molar ratio of each reagent as well as on the method of the addition. Cellulose ethers of moderate to high molecular weight are insoluble in water. As a rule, as the DS increases, the polymers gradually pass through a stage of solubility in dilute alkali (those with a DS of up to about 1.0), then through a water soluble stage (about DS 1.0–2.3), and finally attain an organic-solvent-soluble stage (DS 2.3–3.0). Such DS ranges are of course only approximate and the organic solubility trend is gradual and differs for individual ethers. It has to be noticed that the water-soluble cellulose ethers should not be regarded simply as water-soluble forms of cellulose instead the ethers are derivatives of cellulose, containing only a fraction of the original cellulose structure in their molecular structure.[14]

2.4.1.2 Esterification

Cellulose esters are the next common derivatives of cellulose after cellulose ethers, which have a number of useful properties. Similar to the etherification reactions, cellulose hydroxyl groups can be esterified by treating cellulose with certain acids such as acetic acid, nitric acid, sulfuric acid and phosphoric acid. The reaction is always in equilibrium, and thus removal of water during the reaction forces the reaction to completion and the concentration of the reacting species determines the ultimate degree

of substitution. Cellulose acetate, an important organic ester is accomplished by the reaction of acetic anhydride with cellulose for 8 h to yield the trimester derivatives with a degree of substitution of 2.75. However, cellulose acetates with lower degree of substitution are obtained via hydrolysis of the trimester by hydrochloric acid to yield the desired substitution.

2.4.2 Oxidation

Oxidation of cellulose transforms the hydroxyl groups into carbonyl and carboxyl groups, which modifies the properties of cellulose. Oxidized cellulosics (or oxycelluloses) are cellulose derivatives produced by reacting cellulose with an oxidant such as gaseous chlorine, hydrogen peroxide, peracetic acid, chlorine dioxide, nitrogen dioxide (dinitrogen tetraoxide), persulfates, permanganate, dichromate-sulfuric acid, hypochlorous acid, hypohalites, or periodates. These oxidized cellulosics may contain carboxylic, aldehyde, and/or ketone functionalities, in addition to the hydroxyl groups, depending on the nature of the oxidant and the reaction conditions used in their preparation. Selective oxidation at primary alcohol group is often difficult but can be achieved by stoichiometric as well as catalytic methods. For instance, reaction of nitrogen dioxide with cellulose yields specifically 6-carboxy cellulose with a degree of oxidation 12-18% but some concomitant degradation occurs during the reaction. Catalytic amounts of the water-soluble reagent TEMPO promotes regioselective oxidation of cellulose at 6-hydroxyl groups to carboxylic acid and also minimizes the degradation products.[109]

Periodate oxidation is one example of a quite selective oxidative modification of cellulose without resulting in any side products. In addition to cellulose, the periodate

oxidation approach has also been employed to a number of polysaccharides such as alginate, chitosan, starch, glucosaminoglucans, to name a few. Earlier, periodate oxidation provided a routine method for elucidation of structures in complex carbohydrates, and its applications helped to interpret fundamental structures in many polysaccharides.[110] Fig. 2.12 shows the dialdehyde products obtained from (1-6)-linked, (1-4)-linked, (1-3)-linked, (1-2)-linked, and terminal non-reducing residues, illustrating the number of moles of periodate consumed and the required orientation of a vicinal diols such as equatorial-equatorial or axial-equatorial in order to be consumed by periodate and distinguished from each other.

Reaction of periodates with polysaccharides yields their dialdehyde derivatives, which are easily isolable and a variable degrees of oxidation can be obtained due to the presence of a number of potentially oxidizable units. However, as a result of the oxidation, the probability of hemiacetal and hemialdal formation is very high due to the formation of inter- and intramolecular linkages. For (1-4)-linked polysaccharides, numerous structures of five and six-membered rings for periodate-oxidized product were shown by Fan et al.[111] These rings could form due to the linkages between different hydroxyl units, either in the same chain or different chains although there is no definite evidence as to which one is correct. Fig. 2.13 shows some possible reaction products of an oxidized (1-4)-linked polysaccharides. Periodate oxidation reaction has become the most versatile route to synthesize polysaccharide derivatives with novel functionalities for numerous applications.

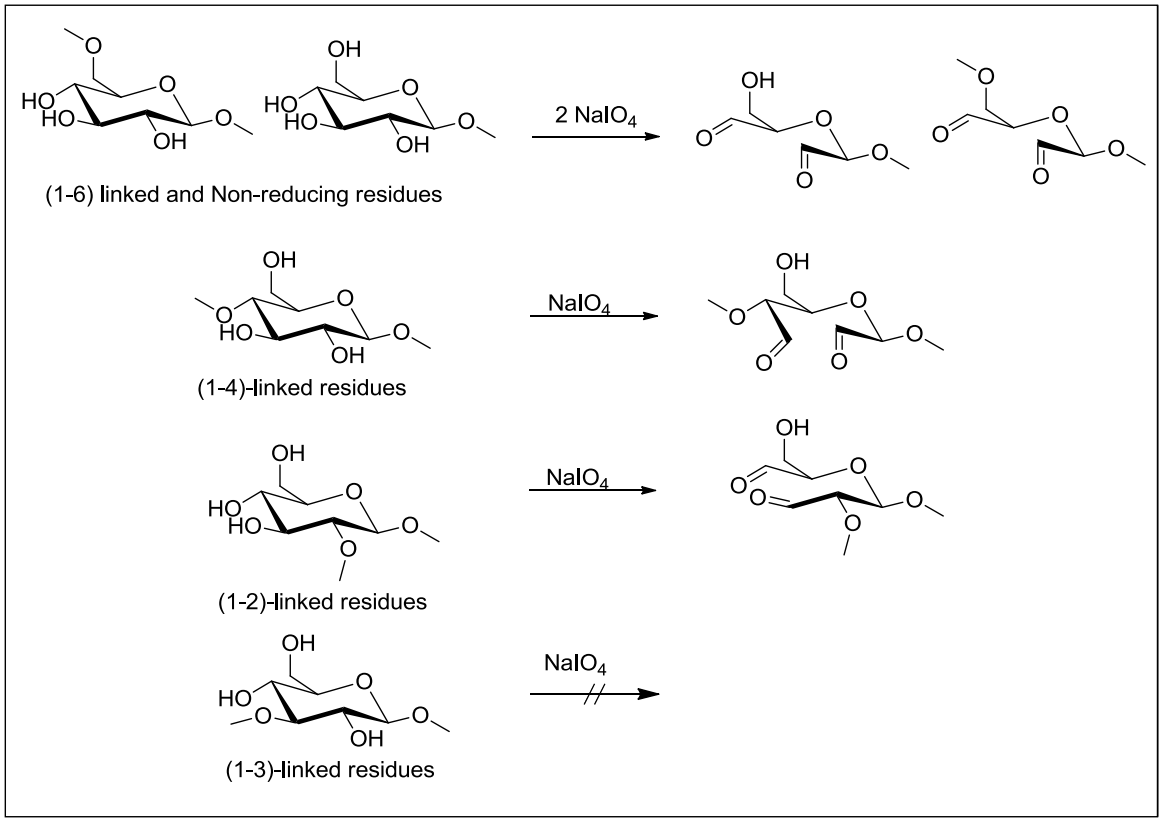

Fig. 2.12 Periodate oxidation of 1-6, 1-4, 1-3, 1-2 linked and non-reducing end residues of polysaccharides.[112-113]

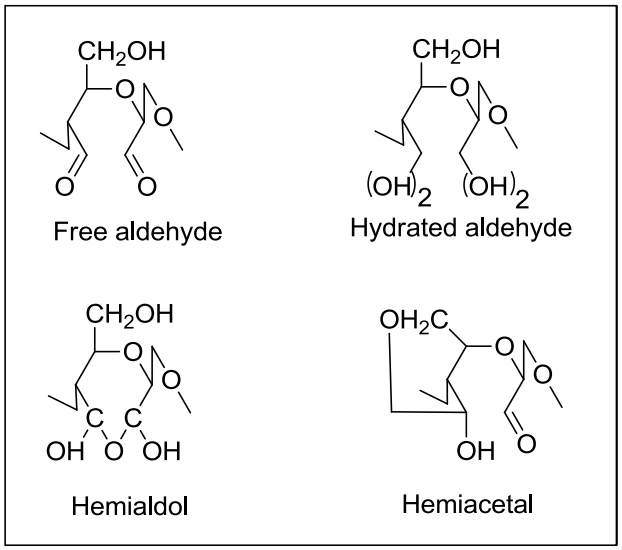

Fig. 2.13 Possible reaction products of an oxidized (1-4)-linked polysaccharides.[110]

2.4.2.1 Mechanism of periodate oxidation

Vicinal alcohols, also known as glycols, undergo oxidative cleavage in the presence of periodate to introduce aldehyde groups at adjacent carbons resulting in a dialdehyde product and this oxidative cleavage is well known for its regioselectivity. The high selectivity of the reaction is easy to explain, which is mainly attributed to the ability of the central atom of the oxidant to complex with the vicinal hydroxyls and effect a two electron transfer.[114] The overall oxidation reaction is thought to proceed via a cyclic diester of periodic acid with vicinal hydroxyls, which subsequently undergoes an intramolecular redox process with C–C bond cleavage according to a concerted mechanism as proposed originally by Criegee et al. (Fig 2.14).[115] It was found that the planar conformation of the cyclic ester is necessary for the cleavage since compounds containing eclipsed hydroxyl groups are the most reactive such as 1,2-acenaphthanediol, methyl 2,6-anhydro-α-D-altropyranoside,[116] and cis-1,2-camphanediol.[117] Examples of slightly less reactive diols include cis-1,2-cyclopentanediol[118] and cis-2,3-tetrahydrofurandiol,[119] which are able to attain the eclipsed condition with little strain.

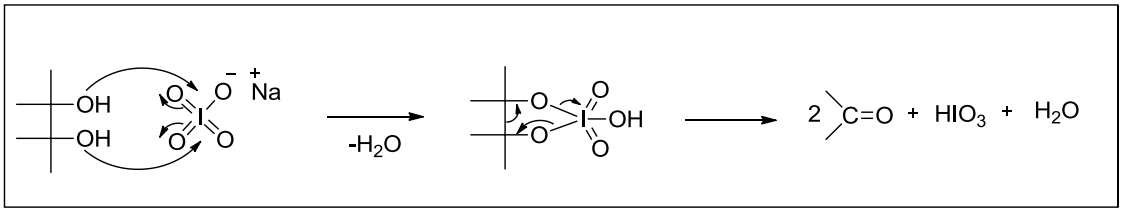

Fig. 2.14 Mechanism of periodate oxidation of glycol.[114]

Apart from vicinal diols, other 1,2-dioxygenated groups such as 2-hydroxyaldehydes,[120-121] 1,2-dicarbonyl compounds,[122] α-hydroxy and α-keto acids[123] and α-amino alcohols[124]

undergo oxidative fragmentation reaction by periodate, although the reaction occurs relatively slowly. In presence of light or oxygen, periodate becomes unstable and decomposes to form radicals. Hence, the oxidation reaction is usually performed in dark condition and in absence of oxygen to avoid any radical induced depolymerization. Other than periodate, lead acetate can also perform the same oxidation reaction through similar mechanism to yield the regioselective dialdehyde product. For a long time, oxidative glycol cleavage has been used as a classical method for the structural determination of complex carbohydrate structures. In this regard, periodate is more popular than lead acetate due to its preferential reactivity in water, where typical polysaccharides reactions are performed.

2.4.2.2 Periodate oxidation of cellulose

As mentioned earlier, regioselective periodate oxidation mechanism requires vicinal hydroxyls and location of such groups at the C-2 and C-3 positions in cellulosics favors formation of cyclic diester of periodic acid, which subsequently undergoes an intramolecular redox process with C–C bond cleavage according to the concerted mechanism as shown in Fig. 2.15. Due to its hydrophilic character, periodate reaction of cellulose proceeds in an aqueous suspension under the controlled condition of temperature, light and concentration of oxidant and the usual periodate oxidation of cellulose in an aqueous medium is considered as a heterogeneous reaction. Aqueous solution of periodates opens the pyranose ring and leads to the introduction of aldehydes at both C-2 and C-3 positions without the simultaneous occurrence of any side reaction and the product is commonly referred to as dialdehyde cellulose (DAC). The

regioselectivity was examined by further studying the hydrolysis product of the dialdehyde cellulose, which gives rise to glyoxal and *n*-erythrose confirmed as *n*-erythronic acid.[125] This finding also proved that periodate oxidation was caused by cleavage of the carbon-carbon linkage containing vicinal hydroxyl groups at the C-2 and C-3 of the anhydro *n*-glucopyranose units and generally accepted structure of other polysaccharides oxidized with periodate.[126] The degree of oxidation can be controlled by the reaction time and the concentration of oxidant.

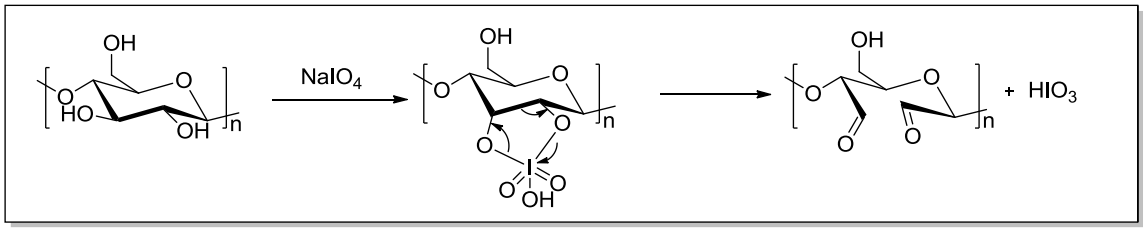

Fig. 2.15 Schematic of periodate oxidation reaction mechanism of cellulose.

Periodate oxidation of cellulose is one of the most extensively and widely studied oxidation reactions compared to other polysaccharides. This is because (i) periodate serves as useful model for oxidizing agents frequently used or encountered in processing of pulps, (ii) minimize degradation and retain the mechanical and morphological properties of the starting material, and (iii) finally the development of novel cellulose derivatives through periodate oxidation. In order to achieve high aldehyde contents, sometimes large amounts of periodate and long oxidation times have to be followed, which results in a decrease in the efficiency of the oxidation and forms a lot of iodine waste. Few attempts were made to improve the reactivity of cellulose with periodates. For instance, Tang et al.[127] treated cellulose fibers with ultrasound before reacting with periodate. Regioselective oxidation reactivity of cellulose towards periodate was

significantly improved showing an increase in cellulose accessibility in terms of water retention value (WRV) with increasing ultrasound treatment time, corresponding to 73.0%, 75.6%, 80.8%, 98.7% and 119.0% after treated for 0, 90, 180, 360 and 720s, respectively. Recently, Juho and coworkers[128] significantly enhanced the periodate oxidation efficiency by using elevated temperatures (55-85 ^{o}C) in the presence of LiCl metal salts as cellulose activators in very short times (less than 2 h). LiCl improved the oxidation efficiency by reducing the inter- and intra-molecular hydrogen bonding between the cellulose chains. Again, they introduced a new approach,[129] i.e simultaneous pulp micronization in a wet stirred media mill and oxidation by sodium periodate to produce dialdehyde cellulose microfibers within short reaction times and in mild condition. Field emission scanning electron micrographs (FESEM) showed that milling completely disintegrated the fiber structure and produced fibrillar particles with a length from 10 to 50 μm and diameters ranging from a few hundreds of nanometers to 1 μm depending on the conditions used. As a result, it significantly enhanced the pulp reactivity towards periodate oxidation and it was also observed that microfibers generated by milling-induced oxidation were thinner and they had better size distribution than the microfibers milled without oxidation.

.

2.4.2.3 Analysis of carbonyl groups in periodate oxidized cellulose

Analysis of the carbonyl group in oxidized cellulose is often complicated. This is due to the presence of hemiacetals resulting from both inter- and intramolecular linkages of the anhydroglucose units in presence of moisture. Fourier transform infrared (FT-IR) spectroscopy is the most frequently used technique for qualitative analysis of oxidized

cellulose, where the samples are always needed to be dried in order to observe the C=O stretching vibration band in FT-IR spectrum. Use of solid state NMR spectroscopy is limited partly due to its characteristic broad peaks and partly due to the formation of hydrates and hemiacetals in DAC samples. On the other hand, the solution NMR method is limited due to the lack of solubility of DAC in common organic solvents.[130-131] Quantitative analysis of the carbonyl groups of the dialdehyde cellulose product was performed by conventional method such as a Tappi standard method known as copper number titration and a second approach called hydroxylamine procedure. In copper number titration, the reducing power of cellulose is measured by reaction with an alkaline Cu^{II} –salt under defined conditions and the generated Cu^{I} ions are titrated after re-oxidation to obtain the copper number. The copper number is then converted to the corresponding carbonyl content using a standard mathematical expression.[132] Hydroxylamine procedure involves the reaction of dialdehyde cellulose with hydroxylamine to form the corresponding oxime and the degree of nitrogen fixation is usually measured by a Kjeldahl procedure or by elemental analysis.[133] However, both the methods seem to have certain limitations, e.g., the copper number data cannot be directly related to the quantity of a specific oxidized function and the hydroxyl amine method is of limited use due to its poor sensitivity, giving rise to only a sum parameter. Additionally, a large quantity of sample is needed for analysis in both the methods.

Considering the lack of a reliable and accurate method for determination of carbonyl content, Potthast et al.[132] first introduced a novel approach based on fluorescence labeling of carbonyls with carbazole-9-carboxylic acid [2-(2-aminooxyethoxy)ethoxy]amide ("CCOA") both in heterogeneous and homogeneous

conditions. The CCOA label contains a fluorophore and a flexible spacer with a reactive oxyamine anchor, which reacts with the aldehyde groups as shown in Fig. 2.16. Due to its fluorescence characteristics, no interference with multi-angle laser light scattering detection (MALLS) detection is encountered. As a result, the carbonyl profile can be determined relative to the molecular weight distribution by gel permeation chromatography (GPC) combined with a multi detector containing fluorescence, MALLS and refractive index (RI) detection. This analytical method was found to be promising and provided the carbonyl content of numerous pulps with precise evaluation of oxidative changes. However, the combination of GPC with fluorescence was limited to only low molecular weight dissolving pulps or rag papers. For high molecular weight pulps such as paper pulps due to their limited solubility in DMAc/LiCl, Potthast et al.[134] used the same CCOA labeling procedure in heterogeneous condition but with slight modification. The modified approach consists of labeling the pulp with CCOA followed by its hydrolysis to release the CCOA and CCOA derived products corresponding to the carbonyl profile to be determined by high pressure liquid chromatography (HPLC). Further investigation on kinetics at low degrees of oxidation using CCOA labeling suggests that 2,3-dialdehyde groups were introduced into high molecular weight areas implying that crystalline regions were attacked at very early stages of oxidation as opposed to the gradual oxidation from amorphous to crystalline region.[135]

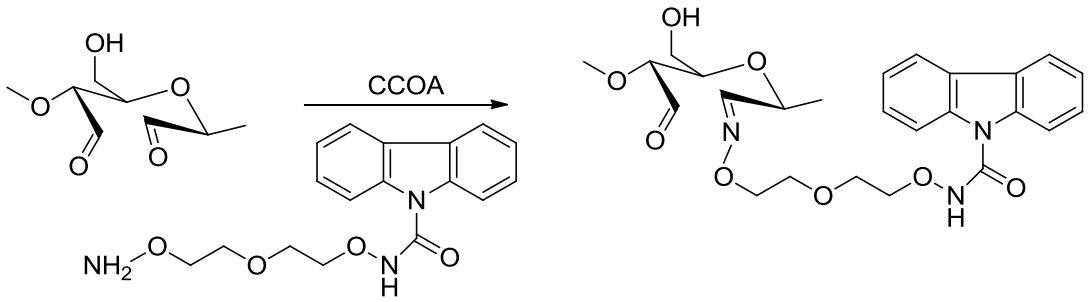

Fig. 2.16 CCOA-labeling of dialdehyde cellulose showing the reaction at C-3.[133]

2.4.2.4 Influence of periodate oxidation on macromolecule properties of cellulose

2.4.2.4.1 Crystallinity

Besides the above mentioned specificity of periodate oxidative reaction of cellulose, it differs from most other oxidizing agents in that it has the property to penetrate and react with the crystalline as well as the amorphous portion of cellulose without causing much degradation under the controlled conditions. With the common types of oxidizing agents, the reaction is virtually confined to the amorphous regions and the surfaces of the crystallites, and the products suffer from unspecific oxidation.[126]

Irrespective of the starting cellulose, periodate oxidation has a prominent effect on the crystallinity of cellulose, since the crystallinity decreases linearly with the degree of oxidation. Varma et al.[130] measured the crystallinity of 2,3-dialdehyde cellulose powders using wide angle XRD technique, showing that crystalline peak almost decreases proportionately with the degree of oxidation of the starting cellulose. Bleached Kraft softwood pulp was oxidized by Hou and coworkers[136] showing similar behavior where a decrease in crystallinity index from 1.40 to 0.88 was observed with the 100% periodate charge on wood fiber after 500 minutes of reaction. The introduction of dialdehyde groups to bacterial cellulose resulted in a decrease in crystallinity from 66% to 56% with

an aldehyde content of 12 % as measured by XRD.[137] Even for the highly crystalline marine alga *Cladophora* cellulose, it follows the similar trend, i.e. crystallinity decreases according to the oxidation level although half-height widths of equatorial diffraction peaks were nearly unchanged.[131] This study also proposed a model explaining that crystalline cellulose was attacked by the oxidant heterogeneously and the oxidation is a self-accelerating process, where oxidation of one glucopyranose ring makes the neighboring group more susceptible to oxidant due to the local loss of crystalline order. The mechanism of oxidation was further investigated by Paolo et al.[138] using both FT-IR and wide-angle X-ray scattering (WAXS), which suggests that periodate oxidizes cellulose in isolated domains leading to decrease of crystallinity.

Cotton fibers oxidized by periodate (1.0 mg/mL) for 1 h had a crystallinity of 65.37%, and the crystallinities of the fibers oxidized by 30.0 mg/ml for 3 h, 5 h and 10 h were 43.79%, 32.16% and 23.76%, respectively, as compared to 62.56% crystallinity for the original cotton fiber.[139] It was proposed that for low periodate concentration, the slight oxidation mainly occurred in the amorphous region of cotton cellulose and the amorphous phase was partially corroded off and dissolved away, resulting in the increase of relative crystallinity for the residual cotton cellulose. However, higher periodate concentration and prolonged reaction time could access into the inner region of cellulose, which would open the pyranose ring and weaken the intermolecular hydrogen bonding. Therefore, the crystalline structure of cotton fiber was broken down and depolymerized, thus significantly reduced the crystallinity of cotton cellulose.

2.4.2.4.2 Chain flexibility

The effect of periodate oxidative cleavage on cellulose chain properties has not been investigated properly due to the insolubility of DAC in common solvents. However, during the carbonyl analysis of dialdehyde cellulose in DMAc/LiCl using a multi detection technique, Potthast et al.[135] provided some additional information on the shape of oxidized cellulose molecules in solution. Typical R_g-M (R_g: radius of gyration, M: molecular weight) relationship i.e. $R_g = KM^{\nu}$ was determined from the angular dependence of light as provided by SEC-MALLS (size exclusion chromatography with multi-angle light scattering detection) data, where ν reflects the overall shape of the polymer varying from 0.33 for compact sphere to 1.0 for completely expanded coils. With an increase in degree of oxidation, there is a decrease in ν down to ~0.4 and a simultaneous increase in molecular weight, suggesting that at higher degrees of oxidation, the radius of the molecules decreases and the molecules become more compact in shape. This phenomenon was further supported by Bouchard et al.[140] as they also observed similar ν values with increasing carbonyl content. The decrease in radius or increase in compactness of oxidized molecules at higher degree of oxidation was believed predominantly due to the inter chain hemiacetal cross-linking, supporting its increased molecular weight.

2.4.2.4.3 Chain degradation

It is well known that β-1,4-linkages in the glucose unit are quite stable and it do not degrade enzymatically in human body. However, the biodegradability of cellulose could be significantly improved by introducing dialdehyde groups into the glucose unit

through periodate oxidation as observed and examined by Singh et al.[141] After studying the degradation process both *in vitro* and *in vivo* and based on the analysis of the degradation products, it was proposed that at physiological pH dialdehyde cellulose degrades hydrolytically into glycolic acid and 2,4-dihydroxybutyric acid by elimination of alkoxyl group as shown in Figure 2.17. Glycolic acid has been reported to be either excreted in urine or participated in glyoxylate metabolism, whereas 2,4-dihydroxybutyric acid participates in in the L-homoserine metabolism in mammalian liver. The degradation process is faster in the first few days followed by a steady and sustained degradation for about a month without producing excessive tissue reaction.[142] Biodegradation of periodate oxidized bacterial cellulose scaffold was studied by Li Jian et al.[143] in water, phosphate buffered saline (PBS) and simulated body fluid (SBF) solutions to increase the potential application of bacterial cellulose in tissue engineering. Faster degradation was occurred in PBS than in water following the same degradation mechanism as mentioned earlier with additional evidence that the degradation began from the amorphous part of the polymer.

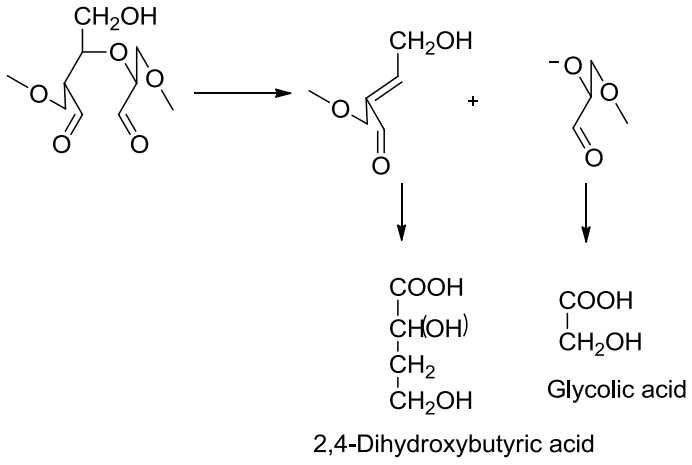

Fig. 2.17 Degradation product of periodate oxidized cellulose.[142]

Dialdehyde cellulose has been the focus of many biomedical studies owing to its biocompatibility and biodegradability. For example, dialdehyde cellulose provided adequate mechanical property combined with bioabsorbability and inherent antimicrobial nature for suture applications.[144] 2,3-Dialdehyde cellulose membranes served as a scaffold for cell attachment and growth, which was evidenced by spreading of fibroblast cells.[145] Further study indicated that freeze drying, porosity and degree of oxidation play a significant role in controlling the biomechanical and viscoelastic properties of the scaffold.[146] Recently, Drogat[147] et al. have shown a new approach to utilize dialdehyde cellulose nanocrystals as a reducing agent and a substrate to form silver nanoparticles on its surface under alkaline condition. These silver nanoparticles have been recognized as excellent candidate for wound dressing and antifouling coatings.

2.4.2.5 Chemical derivatization of periodate oxidized cellulose

The resultant aldehyde groups of the periodated cellulose also considered as ‘‘chemical hooks’’, act as reactive intermediate for further chemical modification, thus increasing the prospects of chemical derivatization of cellulose. There are mainly three different types of subsequent chemical derivatization of dialdehyde cellulose investigated in literature i.e. conversion of dialdehyde to carboxylic acid, Schiff’s base with amines and bisulfite adducts. All these reactions proceed in aqueous solution and under mild reaction condition and therefore are easy to control for varying degree of substitution.[148]

2.4.2.5.1 Oxidation reaction of 2,3-dialdehyde cellulose

Oxidation of the dialdehyde cellulose with sodium chlorite/hydrogen peroxide leads to carboxyl structures at C2 and C3 positions as shown in Fig. 2.18. This was first introduced by Rutherford et al.[149] and later studied and investigated in detail by Hofreiter and coworkers[150] to optimize the reaction conditions. Cellulose was found to be water soluble by introducing 2,3-dicarboxyl groups and hence, the relative chemical shift of C2 and C3 carbons were easily studied by ^{13}C NMR spectroscopy, which in turn provided the evidence for the presence of aldehyde groups at the respective carbons.[131] Moreover, periodate oxidation followed by the carboxylation reaction opened the glucose rings resulting in numerous stereochemical and rotameric configurations, which was reflected in solid state NMR spectrum by the appearance of multiple and broad peaks.[130]

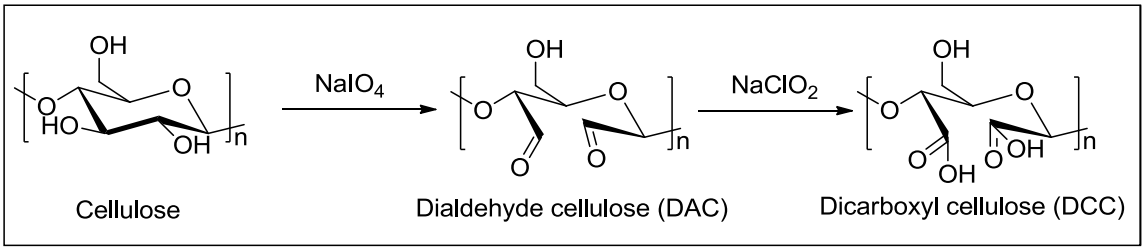

Fig. 2.18 Derivatization of 2,3-dialdehyde cellulose to dicarboxyl product.[130]

2,3-Dicarboxycellulose has been used directly due to its special properties. For example, for 100% oxidation, cellulose is completely soluble in water leading to applications in food, pharmaceuticals and cosmetic industry.[127, 151] Literature study showed that 2,3-dicarboxyl cellulose can complex with various metal ions in the form of metallic salts of carboxylic acids other than alkali metals, which precipitates or solidifies

in exposure to air. Thus, 2,3-dicarboxycellulose was considered as a useful scavenger for the removal of heavy metallic ions under mild conditions.[151] Initial complexation with M^{2+} ions, such as Ca^{2+}, suggests a conformational change in dicarboxyl cellulose with a concomitant reduction in hydrodynamic ratio followed by subsequent gel or solid formation.[152-153] A large number of studies have been dedicated to the calcium binding property of dicarboxy cellulose, a prerequisite for their application as a detergent binder. Introduction of regioselective dicarboxyl groups to spherical cellulose gel led to the preparation of useful cation-exchange chromatographic materials for both aliphatic and aromatic amines. This charged cellulose gels had shown an anomalous pH dependence retention factor for amines with a maximum retention factor at pH 4, which was 4-5 times greater than the conventional gels having similar amount of carboxyls.[154]

2.4.2.5.2 Amination reaction of 2,3-dialdehyde cellulose through Schiff's base reaction

Schiff's base reaction between primary amino functionalities and 2,3-dialdehyde cellulose is a facile and useful chemical derivatization procedure to graft various substituents on to cellulose surface. This has been the most widely studied reaction on dialdehyde cellulose to immobilize various nitrogen containing compounds such as proteins, enzymes, drugs, dyes, as well as aliphatic and aromatic amine compounds to prepare ion-exchange chromatographic materials.[155] As shown in Fig. 2.19, DAC is expected to give its condensation products by reacting with two molar reagents of nitrogen compound per anhydroglucose unit, since it contains two free aldehyde groups in each unit. However, the nucleophilic addition-condensation reaction between a carbonyl group and a basic amine depends on the ease of available hydrogen ion

concentration to the carbony1 oxygen. A high concentration of hydrogen ion contributes greatly to the formation of non nucleophilic R-$N^{+}H_3$ species by the addition of hydrogen ion to amines. Therefore, it is always important to choose the appropriate pH conditions, to promote the formation of the nucleophilic, basic amine, R-NH_2 and to suppress the non-nucleophilic species, R-$N^{+}H_3$.[156-157]

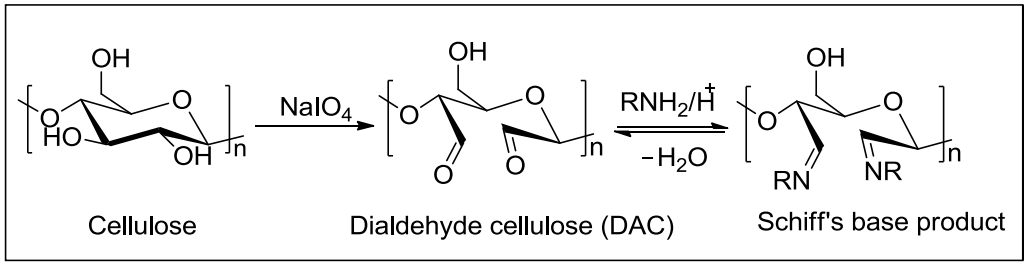

Fig. 2.19 Derivatization of 2,3-dialdehyde cellulose to Schiff's base product.[156]

Kim et al.[148] grafted polyallylamine to size-exclusion graded cellulose gel through periodate oxidation followed by the Schiff's base condensation and subsequent reduction reaction. The ion exchange capacity of these polyallylamine grafted cellulose was found to be remarkably greater than the conventional anion-exchanger material due to the high local density of amino groups introduced at specific position in contrast to the random and sparse charge distribution in conventional exchangers. The same procedure was followed by Wu et al.[158] to prepare ion-exchange material from cellulose fabrics (cotton and rayon-cloths) concluding that the level of grafting is strongly dependent on the concentration, pH of the reaction, and molecular weight of the polyallylamine. The level of cationization was maximized by using high concentration of low molecular weight of (Mw: 1000) amine under high pH.

Partially oxidized lyocell fibers, a regenerated form of cellulose, were shown to have increased amorphous regions and decreased thermal stability with the increase in oxidation level as observed by Han and coworkers.[159] However, after cross-linking with multifunctional amines following Schiff's base reaction, a restriction in the molecular chain mobility occurred, reflecting an improvement in thermal stability and an increase in viscosity-average degree of polymerization. Further study on cross-linking between oxidized lyocell fiber and low molecular weight chito-oligosaccharides through reducctive followed by reductive amination $NaBH_4$ reduction imparted antifibrillation and antimicrobial properties to lyocell fiber.[160] Similarly, grafting of low molecular weight chitosan with bleached Kraft softwood dialdehyde cellulose fiber, cotton fiber and lyocell fiber had exhibited a significant improvement in antimicrobial activity against *Staphylococcun aureus and Escherichia coli*.[161-162]

Another important application of the Schiff's base reaction is to utilize dialdehyde cellulose as a delivery system for amine containing drugs, proteins, enzymes, etc. Most enzymes have versatile application in industry and biomedical field such as hydrolysis, esterification, biotransformations, and racemic resolutions. However, their applications are limited due to their instability and rapid loss in their catalytic activity. Among other methods of enzyme immobilization, covalent immobilization on a suitable carrier represents an effective and attractive alternative because of the following reasons: (1) enzymes do not leak detach from the support during the application; (2) immobilized enzyme can easily make contact with the substrate because it is localized on the support surface; and (3) an increase in heat stability is often observed because of the interaction between the enzyme and support material, thus extending the active life of enzymes.

Trypsin was immobilized on cotton yarn using sodium periodate oxidation followed by the Schiff's base reaction with a maximum loading of 6.1mg/g of cotton.[163] Immobilized trypsin on oxidized cotton yarn retained 90% and 72% of the initial activity at 4 ^{o}C and 25 ^{o}C, respectively, over 60 days of storage in physiological solution. Other examples include immobilization of trypsin and α-chymotrypsin, insulin, collagen on cellulose powders, lipase on regenerated cellulose and glucoamylose on baggase cellulose through the same covalent coupling procedure showing an extended stability of the enzymes.[164-169] p-Amino salicylic acid, an anti-tuberculosis drug molecule was directly immobilized on to dialdehyde cellulose powder followed by its in vivo and in vitro release study, exhibiting the potential use of dialdehyde cellulose as a useful carrier for sustained release. Recently, Dash et al.[170] combined the Schiff's base condensation reaction with subsequent reduction and EDC/NHS esterification to prepare a cellulose nanowhisker based controlled drug delivery system. It is significant in terms of surface grafting of cellulose nanowhiskers through periodate oxidation and amination reaction to synthesize modified nanowhiskers for various structural and biomedical applications.

2.4.2.5.3 Sulfonation reaction

Sulfonation of dialdehyde cellulose is the least studied chemical modification reaction in literature. This is a very simple reaction between 2,3-dialdehyde cellulose and sodium bisulfite in aqueous medium (Fig. 2.20) and the product of the sulfonation reaction is referred as bisulfite adduct or sulfonated product of cellulose.

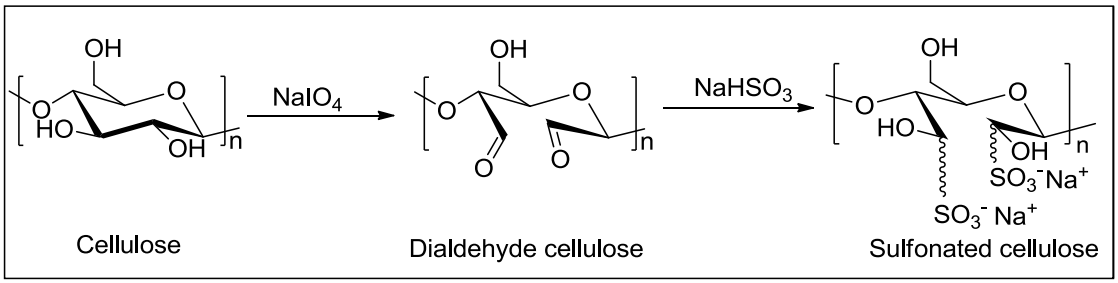

Fig. 2.20 Derivatization of 2,3-dialdehyde cellulose to sulfonate product.[171]

Rahn et al.[172] first studied the reaction in water as well as in a mixture of water/ethanol followed by its characterization using FT-IR and elemental analysis. From sulfur analysis it was observed that the degree of sulfonation can be controlled by the aldehydes to sodium bisulfite ratio and the duration of sulfonation reaction to some extent. Depending on the bisulfite content, the samples were soluble or highly swellable in water. However, a detailed characterization of the sulfonated cellulose was lacking in this study. Shet and Wallajapet[173] investigated the effect of introduction of sulfonate groups on the physical and mechanical properties of cellulose fibers. They reported that the conversion of dialdehyde cellulose to sulfonated cellulose resulted in a significant increase in water absorbency values as well as in both dry and wet tensile strength of the fibers.

Hou et al.[171] demonstrated the effect of periodate oxidation and sulfonation on the water absorbency, dry and rewet tensile strength of the sheets made from softwood pulp. It was concluded that the aldehyde content increases with the oxidant charge and the reaction time. The treatment of the oxidized fibers with sodium bisulfite not only improved the undried fiber water absorbency and swelling but also increased the dry and rewet tensile strengths of test sheets. At 50 wt. % oxidant charge and 240 min oxidation duration time the highest values of 8.30 and 62.94 Nâm/g for both rewet and dry tensile indices of the test sheets were obtained after sulfonation. The observed increase in

bonding strength of test sheets made of oxidized and sulfonated fibers was validated from the special features of AFM topographical images of the test sheets.

2.5 Chemical modification of cellulose nanowhiskers

Recently, cellulose nanowhiskers have attracted significant research attention as a green nanofiller in bionanocomposites because of their superior mechanical properties, high aspect ratio, low density, biocompatibility, high strength, and crystallinity.[43, 174-176] To further broaden its utilization, constant attempts have been made to chemically modify the surface hydroxyl groups of nanowhisker into different polar and non-polar moieties, which have led to an increased interest in synthesis of functionalized nanowhiskers, a relatively new and exciting research arena.

Due to the abundance of reactive hydroxyl groups on CNWs surface, esterification, and etherification are the most common approaches for chemical modification of cellulose whiskers although there are several reports on oxidation, nucleophilic substitution, and silylation reaction. All these modifications are primarily focused on various covalent functionalization of the surface hydroxyl groups considering the need for potential applications. Sassi et al.[177] acetylated valonia and tunicate whisker surface using acetic anhydride in acetic acid involving a non-swelling mechanism only affecting the cellulose chains localized at the surface. Acetylation of whiskers was also carried out in vinyl acetate, alkenyl succinic anhydride (ASA) to improve the dispersion of whiskers in organic solvents.[178-181]

The surface of ramie cellulose whiskers was esterified with organic fatty acids of different chain lengths by reacting with different acid chlorides (hexanoyl, lauroyl and

stearoyl chlorides) to change their hydrophilic surface to hydrophobic by de Menezes et al.[95] The esterification reaction enhanced the non-polarity of nanowhiskers allowing their use as fillers in non-polar low density polyethylene matrix to process the nanocomposite materials. An alternative to regular multistep synthetic approaches, Dorgan et al.[182] conducted simultaneous synthesis and esterification of nanowhiskers using a mixture of acetic acid, HCl and organic acids (acetic and butyric acid) to increase their hydrophobicity. Approximately half of the surface hydroxyl groups of resulting nanowhiskers were found to be esterified, thus improving their dispersion in organic solvents and preventing the formation of strong hydrogen bonding upon drying. L-leucine amino acid was grafted to nanowhisker surfaces through esterification reaction showing a possible nanowhisker platform for introducing biologically active building blocks.[183]

Gousse et al.[184] examined the silylation of the hydroxyl groups on tunicin whiskers using a series of alkyldimethylchlorosilanes such as n-butyl, n-octyl and n-dodecyl silanes. It was observed that silylated whiskers were readily dispersible in THF but their birefringence behavior and morphological integrity was lost at high degree of silylation (DS > 1). Further silylation of sisal nanowhisker by n-octadecyl isocyanate was investigated by Siqueira et al.[185] to reinforce in to polycarpolactone (PCL) based nanocomposites. Trimethylsilylation of the bacterial nanocrystal surface was performed heterogeneously with hexamethyldisilazane to reduce the surface hydrophilicity, which was incorporated in cellulose butyrate matrix to process nanocomposites.

TEMPO oxidation of nanowhisker converts the surface hydroxymethyl groups into their carboxylic form, while maintaining their structural integrity, characteristic birefringence behavior and homogeneous dispersion ability in water. TEMPO mediated

oxidation of CNWs obtained from HCl hydrolysis of cellulose fibers was studied by various groups in order to impart negative charge on whisker surface to obtain a non-flocculated suspension in water.[92, 186-187] Araki et al.[92] further prepared novel sterically-stabilized aqueous whisker suspension combining TEMPO mediated carboxylation and grafting of amine terminated polyethylene glycol (PEG). Followed by TEMPO oxidation, amidation and complexation were performed on nanowhisker surfaces using octadecylamine (ODA) as the modifying compound by Jhonson and coworkers.[188] Both treatments resulted in complete substitution of TONc surface carboxyl groups with ODA, transforming nanowhisker surfaces from hydrophilic to hydrophobic with improved thermal stability. 4-Amino TEMPO was successfully grafted to the TEMPO oxidized nanowhisker surface via an amide coupling without affecting their morphology and crystallinity and the amide coupling was found to reduce the polarity of the nanowhisker surface.[186] Positive charges were also introduced on to cellulose nanowhisker surfaces through nucleophilic coupling of hydroxyl groups with epoxypropyltrimethyl ammonium chloride in presence of alkali as reported by Hassani et al.[189]

Fluorescent cellulose nanocrystals were prepared through a silanization reaction with 3-aminopropyltrimethoxysilane followed by covalent grafting of fluorescein isothiocyanate.[190] Literature reveals several attempts of surface modification of cellulose nanowhisker for potential biomedical applications. For instance, cellulose nanowhisker surfaces were functionalized with gold nanoparticles by Mahmoud et al. and this templated material was demonstrated as an excellent immobilization support for enzymes with high loading capacity.[191] Single stranded oligonucleotides were effectively grafted

on to TEMPO oxidized nanowhisker surfaces, setting a platform for future development of nanodevices from inexpensive and chemically versatile nanowhiskers.[192]

Several other examples of functionalization approach includes grafting-onto and grafting-from whisker surfaces to demonstrate very good compatibility and high adhesion with synthetic polymers.[193-194] These grafting approaches frequently involve functionalization via surface hydroxyl groups to a presynthesized polymer through a coupling agent or to a polymer formed by in-situ polymerization from immobilized initiators on the substrate surface. The literature also shows few studies on modification of CNWs surfaces by coating with surfactants to improve the compatibility with non-polar solvents.[195-198]

CHAPTER 3

EXPERIMENTAL MATERIALS AND PROCEDURES

3.1 Materials

Hard cellulose beads (~100 μm size) made from bleached hard wood chemical pulp were provided by Kobo Products, USA. A commercial fully bleached softwood Kraft pulp was obtained from a southeastern USA manufacturing facility. The cationic starch (Degree of substitution: 0.04-0.05, Mw ~ 3×10^8) was supplied by National Starch and Chemical Company, USA. Poly(diallyldimethylammonium chloride) (Poly-DADMAC, M_w 1-2×10^5, 0.001 N) and potassium polyvinyl sulfate (PVSK, M_w ~1.7×10^5, 0.001 N) solutions were purchased from Nalco, USA. Gelatin (type A, Bloom 300) was purchased from VWR International. All chemicals and solvents were purchased from VWR International and used as received.

3.2 Cellulose nanowhisker preparation

The fully bleached softwood Kraft pulp, obtained from southeastern USA manufacturing facility was ground in a Willy mill and passed through a sieve (0.85 mm) to prepare nanowhiskers. Cellulose nanowhiskers were prepared by sulfuric acid hydrolysis of the pulp based on a literature procedure.[31] In brief, H_2SO_4 solution (64%, w/w) was prepared in an ice bath and then the temperature of the solution was maintained at 45 ^oC in a hot water bath. Pulp (60.00 g) was mixed with the above H_2SO_4 solution (1:10 g/mL) and the mixture was continuously stirred at 45 ^oC for 45 min. The hydrolysis reaction was stopped by adding excess (10-fold) of distilled water. The

sediment was centrifuged at 12,000 rpm for 10 min and the precipitate was collected and dialyzed (MWCO: 12-14,000) with DI water until the solution pH did not change. After dialysis, the content was sonicated in an ice bath for 10 min by a GEX 500 ultrasonic processor with the output power set as 38% and then centrifuged for 5 min at 10,000 rpm. The cloudy supernatant, containing nanowhiskers, was collected and the remaining sediment was again mixed with water, sonicated and centrifuged to obtain additional nanowhisker; this procedure was repeated till the supernatant was clear. Cellulose nanowhiskers were obtained in 20-30% yield.

3.3 Sodium periodate oxidation of cellulose

3.3.1 Sodium periodate oxidation of cellulose fibers

A slurry of cellulosic fibers (6.00 g) and deionized water (DI) (200.00 mL) was treated with sodium periodate (1.20 g, 5.61 mmol) and stirred for three days at room temperature in the absence of light. The product was filtered, repeatedly washed with DI water to remove the spent oxidant, and then air-dried. The same procedure was followed to prepare all the oxidized samples and the isolated mass yields were 95-98%. These samples were named as dialdehyde cellulose (DAC).

3.3.2 Sodium periodate oxidation of cellulose nanowhiskers

A mixture of cellulose nanowhiskers suspension (250.00 mL, 2.00 wt. %, w/v) and sodium periodate (0.60 g, 2.80 mmols) was stirred for two days in the absence of light at room temperature. The product was then placed into dialysis membranes (MWCO: 12-14,000) and dialyzed against DI water for 2 days to remove the spent oxidant, and then freeze-dried providing a gravimetric yield of 98%.

3.4 Sulfonation of 2,3-dialdehyde cellulose

3.4.1 Sulfonation of 2,3-dialdehyde cellulose fibers

The 2,3-dialdehyde cellulose (4.00 g) was dispersed in DI water (100.00 mL) and reacted with sodium bisulfite (6.00 g, 57.65 mmol). After stirring for 72 h at room temperature, the resulting product was dialyzed using cellulose acetate membrane (MWCO: 5000) followed by freeze drying. All the samples were prepared using the same amount of sodium bisulfite and the products were obtained in 87-94% yield. These samples were referred to as sulfonated cellulose (SC).

3.4.2 Sulfonation of 2,3-dialdehyde cellulose beads

2,3-Dialdehyde cellulose beads (6.00 g) were slowly stirred in sodium bisulfite solution (100 mL, 0.48 N) for 24 h. The resulting product was dialyzed using cellulose acetate membrane (MWCO: 5000) against DI water for 2 days, followed by freeze drying and the products were obtained in 87-94% gravimetric yield.

3.5 Reaction of dialdehyde cellulose whiskers with primary amines

The dialdehyde cellulose whisker suspension (100 mL, 2.00 wt. %) was acidified in acetate buffer (100.00 mL, pH 4.5) and stirred for 15 min. Methyl and butyl amine was then slowly added to the suspension (5 eq. per glucose unit) in separate experiments and the mixture was continuously stirred at 45 ^{o}C for 6 h followed by the *in situ* reduction of the resulting imine intermediate at room temperature employing $NaBH_4$ (2.5 eq. per glucose unit) dissolved in 2.00 mL water. After stirring for 3 h, the product was dialyzed

(MWCO: 12-14,000) against DI water until the pH was neutral and subsequently, the slurry was freeze dried to obtain the dry product with a mass yield of 80-90%.

3.6 Reaction of dialdehyde cellulose whiskers with gamma aminobutyric acid (GABA)

A dialdehyde cellulose nanowhisker suspension (20.00 mL, 2.00 wt. %, w/v) was mixed with acetate buffer (20.00 mL, pH 9.0) and stirred for 15 min. Gamma aminobutyric acid was then slowly added to the suspension (10 eq. per glucose unit) and the mixture was continuously stirred at 45 ^{o}C for 24 h followed by the *in situ* reduction of the resulting imine intermediates at room temperature employing $NaCNBH_3$ (2.5 eq. per glucose unit). After stirring for 6 h, the product was dialyzed (MWCO: 12-14,000) against DI water until the pH was neutral and subsequently, the slurry was freeze dried to obtain the dry product with a yield of 80-90%.

3.7 Reaction of DAC-GABA with syringyl alcohol

An aqueous suspension of DAC-GABA (10.00 mL, 2.00 wt.%, w/v), 1-ethyl-3-(3-dimethylaminopropyl) carbodiimide (EDC, 1.87 g, 8.00 mmol), sulfo-N-hydroxysuccinimide (NHS, 0.50 mmol), 4-(dimethylamino) pyridine (DMAP, 1.22 g, 1.00 mmol) and syringyl alcohol (1.60 g, 8.00 mmol) was stirred at room temperature for 24 h. Finally, it was dialyzed against DI water for 3-4 days and freeze dried. The product was obtained in 70-80 % yield.

3.8 Synthesis of chemically cross-linked hydrogels

A solution was prepared by adding gelatin (4.708 g) to water at 40 ^{o}C with slow stirring, and the solution was kept at this condition for 3-4 days to remove all entrained air-bubbles. The oxidized nanowhisker suspension (30 mL, 0.515 g) was degassed to get rid of any bubbles using a water aspirator. Then the nanowhisker suspension was warmed to 40 ^{o}C and slowly added to gelatin solution and mixed for 20 min under constant stirring. The mixed gel was poured onto a Teflon mold at room temperature and after drying for 24 h at room temperature the gels were stored at 4 ^{o}C for 10 days. The gels were punched into samples of 14 mm diameter and 2 mm thickness for further characterization.

3.9 Analysis procedures

3.9.1 Determination of carbonyl content of dialdehyde cellulose by copper number titration

Copper number (Cu #) was measured following Tappi standard method T 430 (Tappi Standard T430). In brief, air-dried fibers (0.30 g) were treated with an aqueous $CuSO_4$ (1.00 mL, 0.40 N) solution and a carbonate-bicarbonate solution (19.00 mL, 2.40 N, 1.04 N). The mixture was heated at 100 °C for 3 h, cooled, filtered, and washed with 5% aqueous Na_2CO_3 solution (20.00 mL) and hot water (50.00 mL). The fibers along with the filter paper were dispersed in 5% phosphomolybdic acid (5.00 mL), stirred, filtered, and then washed thoroughly with water. The filtrate was diluted with DI water (140.00 mL) followed by the titration with 0.05 N $KMnO_4$ to a faint pink end point. A blank test was also performed following the same procedure. For each sample the

experiment was repeated three times to obtain the copper number and the data were reported with an error of less than ±4.0%.

The copper number was calculated using the equation[132]:

Copper number = (6.36 (V-B) N)/W

V = Volume of $KMnO_4$ solution to titrate the filtrate from the specimen, mL.

B = Volume of $KMnO_4$ solution to titrate the blank filtrate, mL.

N = Normality of $KMnO_4$, 0.05 N.

W = Weight of pulp fibers, g.

3.9.2 Conductometric titration of sulfonated cellulose

Conductometric titration was carried out with a model 2052 EC meter at a cell constant of 10 cm^{-1} and the procedure is based on literature methodology.[199] Sulfonated cellulose (0.30 g) was suspended in HCl solution (60.00 mL, 0.10 N) for 1 h, then filtered, and washed with sufficient amount of DI water to remove excess acid. The air-dried samples were dispersed in sodium chloride solution (45.00 mL, 0.001 N) followed by the titration with 0.05 N sodium hydroxide solution with continuous stirring under nitrogen atmosphere. Initially, 0.25 mL of sodium hydroxide was added and the conductance value was recorded every 10 minutes so as to allow sufficient time for the equilibrium to be reached between readings and gradually the alkali addition was decreased to 0.10 mL before taking each measurement. Titration was continued until the conductivity reading was about the same as initial reading. In each case, the titration was conducted three times and the value reported was the average of all the three readings with an error of less than ±2.0%.

3.9.3 Polyelectrolyte titration for surface charge determination

The polyelectric titrations were carried out in a MUTEK particle charge detector based on a published method.[200] Briefly, the sulfonated cellulose beads (0.50 g) were mixed with polydiallyldimethylammonium chloride solution (Poly-DADMAC, 100 mL, 0.001 N) and stirred for 2 h. This mixture was then filtered and 10.00 mL of the filtrate was pipetted into the cell of the detector followed by the titration with 0.001 N of potassium polyvinyl sulfate (PVSK) solution. The specific charge density of the beads was calculated with an error of less than ±0.10% using the formula: ($q = [(Vp - Vb) \times c \times 1000]/w$), where q is specific charge density (mmol/kg), Vp is the volume of titrant used for the specimen (mL), Vb is the titrant consumed by the blank solution (mL), c is the concentration of titrant (N), and w is weight of the sample (g). In each case, the titration was conducted three times and the value reported was the average of all the three readings with an error of less than ±0.5%

3.9.4 Study of interaction between cationic starch and sulfonated cellulose beads

To a solution of sulfonated cellulose beads in water (0.001%, w/v), cationic starch solution (1%, w/v) was added in a petri dish and the interaction was studied immediately using a Leica DM IRM microscope at 15 magnifications at room temperature.

3.9.5 FT -IR spectroscopy

Transmission mode FT-IR spectra were collected with a Nicolet Magna-IR^{TM} 550 spectrometer. Spectra were obtained in 400-4000 cm^{-1} range and for each sample 64

scans were collected at a resolution of 4 cm^{-1}. All the samples were grounded to powder, and pressed into a KBr pellet (1:200) before collecting the spectra.

3.9.6 Gel permeation chromatography analysis of cellulose

The number-average molecular weight (M_n) and the weight-average molecular weight (M_w) were determined by gel permeation chromatography (GPC) after tricarbanilation of celluloseCellulose sample (15 mg) was dried over P_2O_5 under vacuum (762 mm of Hg) at 40 °C for 24 h. Oven-dried cellulosic fiber was reacted with a mixture of anhydrous pyridine (4.00 mL) and excess of phenyl isocyanate (0.50 mL, 4.00 mmol) at 65 ^oC with continuous stirring for 2-3 days. The solution was then cooled followed by the addition of methanol (1.00 mL) to consume the unreacted phenyl isocyanate. The tricarbanilate derivative was precipitated in water-methanol (3:7, 400 mL) mixture and purified by centrifuging at 2500 rpm via repeated washing. Finally, the samples were lyophilized and vacuum dried for analysis.

The cellulose tricarbanilate was analyzed for molecular weight and molecular weight distribution using a Hewlett Packard 1090 series HPLC system consisting of an auto-sampler, a UV detector, and three columns of Styragel HR1, HR3, and HR4 (Waters Inc., USA) linked in series using tetrahydrofuran (THF) as the eluent. The derivatized cellulose was dissolved in THF (1 mg/mL), and the solution was filtered through a 0.45 μm filter. Then the filtered solution (20 μL) was injected into the HPLC system and was detected using the UV detector at 236 nm. Standard narrow polystyrene samples were used in order to construct a calibration curve. Data were collected with Agilent ChemStation Rev. A.10.01 and analyzed with Agilent GPC Addon Rev. A.02.02

software. The values M_n and M_w were calculated using the GPC software, and the weight-average degree of polymerization (DP) was obtained by dividing M_w by 519, the molecular weight of the cellulose tricarbanilate monomer.

3.9.7 Gel permeation chromatography analysis of sulfonated cellulose

Sulfonated cellulose (1.00 mg) was dissolved in DI water (1.00 mL) and GPC was carried out using an aqueous column (Ultrahydrogel, 7.8×300 mm) at a flow rate of 0.80 cm^3/min. Chromatograms were recorded by using a refractive index detector. Calibration was carried out with pullulan standard (Standard P-82, Showa Denko, Co., Japan). Data were collected with Agilent ChemStation Rev. A.10.01 and analyzed with Agilent GPC Addon Rev. A.02.02 software. The results had an error of less than ±3.0%.

3.9.8 NMR spectroscopy

All NMR experiments were performed with a Bruker Avance-400 spectrometer (Billerica, MA, USA). Data analysis was accomplished using Mnova NMR Data Processing software (Mestrelab Research SL, Santiago de Compostela, Spain).

3.9.8.1 ^{1}H, ^{13}C, DEPT 135 and Heteronuclear Single Quantum Coherence (HSQC) NMR spectroscopy of sulfonated cellulose

Sulfonated samples were dried under vacuum at 40 ^{o}C overnight and then dissolved in a D_2O-DMSO-*d6* (0.70 mL, 200:1, w/w) mixture with constant stirring at 40 ^{o}C for 24 h. An aliquot of this sample solution (0.50 mL) was transferred to a NMR tube. DMSO was used as an internal standard (δ 2.50 ppm). 128 scans were collected at 40 ^{o} C

for ^{1}H spectra and 30,000 scans for ^{13}C spectra. HSQC spectra were obtained using a Bruker DRX 500 MHz spectrometer using standard pulse sequences. It has to be noted that our further experiments show that the addition of 0.5 wt.% DMSO-d_6 in D_2O has no effect on the solubility of sulfonated cellulose. DEPT spectra were acquired using 135° pulse angle, 3-s pulse delay, and 8192 scans. The acquisition temperature is 45 °C with no zero filling and 5.0 Hz line broadening.

3.9.8.2 ^{13}C NMR spectroscopy of cellulose nanowhisker derivatives

Freeze dried aminated samples (0.05 g) were dissolved in DMSO-d_6 (0.60 mL) with constant stirring at 45 ^{o}C for 3 h. An aliquot of this sample solution (0.50 mL) was transferred to a NMR tube and 30,000 scans were collected for each spectrum at 45 ^{o}C with zero filling of 32K, 10Hz line broadening and 1 sec pulse delay.

3.9.8.3 Diffusion ordered NMR spectroscopy

The DOSY experiments were conducted using the bipolar pulse pair (BPP) pulse sequence. Field gradient calibration was accomplished using the self-diffusion coefficient of pure water at 25 ° C ($2.299 * 10^{-9}$ m^2s^{-1}). The gradients were applied for 3.2 ms and the diffusion time was 80 ms. Homospoil gradients were applied for 600 μs during diffusion and eddy current settling durations. The gradients were incremented 16 times from 1.7 G/cm to 63.0 G/cm. A total of 64 free induction decays containing 8 K complex data points were collected at each gradient with a spectral sweep width of 15.0 ppm. The recycle delay was 5 s.

3.9.8.4 Solid state NMR spectroscopy of aminated cellulose nanowhiskers

For solid-state ^{13}C NMR experiments, the samples were added into 4-mm cylindrical ceramic MAS rotors. CP-MAS experiments utilized 10 kHz MAS probe head spinning speed, a 5μs (90 deg) proton pulse, 1.5 ms contact pulse, 4 s recycle delay and 2 K scans. All spectra were recorded on pre-wet samples with 40-60% water content and the data processing was performed offline using the NUTS software (Acorn NMR Inc.).

3.9.8.5 ^{1}H spin-spin (T_2) NMR experiments of hydrogel

^{1}H spin-spin (T_2) NMR experiments on samples swollen in 100% D_2O were performed on a Bruker DSX-400 spectrometer, operating at a frequency of 399.875 MHz for ^{1}H NMR in a Bruker double-resonance MAS probe head at spinning speed of 2 kHz at room temperature. A standard Carr-Purcell-Meiboom-Gill (CPMG) sequence with a τ = 500 μs, utilized a 5 μs (90°) proton pulse, 10 s recycle delay and 128 scans. The CPMG experiment was collected 26 data points between 0.002-10 s.

3.9.9 Scanning electron microscopy

Surface morphology of samples was studied by Hitachi S-800 and JEOL-1530 thermally-assisted field emission (TFE) scanning electron microscope at the required magnifications. Before acquiring images, the surfaces of all the samples were coated with gold in a sputter coater.

3.9.10 X-ray photoelectron spectroscopy (XPS) analysis

X-ray photoelectron spectra of unmodified and modified whiskers were collected on a Thermo K-alpha XPS spectrometer with a monochromatic aluminum Kα source operated at 12 kV and 6 mA under a pressure of 10^{-8} mbar. The binding energy scale was shifted to ensure that the main C-C/C-H contribution to the C1s signal occurred at 285.0 kV.

3.9.11 TEM experiment

Transmission electron micrographs of cellulose nanowhisker samples were taken in a JEOL 100CX-2 transmission electron microscope at an accelerating voltage of 100 kV. Sample solutions (0.02 %, w/v) were deposited on a carbon coated grid and allowed to dry followed by staining with 2 wt. % aqueous uranyl acetate solution.

3.9.12 AFM experiment

AFM experiments were conducted on a Veeco, NanoScope 3100 scanning probe microscope with a NanoScope IIIa controller. Amplitude images were obtained on air dried suspensions in tapping mode, using a 1-10 Ohm-cm phosphorus (n) doped Si tip, with a nominal frequency of 150 kHz.

3.9.13 Determination of degree of cross-linking of the hydrogels

The degree of cross linking of the hydrogels was determined by Ninhydrin (2,2-dihydroxy-1,3-indanedione) assay.[201] Lyophilized gels were ground to powder and to 5 mg of the samples in a test tube, 1.00 mL of Ninhydrin solution (1.5 % in ethanol w/v) were added followed by heating the mixture for 25 min at 80 ^{o}C. After cooling to room

temperature for 1 h, it was diluted with DI water and the optical absorbance was measured using PerkinElmer Lambda 35 UV-visible spectrometer at λ 570 nm against a blank solution without gels, which had been treated exactly the same way as the cross-linked gels. Glycine was used as standards to obtain a calibration curve to determine the total number of free amine groups in the gelatin hydrogels. The experiment was repeated three times for each sample and the data were reported with an error of less than ±5.0%. Degree of cross linking was determined by following the equation:

Degree of cross-linking (%) =

{1- (Absorbance of cross-linked gel/Absorbance of non-cross-linked gel)} × 100

3.9.14 Study of swelling properties of hydrogels

Swelling properties of the chemically cross-linked hydrogels were studied by incubating in water for 2 days at room temperature and then the gels were gently blotted and finally weighed.[202] The dry weight of the gel was determined by drying the gel in vacuum oven at 50 ^{o}C till constant weight was obtained. The experiment was repeated three times for each sample and the data were reported with an error of less than ±2.0%. Then the equilibrium fluid content was calculated from the following equation:

Equilibrium fluid content (%) = {1- (weight of dry gel/weight of swollen gel)} × 100

3.9.15 Rheological experiments of hydrogels

Hydrogels were equilibrated in water at room temperature for 2 days before the rheological measurements were taken. The rheological experiments at oscillatory shear deformation of the gelatin hydrogels were carried out with AR2000 rheometer parallel

plates of 14 mm diameter. The storage (elastic) G' and loss (viscous) G" moduli were recorded at constant temperature (27 °C) and at shear strain of 0.05% in a range of frequency from 0.1 to 10 Hertz.[203,204] The temperature dependence of the storage modulus was determined by oscillatory shear deformation and temperature ramp of 27 to 50 °C with a heating rate of 1.5 °C/min at a constant frequency 1 Hz and constant shear rate of 0.05. The experiment was repeated three times for each sample and the data were reported with an error of less than ±5.0%.

CHAPTER 4

SYNTHESIS OF NOVEL WATER SOLUBLE SULFONATED CELLULOSE[1]

4.1 Introduction

Cellulose, one of the most chemically uniform biopolymers synthesized in nature, is also one of the most abundant and important renewable biopolymers in nature. Due to the presence of ordered hydrogen bonds it forms various supramolecular crystalline structures, which are essential for many of its native and commercial fibrous applications. In addition, cellulose's special properties such as hydrophilicity, biocompatibility, and chirality have made it a natural bioresource for advanced bioactive, biocompatible materials, and sensor matrices.[28, 205] A limitation of cellulose is its insolubility in water, and this has been commonly addressed by derivatizing cellulose such as sulfoethylated or carboxymethylated products.[206-207]

It is well known that both the degree of substitution and distribution of functional groups influence the properties of cellulose. Therefore, many attempts have been made to prepare regioselectively functionalized cellulose derivatives.[28, 208] Among these derivatization approaches, periodate oxidation of cellulose[131, 209-212] is significant because

[1] This manuscript was accepted for publication in Carbohydrate Research, 2010. It is entitled as "Synthesis of Novel Water Soluble Sulfonated Cellulose". The other authors are Nan Jiang from the Institute of Paper Science and Technology at Georgia Institute of Technology, Gelbaum Leslie from School of Chemistry and Biochemistry at Georgia Institute of Technology and Arthur J. Ragauskas from the Institute of Paper Science and Technology and School of Chemistry and Biochemistry at Georgia Institute of Technology.

it selectively cleaves the C2-C3 bond of underivatized cellulose to yield the corresponding 2,3-dialdehyde product. Due to the specificity and selectivity of this oxidation reaction, it has been extensively studied for many years and the product has been well characterized by several analytical techniques.

Varma and Kulkarni[213] studied the reactivity of cellulose with periodate and reported that the two key factors contributing towards the extent of oxidation were the concentration of periodate and temperature. Morooka et al.[214] have reported the homogeneous periodate oxidation reaction of methylol cellulose and compared it with conventional heterogeneous condition. A significant increase in oxidation level was found with solubilized methylol cellulose compared with the heterogeneous reaction. Other studies[131, 215] on the relative crystallinity of dialdehyde cellulose have reported that the crystallinity is significantly decreased and the morphology of cellulose is also changed after oxidation. Kim et al.[216] have found that the dialdehyde cellulose obtained by extensive oxidation of cellulose dissolves in hot water but was degraded at elevated temperatures and long treatment times. Tang et al. have shown that treating fibers with ultrasound prior to periodate oxidation enhances the water retention value of the oxidized product.[127]

The reactive dialdehyde cellulose product from periodate oxidation provides a facile route to a number of other functional groups such as carboxylic acids, imines sulfonates.[35, 156-157, 217-219] This approach to cellulose functionalization can yield a high molecular weight polymer with unique properties, such as fluorescence, energy storing, drug release, and chromatography.[154, 172, 220] Periodate oxidation followed by the sulfonation to obtain disulfonated derivatives of cellulose has not been explored in detail

in the literature. In 1998, Rahn et al.[172] first reported the synthesis of a disulfonated derivative of cellulose followed by its characterization using FT-IR spectroscopy and elemental analysis. It was concluded that the degree of conversion can be controlled by the reaction time, aldehyde to bisulfite ratio and the subsequent regeneration process of the product. Additionally, depending on the bisulfite content, the samples were soluble or highly swellable in water, however, a detailed characterization was lacking in this study. Shet and Wallajapet[173] investigated the effect of introduction of sulfonate groups on the physical and mechanical properties of cellulose fibers. They reported that the conversion of dialdehyde cellulose to sulfonated cellulose resulted in a significant increase in water absorbency values as well as both dry and wet tensile strength improvements for sulfonated cellulose fibers. Oxidation and subsequent sulfonation of bleached softwood Kraft pulp were also studied by Hou et al.[136] They have shown an increase in the water absorbent properties of undried fibers by 25.0-189.0%, significant improvement in tensile strength and reduction in cellulose fiber length after oxidation and sulfonation treatment.

Previously, Zhang et al. have reported that periodate oxidation and sulfonation of bleached hardwood Kraft pulp and nanocellulosic structures exhibit enhanced water absorbency by 10-199% depending upon the degree of oxidation.[221] These studies also demonstrated that cellulose whiskers and nanospheres exhibited enhanced water absorption with respect to conventional fibers. This oxidation/sulfonation sequence was carried out by employing relatively low molar application levels of periodate. The current study investigates the effect of high charges of periodate oxidation on cellulosic fiber followed by sulfonation and the corresponding water solubility properties of this modified fiber along with a detailed characterization of the sulfonated product.

4.2 Experimental

4.2.1 Sodium periodate oxidation of cellulose

Cellulose fibers were oxidized in presence of sodium periodate as described in Chapter 3 (3.3.1 Sodium periodate oxidation of cellulose fibers). The samples were named as DAC0.2, DAC0.3, DAC0.4, DAC0.7, and DAC1.0 (i.e., DAC= dialdehyde cellulose, 0.2, 0.3, 0.4, 0.5, 0.7, 1.0 = mass ratio of sodium periodate to cellulose).

4.2.2 Sulfonation of 2,3-dialdehyde cellulose

The 2,3-dialdehyde cellulose was reacted with sodium bisulfite as described in Chapter 3 (3.4.1 Sulfonation of 2,3-dialdehyde cellulose fibers). The samples were referred to as SC0.2, SC0.3, SC0.4, SC0.5, SC0.7, and SC1.0 (SC: sulfonated cellulose, 0.2, 0.3, 0.4, 0.5, 0.7, 1.0 = mass ratio of sodium periodate to cellulose). A schematic reaction pathway for oxidation and sulfonation of cellulose is shown in Fig. 4.1.

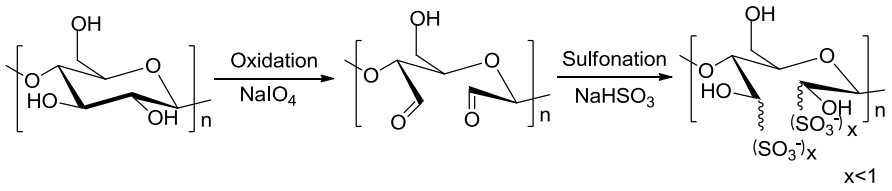

Fig. 4.1 Oxidation and sulfonation of cellulose.

4.2.3 Determination of carbonyl content of dialdehyde cellulose

Carbonyl content was measured following Tappi standard method T430 as described in Chapter 3 (3.9.1 Determination of carbonyl content of dialdehyde cellulose by copper number titration).

4.2.4 Conductometric titration of sulfonated cellulose

Conductometric titration was carried out with a model 2052 EC meter at a cell constant of 10 cm^{-1} as described in Chapter 3 (3.9.2 Conductometric titration of sulfonated cellulose) to determine the bulk sulfonic acid content.

4.2.5 FT-IR spectroscopy

Transmission mode FT-IR spectra were collected with a Nicolet Magna-IR^{TM} 550 spectrometer as described in Chapter 3 (3.9.5 FT-IR spectroscopy). The oxidized samples were grounded to powder, dried at 105 °C for 12 h, cooled, and pressed into a KBr pellet (1:200).

4.2.6 Gel permeation chromatography of oxidized and sulfonated cellulose

The number-average molecular weight (M_n) and the weight-average molecular weight of oxidized and sulfonated cellulose samples (M_w) were determined by GPC as described in Chapter 3 (3.9.6 Gel permeation chromatography analysis of cellulose and 3.9.7 Gel permeation chromatography analysis of sulfonated cellulose).

4.2.7 Scanning electron microscopy of cellulose and its derivatives

Surface morphology of cellulosic fiber, dialdehyde cellulose, and sulfonated cellulose was studied by using Hitachi S-800 scanning electron microscope as described in Chapter 3 (3.9.9 Scanning electron microscopy). The images were taken at 1000X magnifications.

4.2.8 NMR spectroscopy of sulfonated cellulose

^{1}H, ^{13}C and DEPT 135 NMR spectra were obtained using a Bruker Avance 400 MHz spectrometer at 30 ^{o}C as described in Chapter 3 (3.9.8.1 ^{1}H, ^{13}C, DEPT 135 and Heteronuclear Single Quantum Coherence (HSQC) NMR spectroscopy of sulfonated cellulose).

4.3 Results and discussion

The sulfonation of cellulose was accomplished by selectively generating the C2,3-dialdehyde of cellulose by periodate oxidation followed by treatment with sodium bisulfite. As summarized in Table 4.1, the sodium periodate oxidation of cellulose was obtained with varying mass ratios. First, copper number was determined experimentally from the reductive reaction of dialdehyde cellulose with $CuSO_4$ and then it was converted to carbonyl content using equation 1 as proposed by Rohrling et al.[132] It can be observed from Table 4.1 that as the ratio of sodium periodate to cellulosic fiber increased, the carbonyl group content of oxidized fiber also increased. However, a very low degree of oxidation (~5%) was observed which could be attributed to the non-uniform distribution of oxidation over fiber surface.[131]

Carbonyl Group Content (mmol /100 g o.d. pulp) = $(Cu^{\#} - 0.07) / 0.6$ (1)

Table 4.1 Copper number and carbonyl content of oxidized cellulose samples.

Samples	$NaIO_4$/Cellulose (w/w)	Copper number[a] (mmol g^{-1})	Carbonyl content (mmol g^{-1})
Starting Cellulosic	0.0	0.037	0.002
DAC0.2	0.2	1.20	0.12
DAC0.3	0.3	1.41	0.14
DAC0.4	0.4	1.67	0.17
DAC0.5	0.5	1.74	0.18
DAC0.7	0.7	2.10	0.22
DAC1.0	1.0	2.66	0.28

Note: 3 days of stirring at room temperature, a: % Error (±)4.0

The presence of the aldehyde group in oxidized fiber was further verified by using FT-IR spectroscopy. A detailed infrared assignment of cellulose vibration bands is summarized in Table 4.2. Figure 4.2 presents the spectra of the fibers before and after treating with sodium periodate. The characteristic band for the carbonyl group at 1736 cm^{-1} and for the hemiacetal structure at 880 cm^{-1} in the spectra of oxidized fibers clearly indicates the formation of dialdehyde cellulose after periodation.[216] In the case of cellulose a band also appears at 900±20 cm^{-1} due to the vibration of C5C6H and O6C6H groups[222] which overlaps with hemiacetal band of dialdehyde cellulose. Thus, both the copper number calculation and FT-IR spectroscopy confirm the conversion of cellulose to dialdehyde cellulose. It is also evident from the FT-IR spectra that by increasing the concentration of sodium periodate the oxidized product exhibits a gradual enhancement in carbonyl band intensity.

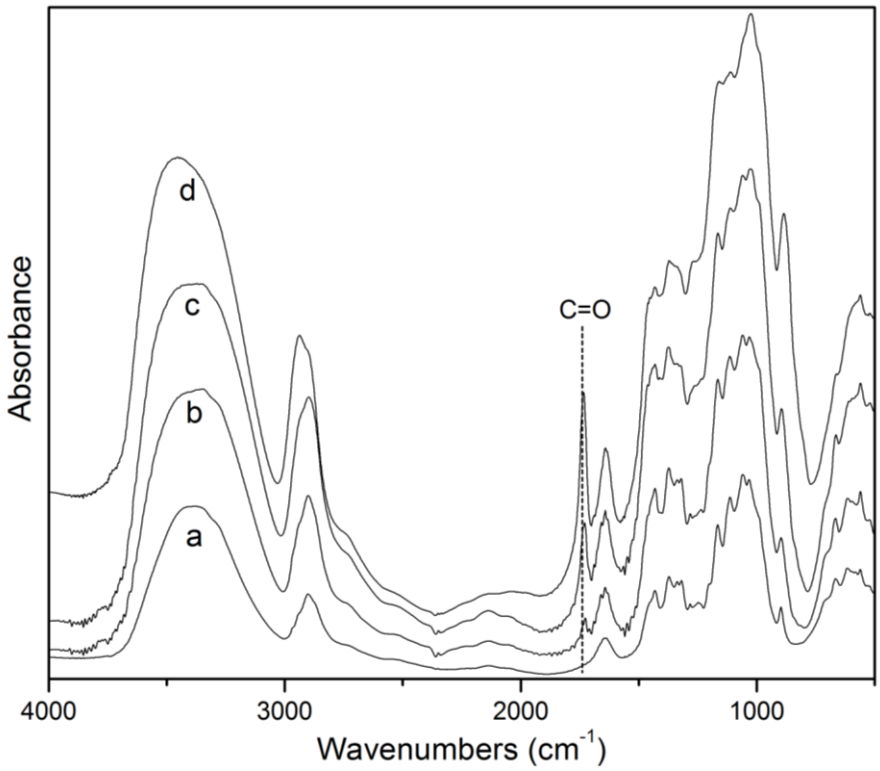

Fig. 4.2 FT-IR spectra of (a) cellulose (b) DAC0.2 (c) DAC0.4 and (d) DAC1.0 samples.

Table 4.2 Infrared assignment of cellulose.[222-223]

Frequency (cm^{-1})	Assignment
650	O-H out of plane deformation
895	Antisymmetric out of phase stretching
910	Vibration of C5C6H and O6C6H groups
965, 988, 1005, 1030, 1069, 1078	CO and CC stretching, CH_2 rocking
1106	Antisymmetric in phase ring stretching
1161	Antisymmetric oxygen bridge stretching
1204, 1232, 1249, 1275	CH_2 wagging, CH and OH deformation
1310	$CH_{\perp}$ deformation
1335	CH in-plane deformation
1365	$CH_{\parallel}$ deformation
1426	CH_2 symmetric bending
1446	OH in-plane deformation
1640	Adsorbed H_2O
2851	CH_2 $_{\parallel}$ symmetric stretching
2907	CH_2 $_{\perp}$ stretching
2967	CH_2 antisymmetric stretching
3300	$OH_{\parallel}$ stretching
3400	$OH_{\perp}$ stretching

Dialdehyde cellulose samples were treated with sodium bisulfite to yield the corresponding sulfonated product. The sulfonic acid group content in each sample was determined by conductometric titration (Table 4.3), and the results indicate an increase in sulfonic acid content from 0 to 0.16 (mmol g^{-1}) with the charge of sodium periodate employed. It can also be noticed that the samples having higher carbonyl content afforded sulfonated cellulose with higher amounts of sulfonic acid groups. In solution, SC0.7 and

SC1.0 samples remain as particles and adhere to the electrode causing instability in the conductance reading. Therefore, sulfonic acid group content was calculated only up to SC0.5.

Table 4.3 Sulfonic acid group content of oxidized and sulfonated cellulose samples.

Samples	Sulfonic acid content[a] (mmol g^{-1})
Starting Cellulosic	0.00
SC0.2	0.09
SC0.3	0.10
SC0.4	0.14
SC0.5	0.16

a: % Error (±)2.0

Figure 4.3 (a)-(g) shows the SEM images of the initial fibers and its oxidized product. Cellulosic fibers appear long, well separated from each other and are in the range of 15-18 µm in width. In the case of oxidized samples, the fibrous form is retained but the thickness of the fibers is greater than that of the cellulosic fibers, a distribution of fiber width from 15 to 40 µm (b)-(g). However, conversion of dialdehyde cellulose to sulfonated cellulose exhibits a significant change in surface morphology (Fig. 4.4), which could be due to the mass losses during the sulfonation process. These samples have a smooth surface compared to both initial fiber and dialdehyde cellulose. In conclusion, the surface morphology of cellulose fibers has been affected by the oxidation/sulfonation sequence.

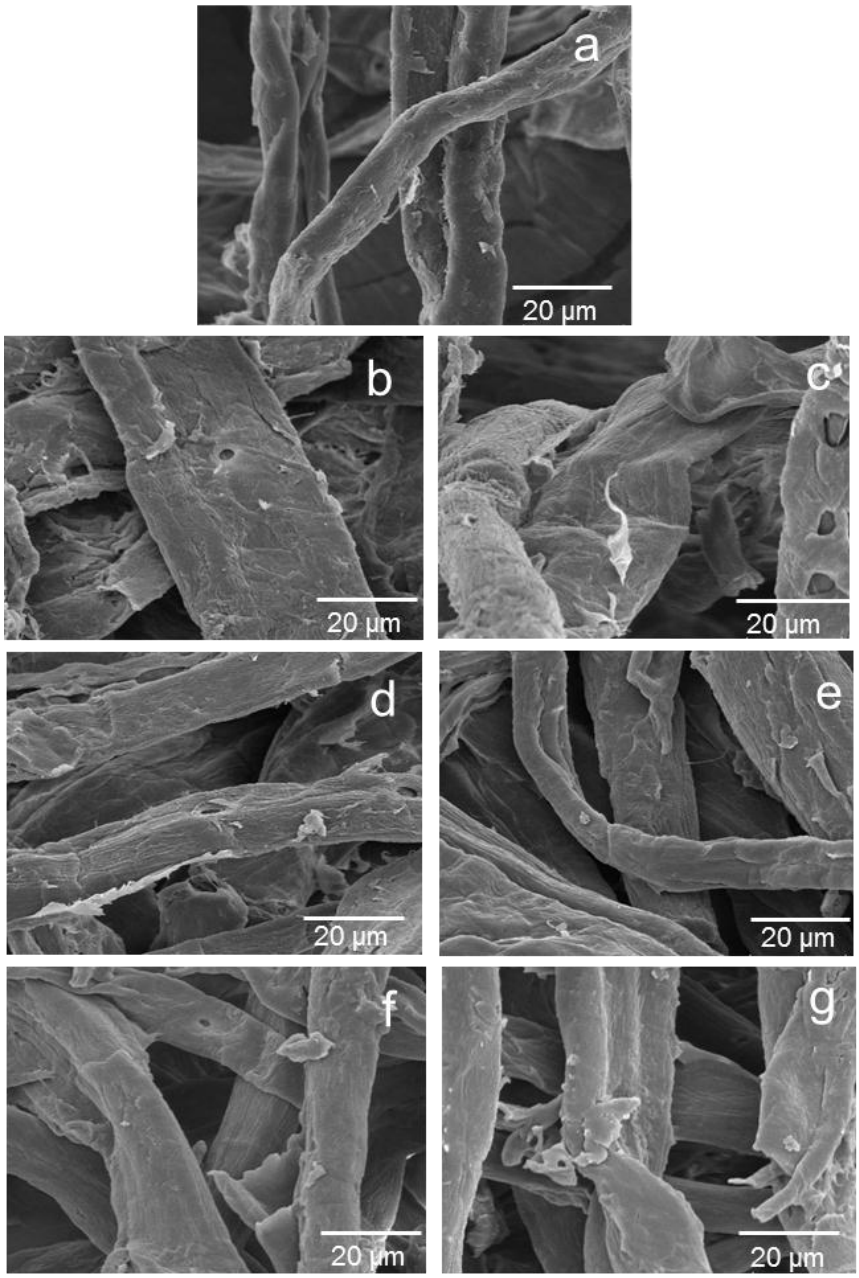

Fig. 4.3 SEM images of (a) cellulose (b) DAC0.2 (c) DAC0.3 (d) DAC0.4 (e) DAC0.5 (f) DAC0.7 (g) DAC1.0.

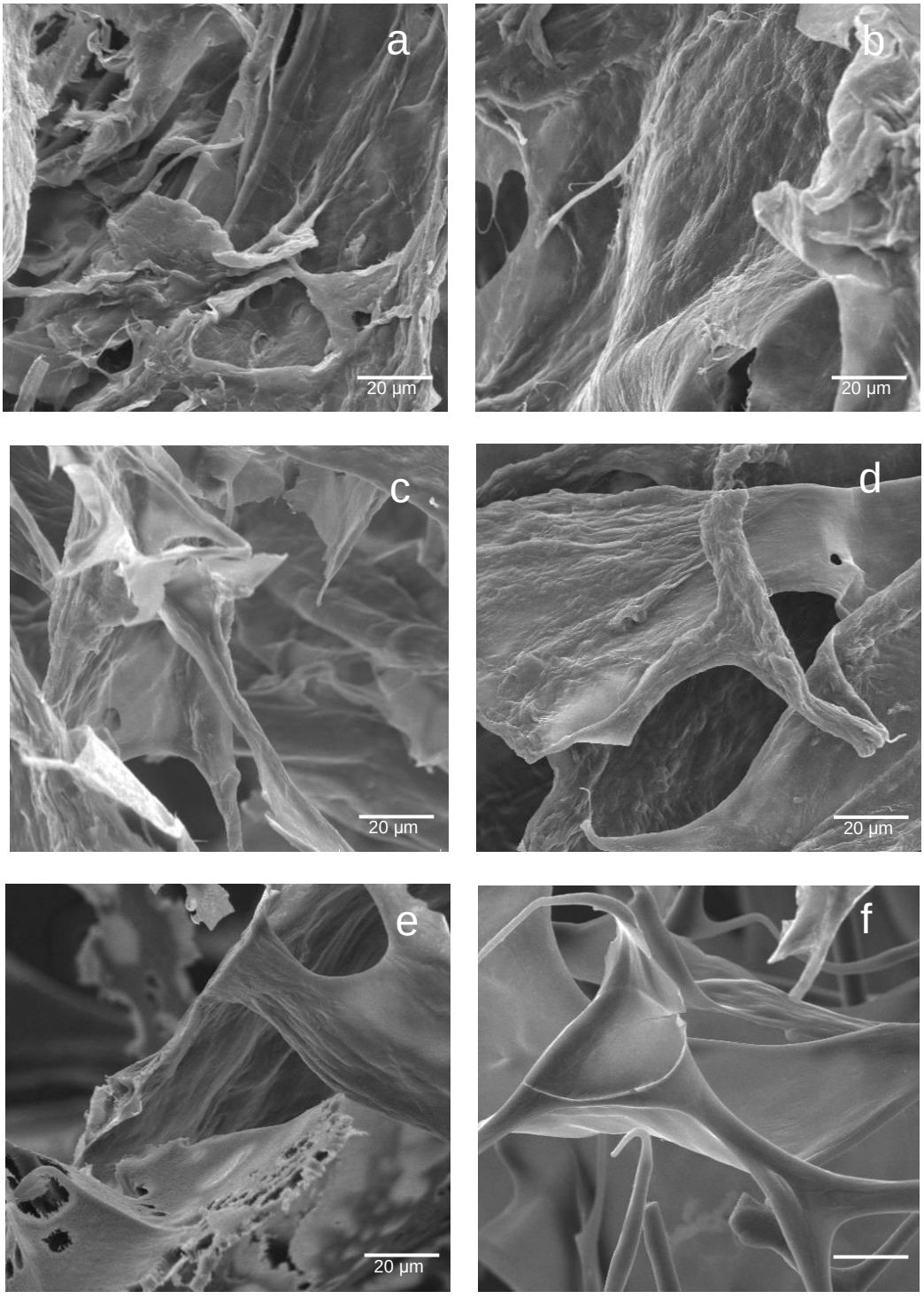

Fig. 4.4 SEM images of (a) SC0.2 (b) SC0.3 (c) SC0.4 (d) SC0.5 (e) SC0.7 (f) SC1.0.

Determination of the solubility of sulfonated cellulose samples in water was accomplished using ^{1}H NMR with DMSO as an internal standard. Solubility was calculated based on the integration ratio of the sample signal (3-4ppm) to the internal standard signal. It is interesting to note that the solubility of cellulose increases dramatically from 2.85 to 28.57 g/L with the increased level of oxidation and sulfonation (Fig. 4. 5) due to the incorporation of sulfonic acid groups in to the cellulose chain.

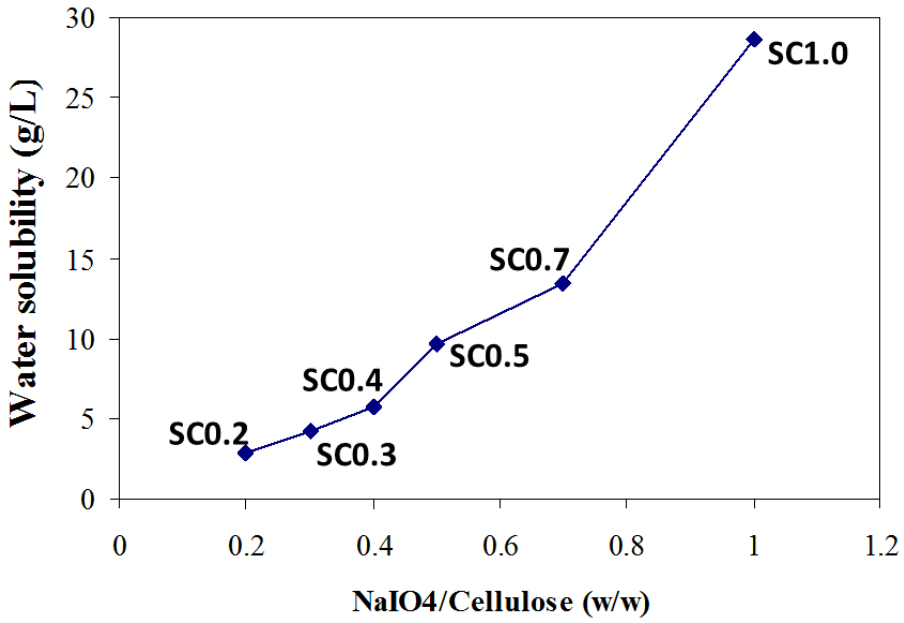

Fig. 4.5 Solubility of oxidized and sulfonated cellulose samples determined from ^{1}H NMR spectra with the level of oxidation and sulfonation.

Carboxymethylcellulose (CMC), the most commonly used water soluble cellulose ether, is available in a wide range of degree of substitutions. It is known that CMC is readily soluble in water at a DS above 0.4. However, the rate of dissolution also increases with increasing DS and decreasing molecular weight. For example, commercial CMC with molecular weight of 9×10^{4} g/mol and DS of 0.65-0.90 have a solubility of

40mg/mL, whereas a molecular weight of 7×10^5 g/mol and DS 0.65-0.85 shows a solubility of 10mg/mL. The most widely used types are in the 0.7 to 1.2 DS range. For similar order of molecular weight (2.77×10^5 g/mol) of sulfonated cellulose, we obtained a solubility of 28 mg/mL at 0.05 DS. The DS herein is the moles of sulfonic acid groups per mol of glucose unit in cellulose assuming complete conversion of carbonyl to sulfonate groups.

The molecular weight and polydispersity index of cellulosic fiber and sulfonated samples were obtained by size exclusion chromatography (Table 4.4). Due to the limited solubility of lower degree sulfonated samples in water, the data were only obtained for the samples having high sulfonic acid content. An increase in the molecular weight of sulfonated samples compared to that of the starting material indicates the addition of sulfonic acid group to the cellulose chain through oxidation/sulfonation reaction.

Table 4.4 Molecular weight and polydispersity index of oxidized and sulfonated cellulose samples by size exclusion chromatography.

Samples	Number average molecular weight Mn (g/mol)	Weight average molecular weight Mw (g/mol)	Polydispersity index
Starting cellulose	1.87×10^5	7.66×10^5	4.09
SC0.5	2.44×10^5	1.68×10^6	6.87
SC0.7	2.34×10^5	1.72×10^6	7.38
SC1.0	2.77×10^5	1.76×10^6	6.36

Structural characterization of the solubilized sulfonated cellulose was carried out by means of NMR spectroscopy. As shown in Fig. 4.6 (a), ^{13}C and ^{1}H NMR spectra of sulfonated cellulose exhibits broad overlapping peaks. Therefore, we collected HSQC

spectra of the oxidized and sulfonated cellulose in order to resolve and assign all the peaks (Fig. 4.7). Based on literature values[224-226] the signals centered at δ 103, 73, 74, 81, 76, and 60 were readily assigned to C1, C2, C3, C4, C5 and C6 of the glucopyranoside ring in sulfonated cellulose, respectively and hence, the signals were correspondingly assigned in the HSQC spectra. A DEPT 135 NMR confirmed the C6 assignment of the glucopyranoside ring (Fig. 4.6 b). Another methylene signal at δ 70.0 was then assigned to the CH_2-OH of the glucose ring that had undergone periodate oxidation and sulfonation. The oxidation/sulfonation of C2/3 was anticipated to shift these signals and the adjacent carbons downfield, hence the signals at 99/5.4, 94/5.3, 96/4.8, 88/5.0, and 70/4.0 could be assigned to C1'/H1', C2'/H2', C3'/H3', C4'/H4' and C6'/H6', respectively.

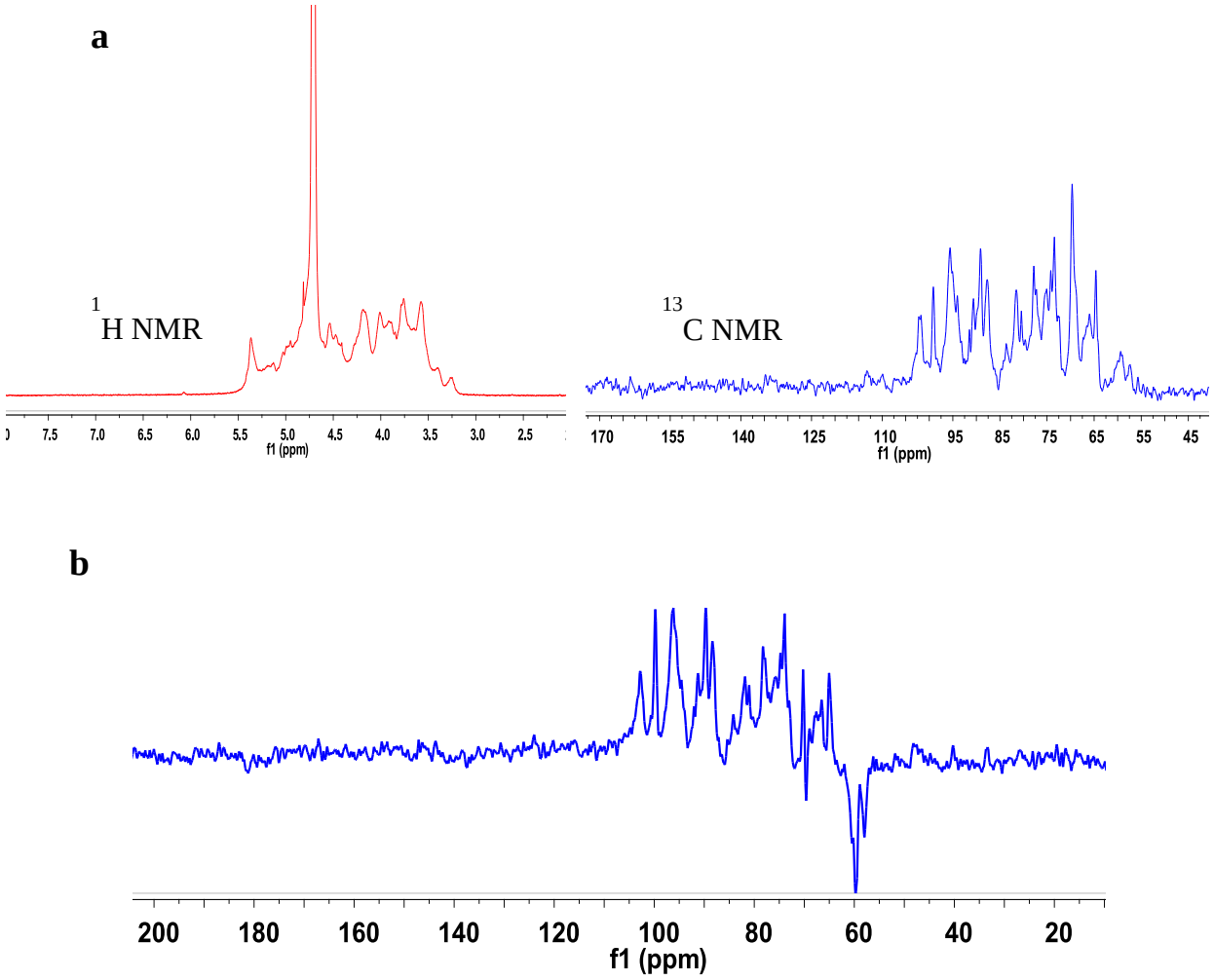

Fig. 4.6 (a) ^{1}H NMR (left) and ^{13}C (right) NMR spectra (b) DEPT-135 NMR spectra of oxidized and sulfonated cellulose (SC1.0) sample in D_2O.

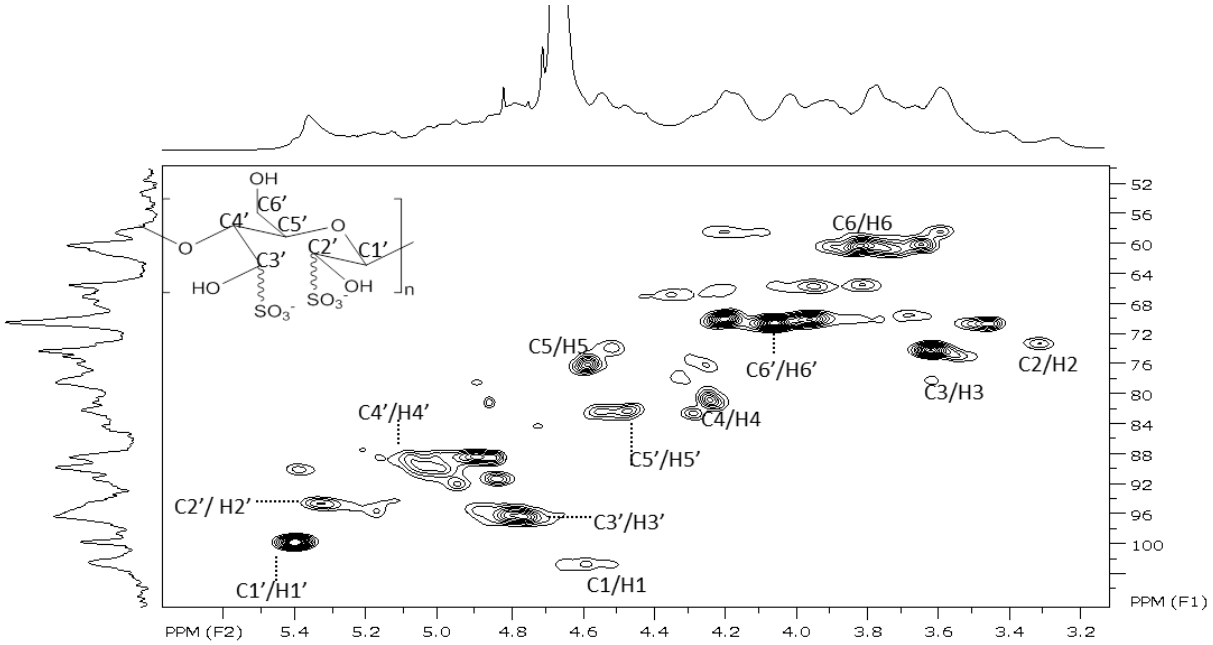

Fig. 4.7 Typical HSQC spectra of oxidized and sulfonated cellulose (SC1.0) sample in D_2O.

4.4 Conclusions

A series of sulfonated cellulose samples were successfully prepared by following standardized sodium periodate oxidation and sodium bisulfite sulfonation of bleached hardwood Kraft fibers. Six levels of oxidations were carried out using 0.93-4.67 mmol of periodate per gram of pulp and products were obtained in 95-98% yield. The aldehyde and sulfonic acid content, surface morphology, and water solubility of these treated fibers were characterized. It was found that the carbonyl group content increased (0.12-0.28 mmol/g) with the periodate charge and so did the sulfonic acid content in subsequent sulfonation step. Scanning electron microscopy images showed that periodate oxidation of cellulose does not affect the morphologies of cellulose fibers, whereas a significant change in surface morphology of the fibers were observed in case of sulfonated samples. A complete structural characterization of the sulfonated product was done combining ^{13}C NMR and DEPT-135 NMR spectra and eventually assigning all the carbon atoms in 2D

HSQC spectra. Solubility of sulfonated cellulose in water was determined from quantitative ^{1}H NMR spectra and the resulting product was shown to have water solubility properties provided that the sulfonic acid content is above 0.16 mmol g^{-1} of the sample. A solubility of 28.57 g/L was found when cellulose was oxidized with 4.67 mmol periodate per gram cellulose followed by the sulfonation reaction.

Water soluble derivatives of cellulose have been prepared by etherification reaction of cellulose and thus, for the first time, a novel water soluble derivative of cellulose was successfully prepared at room temperature through periodation/sulfonation sequence under mild reaction conditions, which has a promising future as a biocompatible and biodegradable material in pharmaceutical, food and in personal care industry applications. The oxidation/sulfonation scheme provided a facile approach not only to synthesize a water soluble derivative of cellulose, but also to introduce negatively charged sulfonic acid groups on cellulose surface and considering the potential applications of anionic bead cellulose, this method was used in the next study to synthesize 2,3-disulfonated bead cellulose.

CHAPTER 5

CHARGING CELLULOSE SPHERES: SYNTHESIS OF 2,3-DISULFONATED CELLULOSE IN BEAD FORM[2]

5.1 Introduction

Naturally occurring polysaccharides containing negatively charged functional groups are known to exhibit valuable chemical and biological properties.[227-230] In this regard, cellulose derivatives having carboxyl, carboxymethyl, phosphate, and sulfonic groups are often synthesized with controlled reaction conditions to regulate the distribution of these substituents for various applications. For example, sulfonated cellulose derivatives have been utilized as catalysts, stationary phases for chromatography, as well as for protein separation and removal of metals.[231-234] Recently, it has been found that sulfonated cellulose and carboxylated cellulose sulfates exhibit unique wound healing, anticoagulant and antiviral properties.[235-238] The mechanism contributing to these biological properties involves an electrostatic interaction between the positively charged amino acids present in the proteins and the negatively charged sulfonic residues.[239] These beneficial properties have been reported to vary with the degree of sulfonation and the spatial position of the sulfonic groups.[28, 240-242]

---

[2]This manuscript was accepted for publication in Journal of Biobased Mater. Bioenergy, 2010. It is entitled as "Charging cellulose spheres: Synthesis of 2,3-disulfonated cellulose in bead form". The other author is Arthur J. Ragauskas from the Institute of Paper Science and Technology and School of Chemistry and Biochemistry at Georgia Institute of Technology

The literature reveals a number of methods to synthesize sulfonated cellulose but the most common method has been reported as the reaction of cellulose with chlorosulfonic acid or sulfuric acid in DMF at 30-50 ^{o}C. Various other methods include pyridine-sulfur trioxide complex in DMF, sulfur trioxide-trimethylamine complex, and sulfuric acid mediated by dicyclohexylcarbodiimide (DCC) as the sulfonating reagent. Depending on the reaction condition the degree of cellulose substitution can vary from 0.25-3.0 per glucopyranoside unit.[243-245]

Cellulose beads are valuable renewable material that can be manufactured with a well defined particle size and pore structure exhibiting high mechanical strength, surface area, and chemical reactivity. Spherical cellulose is usually prepared by regenerating cellulose typically dissolved in NMMO, DMAC, NaOH/urea, NaOH/thiourea, or calcium thiocyanate. Chemical modification of cellulose beads is of growing research interest and anionically charged beads have been accomplished by sulfoethylation, sulfonation, phosphonation, or oxidation.[58, 245-246] Negatively charged cellulose beads, with micron size diameter have been used for solid phase synthesis, supports for chromatography, removal of heavy metals, immobilization of enzymes, drugs, and blood purification.[76, 247-248]

This study presents the application of a sequence of heterogeneous reactions (i.e. periodate oxidation and sulfonation to functionalize cellulosic spheres). This reaction sequence has been frequently used in the derivatization of carbohydrates because of its high selectivity and absence of any significant side reactions.[131, 135-136, 249] Hard cellulose beads were activated by three different levels of periodate oxidation followed by the sodium bisulfite sulfonation reaction to obtain its disulfonated derivative. Physical and

chemical properties of the sulfonated beads were studied by FT-IR, SEM, and by titration of sulfonic groups on the bead surface.

5.2 Experimental

5.2.1 Sodium periodate oxidation of cellulose beads

Sodium periodate oxidation of cellulose bead was carried out based on published literature.[135,131,249] In brief, a mixture of cellulose beads (15.00 g) and sodium periodate (0.90 g, 4.20 mmol) was dispersed in deionized (DI) water (150.00 mL) and stirred for three days in the absence of light at room temperature. The product was filtered, repeatedly washed with DI water to remove the spent oxidant, and then air-dried providing a gravimetric yield of 98%. The same procedure was then repeated using 8.41 and 16.83 mmol of sodium periodate providing 95 and 97% yield of the oxidized cellulose beads, correspondingly. These samples were named DAC1, DAC2, and DAC3, where DAC= dialdehyde cellulose beads and 1, 2, 3 corresponds to 4.20, 8.41 and 16.83 mmols of sodium periodate employed, respectively.

5.2.2 Sulfonation of 2,3-dialdehyde cellulose beads

2,3-Dialdehyde cellulose beads were sulfonated with sodium bisulfite as described in Chapter 3 (3.4.2 Sulfonation of 2,3-dialdehyde cellulose beads). These samples were named as SC1, SC2, SC3 corresponding to DAC1, DAC2, and DAC3 samples where SC represents to sulfonated cellulose products.

5.2.3 Determination of carbonyl groups of 2,3-dialdehyde bead cellulose

The carbonyl group content of the starting and oxidized beads was determined following Tappi standard method T430 as described in Chapter 3 (3.9.1 Determination of carbonyl content of dialdehyde cellulose by copper number titration).

5.2.4 Conductometric titration for bulk charge determination

Conductometric titration of SC1-SC3 was carried out using a 2052 EC meter conductivity instrument at a cell constant of 10 cm^{-1} as described in Chapter 3 (3.9.2 Conductometric titration of sulfonated cellulose) to determine the bulk sulfonic acid content.

5.2.5 Polyelectrolyte titration for surface charge determination

The polyelectric titrations were carried out in a MUTEK particle charge detector as described in Chapter 3 (3.9.3 Polyelectrolyte titration for surface charge determination).

5.2.6 Study of interaction between cationic starch and sulfonated cellulose beads

The interaction between cationic starch and sulfonated cellulose beads was studied on a Leica DM IRM microscope as described in Chapter 3 (3.9.4 Study of interaction between cationic starch and sulfonated cellulose beads).

5.2.7 FT-IR Spectroscopy

Transmission mode FT-IR spectra were collected with a Nicolet Magna-IR^{TM} 550 spectrometer as described in Chapter 3 (3.9.5 FT-IR spectroscopy). The oxidized beads were dried at 105 °C for 12 h, cooled, and pressed into a KBr pellet (1:200).

5.2.8 Scanning electron microscopy

Surface morphology of cellulose beads and its derivatized products were studied by JEOL-1530 thermally-assisted field emission (TFE) scanning electron microscope as described in Chapter 3 (3.9.9 Scanning electron microscopy) and then SEM images were acquired at 100x magnifications. The size of the beads was measured by image plus software.

5.3 Results and discussion

Cellulose beads were treated with sodium periodate to obtain the 2,3-dialdehyde cellulose and the corresponding carbonyl contents of the resulted products were determined. As shown in Table 5.1, the increase in periodate charge leads to a corresponding increase in the carbonyl content. The presence of an aldehyde band at 1736 cm^{-1} in the FT-IR spectra of the periodate treated cellulose beads (Fig.5.1) confirms the oxidative fragmentation of glucopyranoside units and the spectral data exhibits an increase in signal intensity with increasing periodate charge.

Table 5.1 Copper number and carbonyl content of oxidized cellulose beads.

Samples	$NaIO_4$/Cellulose (w/w)	Copper number[a] (mmol g^{-1})	Carbonyl content (mmol g^{-1})
Starting Cellulose beads	0.0	0.045	0.003
DAC1	0.06	0.94	0.10
DAC2	0.12	1.18	0.12
DAC3	0.24	1.40	0.14

Note: 3 days of stirring at room temperature, *a*: % Error (±)4.0

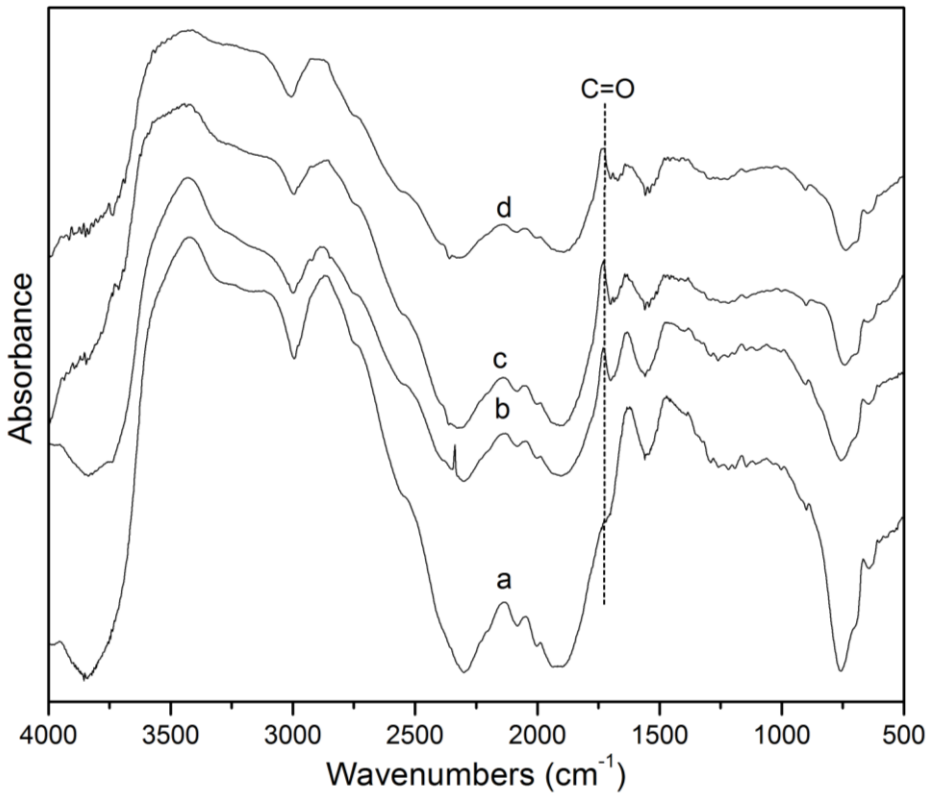

Fig. 5.1 Transmission FT-IR spectra of (a) Starting cellulose beads, (b) DAC1, (c) DAC2, and (d) DAC3.

Sulfonated cellulose beads were prepared by the reaction of oxidized beads with an aqueous solution of sodium bisulfite. The overall chemical process is summarized in Fig. 5.2. Both bulk charge and surface charge density were determined by conductometric and polyelectrolytic titration, respectively. Bulk sulfonic acid group content (Table 5.2) increased with the periodate charge employed and so also was the case for the surface charge density (Table 5.3). Comparing both the surface and bulk charge density it was found that most of the acidic groups are present in the bulk of the cellulose beads.

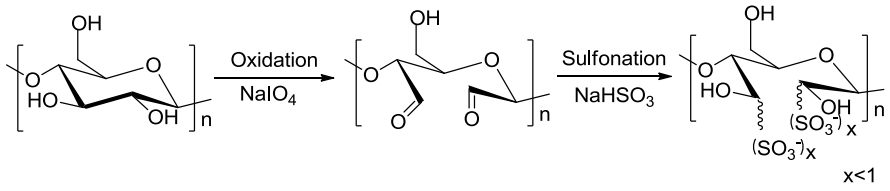

Fig. 5.2 Oxidation and sulfonation of cellulose beads.

Table 5.2 Sulfonic acid group content of oxidized and sulfonated cellulose beads.

Samples	Sulfonic acid content[a] (mmol g^{-1})
Starting Cellulose beads	0.00
SC1	0.08
SC2	0.12
SC3	0.13

a: % Error: ±2%

Table 5.3 Surface charge density of sulfonated cellulose beads.

Samples	Surface charge density[a] (mmol g^{-1})	Surface:bulk charge
Starting Cellulose beads	0.00	0.00
SC1	0.001	0.012
SC2	0.005	0.041
SC3	0.007	0.053

a: % Error: ± 0.1%

Figures 5.3 and 5.4 show the SEM images of the starting, oxidized and sulfonated cellulose beads. The results of this analysis indicate that the size of both the oxidized and sulfonated beads increased by ~20-50 μm with respect to the initial beads. This was attributed to the hydrophilic nature of initial cellulose beads and also an increase in water absorbency of the beads following oxidation/sulfonation.[221] These images also indicate that the spherical shape of the beads was retained after oxidation and sulfonation steps except for Fig. 5.4(d), where the beads start to collapse after being stirred vigorously during the reaction. Indeed, it was determined that in order to maintain the spherical shape of cellulose beads the oxidized products should be stirred gently in the reaction medium during the sulfonation reaction.

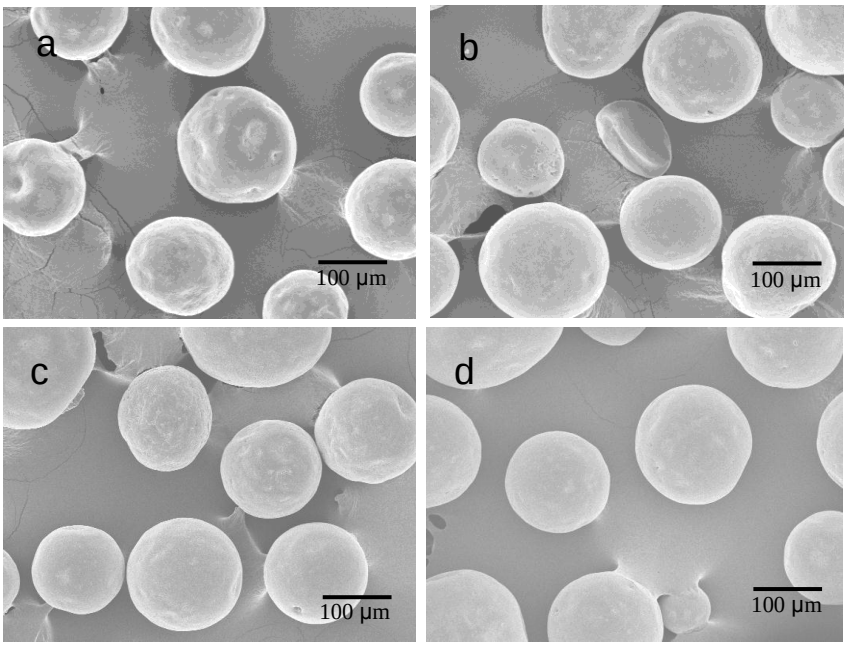

Fig. 5.3 SEM images of (a) starting beads, (b) DAC1, (c) DAC2, and (d) DAC3.

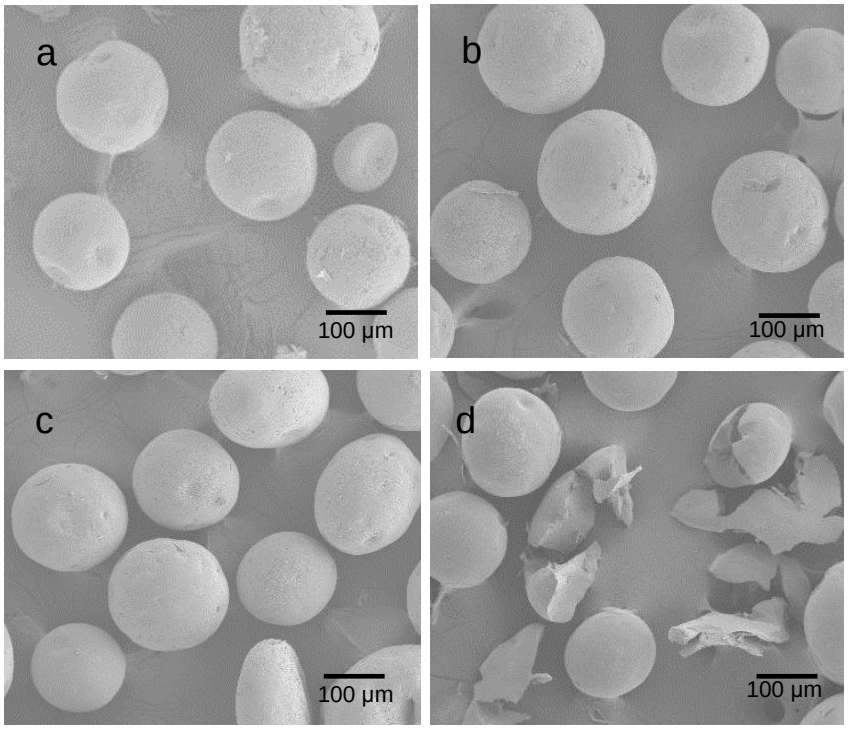

Fig. 5.4 SEM images of sulfonated beads (a) SC1, (b) SC2, (c) SC3, and (d) sulfonated beads after stirring vigorously.

The electrostatic interaction of sulfonated cellulose beads with cationic starch was investigated by optical microscope. As shown in Fig. 5.5 (a-c), as soon as a cation starch solution was added to the beads, the particles started moving towards the bead surfaces. The electrostatic attraction results in aggregation between the cationic starch polymer and anionic cellulose beads as shown in Fig. 5.5 (d). As a control experiment, oxidized/sulfonated beads were found not to agglomerate when mixed with a neutral starch solution. Hence, the aggregation phenomena with a cationic starch can be attributed to electrostatic interactions.

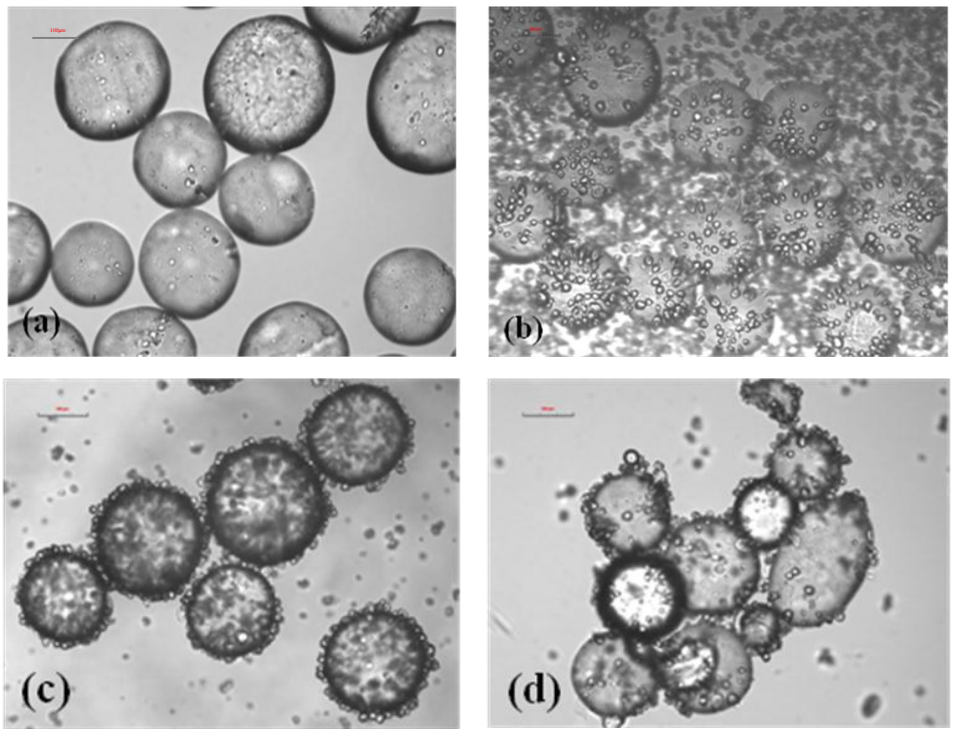

Fig. 5.5 Microscope images of (a) beads in water, (b) after adding starch solution, (c) beads separated from starch solution, and (d) aggregation of beads; Scale bar: 100μm.

5.4 Conclusions

Polyanionic polysaccharides exhibit interesting chemical and biological properties that are dependent on the presence and spatial position of anionic groups. In this study, regioselective oxidation of ~100 μm cellulose beads was accomplished using 4.20-16.83 mmols of sodium periodate yielding the corresponding 2,3-dialdehyde cellulose product in 95-98% gravimetric yields. The corresponding oxidized cellulose beads exhibited a 0.10-0.14 mmol of carbonyl groups per gram of beads as determined by Cu^{2+} titration. Upon sulfonation of the oxidized beads with 0.48 N sodium bisulfite solution the corresponding 2,3-disulfonated cellulose beads were obtained and depending on the

degree of oxidation, the sulfonic charge of the beads was determined to range from 0.08 - 0.13 mmols per gram of cellulose. The size and shape of both unmodified and modified beads were studied by scanning electron microscope. The oxidized/sulfonated beads were shown to aggregate in an aqueous solution when mixed with a cationic starch as observed by optical microscopy.

Therefore, this study demonstrates that anionic 2,3-disulfonated cellulose beads can be successfully prepared by periodate oxidation of cellulose beads to obtain DAC beads, which act as a reactive intermediate to introduce negative chage on its surface through sulfonation reaction and control the charge on the beads. Considering the applications of spherical form of cellulose, the beads should be carefully agitated during the reaction in order to preserve their shapes. In conclusion, this method of generating anionically charged cellulose beads has the advantages of a simple reaction procedure that is high yielding, and regioselective. The resulting product was shown to exhibit an electrostatical affinity to cationic starch and future applications could include their usage to agglomeriate cationally charged proteins and also to remove cationic metals and the chromatography of biological molecules. In our next studies, we utilized the periodate oxidation approach to chemically modify cellulose nanowhisker surfaces to synthesize novel materials.

CHAPTER 6

GRAFTING OF MODEL PRIMARY AMINE COMPOUNDS TO CELLULOSE NANOWHISKERS THROUGH PERIODATE OXIDATION[3]

6.1 Introduction

Cellulose is the most abundant and sustainable polymeric raw material in nature, obtained from different vegetal, bacterial and animal sources. Formed by repeated units of glucose monomers, it has led to a global renaissance of interdisciplinary cellulose research because of its unique characteristics. For the past few decades, cellulose has attracted the attention as one of the promising polysaccharides for accomplishing highly engineered nanoparticles, which can be significantly modified to tailor its properties for many potential applications.[50, 250-252]

Controlled acid hydrolysis of cellulosic fibers exploits the hierarchical structure of cellulose by selectively hydrolyzing the amorphous regions and leaving behind the less reactive crystalline regions called cellulose nanowhiskers (CNWs). These nanowhiskers are defined as elongated rod-like nanoparticles with typical dimension of 100-1000 nanometers in length and 5-50 nanometers in width depending on their source as well as the hydrolysis conditions.[12, 41, 102, 253] Recently, cellulose nanowhiskers have attracted research attention as a green nanofiller in bionanocomposites because of their superior

[3] This manuscript was accepted for publication in Cellulose, 2012. It is entitled as "Grafting of Model Primary Amine Compounds to Cellulose Nanowhiskers through Periodate Oxidation". The other authors are Thomas Elder from USDA-Forest Service, Pineville, LA and Arthur J. Ragauskas from the Institute of Paper Science and Technology and School of Chemistry and Biochemistry at Georgia Institute of Technology

mechanical properties, high aspect ratio, low density, biocompatibility, high strength, and crystallinity.[43, 83, 174-175] To further broaden their applications furthermore, attempts were made to transform the hydroxyl groups into different polar and non-polar moieties which have led to an increased interest in synthesis of functionalized nanowhiskers.

Due to the abundance of reactive hydroxyl groups at the surface of CNWs, esterification, and etherification are the most common approaches for chemical modification of cellulose whiskers although there are several reports on oxidation and nucleophillic substitution reaction. In fact, all these modifications are focused on the covalent functionalization of the surface hydroxyl groups. For example, Sassi et al.[177] acetylated valonia and tunicate whisker using acetic anhydride in acetic acid only affecting the cellulose chains localized at the surface. Acetylation of whiskers was also carried out in vinyl acetate, alkenyl succinic anhydride (ASA) to improve the dispersion of whiskers in organic solvents.[178-181]

Gousse et al. examined the silylation of the hydroxyl groups on tunicin whiskers using a series of alkyldimethylchlorosilanes such as *n*-butyl, *n*-octyl and *n*-dodecyl silanes.[184] It was observed that silylated whiskers were readily dispersible in THF but their birefringence behavior and morphological integrity was lost at high degrees of silylation (DS >1). The TEMPO-mediated oxidation of CNWs, obtained from HCl hydrolysis of cellulose fibers, was studied by various groups to impart negative charge on nanowhisker surface.[92, 187, 254] Araki et al.[92] further prepared novel sterically-stabilized aqueous whisker suspension combining TEMPO-mediated carboxylation and grafting of amine terminated polyethylene glycol (PEG). Nucleophilic coupling of hydroxyl groups of cellulose nanowhiskers with epoxypropyltrimethyl ammonium chloride in presence of

alkali was reported by Hasani et al.[189] that introduced positive charges at the whisker surfaces. Several other examples of functionalization approach include grafting-onto and grafting-from whisker surfaces to demonstrate very good compatibility and high adhesion with synthetic polymers.[193-194] These grafting approaches frequently involve functionalization via surface hydroxyl groups to a presynthesized polymer through a coupling agent or to a polymer formed by *in situ* polymerization from immobilized initiators on the substrate surface.

The periodate oxidation approach offers a facile and important method for functionalization of hydroxyl groups in cellulose nanowhiskers. It is well known for its highly selective oxidative fragmentation of the C-2 and C-3 glycol bond of the glucose ring in to C-2/C-3 dialdehyde product, which acts as a reactive intermediate for further derivatization.[113, 135, 221] Cellulose fibers, containing active amine groups have been known for their antimicrobial properties and irreversible chemical attachment resulting from covalent bonding are highly effective and preferable method to introduce amines onto cellulose surfaces.[255-258] The purpose of the present work is to utilize the facile periodate oxidation approach in order to incorporate model primary amine compounds to cellulose nanowhisker surfaces. In brief, cellulose nanowhiskers resulting from H_2SO_4 hydrolysis of bleached softwood pulp were oxidized in presence of sodium periodate to obtain the dialdehyde cellulose whisker product. These oxidized nanowhiskers were then grafted with methyl and butyl amine to obtain the corresponding amine derivatives employing a reductive amination treatment. This chapter highlights our studies on the chemistry and the characterization of the modified nanowhiskers by copper titration, FT-IR, NMR and AFM.

6.2 Experimental

6.2.1 Preparation of H_2SO_4-hydrolyzed cellulose nanowhiskers

Cellulose nanowhiskers were prepared by sulfuric acid hydrolysis of a bleached softwood Kraft pulp as described in Chapter 3 (3.2 Cellulose nanowhisker preparation).

6.2.2 Sodium periodate oxidation of cellulose nanowhiskers

Sodium periodate oxidation of cellulose nanowhiskers was carried out as described in Chapter 3 (3.3.2 Sodium periodate oxidation of cellulose nanowhiskers). These samples were named as DAC1, DAC2, and DAC3, where DAC= dialdehyde cellulose and 1, 2, 3 corresponds to 2.80, 8.40 and 10.02 mmols of sodium periodate employed, respectively.

6.2.3 Reaction of dialdehyde cellulose whiskers with amines

Dialdehyde cellulose nanowhiskers were reacted with amines following the procedure as described in Chapter 3 (3.5 Reaction of dialdehyde cellulose whiskers with primary amines). A schematic pathway for oxidation and reductive-amination of cellulose nanowhiskers is shown in Fig. 6.1.

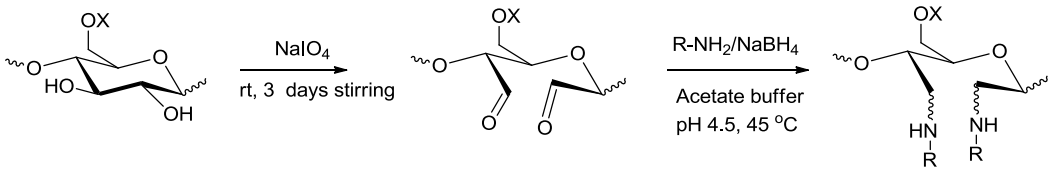

X = H, SO_3H R= methyl and butyl

Fig. 6.1 Oxidation and reduction reaction of cellulose nanowhiskers.

These samples were named as DACX-MA, DACX-BA, where DAC= dialdehyde cellulose, MA= methyl amine, BA= butyl amine and X= 1, 2, 3 corresponds to three levels of oxidation, respectively.

6.2.4 Determination of carbonyl groups by copper titration

The carbonyl group content of the starting and oxidized whiskers was determined following Tappi standard method T430 as described in Chapter 3 (3.9.1 Determination of carbonyl content of dialdehyde cellulose by copper number titration).

6.2.5 FT-IR spectroscopy of cellulose nanowhiskers and their derivatives

Transmission mode FT-IR spectra were collected with a Nicolet Magna-IR^{TM} 550 spectrometer as described in Chapter 3 (3.9.5 FT-IR spectroscopy). The starting whisker and oxidized samples were dried at 105 °C for 6 h and then cooled to room temperature for FT-IR analysis. The oven dried CNWs, periodate oxidized CNWs and freeze dried amine derivatives were pressed into KBr pellets (1:200).

6.2.6 NMR spectroscopy

Amine derivatives of cellulose nanowhiskers were characterized by ^{13}C NMR and solid state NMR spectroscopy as described in Chapter 3 (3.9.8.2 ^{13}C NMR spectroscopy of cellulose nanowhisker derivatives and 3.9.8.4 Solid state NMR spectroscopy of aminated cellulose nanowhiskers).

6.2.7 X-ray photoelectron spectroscopy analysis

X-ray photoelectron spectra of cellulose nanowhiskers and their derivatives were collected on a Thermo K-alpha XPS spectrometer as described in Chapter 3 (3.9.10 X-ray photoelectron spectroscopy (XPS) analysis).

6.2.8 AFM experiment

AFM experiments were conducted on a Veeco, NanoScope 3100 scanning probe microscope with a NanoScope IIIa controller as described in Chapter 3 (3.9.12 AFM experiment).

6.3 Results and discussion

Cellulose nanowhiskers were oxidized in presence of sodium periodate to yield the corresponding C-2/C-3 dialdehyde product and the carbonyl content was determined by Cu^{2+} titration (Table 6.1). The results indicated a corresponding increase in carbonyl content with increasing sodium periodate equivalents, although a very low degree of oxidation (2.3%) was observed, which was attributed to the non-uniform distribution of oxidation over fiber surface.[131] Further evidence of carbonyl group was obtained from the transmission mode FT-IR spectra, as shown in Fig. 6.2. The characteristic C=O stretching vibration band of the dialdehyde cellulose nanowhiskers appeared at 1740 cm^{-1} and this spectral data confirms a gradual oxidation of nanowhiskers as the intensity of the carbonyl band increases with increased oxidant.

Table 6.1 Carbonyl content of oxidized cellulose nanowhiskers.

Samples	$NaIO_4$ mmols	Carbonyl content (mmol g^{-1})
CNWs	0.00	0.006
DAC1	2.80	0.062
DAC2	8.40	0.114
DAC3	10.02	0.141

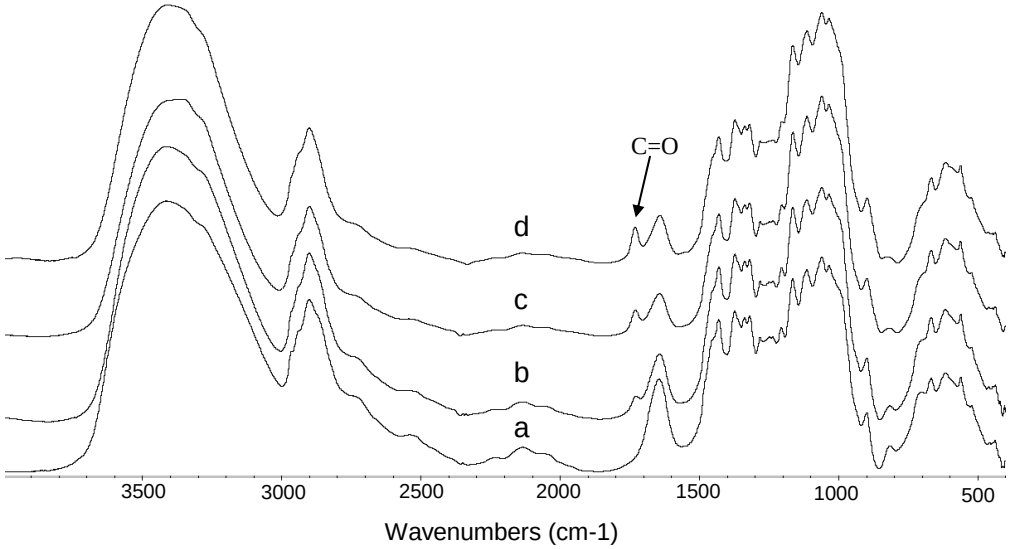

Fig. 6.2 FT-IR spectra (a) nanowhiskers (b) DAC1 (c) DAC2 and (d) DAC3.

The dialdehyde cellulose nanowhiskers were then reacted with methyl amine and butyl amine to generate *in situ* the corresponding imines followed by sodium borohydride reduction to yield the amine derivatives. The presence of the amine functionality grafted to the cellulose whiskers was evidenced from FT-IR spectra (Fig. 6.3 and 6.4) as indicated by the appearance of a new absorption band at 1564 cm^{-1} corresponding to N-H bending vibration. This result was further supported by ^{13}C solution NMR spectra (Fig. 6.5 and 6.6) as a result of their partial solubility in DMSO, possibly due to the incorporation of non-polar small chains on to the surface of nanowhiskers. NMR spectra

exhibited chemical shifts arising from the respective amine carbons as well as a peak at 172 ppm arising from aldehyde carbonyl carbon after adding 5 equivalents of amines per glucose unit, suggesting the presence of residual carbonyl group in the sample. Additional evidence was obtained from copper titration result of these amine grafted nanowhiskers (Table 6.2) showing the remaining unreacted carbonyls. However, with excess equivalents of amine (1:20) the carbonyl peak in NMR spectra disappears as shown in Fig. 6.7 and this was again supported from carbonyl content (Table 6.2) estimation through copper titration. The absence of carbonyl groups in amine grafted samples could be explained to their reduction to amine derivatives and to some extent the possible reduction by sodium borohydride. As a control experiment, cellulose nanowhiskers and the oxidized products were found to be insoluble in DMSO. The samples were further characterized by XPS in order to confirm the presence of amines on the surface of nanowhiskers.

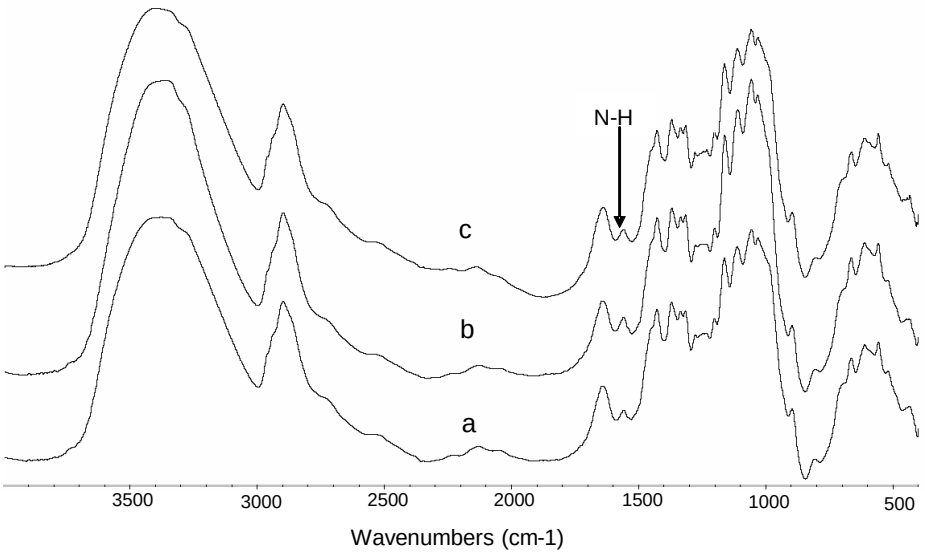

Fig. 6.3 FT-IR spectra (a) DAC1-MA (b) DAC2-MA and (c) DAC3-MA.

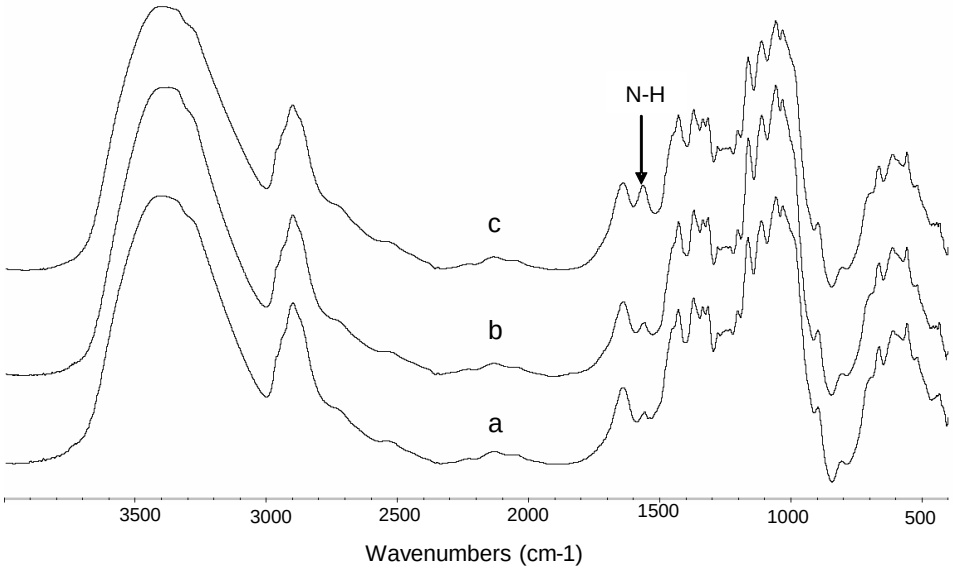

Fig. 6.4 FT-IR spectra (a) DAC1-BA (b) DAC2-BA (c) DAC3-BA.

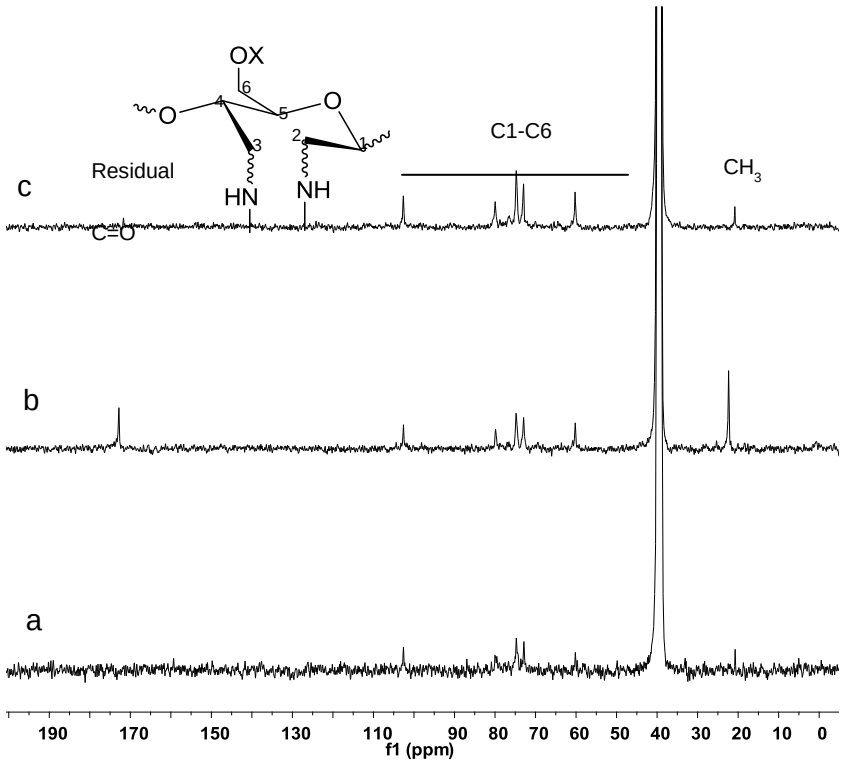

Fig. 6.5 ^{13}C NMR spectra of nanowhiskers after adding (1:5 eq) of methyl amine (a) DAC1-MA (b) DAC2-MA and (c) DAC3-MA.

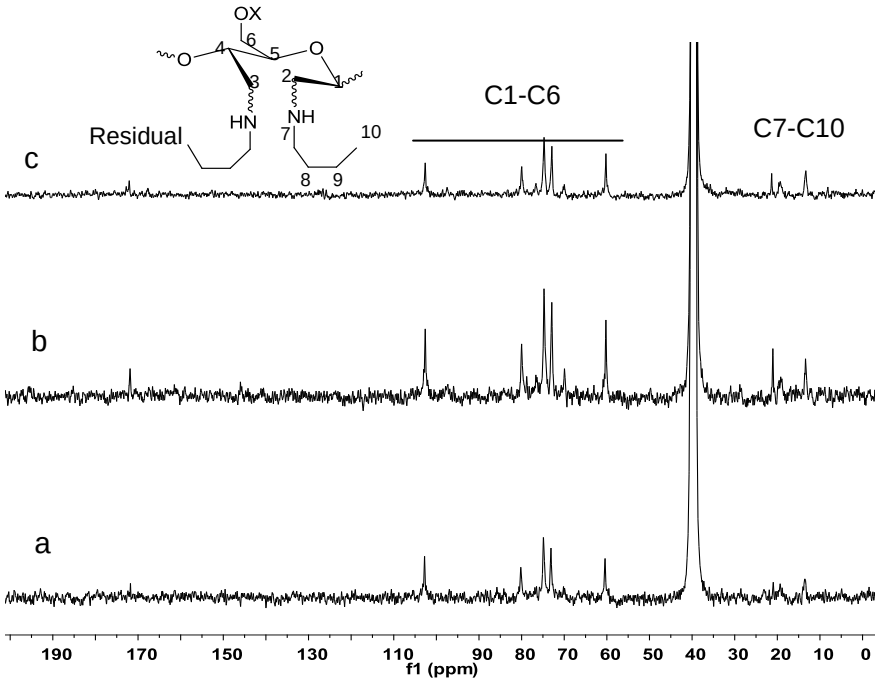

Fig. 6.6 ^{13}C NMR spectra of nanowhiskers after adding (1:5 eq) of butyl amine (a) DAC1-BA (b) DAC2-BA and (c) DAC3-BA.

Table 6.2 Carbonyl content of amine grafted nanowhiskers determined by copper number titration.

Samples	Initial carbonyl content (mmol g^{-1})	Carbonyl content (1:5 eq amines) (mmol g^{-1})	Carbonyl content (1:20 eq amines) (mmol g^{-1})
DAC1	0.062	0.021	0.001
DAC2	0.114	0.060	0.002
DAC3	0.141	0.103	0.002

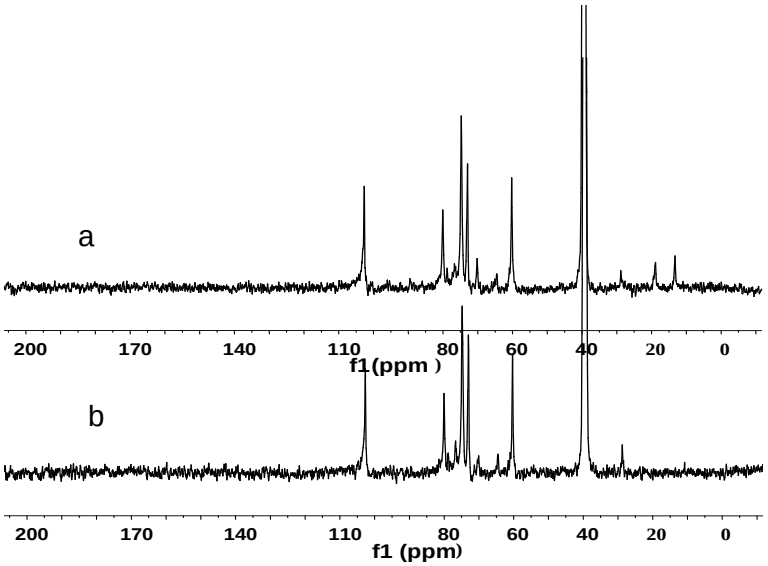

Fig. 6.7 Typical ^{13}C NMR spectra of nanowhiskers after adding excess (1:20 eq) of amine (a) DAC-MA (b) DAC-BA.

Surface elemental composition of unmodified and modified cellulose nanowhiskers determined from XPS analysis is summarized in Table 6.3, which only investigates the sample surface (~10 nm deep).[259] As expected, pure nanowhiskers

consist of mainly carbon and oxygen. After grafting with methyl and butyl amines, the nanowhisker surface shows the presence of nitrogen along with carbon and oxygen. The treatment of cellulose nanowhiskers with methyl and butyl amines caused an increase in the concentration of carbon and nitrogen, which is a clear indication of the attachment of the primary amines to the whisker surface. We observed a maximum of 1.3% and 2.1% of nitrogen in DAC3-MA and DAC3-BA samples respectively. However, DAC1-MA and DAC1-BA samples did not exhibit any nitrogen content on the surface possibly due to its low degree of substitution.

Table 6.3 Surface elemental composition of cellulose nanowhiskers before and after chemical modification.

Sample	Elemental composition (%)			Sample	Elemental composition (%)		
	O	C	N		O	C	N
Nanowhiskers	38.6	53.25	0				
DAC1-MA	37.9	55.1		DAC1-BA	37.4	54.5	
DAC2-MA	37.2	55.2	0.5	DAC2-BA	37.5	54.5	0.6
DAC3-MA	33.4	58.0	0.9	DAC3-BA	34.0	56.3	1.2
DAC3-MA (1:20)	32.6	58.6	1.3	DAC3-BA (1:20)	33.6	57.2	2.1

Investigation of surface morphology of cellulose nanowhisker and its derivatives was carried out by AFM as shown in Fig. 6.8. AFM images show that the nanowhiskers maintained their characteristic morphology even after grafting with amines. Nanowhiskers seem to be agglomerated before chemical modifications but they were found to be separated from each other after chemical modification due to the incorporation of relatively hydrophobic groups on the surfaces.

Determination of crystallinity using different techniques has been extensively studied in literature and it has been concluded that the crystallinity index (CrI) varies substantially depending on the choice of instrument and data analysis technique implemented. The two most commonly used techniques for determining the crystallinity index are NMR and XRD. However, the XRD method always shows significantly higher crystallinity values than NMR although the trend of CrI is consistent in each measurement.[260]

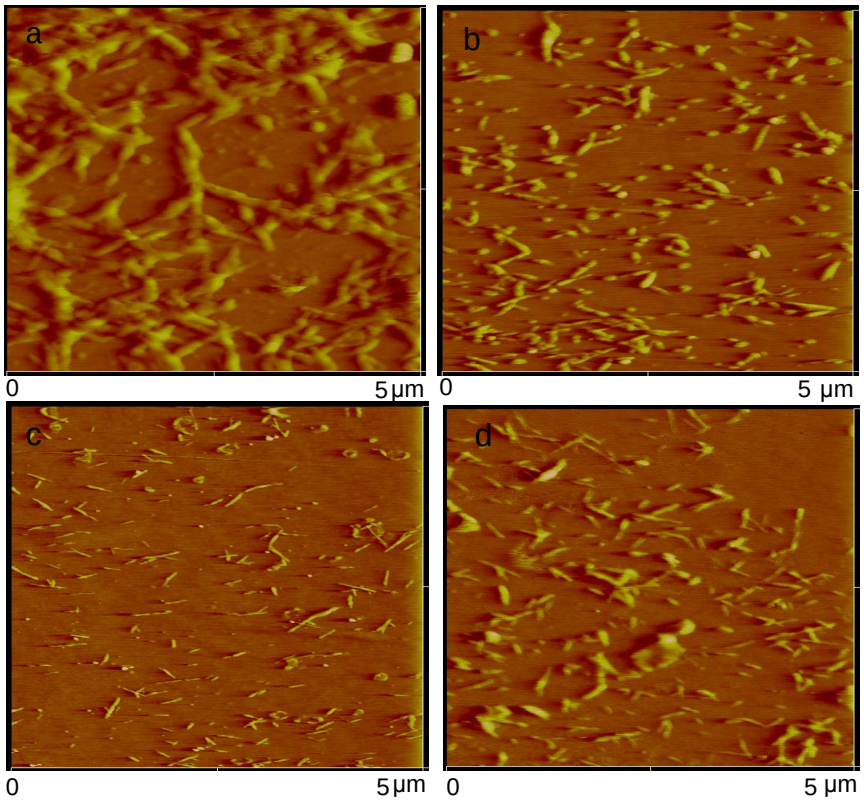

Fig. 6.8 AFM image of 0.001 wt. % suspensions (a) nanowhiskers, (b) DAC3, (c) DAC3-MA and (d) DAC3-BA.

We have used solid-state ^{13}C NMR method to measure the crystallinity index, where spectra of all the samples were analyzed using line shape analysis based on the method outlined by Larsson et al.[261] Crystallinity index was calculated from the ratio of the peak areas in crystalline region to the peak areas in non-crystalline regions with an error of approximately 3%. It was observed that CrI of nanowhiskers was preserved even after the oxidation-reduction reaction (Table 6.4), which could be due to the grafting of small molecules onto the whiskers. Similar observation was made in the literature, where morphology and crystallinity of nanowhiskers is retained after chemical modification.[181]

Table 6.4 Crystallinity index of cellulose nanowhiskers before and after chemical modification.

Samples	Crystallinity Index (CrI)
CNWs	56.5
DAC1	55.5
DAC2	57.2
DAC3	57.0
DAC3-MA	55.9
DAC3-BA	57.7

6.4 Conclusions

Cellulose nanowhiskers were prepared by sulfuric acid hydrolysis of bleached softwood pulp followed by their regioselective oxidation using 2.80-10.02 mmols of sodium periodate per 5g of whisker. Finally, dialdehyde cellulose nanowhiskers were successfully grafted with model amine compounds such as methyl and butyl amines

through a Schiff base condensation and sodium borohydride reduction reaction in aqueous media to obtain their amine derivatives in 80-90% yield. We found a corresponding increase in carbonyl content (0.06-0.14 mmols/g) of the oxidized nanowhisker products with the increase in oxidant as measured by titrimetric analysis and this was further evidenced by FT-IR spectroscopy.

Interestingly, the amine grafted nanowhiskers were found to be partially soluble in DMSO even at a low content of amine groups. Occurrence of partial non-polar moieties on nanowhisker surfaces by introducing alkyl chains is the most likely reason. As a consequence, the effective grafting of amines to whiskers was demonstrated by ^{13}C NMR with additional evidence from FT-IR and copper titration experiments. The reduction reaction between amines and carbonyl groups was further confirmed by XPS analysis due to the presence of nitrogen on nanowhisker surface. Morphological integrity and crystallinity of the nanowhiskers was maintained after the chemical modification as studied by AFM and solid-state ^{13}C NMR, respectively.

In conclusion, periodate oxidation and reductive amination showed a promising path to attach various amine containing compounds such as enzymes, antibiotics to the nanowhisker surface, a renewable source of raw material for potential biomedical applications. Therefore, in our next study we utilized this oxidation and reduction methodology to synthesize cellulose nanowhisker carrier molecules for drugs and biomolecules as well as to prepare chemically cross-linked gelatin hydrogels. [170] [131] [171] [131] [171] [131] [263] [186]

CHAPTER 7

SYNTHESIS OF A NOVEL CELLULOSE NANOWHISKER BASED DRUG DELIVERY SYSTEM[4]

7.1 Introduction

Development of nanoparticle delivery systems for drugs, proteins, and enzymes remains an important challenge in biomedical research on account of the effective delivery and release of the carrier molecules at the target site. Over past few decades, extensive studies have been performed on both synthetic and natural polymer based nano carriers and several of them are already in clinical use.[262-264] Of the readily available natural polymers, polysaccharide nanoparticles, especially cellulose nanowhiskers (CNWs) have attracted increasing attention as a promising delivery system for drugs due to their outstanding properties such as nano dimension, high surface area, hydrophilicity, biocompatibility, and biodegradability.[43, 252]

Cellulose nanowhiskers are defined as elongated rod-like crystals with a dimension of 100-1000 nanometers in length and 5-50 nanometers in diameter, typically obtained by acid hydrolysis of cellulose fibers. Significant efforts have been dedicated to explore the preparation and properties of cellulose nanowhiskers from various cellulosic sources.[12, 41, 102, 180, 253] It was observed that the dimensions and properties of nanowhiskers vary depending on their sources as well as the hydrolysis conditions

[4] This manuscript was accepted for publication in RSC Advances, 2012. It is entitled as "Synthesis of a novel cellulose nanowhisker based drug delivery system". The other author is Arthur J. Ragauskas from the Institute of Paper Science and Technology and School of Chemistry and Biochemistry at Georgia Institute of Technology

employed. Several recent studies on cellulose nanowhiskers and their derivatives indicate the potential biomedical applications of cellulose nanowhiskers. For example, Dong et al.[190] have chemically labeled nanowhiskers with fluorescein isothiocyanate (FITC) fluorophore through a three-step reaction path way and evaluated it for fluorescence bioassay and bioimaging applications. Cellulose nanowhisker surfaces have also been successfully modified using L-leucine amino acid showing a possible platform for introducing biologically active building blocks.[183]

A supramolecular hydrogel based on cyclodextrin/polymer inclusion was prepared by Zhang and coworkers[265] and it was shown that incorporation of cellulose nanowhiskers in to the hydrogel enhances its gelation, mechanical strength and facilitates sustained release of drugs. Further evaluation of the hydrogel on cell viability did not indicate any additional cytotoxicity implying a potential candidate for smart delivery and sustained release applications. Cellulose nanowhisker surfaces were functionalized with gold nanoparticles by Mahmoud et al. and this templated material was demonstrated as an excellent immobilization support for enzymes with high loading capacity.[191] Single stranded oligonucleotides were effectively grafted on to TEMPO oxidized nanowhisker surfaces, setting a platform for future development of nanodevices from inexpensive and chemically versatile nanowhiskers.[192]

The toxicity assessment of cellulose nanowhiskers has been examined by interacting with microvascular endothelial cells, rainbow trout hepatocytes, and other aquatic species.[266-267] It was concluded that cellulose nanowhiskers are non-toxic to cells and could be considered for the delivery of biomolecules and therapeutics. Dugan and coworkers examined the bioactivity of nanowhiskers by interacting them with myoblast

cells, which showed that patterned CNWs surfaces actively direct the growth of tissue leading to future applications in tissue engineering and also nanowhiskers exhibited non-cytotoxicity and non-immunogenicity even at relatively high concentrations.[268-269] Additionally, due to the presence of abundant hydroxyl groups, cellulose nanowhiskers are hydrophilic in nature, thus exhibit low protein adsorption, ensuring a long blood circulation half-life and delaying initial clearance from the blood stream.[270]

Besides these biomedical properties, cellulose nanowhiskers are easy to prepare, form a colloidal suspension in water and mild reaction condition can be followed to functionalize CNWs, which motivated us to examine the synthesis of a nanowhisker based drug delivery system through their surface chemical modification. Typical drug delivery systems involve natural or synthetic biocompatible polymers, which are coupled to the targeting moiety directly or via a spacer arm. Releasable PEGylation (rPEGylation) is one of the extensively studied and promising drug delivery technologies for amine containing drugs or biologically active agents, where the drug carrier design constitutes a "trigger" or a "spacer" element attached to polyethylene glycol (PEG) backbone to provide the specific initiation and rate of release path way, followed by a "linker" molecule. The linkers comprise a series of customized aliphatic and aromatic molecules known as releasable PEG (rPEG) linkers and they play a key role in achieving controlled delivery.[271]

The release sequence involves a base or enzyme cleaved initiation step to separate the PEG followed by a second faster step through molecular decomposition of the linkers to deliver the unmodified and fully active drug. We examined the use of an aromatic linker, known as benzyl elimination linker, in designing our nanowhisker delivery system

since it relies on a classic and rapid 1,4-or 1,6-benzyl elimination reaction and molecular decomposition to regenerate the amine group of conjugated drug/biomolecule, (Fig. 7.1). A detailed study of the structure and release mechanism of other linker molecules can be found in literature.[272-273]

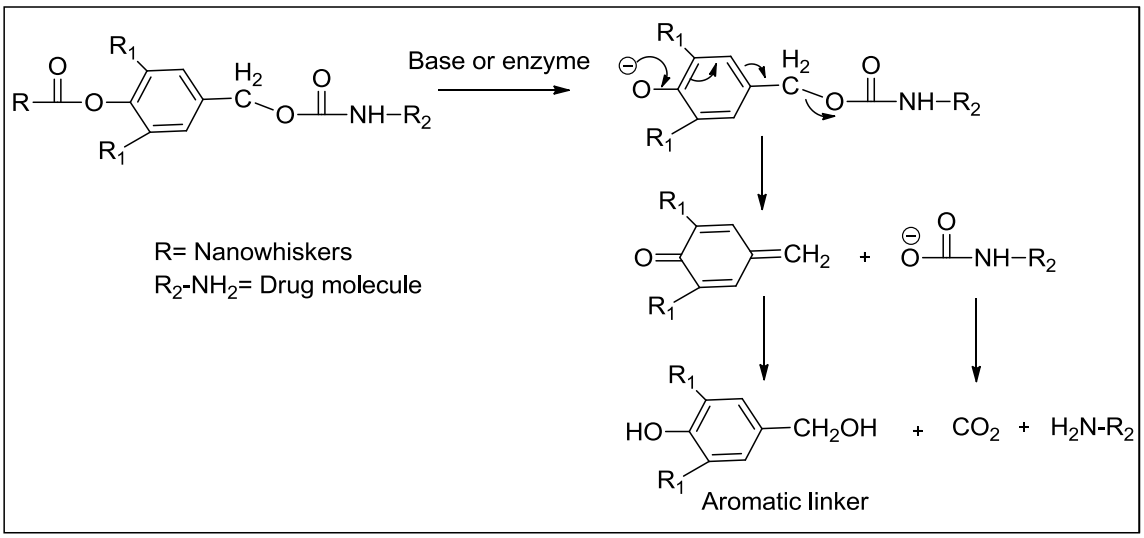

Fig. 7.1 1,6-Benzyl elimination reaction mechanism of aromatic linker.

In this study, we combined the aromatic linker and cellulose nanowhiskers to synthesize a novel delivery system for amine containing biologically active compounds and drug molecules. Based on our previous study focused on grafting of small chain primary amines to nanowhiskers employing a sequence of oxidation, condensation and *in situ* reduction reactions, gamma aminobutyric acid, a spacer molecule was grafted to nanowhisker surface. Gamma aminobutyric acid was chosen as a spacer molecule because of its biocompatibility and ease of availability. In the next step, syringyl alcohol was used as an aromatic linker and attached to the carboxylic group of amino acid. The effective grafting of spacer and linker molecules to the nanowhisker surfaces was

investigated by a series of characterization techniques including FT-IR, NMR, XPS and TEM.

7.2 Experimental

7.2.1 Preparation of cellulose nanowhiskers

Cellulose nanowhiskers were prepared by sulfuric acid hydrolysis of a bleached softwood Kraft pulp as described in Chapter 3 (3.2 Cellulose nanowhisker preparation).

7.2.2 Sodium periodate oxidation of cellulose nanowhiskers

Sodium periodate oxidation of cellulose nanowhiskers was carried out as described in Chapter 3 (3.3.2 Sodium periodate oxidation of cellulose nanowhiskers). These sample was designated as DAC, where DAC= dialdehyde cellulose nanowhisker.

7.2.3 Reaction of dialdehyde cellulose whiskers with gamma aminobutyric acid

Dialdehyde cellulose nanowhiskers were grafted with GABA as described in Chapter 3 (3.6 Reaction of dialdehyde cellulose whiskers with gamma aminobutyric acid (GABA)). The sample was referred as DAC-GABA.

7.2.4 Reaction of DAC-GABA with syringyl alcohol

DAC-GABA was reacted with syringyl alcohol as described in Chapter 3 (3.7 Reaction of DAC-GABA with syringyl alcohol). The product was referred as DAC-GABA-SA. A schematic representation of the reaction is shown in Fig. 7.2.

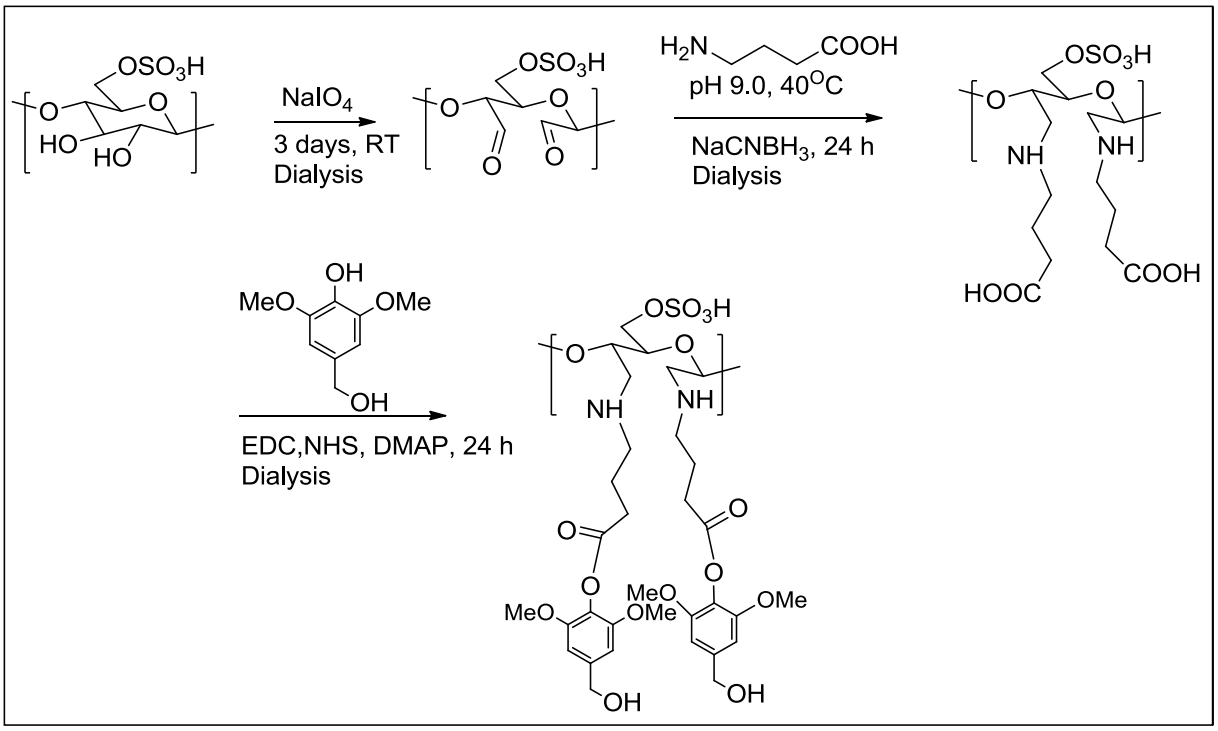

Fig. 7.2 Reaction path followed to modify the cellulose nanowhisker surfaces.

7.2.5 FT-IR Spectroscopy

Transmission mode FT-IR spectra were collected with a Nicolet Magna-IR^{TM} 550 spectrometer as described in Chapter 3 (3.9.5 FT-IR spectroscopy). The oven dried CNWs, periodate oxidized CNWs and freeze dried DAC-GABA, DAC-GABA-SA samples were pressed into KBr pellets (1:200).

7.2.6 NMR spectroscopy

^{13}C NMR spectra were obtained on a Bruker Avance-400 spectrometer operating at a frequency of 100.55 MHz at 45 ^{o} C as described in Chapter 3 (3.9.8.2 ^{13}C NMR spectroscopy of cellulose nanowhisker derivatives).

The DOSY experiments were conducted using the bipolar pulse pair (BPP) pulse sequence as described in Chapter 3 (3.9.8.3 Diffusion ordered NMR spectroscopy).

7.2.7 X-ray photoelectron spectroscopy analysis

X-ray photoelectron spectra of cellulose nanowhiskers and their derivatives swere collected on a Thermo K-alpha XPS spectrometer as described in Chapter 3 (3.9.10 X-ray photoelectron spectroscopy (XPS) analysis).

7.2.8 TEM experiment

Transmission electron micrographs of cellulose nanowhisker samples were taken in a JEOL 100CX-2 transmission electron microscope at an accelerating voltage of 100 kV as described in Chapter 3 (3.9.11 TEM experiment).

7.3 Results and discussion

The purpose of the following chemical modifications is to synthesize a drug delivery system based on cellulose nanowhiskers without the conjugation of the active agent and we expect this synthetic strategy will open their use as a vehicle for drugs, enzymes and other biomolecules. Cellulose nanowhiskers prepared by the sulfuric acid hydrolysis of the softwood kraft pulp were oxidized in presence of sodium periodate. Periodate oxidation of nanowhiskers selectively cleaves the C2-C3 bond and introduces carbonyl groups at respective carbon atoms of the glucose ring which was confirmed from the FT-IR spectra due to the appearance of carbonyl band at 1734 cm^{-1} (Fig. 7.3). Oxidized nanowhiskers were further grafted with the spacer molecule, gamma

aminobutyric acid following Schiff's base reaction and *in situ* sodium cyanoborohydride reduction. As a result, the carbonyl band disappeared and an additional band at 1568 cm^{-1} appeared indicating successful amination-reduction reaction between the carbonyl and amine groups. The final step involved the activation of carboxylic group of the amino acid by EDC in presence of NHS followed by the esterification with syringyl alcohol. As observed in the FT-IR spectra, the presence of an ester C=O at 1680 cm^{-1}, in addition to a characteristic C=C band of benzene ring at 1609 cm^{-1} supports the esterification reaction. The results from FT-IR spectra support the sequence of changes that occurred during the series of reactions.

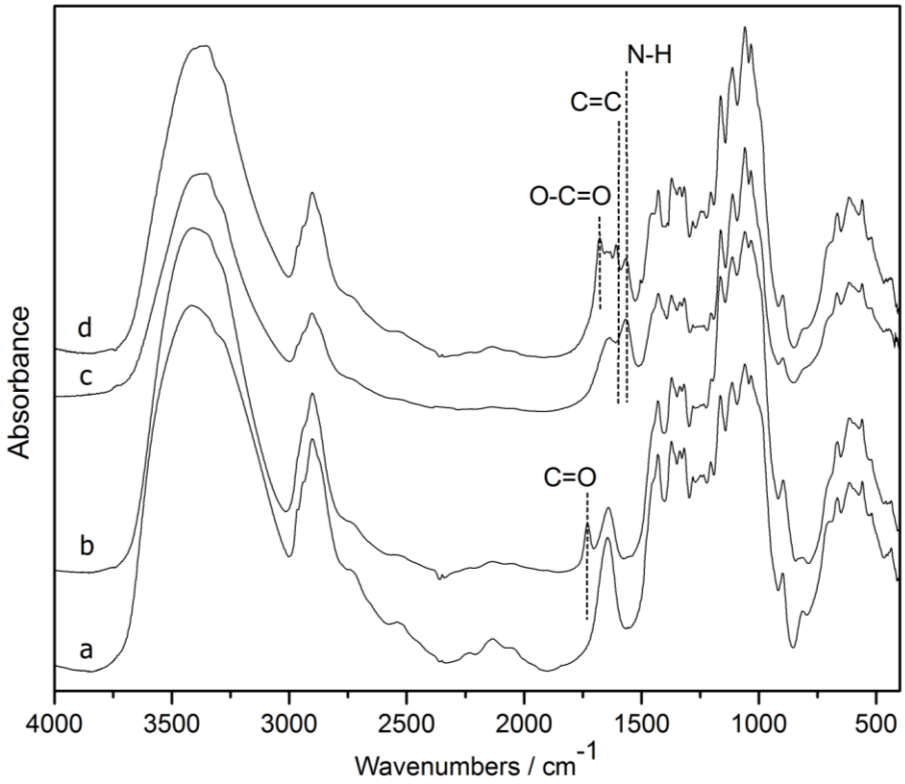

Fig. 7.3 FT-IR spectra of (a) nanowhiskers (b) DAC (c) DAC-GABA (d) DAC-GABA-SA.

Cellulose nanowhisker derivatives were further characterized by NMR spectroscopy. DAC-GABA sample was found to be insoluble in DMSO-d_6; hence it was dissolved in a mixture of predeuterated pyridinium ionic liquid and DMSO-d_6 (1:4) to study the structural changes by ^{13}C NMR.[274] As shown in Fig. 7.4, the signals centered at δ 103.5, 73.4, 74.6, 81, 76.4, and 60.2 were readily assigned to C1, C2, C3, C4, C5, and C6 of glucopyranoside ring in cellulose nanowhiskers, respectively. The peaks corresponding to carboxylic group and the alkyl chain of gamma aminobutyric acid appeared at 172.4 and 20-35 ppm respectively, suggesting its attachment to nanowhiskers. Signals in the region of 120-150 ppm belong to the ionic liquid. DAC-GABA-SA sample was found to be soluble in DMSO-d_6 possibly, due to the incorporation of non-polar moieties on to the surface of nanowhiskers. So, the NMR spectra were collected in DMSO to avoid the interference of peaks from ionic liquid with the syringyl group. As shown in Fig. 7.5, signals at δ 57.3, 63.5, 102.9, 142.6, 152.4, 157.2, and 174.5 correspond to C16, C15, C13, C11, C14, C12, and C10 of syringyl group, respectively, indicating the chemical modification of DAC-GABA by syringyl alcohol molecule.

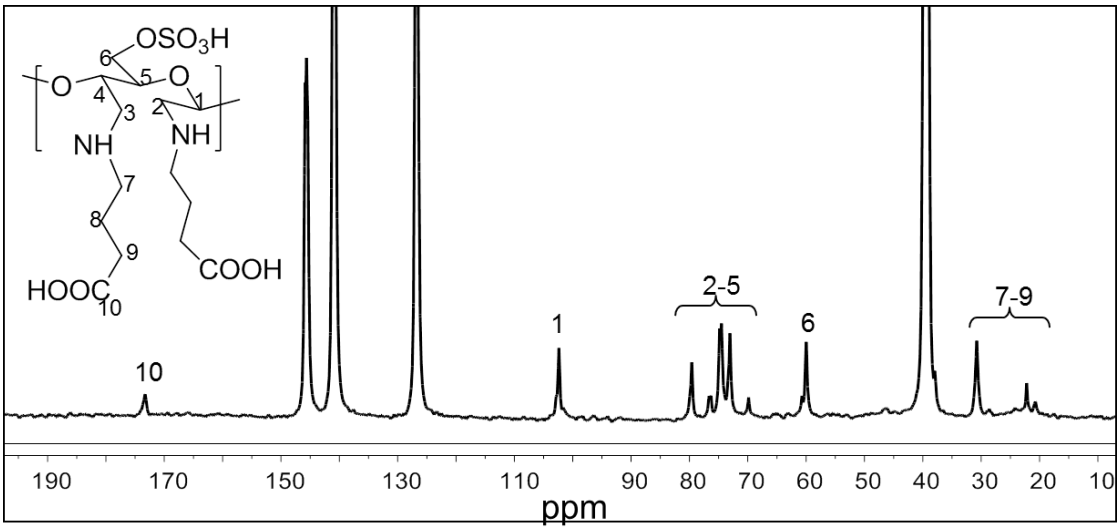

Fig. 7.4 ^{13}C NMR spectrum of DAC-GABA in predeuterated pyridinium ionic liquid-DMSO-d_6.

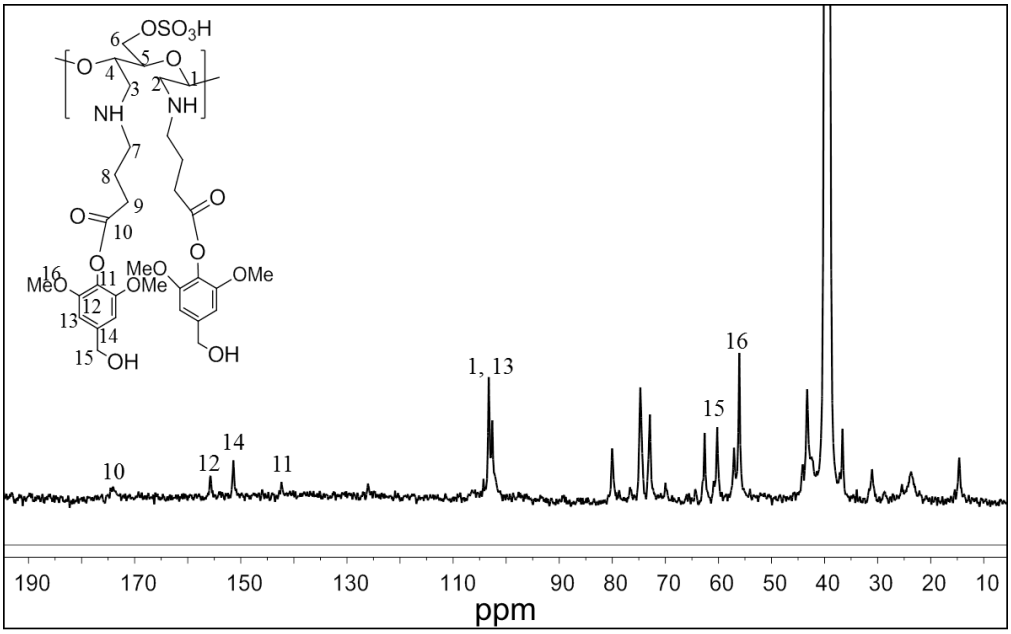

Fig. 7.5 ^{13}C NMR spectrum of DAC-GABA-SA in DMSO-d_6.

In order to confirm that the ^{13}C NMR spectrum of DAC-GABA-SA is a consequence of effective chemical attachment of spacer and linker molecule to the nanowhiskers, we further collected its 2D DOSY spectrum. DOSY is a powerful technique to study the interactions between the components in a solution based on their difference in apparent diffusion coefficients. Diffusion ordered spectroscopy employs pulsed field gradient (PFG) to acquire a series of diffusion-attenuated 1D PFG-spin echo experiments. A suitable Laplace transform of the decaying signal results in a 2D spectrum with chemical shift on one axis and the distribution of diffusion coefficients on the other axis.[275-276]

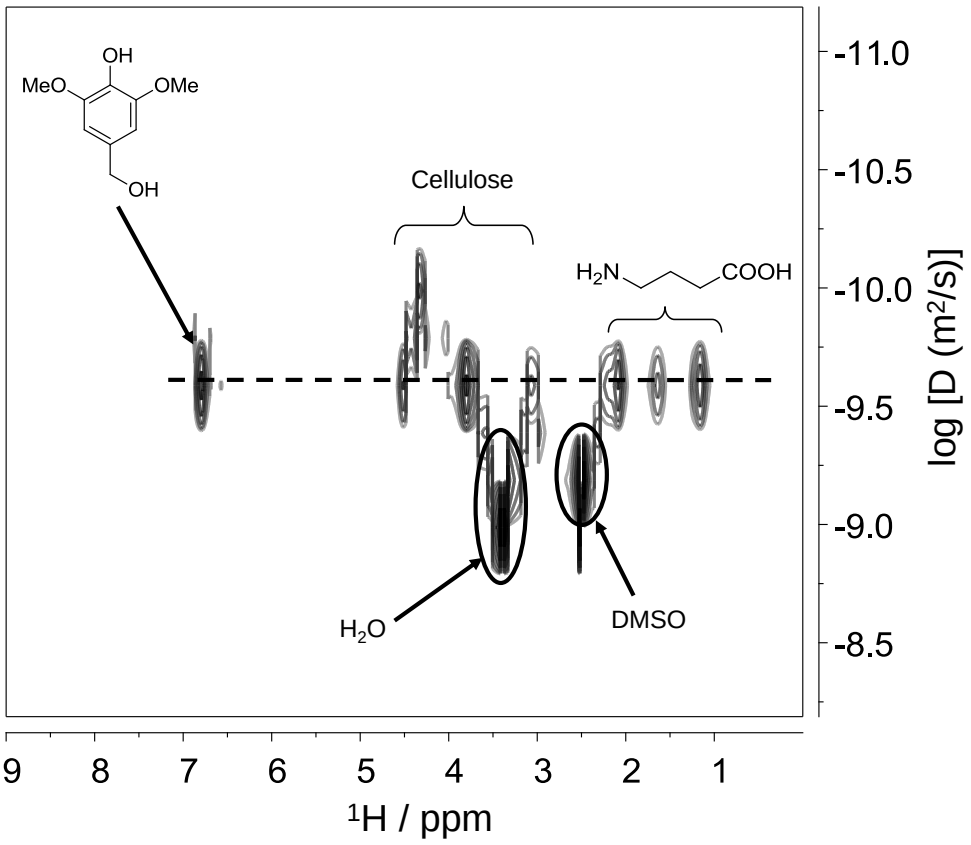

Fig. 7.6 Contour-plot ^{1}H NMR DOSY spectrum of DAC-GABA-SA in DMSO-d_6.

Interaction between the molecules will be determined by comparing their diffusion coefficients at their chemical shifts; for instance, if the molecules with different diffusion coefficients are chemically associated with each other then they will diffuse at the same rate whereas, no interaction will give rise to separate diffusion coefficients at their respective chemical shifts. As shown in Fig. 7.6, signals belonging to cellulose nanowhiskers, amino acid and syringyl molecule are aligned at same diffusion coefficients, confirming that the three molecules diffuse together, which suggests they are chemically bonded to each other.

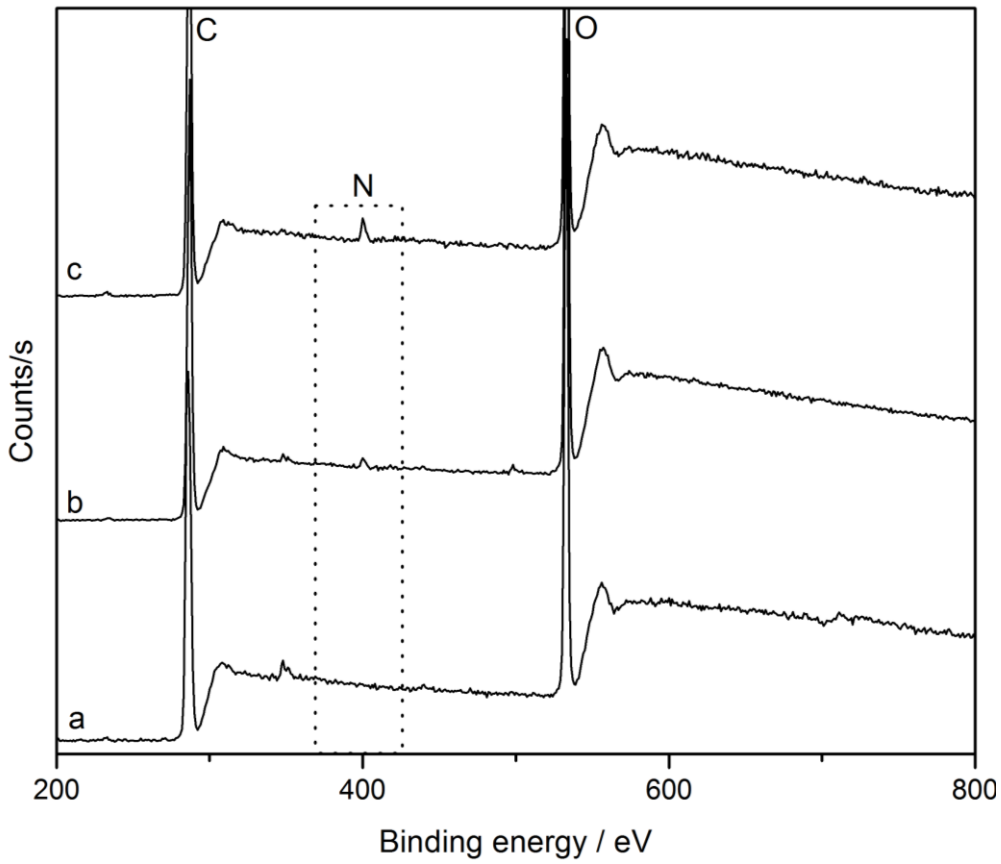

Fig. 7.7 XPS spectra of (a) nanowhiskers (b) DAC-GABA (c) DAC-GABA-SA.

Table 7.1 Surface elemental composition of cellulose nanowhiskers before and after chemical modification.

Sample	Elemental composition (%)		
	O	C	N
Nanowhiskers	37.61	53.25	0
DAC-GABA	36.43	55.92	1.47
DAC-GABA-SA	37.22	56.83	1.80

Surface elemental composition of pure cellulose nanowhiskers and their derivatives was studied by XPS spectroscopy. As expected, spectrum of pure nanowhiskers (Fig. 7.7) exhibits two peaks at 285 and 532.6 eV which correspond to carbon and oxygen respectively. After treating with gamma aminobutyric acid and syringyl alcohol the nanowhisker surface shows the presence of nitrogen at 400 eV in addition to carbon and oxygen. As summarized in Table 7.1, coupling of cellulose nanowhiskers with the spacer and linker molecule caused an increase in the concentration of carbon and nitrogen which is a clear indication of their attachment to the nanowhisker surface.

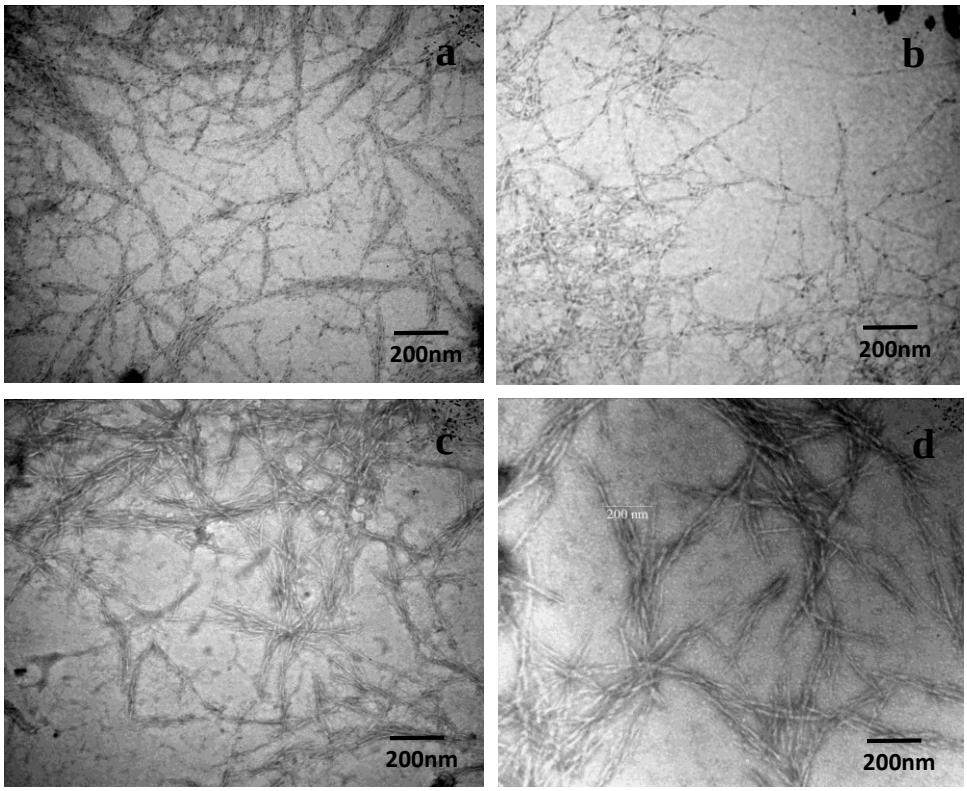

Fig. 7.8 TEM images of 0.02 wt% suspensions (a) nanowhiskers (b) DAC (c) DAC-GABA (d) DAC-GABA-SA.

Surface morphology of cellulose nanowhiskers and their derivatives was investigated by TEM as shown in Fig. 7.8. TEM images show that the nanowhiskers maintained their rod-like characteristic morphology even after the series of reactions. The dimensions of CNWs and their derivatives were found to be in the range of 150-300 nm in length and 4-8 nm in diameter.

7.4 Conclusions

In this work, we successfully prepared a novel nanometeric drug delivery molecule for amine containing biologically active molecules or drugs employing functionalized cellulose nanowhiskers. The nanowhiskers were grafted with a spacer molecule (gamma aminobutyric acid) following a well-established periodate oxidation and Schiff's base condensation reaction. To achieve controlled and rapid delivery of the carrier molecule, syringyl alcohol, a releasable linker was then attached to it. All the reactions were carried out in aqueous media and the resulting products were characterized by FT-IR, NMR, XPS, and TEM experiments to evaluate the functional groups, structure, and morphology respectively. The coupling of spacer and the linker molecule to nanowhiskers was confirmed from the sequential changes in functional groups and structure through FT-IR, ^{13}C NMR and XPS spectroscopy.

Further, their effective binding to cellulose nanowhiskers surface was evidenced from the single diffusion coefficient the final product by 2D-DOSY NMR spectroscopy. TEM observations showed no change in size and shape of nanowhiskers after the series of reactions, which is substantial for a delivery system. In conclusion, the unique assembly of cellulose nanowhiskers attached to a syringyl alcohol linker through gamma aminobutyric acid spacer molecule enables to successfully synthesize a novel cellulose nanowhisker based delivery system by following a series of oxidation, reductive amination and esterification reactions in aqueous media. The concept of carrier molecule from a renewable, biocompatible and biodegradable resource provides a platform that could be widely adapted for the controlled delivery of enzymes, proteins and amine containing drugs with the selection of desired linker molecules.

CHAPTER 8

CHEMICAL CROSS-LINKING OF GELATIN HYDROGELS BY PERIODATE OXIDIZED CELLULOSE NANOWHISKER[5]

8.1 Introduction

Hydrogels represent an interesting class of polymer networks, which have received a substantial amount of interest in pharmaceutical and biomedical applications including contact lens materials, artificial tendons, matrices for tissue engineering and drug delivery systems. Development of hydrogels is a rapidly growing research arena and a number of synthetic, as well as, naturally derived materials have been studied and reported in literature to form well-characterized hydrogels.[277-278] Among those, gelatin is a widely used material to form hydrogels for numerous biomedical applications such as wound dressing, plasma expander, adhesive and adsorbent material, vascular prostheses and in drug delivery as hard or soft capsules, hydrogels, or microspheres due to its high water content capacity, biocompatibility, biodegradability and non-immunogenicity.[279-282]

Gelatin is a protein obtained by de-naturing the triple-helix structure of collagen into single strain molecules. Upon cooling the aqueous solution of gelatin below 35 ^{o}C, it forms physical thermo-reversible gels due to partial recovery of collagen triple-helix structure by disorder-order rearrangement.[283-285] However, the application of gelatin is

---

[5] This manuscript was accepted for publication in Carbohydrate Polymers, 2012. It is entitled as "Improving the Mechanical and Thermal Properties of Gelatin Hydrogels Cross-Linked by Cellulose Nanowhiskers". The other authors are Marcus Foston from the Institute of Paper Science and Technology at Georgia Institute of Technology and Arthur J. Ragauskas from the Institute of Paper Science and Technology and School of Chemistry and Biochemistry at Georgia Institute of Technology

typically limited at higher temperature (above 35 ^{o}C), where breaking of the secondary bonding structure destroys the physical network. This leads to poor thermal and mechanical properties, and has thus far limited gelatin, a readily available and relative cheap material from further application. Therefore, chemical cross-links between the protein chains of gelatin are used to stabilize these gels, often refer to a chemical gelatin gels.[203] Various cross-linking agents including carboiimides,[202] formaldehyde,[286] glutaraldehyde,[287-288] oxidized polysaccharides such as dextran,[203, 289] chondroitin sulfate[290-291] and starch[292] have been used to chemically cross-link gelatin chains in order to improve the gel stability, increasing the resistance to thermal degradation and improving mechanical properties.

Recently, rod-like polysaccharide nanoparticles known as cellulose nanowhiskers, have gained considerable interest as a promising biomaterial due to their outstanding properties such as high surface area, high mechanical property, hydrophilicity, biocompatibility, and biodegradability.[83, 176] Cellulose nanowhiskers are usually obtained by the controlled acid hydrolysis of native cellulose fibers, where the size and mechanical characteristics of the resulting nanowhiskers depend on the source and hydrolysis conditions of cellulose fibers. The typical dimension of wood-based nanowhiskers is 5-10 nm in width and 100-300 nm in length.[43, 252-253] Because of their unique characteristics, cellulose nanowhiskers have been incorporated as fillers in several polymeric hydrogel matrices. For instance, supramolecular hydrogels based on cyclodextrin/polymer inclusion was prepared by Zhang and coworkers[265] and it was shown that incorporation of cellulose nanowhiskers into these hydrogels enhance gelation, mechanical strength and facilitates sustained release of drugs. Goetz et al.[293]

synthesized hydrogels by co-cross-linking a poly(methyl vinyl ether co maleic acid) (PMVEMA)-polyethylene glycol (PEG) matrix with cellulose nanowhiskers, again resulting in a significant improvement in mechanical and swelling properties. Other examples of composite hydrogels include CNW-reinforced with various polymer matrices such as agarose,[294] regenerated cellulose,[295] poly(acrylamide-co-acrylate),[296] hemicellulose[297] and chitosan-graft-poly(acrylic acid) copolymer.[298] Nevertheless, there has been no attempt so far on the employment of cellulose nanowhisker as a renewable, non-toxic and inexpensive cross-linker in gelatin matrix to enhance the material's hydrogel properties.

In presence of periodic acid, cellulose nanowhiskers undergo oxidative cleavage at the C_2-C_3 glycol bond resulting in dialdehyde groups at the respective carbon atoms. These aldehyde groups could act as a potential cross-linker since they will react with free amine groups of gelatin through Schiff's base formation. In this study, we present chemical cross-linking of gelatin by periodate oxidized nanowhiskers containing different amounts of aldehyde groups. To investigate the effect of cross-linking on the gel properties, physicochemical, thermal and mechanical properties of the formulated hydrogels were studied using a variety of advanced techniques. We observed a significant improvement in mechanical and thermal properties of the cross-linked gels compared to neat gelatin gels, which could broaden the use of gelatin hydrogels in various biomedical applications.

8.2 Experimental

8.2.1 Preparation of cellulose nanowhiskers

Cellulose nanowhiskers were prepared by sulfuric acid hydrolysis of a bleached softwood Kraft pulp as described in Chapter 3 (3.2 Cellulose nanowhisker preparation).

8.2.2 Sodium periodate oxidation of cellulose nanowhiskers

Sodium periodate oxidation of cellulose nanowhiskers was carried out as described in Chapter 3 (3.3.2 Sodium periodate oxidation of cellulose nanowhiskers). These samples were named as DAC1, DAC2, DAC3 and DAC4, where DAC= dialdehyde cellulose and 1, 2, 3, and 4 corresponds to 0.1, 0.3, 0.5 and 0.7, weight ratio of sodium periodate to nanowhiskers, respectively.

8.2.3 Synthesis of cross-linked hydrogels

Cross-linked hydrogels were prepared by following the procedure as described in Chapter 3 (3.8 Synthesis of chemically cross-linked hydrogels).

8.2.4 Determination of carbonyl groups by copper titration

The carbonyl group content of the starting and oxidized whiskers was determined following Tappi standard method T430 as described in Chapter 3 (3.9.1 Determination of carbonyl content of dialdehyde cellulose by copper number titration).

8.2.5 FT-IR spectroscopy

Transmission mode FT-IR spectra were collected with a Nicolet Magna-IR^{TM} 550 spectrometer as described in Chapter 3 (3.9.5 FT-IR spectroscopy). The oven dried CNWs, periodate oxidized CNWs and freeze dried cross-linked gels were pressed in to KBr pellets (1:200).

8.2.6 Determination of degree of cross-linking

The degree of cross-linking of the hydrogels was determined by Ninhydrin (2,2-dihydroxy-1,3-indanedione) assay as described in Chapter 3 (3.9.13 Determination of degree of cross-linking of the hydrogels).

8.2.7 Swelling properties of the hydrogels

Swelling properties of the chemically cross-linked hydrogels were studied as described in Chapter 3 (3.9.14 Study of swelling properties of hydrogels).

8.2.8 NMR experiments

^{1}H spin-spin (T_2) NMR experiments on samples swollen in 100% D_2O were performed on a Bruker DSX-400 spectrometer as described in Chapter 3 (3.9.8.5 ^{1}H spin-spin (T_2) NMR experiments of hydrogel). The resulting T_2 decay profiles were analyzed using a two-component Gaussian-exponential model in IgorPro® software.

8.2.9 Rheological study

The rheological experiments at oscillatory shear deformation of the gelatin hydrogels were carried out with AR2000 rheometer parallel plates of 14 mm diameter as described in Chapter 3 (3.9.15 Rheological experiments of hydrogels).

8.2.10 Scanning electron microscopy

Swollen gels were quickly frozen using liquid nitrogen and freeze-dried for 3-4 days. Surfaces of all the samples were coated with gold in a Quorum Q150T ES sputter coater for 10 min. Surface morphology of lyophilized non-cross linked and cross-linked hydrogels was studied by Hitachi S-800 scanning electron microscope at 500X magnifications.

8.3 Results and discussion

Cellulose nanowhiskers were oxidized in the presence of sodium periodate to yield the corresponding C_2/C_3 dialdehyde product and the carbonyl content was quantified by Cu^{2+} titration (Table 8.1). The increase in sodium periodate equivalents for the oxidative treatment of cellulose nanowhiskers resulted in a corresponding increase in carbonyl content, which was evident in the transmission mode FT-IR spectra, as shown in Fig. 8.1. The characteristic C=O stretching vibration band of the dialdehyde cellulose nanowhisker appeared at 1740 cm^{-1} and this spectral data confirms a gradual oxidation of nanowhiskers as the intensity of the carbonyl band increases with increased oxidant.

Table 8.1 Carbonyl content of oxidized cellulose nanowhiskers.

Samples	$NaIO_4$/CNWs (w/w)	Carbonyl content (mmols g^{-1})
CNWs	0.00	0.006
DAC1	0.10	0.060
DAC2	0.30	0.114
DAC3	0.50	0.150
DAC4	0.70	0.231

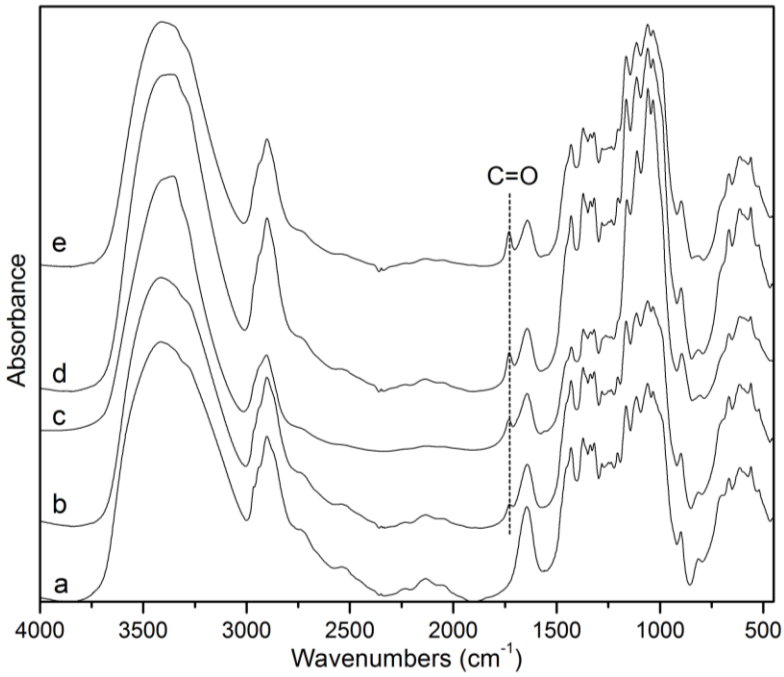

Fig. 8.1 FT-IR spectra of (a) nanowhiskers, (b) DAC1, (c) DAC2, (d) DAC3 and (e) DAC4.

Aqueous solutions of gelatin were then cross-linked with oxidized cellulose nanowhiskers containing varying amount of aldehydes to obtain the chemical hydrogels. It was observed that the hydrogels composed of only gelatin are transparent, whereas the cross-linked hydrogels are slightly yellowish in color and semi-transparent. As shown in FT-IR spectra (Fig. 8.2), the presence of cellulose nanowhisker in the cross-linked gel

can be evidenced from the appearance of nanowhisker bands in the region 3300-3500 cm^{-1} and 1000-1200 cm^{-1}. The cross-linking reaction occurs between the aldehyde group in nanowhiskers and the free ε-amino groups of the lysine and hydroxylysine residues present in gelatin as shown in Fig. 8.3. The coupling was favored by the disappearance of the carbonyl band of oxidized nanowhisker indicating the occurrence of chemical interaction between nanowhisker and gelatin.

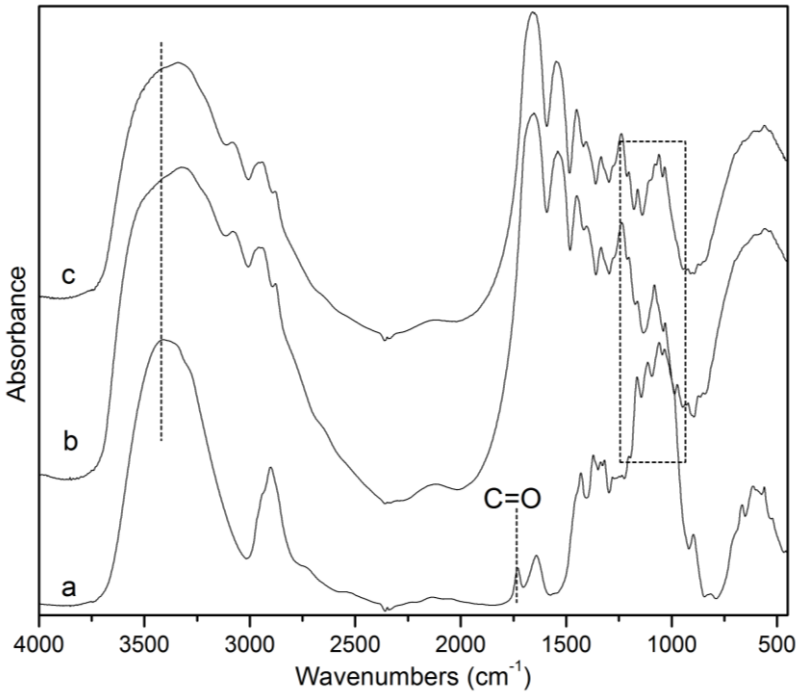

Fig. 8.2 FT-IR spectra of (a) DAC4, (b) gelatin and (c) cross-linked hydrogels.

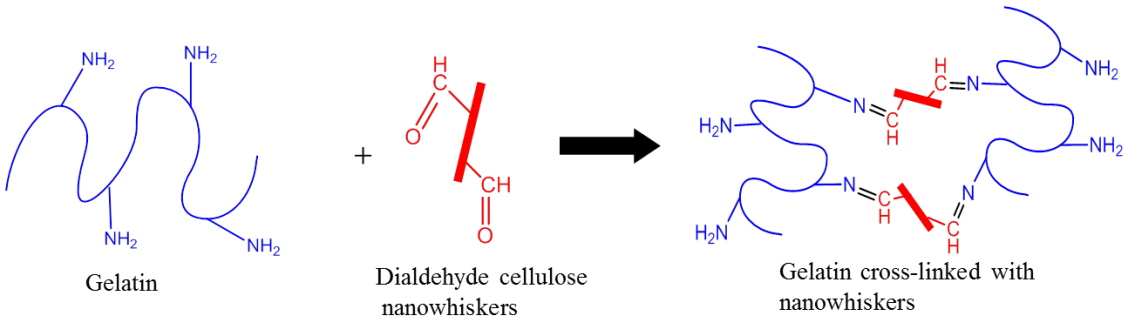

Fig. 8.3 Schematic representation of cross-linked hydrogels.

In order to determine the reaction efficiency between gelatin and dialdehyde cellulose nanowhiskers, the amount of the unreacted free amines in the chemically cross-linked samples was measured by spectrophotometrically following a Ninhydrin assay with the function of oxidized nanowhisker. The degree of cross-linking was calculated by comparing the absorbance of cross-linked samples with the control sample i.e. gelatin gels in the absence of oxidized nanowhiskers. The degree of cross-linking was found to increase from 0.14 to 17 % (Fig. 8.4) as a function of the oxidation level due to the presence of an increased amount of aldehyde groups to chemically react with the available free amine. The maximum theoretical degree of cross-linking was obtained by comparing with standard glycine samples and it was found to be 17%, which agrees with the experimental value.

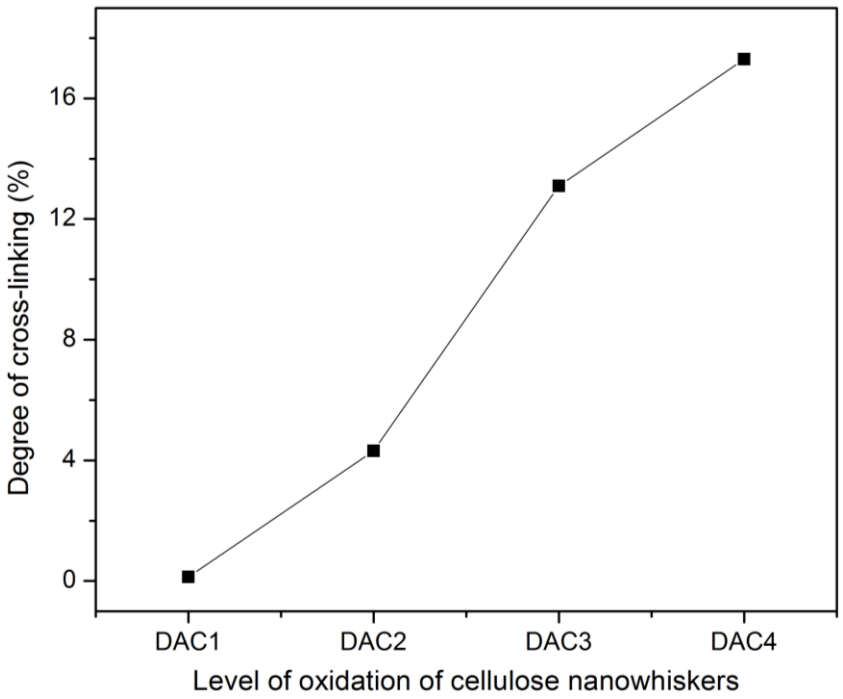

Fig. 8.4 Degree of cross-linking of hydrogels as a function of oxidized nanowhiskers.

^{1}H spin-spin relaxation (T_2) NMR experiments were carried out to analyze the effect of cross-linking on molecular mobility in an effort to further characterize gel properties. Since T_2 relaxation decay intensity is sensitive to local chain dynamics in the polymer/gel matrix, the T_2 relaxation behavior can be used to describe molecular motion, determining the relative amounts of rigid and mobile components within the hydrogel network before and after cross-linking.[299] In general, the faster the rate of T_2 relaxation the more rigid or fewer degrees of freedom the chemical group associated with that chemical shift has. In this experiment, T_2 data were collected using a Carr-Purcell-Meiboom-Gill (CPMG) sequence, which utilizes the application of a train of 180° pulses subsequent to the initial 90° excitation pulse, designed to eliminating the effects T_2 relaxation due to different chemical shift, J-coupling and magnetic field inhomogeneity

for materials that display increased diffusion without exhibiting isotopic.[300] Since typical Gaussian relaxation behavior is associated with rigid polymer systems and exponential behavior with more mobile structures, the T_2 relaxation behavior was analyzed using the two-component Gaussian-exponential model shown below (Eq. 1).[301]

$$I(t) = \%\,Ridge * \exp\left(\left[\frac{-t}{T_{2,Rigid}}\right]^2\right) + \%\,Mobile * \exp\left(\frac{-t}{T_{2,Mobile}}\right) + Offset \qquad \text{Eq. 1}$$

In utilizing this two component model, the Gaussian component should indicate the relative proportion of protons belonging to rigid repeat units in cross-linking junction points, while the exponential component should describe the amount of more mobile repeat units belonging to chains outside or between junctions of cross-linking points.

The ^{1}H MAS NMR spectra obtained for the cross-linked hydrogels composed of gelatin and dialdehyde cellulose nanowhiskers swollen in D_2O and spun at 2 kHz showed a series of fairly resolved peaks between ~4.75–0.8 ppm. The appearance of the pure gelatin is identical to that of the hydrogel with dialdehyde cellulose nanowhiskers (Appendix A Fig. A.1), which was expected based on a rough calculation showing ~90% of the total protons in the gelatin/cellulose nanowhisker system belong to gelatin. In addition, the spectrum of pure cellulose nanowhiskers displays a broad peak, due to crystalline nature of the cellulose and extremely fast T_2 relaxation, centered at ~3.50 ppm [299] manifesting as a minor background feature of the hydrogel spectrum.

Table 8.2 represents the resulting percent rigid and mobile proton in the cross-linked hydrogels based on the ^{1}H spectral integrations from ~4.75–0.8 ppm and defined by non-linear least squared fit of the T_2 relaxation model in Equation 1 (Appendix A Fig. A.2). The hydrogels composed of both gelatin and cellulose nanowhisker in general displays a relatively higher chain rigidity, greater relative number of cross-linking

junction points and a corresponding lower proportion of mobile protons. The consistent ~30-35% increase in rigid proton content is greater than the ~10% proton due to the addition of cellulose nanowhiskers which indicates the existence of chemical linkages between the gelatin matrix and nanowhisker and demonstrates this cross-linking affects the local molecular mobility of the chains. An average T_2 value of 4.4 ms and 21.0 ms was calculated for the rigid and mobile components respectively for all the hydrogels. We did expect the T_2 values to decrease when comparing the neat gelatin and gelatin/cellulose nanowhisker systems however the difference between T_2 values were statistically insignificant.

Table 8.2 Relative rigid and mobile component intensities based on a Gaussian-exponential model of the hydrogels determined by ^{1}H spin-spin relaxation (T_2) NMR experiments.

Degree of chemical cross-linking (%)	% Rigid	% Mobile
0	35	65
0.14	44	56
4.3	42	58
13	50	50
17	50	50

The swelling properties of the hydrogels prepared from the interaction of dialdehyde cellulose nanowhisker and gelatin were evaluated from their water uptake value. It was found that all the gels attained the equilibrium swelling in 2 days. As shown in Fig. 8.5, the equilibrium water content was decreased with the increase in the level of

oxidation of cellulose nanowhiskers, which is attributed to the increased degree of cross-linking. Similar behavior was also observed for gelatin gels cross-linked with glutaraldehyde and plant polyphenols, periodated alginate.[285, 302-303] The swelling behavior was further explained as a result of the formation of rigid network after cross-linking, observed by NMR experiments, which consequently has less ability to uptake water. Equilibrium fluid content was calculated to be decreased from 92.50 to 87.60 % with the increase in degree of cross-linking. The small difference in the water uptake value could be due to the presence of characteristic gelatin network resulting from gelatin-gelatin physical structuring in the cross-linked gels.

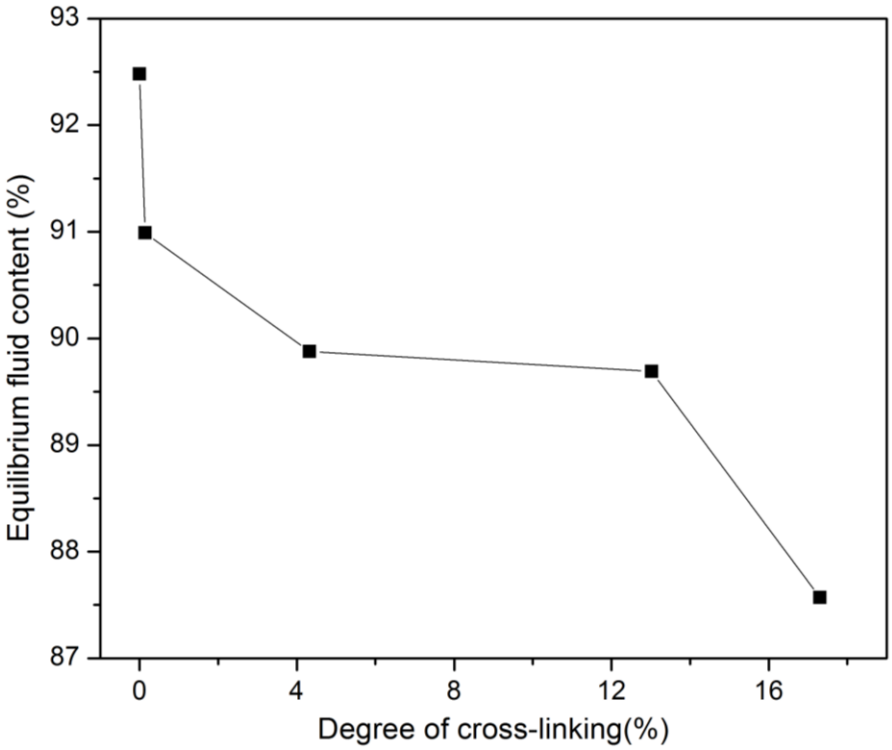

Fig. 8.5 Equilibrium fluid content of cross-linked hydrogels.

Hydrogel formation of gelatin below its melting temperature primarily involves the gelatin-gelatin physical interaction as a result of structuring of helical configuration.

However, hydrogel formation between gelatin and dialdehyde cellulose nanowhisker involves two different interactions; one is associated with the chemical cross-links between gelatin and oxidized nanowhisker and the second one is due to the formation of physical cross-links between the gelatin chains. Viscoelastic properties of the hydrogels were measured from the mechanical response of the samples as they are deformed under periodic strain.

The elastic modulus *G*' and the viscous (also imaginary or loss) modulus *G*" of the physically cross-linked gels at room temperature are presented in Fig. 8.6. It was found that G" component is considerably smaller than G' component, exhibiting the formation of an elastic network. However, there is a significant increase in storage modulus of chemically cross-linked hydrogels compared to the physical gel and the increase in degree of cross-linking led to an increase in storage modulus of the cross-linked gels as shown in Fig. 8.7, which is attributed to the influence of chemical interaction between gelatin and dialdehyde nanowhiskers. A tan δ =G"/G' plot is shown in Fig. 8.8 and tan δ value decreases with increase in cross-linking, reflecting the elastic behavior of the gels. It has to be noticed that when the degree of cross-linking was increased from 4-13%, there is a small increase in storage modulus, which could be due to a partial microphase separation of the hydrogels. Schacht et al. prepared hydrogels from gelatin and dextran dialdehyde (1:1 w/w) and the degree of oxidation of dextran dialdehye was varied from 5 to 20%.[304] They had shown that when the degree of oxidation was below 20%, the storage modulus of cross-linked gels were lower than the gelatin hydrogels. We find a huge increase (150%) in case of dialdehyde cellulose nanowhisker cross-linked hydrogels for ~4% degree of oxidation.

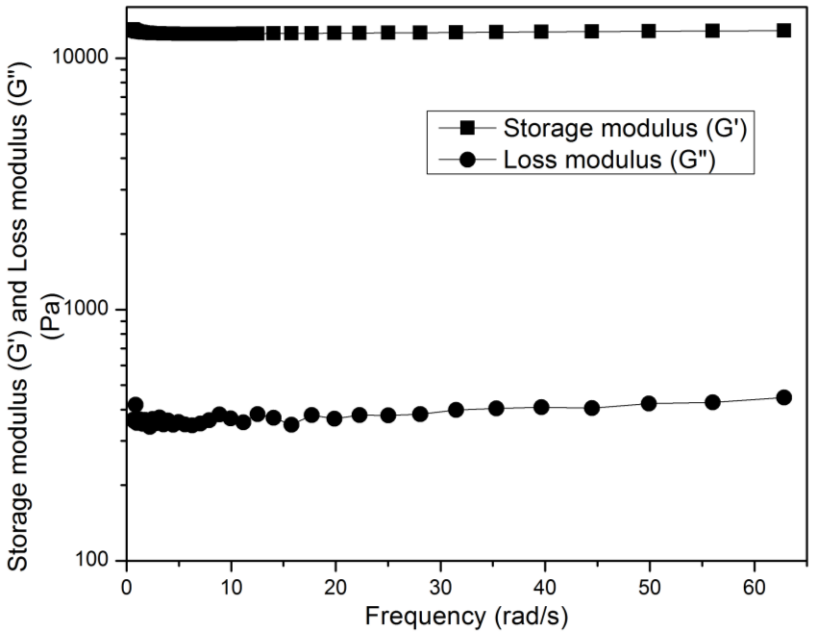

Fig. 8.6 Dynamic rheological observations of the gelatin gels.

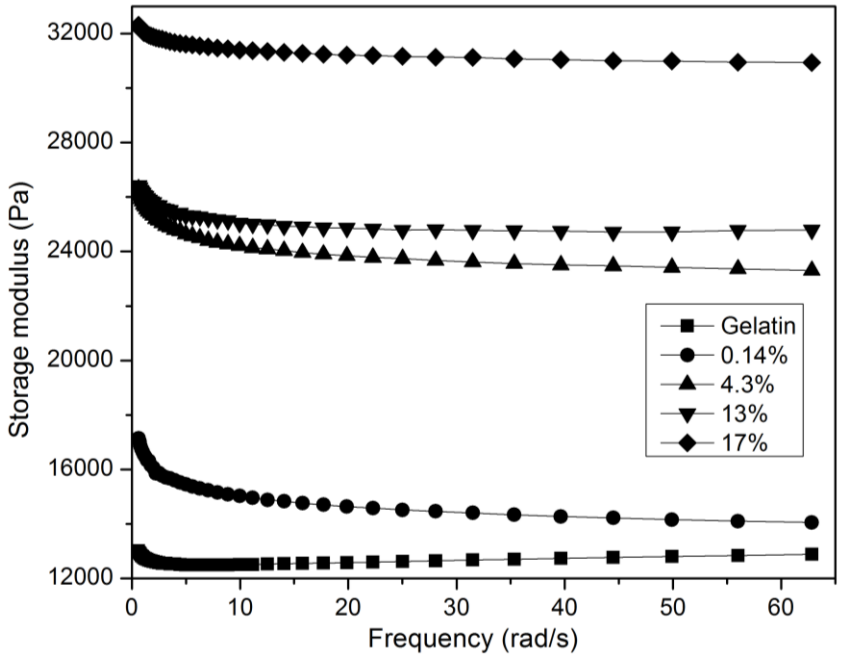

Fig. 8.7 Effect of chemical cross-linking on the storage modulus of the gelatin gels.

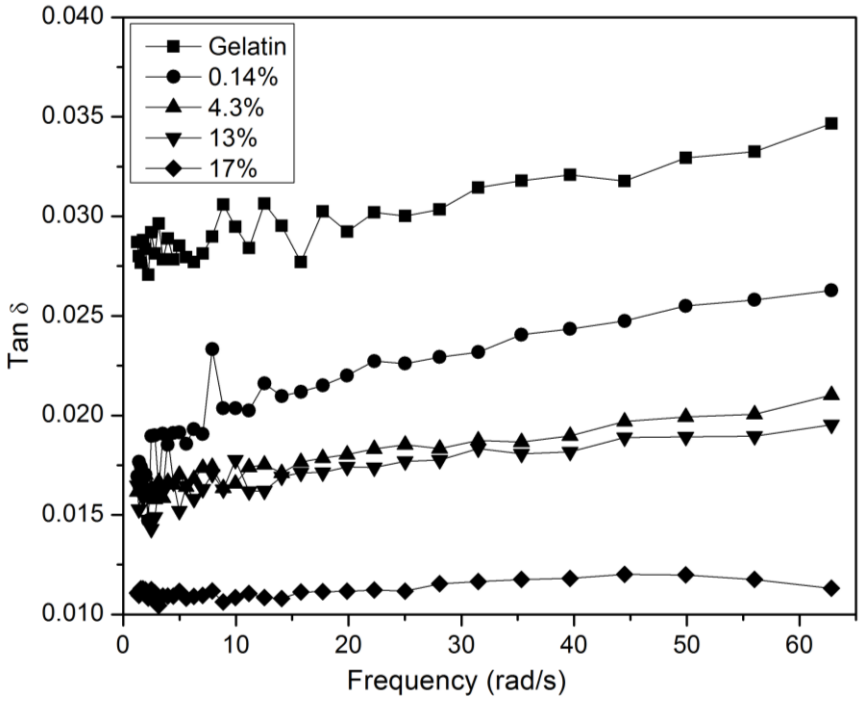

Fig. 8.8 tan δ plot of the cross-linked gelatin gels.

Thermal scanning experiments were performed from 27-50 ^{o}C in order to study and differentiate the contribution of physical and cross-linking below and above the melting point. As shown in Fig. 8.9, the storage modulus of gelatin gels decreases rapidly to very low values until the melting point (35 ^{o}C) indicating the breaking of the physical linkages in gelatin. However, above the melting point there is a rapid increase in G', which could be explained due to the melting of gelatin, subsequently affecting the area between the plates of the rheometer and this leads to a sharp increase in G' to above its initial value. At the same time the viscous or loss modulus (G") clearly increases with temperature, suggesting that the gel becomes more liquid like due to melting of gelatin.

Fig. 8.10 shows the effect of temperature on storage modulus of chemically cross-linked gels with the degree of cross-linking compared to gelatin gels. The initial decrease

in G’ value before the melting point is possibly due to the breaking of the physical attachments. It can be observed that there is a gradual improvement in the melting behavior and G’ of the hydrogels with the degree of cross-linking. For lower degree of cross-linking (0.14%) samples exhibited similar thermal behavior as gels prepared from gelatin, whereas for 4.3 and 13% cross-linked samples, the elastic modulus value stays higher than the gelatin samples even above the melting point of gelatin and they became stable until 45 ^{o}C, suggesting a significant contribution from chemical cross-linking. Samples with 17% degree of cross-linking were found to be stable until 50 ^{o}C with a high storage modulus due to the presence of more chemical bonds resulting from higher degree of cross-linking. The higher G’ value of chemical gels at below and above the melting temperature of gelatin indicates the existence of a stable elastic network at higher temperature because of the chemical cross-linking between gelatin and oxidized CNWs.

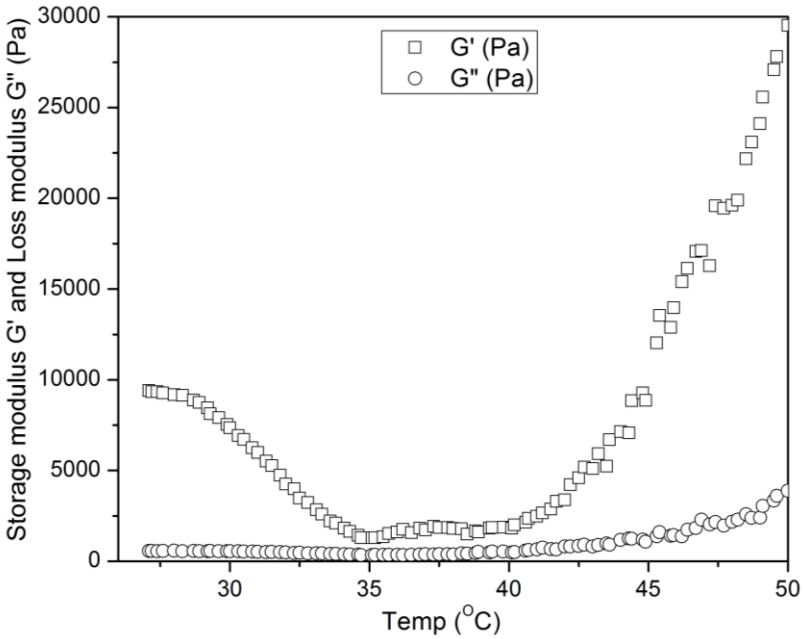

Fig. 8.9 Effect of temperature on dynamic rheological behavior of the physically cross-linked gelatin gels.

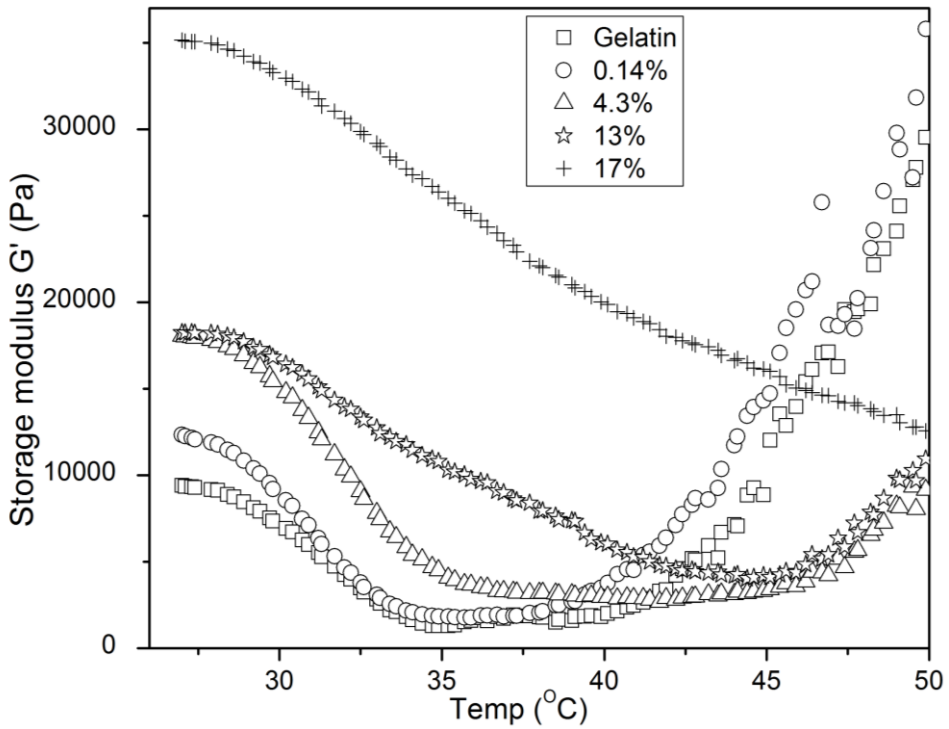

Fig. 8.10 Effect of temperature on storage modulus of chemically cross-linked gelatin gels.

The changes in morphology of gelatin hydrogels cross-linked by oxidized nanowhiskers were investigated through SEM images. In order to preserve better morphology, the swollen hydrogels were quickly frozen in liquid nitrogen and then freeze dried as reported in literature and this technique has been found to be very useful to reveal the interior morphology of the swollen hydrogels with minimal artifact.[285, 305] Fig. 8.11 shows the images of the transverse cross-sectional surfaces of the gels with different degree of cross-linking and pore structures are observed to be different depending on the degree of cross-linking. A relatively open network structures with interconnected pores of various size were observed for gelatin samples. However, cross-linking affected the openness of the network structure as the pore size of the cross-linked gels became smaller and more regular in shape than the control samples. For 17% cross-linking, the interior

appeared to be more compact with the smallest pore size. The gradual decrease in pore size and increase in compactness of the cross-linked gels is attributed to the effect of increased degree of cross-linking with additional support from our NMR experiments illustrating the formation of rigid structure after cross-linking. Similar findings were reported by Kim et al.[306] and Liao et al.[285] that the cross-linking offers more intermolecular association forming more number of junction points, which in turn affects the pore structure, size and its distribution.

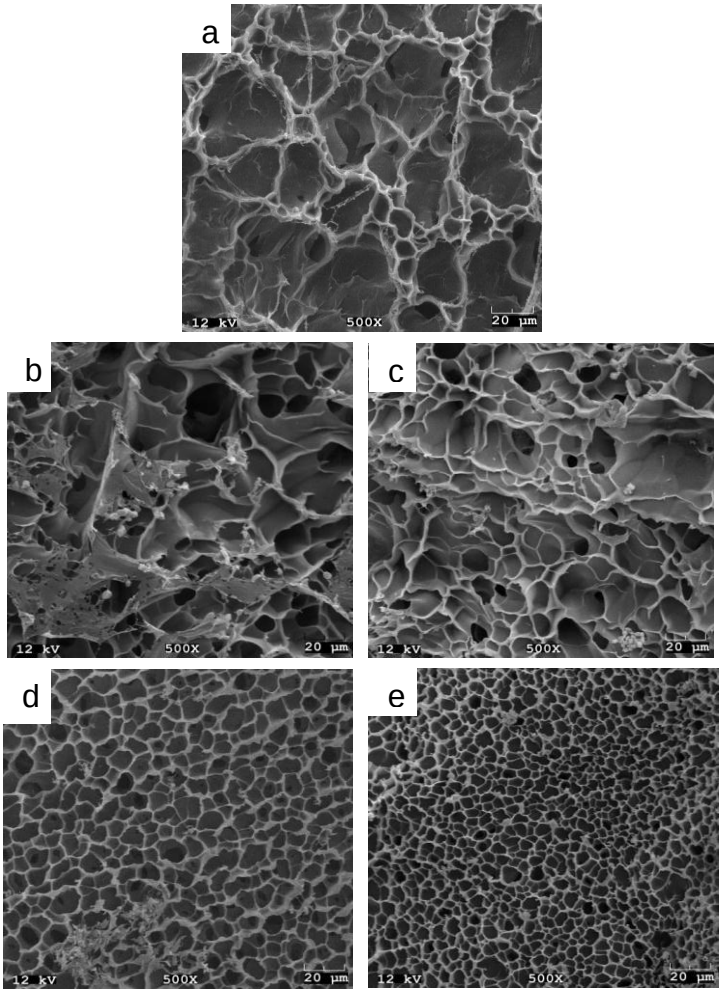

Fig. 8.11 Cross-sectional morphologies of (a) gelatin and (b) 0.14%, (c) 4.3%, (d) 13%, and (e) 17% cross-linked gels (scale bar 20 µm).

8.4 Conclusions

This work reports the first successful study on the synthesis and characterization of a renewable and biocompatible gelatin hydrogels chemically cross-linked by dialdehyde cellulose nanowhiskers containing varying amounts of aldehyde groups. We found an increased degree of chemical cross-linking (0.14-17%) between gelatin and nanowhiskers with the increased amount of aldehyde content (0.062-0.230 mmols/g). ^{1}H nuclear magnetic resonance (NMR) T_2 relaxation experiments on D_2O swollen hydrogels demonstrated that systems consisting of both gelatin and cellulose nanowhiskers displayed a higher percentage of "ridge" protons, attributed to increasing chemical cross-linking junction points between gelatin and nanowhiskers. This increase in hydrogel rigidity not only modified local chain dynamics but also influenced gel swelling, showing relatively reduced water uptake ability than that of the neat gelatin.

Rheological measurements confirmed an increasing trend in storage modulus with the degree of chemical cross-linking, showing an improvement of 150% in storage modulus (G') compared to neat gelatin. Chemical cross-linking also enhanced the resistance of the gels towards thermal degradation above the melting temperature of gelatin as observed by thermal scanning experiments and reduced the pore size of the hydrogels as evidenced by SEM micrographs. The improvement in mechanical and thermal properties of the gelatin hydrogels due to chemical cross-linking by cellulose nanowhiskers would broaden the biomedical applications of the gelatin hydrogels in wound dressing, tissue engineering and sustained release applications.

CHAPTER 9

Overall Conclusions

The primary goal of the thesis was to explore the versatility of cellulose, a renewable and inexhaustible resource of raw material by utilizing periodate oxidative fragmentation methodology. Chapter 4 of the thesis studied the synthesis of novel water soluble cellulose products employing periodate oxidation followed by sulfonation reaction. This study investigated the effect of increase in the level of oxidation/sulfonation reaction on the structure, morphology and water solubility of bleached hardwood Kraft pulp. It was found that carbonyl group content increased (0.12-0.28 mmols/g) with the periodate charge, which led to an increase in sulfonic acid content as determined by the conductometric titration. Solubility of sulfonated cellulose in water was determined from quantitative ^{1}H NMR spectra and a solubility of 28.57 g/L was obtained when cellulose was oxidized with 4.67 mmols of periodate per gram cellulose followed by the sulfonation reaction. Further, structural characterization was carried out by HSQC NMR indicating a mixture of both initial and sulfonated fiber as a result of the partial oxidation and sulfonation reaction. Periodate oxidation did not affect cellulose fiber morphology but upon sulfonation a significant change in surface morphology was observed, showing a complete destruction of fibrous structure as observed by SEM even at lower level of oxidation and sulfonation.

In Chapter 5, the same oxidation and sulfonation methodology was further applied to bead cellulose in order to prepare negatively charged beads. 2,3-disulfonated bead cellulose was synthesized with sulfonic acid content from 0.08 - 0.13 mmols per gram of

beads. The SEM images of the modified beads emphasized that during the chemical modification, gentle stirring is required to maintain the shape of the beads for specific applications. The oxidized/sulfonated beads were shown to aggregate in an aqueous solution when mixed with a cationic starch as observed by optical microscope due to the electrostatic interaction between negatively charged bead surface and positively charged starch, exhibiting their future applications to agglomerate cationically charged proteins, metals and biological molecules.

In Chapter 6, periodate oxidation was applied to cellulose nanowhiskers to prepare their novel derivatives. First of all, cellulose nanowhiskers were prepared by sulfuric acid hydrolysis of bleached softwood Kraft pulp with a dimension of 100-300 nm in length and 10-20 nm in width as measured by AFM. Chapter 6 investigated the grafting of model small chain amine compounds such as methyl and butyl amine onto the nanowhisker surfaces. Three different levels of oxidized nanowhisker samples with 0.062-0.141 mmol/g carbonyl groups were prepared following periodate oxidation. The oxidized samples were then reacted with methyl and butyl amines through Schiff's base condensation reaction followed by sodium borohydride reduction of the resulting imines to obtain their amine derivatives. Aminated derivatives of cellulose nanowhiskers were fully characterized by FT-IR, NMR, XPS, AFM as well as by titrimetric analysis.

This study showed that an excess (1:20) of amine compounds are required to convert all the carbonyl groups of dialdehyde cellulose nanowhisker to the amine product. Presence of non-polar alkyl chains modified nanowhisker surfaces resulted into slightly hydrophobic to obtain a partially soluble product in DMSO, which was easily characterized by ^{13}C NMR. The chemical modification was additionally supported from

XPS data due to the presence of surface nitrogen (~2%), and also from FT-IR and copper titration results. AFM study showed no change in surface morphology of nanowhiskers after grafting with the amines. It was observed from CP-MAS NMR that the crystallinity of cellulose nanowhisker was also maintained, possibly due to the incorporation small chain molecules.

Based on the preliminary study on grafting of amines to nanowhiskers, the next study (Chapter 7) reported the successful synthesis of a drug delivery system from cellulose nanowhiskers. The oxidation and reductive amination mechanism from the previous study was followed to attach a spacer molecule (i.e gamma aminobutyric acid onto cellulose nanowhiskers, considering its biocompatibility and ease of availability). In order to obtain a controlled release of the drug molecule, they were further reacted with a releasable linker (i.e. syringyl alcohol through an esterification reaction). All the reactions were carried out in aqueous media and the successful grafting of the spacer and linker molecule was evidenced by various characterization techniques. FT-IR and NMR spectra confirmed the functional and structural changes in cellulose nanowhiskers after the series of chemical modifications. Single diffusion coefficient value from 2D DOSY experiments confirmed the effective covalent bonding of both the spacer and linker molecule to nanowhiskers. TEM micrographs showed that the size and shape of the nanowhiskers was retained after attaching spacer and linker molecules.

The last study (Chapter 8) investigated the utilization of periodate oxidized cellulose nanowhiskers as cross-linker moieties to stabilize gelatin protein chains. Aqueous solution of gelatin was cross-linked with 10 wt. % oxidized cellulose nanowhiskers containing 0.060-0.231 mmols/g of aldehyde groups through Schiff's base

condensation reaction. It was observed that the increase in carbonyl content increased the degree of chemical cross-linking between gelatin and nanowhisker as the degree of cross-linking was increased from 0.14-17%. ^{1}H spin-spin relaxation (T_2) NMR experiments were carried out to analyze the effect of cross-linking on molecular mobility, showing a relatively higher chain rigidity corresponding to greater relative number of cross-linking junction points in chemically cross-linked gels compared to physical gels. Equilibrium fluid content was found to be decreased from 92.50 to 87.60 % with the increase in degree of cross-linking. Rheological study showed a significant improvement in storage modulus of chemical gels by 150% as a result of chemical cross-linking. Finally, chemical cross-linking increased the thermal stability of the gels above the melting point of gelatin as the gels did not degrade until 50 ^{o}C.

In conclusion, periodate oxidation method was extensively utilized to oxidize cellulose fibers, bead cellulose and cellulose nanowhiskers to their corresponding dialdehyde derivatives. Further reactivity towards sulfonation and amination reaction led to the successful synthesis of a wide range of novel cellulose based materials, increasing the versatility of cellulose to significantly contribute towards a sustainable future.

CHAPTER 10

RECOMMENDATIONS FOR FUTURE WORK

Several studies might be conducted to further extend the application of the developed novel materials from cellulose through periodate oxidative fragmentation approach in this thesis. Some particularly attractive options are as follows:

- Periodate oxidation and sulfonation of cellulose fibers led to the synthesis of a novel water soluble derivative of cellulose. However, a higher degree of substitution is worth studying to improve the solubility of cellulose followed by the investigation of its solution property for many commercial applications.
- Recently, cellulose nanowhiskers have attracted the attention as "green" nanofiller in bionanocomposites because of their superior mechanical properties, high aspect ratio, low density, biocompatibility, high strength, and crystallinity. However, a major limitation for efficient utilization of nanowhisker lies in poor dispersion with non-polar solvents/matrix. To overcome this challenge, periodate oxidation and reductive amination could be a facile and promising path to transform polar reactive hydroxyl groups into non-polar moieties for various structural applications.
- The development of drug delivery system can be further explored by attaching amine containing drugs followed by their release

study in phosphate buffer saline (PBS) solution. Additionally, a various range of release rates can be obtained by customizing and designing the ortho side groups of the aromatic syringyl linker.

APPENDIX A

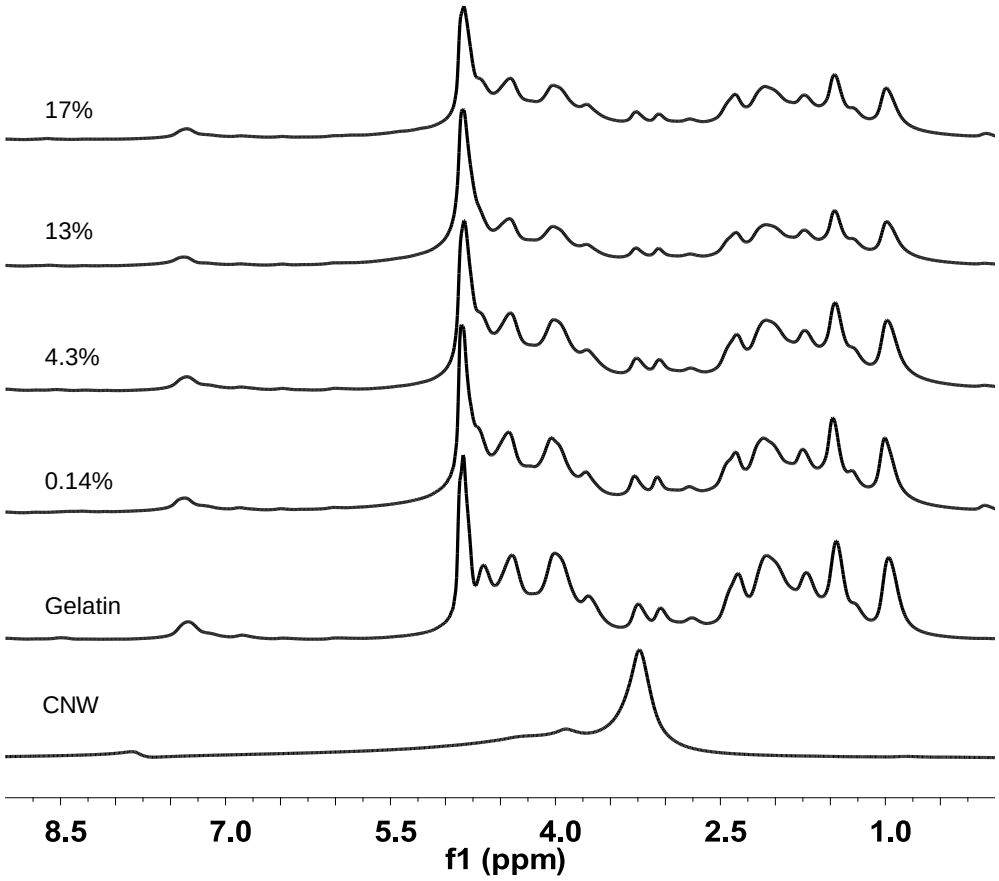

Fig. A.1 ^{1}H MAS 2 kHz spectra of hydrogels with different degrees of cross-linking swollen in D_2O at room temperature.

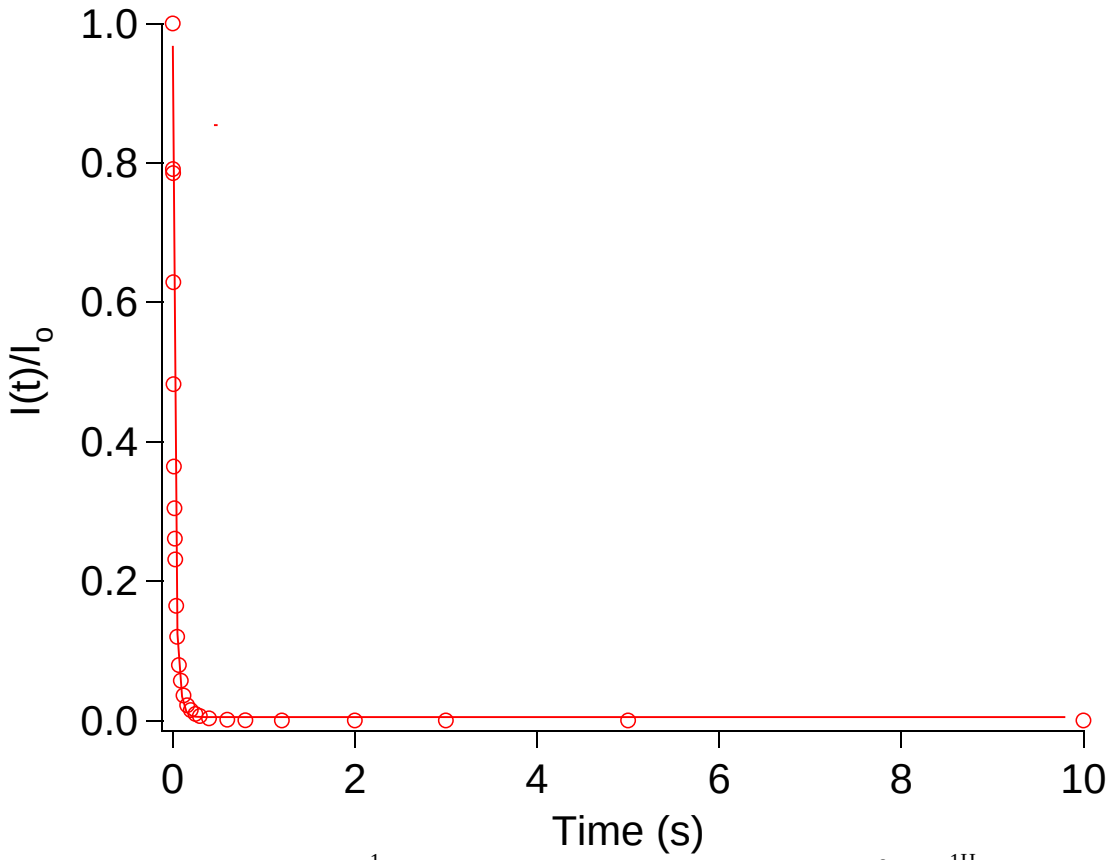

Fig. A. 2 A representative ^{1}H spin-spin relaxation plot resulting from ^{1H} MAS 2 kHz spectra of cross-linked hydrogel (17% degrees of cross-linking) swollen in D_2O at room temperature integrated from ~4.75–0.8 ppm. (Circles) T_2 attenuation data points (solid line) two-component Gaussian-exponential fit.

APPENDIX B

B. CELLULOSE NANOWHISKER FOAMS BY FREEZE CASTING[6]

B.1 Introduction

Fabrication of materials with homogeneous and well defined architectures has received increasing research interest owing to their broad applications such as tissue engineering, delivery matrices, green packaging, nanocomposites, and automotive industry.[307-310] Several methods including spin coating, layer-by-layer, freeze casting, and eutectic growth in two phase system has been utilized to organize micron/nano size particles to obtain ordered structures. Among the different techniques used, freeze casting has been shown as a versatile, easily implemented, and promising technique to build structures such as scaffolds, porous nanocomposites, and microwire networks with well aligned and controlled porosity.[311-313]

Freeze casting technique involves freezing a liquid suspension and sublimation of the solvent there after under reduced pressure. During the freezing process, the suspended particles are organized by rejection from the growing ice crystal front to the intervening space, which results in an ordered structure after sublimation. Fabrication of various materials by this technique suggests that the underlying principle of freeze casting is strongly dependent on simple physics of ice crystals and the physical interaction between the growing solidification front and the inert particles of the slurry.[314-316] Depending on

---

[6] This manuscript was accepted for publication in Carbohydrate Polymers, 2012. It is entitled as "CelluloseNanowhisker Foams by Freezing Casting". The other authors are Yang Li and Arthur J. Ragauskas from the Institute of Paper Science and Technology and School of Chemistry and Biochemistry at Georgia Institute of Technology.

the choice of solvent, slurry formulation, and solidification conditions, the final porosity and pore morphologies can be readily tuned. However, the solidification conditions remain as the key factor since all the features of porosity are created during this stage and thereby, controlling the formation and growth of ice crystals would yield materials with specific microstructure. For instance, in case of unidirectional freezing, a porous structure with unidirectional channel is obtained. In fact, this approach has been utilized to prepare variety of ceramic structures such as silica fiber bundles, tubular supports with radially aligned pores, micro-honeyecombs as well as polymeric scaffolds.[317-319]

Cellulose nanowhiskers, derived sustainably from biomass represent a relatively new raw material that has gained significant attention due to their intrinsically appealing physical, chemical as well as mechanical properties.[43, 83, 102, 320] Cellulose nanowhiskers designate a class of rod like nanoparticles which are mainly prepared by controlled acid hydrolysis of native cellulose fibers. The size and properties of nanowhiskers depend on the source and hydrolysis conditions of cellulose fibers and typically are 5-10 nm in width and 100-300 nm in length for wood-based nanowhiskers.[31, 41] A number of non-periodic highly porous structures known as aerogels from micro and nano cellulose fibers as well as cellulose derivatives has been reported in literature and they are commonly prepared by solvent exchange of a wet gel followed by supercritical CO_2 drying.[320-323] However, porous structures with regular pattern can be obtained by controlling the freezing temperature of the slurry followed by subsequent freeze drying.

Recently, Deng et al.[324] reported the preparation of layered cellulose foams through directional freezing technique emphasizing the effect of fiber concentration and freezing temperature on the microstructure and mechanical properties of microfibril

foams. They have also measured the compressive strength of cellulose nanowhisker foams but a detailed examination on their microstructure is lacking. Utilizing the facile freeze casting technique, we attempt to fabricate aligned porous cellulose nanowhisker structures and investigate the relationship between the freezing conditions and the microstructures obtained, which has not been reported so far. We expect that ice growth strategy of freeze casting technique will allow the fabrication of well ordered cellulose nanowhisker structures, opening their use as a template for layered composites, filters, and storage material.

B.2 Experimental

B.2.1 Materials

A fully bleached commercial softwood Kraft pulp was used as a source for cellulose nanowhiskers preparation. Polyvinyl alcohol (PVA) was purchased from VWR International (M_w: 15000, Degree of hydrolysis: 87-89%).

B.2.2. Preparation of H_2SO_4-hydrolyzed cellulose nanowhiskers

The cellulose nanowhiskers were prepared by sulfuric acid hydrolysis of a bleached softwood pulp based on a literature procedure.[31] In brief, 60.00 g (oven dried weight) of the pulp was mixed with H_2SO_4 solution (64%, w/w, 1:10 g mL^{-1}) with continuous stirring at 45 ^{o}C for 45 min. The hydrolysis reaction was halted by adding excess (10-fold) of distilled water followed by the removal of acidic solution through successive centrifugation at 12,000 rpm for 10 min until the supernatant became turbid. The sediment was collected and dialyzed (MWCO: 12-14,000) against tap water until the

solution pH did not change anymore. After dialysis, the content was sonicated for 10 min and centrifuged for 5 min at 10,000 rpm. The cloudy supernatant, containing nanowhiskers, was collected and the remaining sediment was again mixed with distilled water, sonicated, and centrifuged to obtain additional nanowhisker; this step was repeated till the supernatant was clear.

B.2.3. Preparation of porous samples

Porous cellulose nanowhisker samples were prepared by freezing a suspension of nanowhiskers and polyvinyl alcohol under different freezing conditions and then drying under vacuum. Cellulose nanowhisker suspension (10mL, 2 wt %) was mixed with different amounts of PVA (20% and 50%, w/w) and slowly stirred at room temperature for 4 h in order to avoid the generation of bubbles. Then, the mixture was poured in to small glass vials and freezed by two methods: (i) dipping in liquid nitrogen (ii) placing these vials in two different freezers for 2 h, where the cooling rates were measured to be 4.5 and 13 ^{o}C min^{-1}, respectively. Frozen solids were subsequently dried in a freeze dryer for 24 h to sublimate the water under vacuum. Control samples were prepared in absence of PVA.

B.2.4 Characterization

Surface morphology of the porous samples was studied by JEOL-1530 thermally-assisted field emission (TFE) scanning electron microscope (SEM). Before acquiring images, the surfaces of all the samples were coated with gold in a sputter coater.

B.3 Results and discussion

Cellulose nanowhisker suspension was mixed with PVA and solidification of the slurry was carried out by two ways: (i) quenching the slurry in liquid nitrogen (ii) freezing the slurry at two different cooling rates, i.e., 13 ^{o}C min^{-1} and 4.5 ^{o}C min^{-1}. Freeze drying of the solvent created the final nanowhisker porous structure as a replica of ice crystals that generated during freezing. PVA was used as a binder due to its solubility in water and its compatibility with cellulose nanowhiskers.[325] Cellulose whisker concentration (2.0 wt. %) was chosen as an attempt to be in semi-dilute concentration range especially to obtain a template for potential multilayered nano-composite applications.

It was observed that irrespective of the cooling rate, when compared to the samples in PVA, the samples prepared in absence of PVA (Fig. B.1a) collapsed during the sublimation process resulting in a structure with no particular alignment of the pores created. It suggests that PVA acts as a support to the nanowhiskers, which could be due to the hydrogen bonding between PVA and nanowhiksers, facilitating the formation of a stable oriented porous architecture. The influence of PVA content on the microstructure of the nanowhisker materials prepared was also studied. The images of the samples freezed at 13 ^{o}C min^{-1} cooling rate are shown here (Fig. B.1). At 20 wt. % PVA content, the samples exhibited a well oriented porous structure with equally spaced lamellar walls (Fig. B.1b), while at 50 wt. % of PVA, a dense structure with some locally aligned pores were found (Fig. B.1c) instead of the long range order lamellar walls. The possible physical interactions among nanowhiskers and between nanowhiskers and the growing solidification fronts during the freezing leads to different growth mechanisms, which

could be the reason for the loss in alignment at high slurry concentrations. Similar phenomenon was also observed for samples prepared at 4.5 ^{o} C min^{-1} cooling rate, however, for samples freezed in liquid nitrogen, the effect of PVA concentration on the alignment of pores and its morphology was found to be insignificant.

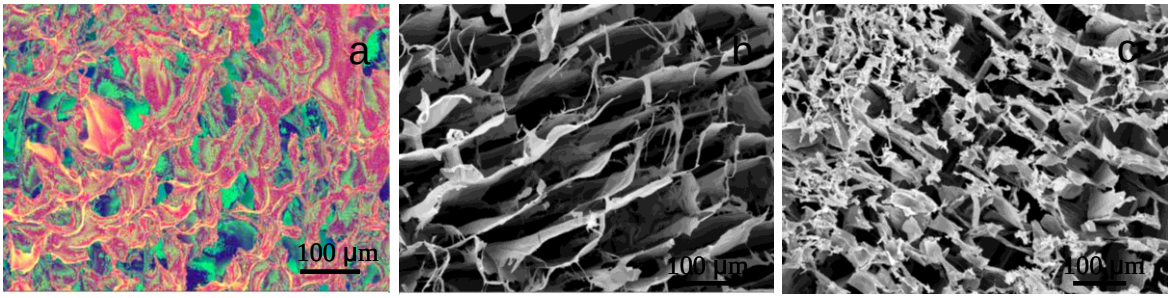

Fig. B.1 Morphology of cellulose nanowhisker samples freezed at 13 ^{o} C min^{-1} cooling rate (a) 0 wt. %, (b) 20 wt. % and (c) 50 wt. % of PVA.

An overview of the porous cellulose nanowhisker material and its microstructure is shown in Fig. B.2a. The bottom part of the microstructure can be characterized as a dense cellular structure with some randomly distributed pores whereas the upper part exhibits an oriented and highly porous structure. It implies that after growth initiation step at the bottom, the ice crystals started growing regularly in a vertical direction leaving behind open pore channels after sublimation. Eventually, the growth was terminated at the top of the suspension and formed a surface which has a different microstructure (Fig. B.2c) as compared to the outer side of the sample, where open, uniform, and oriented pores were observed as shown in Fig. B.2b. Based on the detailed microstructural observation of the sample a schematic diagram is shown in Fig. B.2d simply indicating the growth pattern of ice crystals.

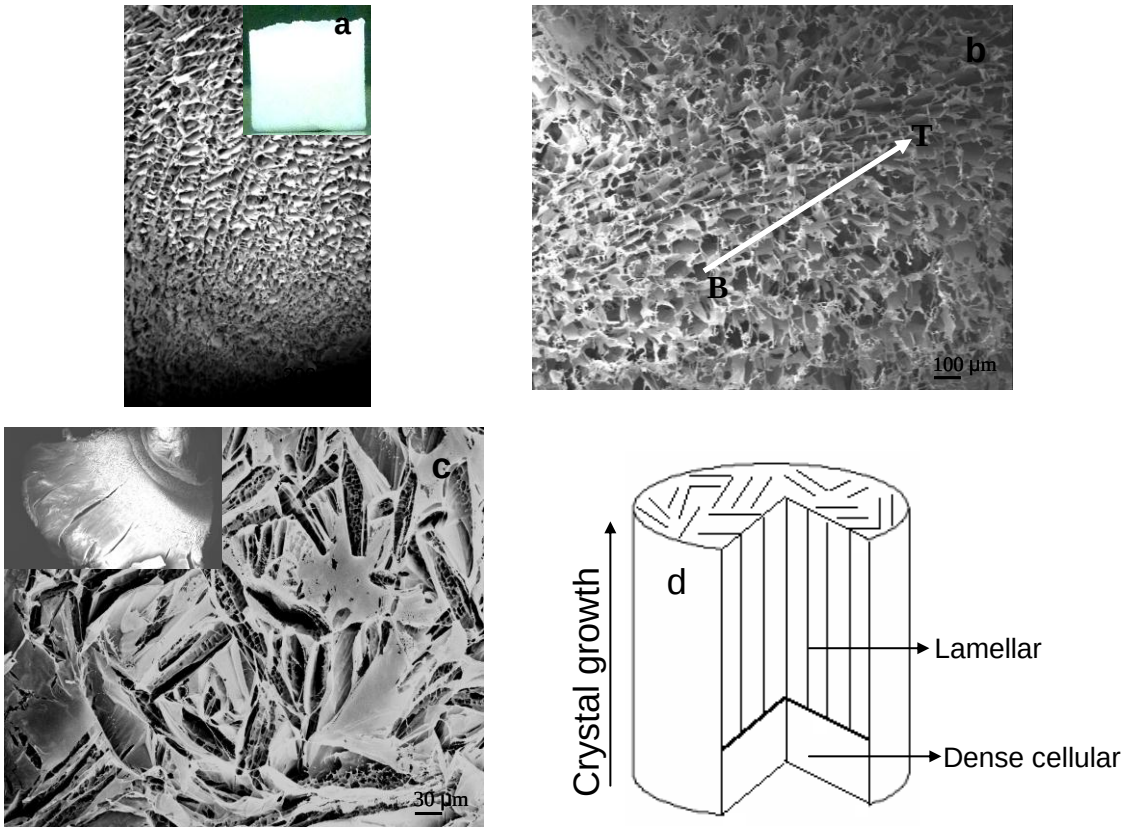

Fig. B.2 (a) Overview of the sample and its microstructure. (b) side (B: bottom and T:Top of the sample) and (c) top view of the porous nanowhisker structure and (d) schematic diagram showing the growth pattern of ice crystals.

Studies on various materials including ceramic and metallic particles reveal that solidification has a critical role in determining the final pore morphology and microstructure of the porous materials.[326-327] Our results are well consistent with literature results as the pore size of the resulted cellulose nanowhisker structure and the pore orientation were both affected by the cooling rate. It was observed that freezing the slurry in liquid nitrogen created a fine and perfectly aligned lamellar structure in the vertical direction with a small pore size of 10-20 µm. The lamellae walls are thinner and inter

lamellae spaces are smaller at this fast freezing condition (Fig. B.3a), whereas a decrease in cooling rate gradually increased the pore size (~100 μm) and lamellae thickness as observed in Fig. B.3b and 3c. Similar behavior was also found in other polymeric and ceramics materials; as faster the freezing rate, finer the resulting structure, on the other hand slow cooling noticeably scaled up the microstructure.[312]

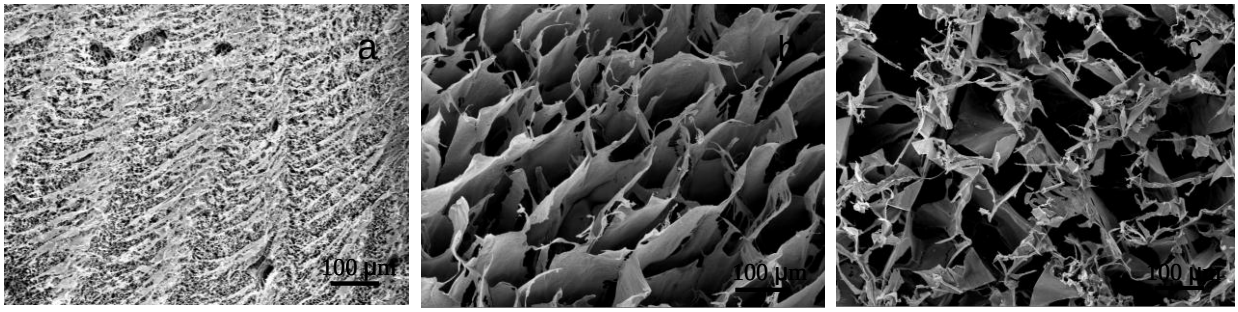

Fig. B.3 Effect of cooling rate on the pore structure of 20 wt. % PVA samples (a) Liquid nitrogen, (b) 13 ^{o}C min^{-1} and (c) 4.5 ^{o}C min^{-1}.

In each case, the cellulose nanowhiskers and PVA slurries were frozen at a constant cooling rate starting from room temperature. As a consequence, the subsequent drying process resulted in a lamellar porous microstructure with long range order (Fig. B.4). This is a typical phenomenon observed under steady state freezing conditions as well as in cases where water is being used as a solvent. The mechanism of lamellar structure formation can be well understood through the basic physics of water freezing which has been already explained in literature.[312, 326] Moreover, the lamellar surface exhibits two different types of surface dendrites. The first type of dendrite grows in between the lamellae whereas the second type corresponds to a fine tortuous morphology protruding from the top of the lamellae. The relative size of these dendrites depends not

only on different freezing conditions applied to the suspension but also on the concentration of the solution. For instance, faster cooling rates with liquid nitrogen leads to finer and smaller dendrites while the dendrite size increases in case of slow cooling or with a more concentrated solution. The formation of the dendritic feature was also observed in porous ceramic structures and it was proposed to be influenced by a number of factors such as nature of the solvent, freezing conditions, and the characteristics of starting powder.[328-329]

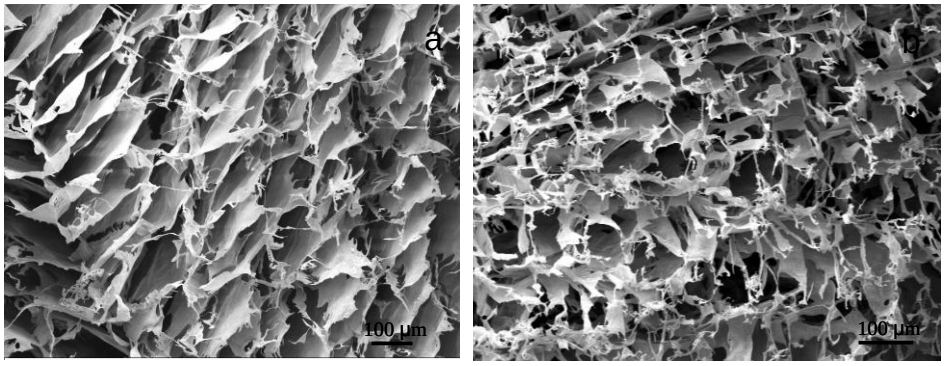

Fig. B.4 Microstructure showing (a) lamellar walls and (b) surface dendrites.

B.4 Conclusions

In conclusion, our results illustrate a simple approach to produce long range ordered porous cellulose nanowhisker structure with PVA as a support material. The resultant microstructure and pore morphology can be controlled by modifying the freezing rate and the slurry concentration. Finally, considering their lamellar and interconnected pore structure combined with the renewable nature of cellulose, ordered cellulose nanowhisker based materials with designed orientation of pore channels can be prepared through precise control of thermal gradients, which has potential applications

especially as a template for layered composites, molecular filtration, delivery matrix, and tissue engineering scaffold.

APPENDIX C

COPYRIGHT PERMISSIONS

ELSEVIER LICENSE
TERMS AND CONDITIONS

Jul 25, 2012

This is a License Agreement between Rajalaxmi Dash ("You") and Elsevier ("Elsevier") provided by Copyright Clearance Center ("CCC"). The license consists of your order details, the terms and conditions provided by Elsevier, and the payment terms and conditions.

All payments must be made in full to CCC. For payment instructions, please see information listed at the bottom of this form.

Supplier	Elsevier Limited The Boulevard,Langford Lane Kidlington,Oxford,OX5 1GB,UK
Registered Company Number	1982084
Customer name	Rajalaxmi Dash
Customer address	1012 Center St. NW Atlanta, GA 30318
License number	2956200671468
License date	Jul 25, 2012
Licensed content publisher	Elsevier
Licensed content publication	Colloids and Surfaces A: Physicochemical and Engineering Aspects
Licensed content title	Flow properties of microcrystalline cellulose suspension prepared by acid treatment of native cellulose
Licensed content author	Jun Araki,Masahisa Wada,Shigenori Kuga,Takeshi Okano
Licensed content date	30 November 1998
Licensed content volume number	142
Licensed content issue number	1
Number of pages	8
Start Page	75
End Page	82
Type of Use	reuse in a thesis/dissertation
Portion	figures/tables/illustrations
Number of figures/tables/illustrations	1

Format	electronic
Are you the author of this Elsevier article?	No
Will you be translating?	No
Order reference number	
Title of your thesis/dissertation	Synthesis and characterization of novel cellulosics
Expected completion date	Aug 2012
Estimated size (number of pages)	200
Elsevier VAT number	GB 494 6272 12
Permissions price	0.00 USD
VAT/Local Sales Tax	0.0 USD / 0.0 GBP
Total	0.00 USD
Terms and Conditions	

INTRODUCTION

1. The publisher for this copyrighted material is Elsevier. By clicking "accept" in connection with completing this licensing transaction, you agree that the following terms and conditions apply to this transaction (along with the Billing and Payment terms and conditions established by Copyright Clearance Center, Inc. ("CCC"), at the time that you opened your Rightslink account and that are available at any time at http://myaccount.copyright.com).

GENERAL TERMS

2. Elsevier hereby grants you permission to reproduce the aforementioned material subject to the terms and conditions indicated.

3. Acknowledgement: If any part of the material to be used (for example, figures) has appeared in our publication with credit or acknowledgement to another source, permission must also be sought from that source. If such permission is not obtained then that material may not be included in your publication/copies. Suitable acknowledgement to the source must be made, either as a footnote or in a reference list at the end of your publication, as follows:

"Reprinted from Publication title, Vol /edition number, Author(s), Title of article / title of chapter, Pages No., Copyright (Year), with permission from Elsevier [OR APPLICABLE SOCIETY COPYRIGHT OWNER]." Also Lancet special credit - "Reprinted from The Lancet, Vol. number, Author(s), Title of article, Pages No., Copyright (Year), with permission from Elsevier."

4. Reproduction of this material is confined to the purpose and/or media for which

permission is hereby given.

5. Altering/Modifying Material: Not Permitted. However figures and illustrations may be altered/adapted minimally to serve your work. Any other abbreviations, additions, deletions and/or any other alterations shall be made only with prior written authorization of Elsevier Ltd. (Please contact Elsevier at permissions@elsevier.com)

6. If the permission fee for the requested use of our material is waived in this instance, please be advised that your future requests for Elsevier materials may attract a fee.

7. Reservation of Rights: Publisher reserves all rights not specifically granted in the combination of (i) the license details provided by you and accepted in the course of this licensing transaction, (ii) these terms and conditions and (iii) CCC's Billing and Payment terms and conditions.

8. License Contingent Upon Payment: While you may exercise the rights licensed immediately upon issuance of the license at the end of the licensing process for the transaction, provided that you have disclosed complete and accurate details of your proposed use, no license is finally effective unless and until full payment is received from you (either by publisher or by CCC) as provided in CCC's Billing and Payment terms and conditions. If full payment is not received on a timely basis, then any license preliminarily granted shall be deemed automatically revoked and shall be void as if never granted. Further, in the event that you breach any of these terms and conditions or any of CCC's Billing and Payment terms and conditions, the license is automatically revoked and shall be void as if never granted. Use of materials as described in a revoked license, as well as any use of the materials beyond the scope of an unrevoked license, may constitute copyright infringement and publisher reserves the right to take any and all action to protect its copyright in the materials.

9. Warranties: Publisher makes no representations or warranties with respect to the licensed material.

10. Indemnity: You hereby indemnify and agree to hold harmless publisher and CCC, and their respective officers, directors, employees and agents, from and against any and all claims arising out of your use of the licensed material other than as specifically authorized pursuant to this license.

11. No Transfer of License: This license is personal to you and may not be sublicensed, assigned, or transferred by you to any other person without publisher's written permission.

12. No Amendment Except in Writing: This license may not be amended except in a writing signed by both parties (or, in the case of publisher, by CCC on publisher's behalf).

13. Objection to Contrary Terms: Publisher hereby objects to any terms contained in any purchase order, acknowledgment, check endorsement or other writing prepared by you, which terms are inconsistent with these terms and conditions or CCC's Billing and

Payment terms and conditions. These terms and conditions, together with CCC's Billing and Payment terms and conditions (which are incorporated herein), comprise the entire agreement between you and publisher (and CCC) concerning this licensing transaction. In the event of any conflict between your obligations established by these terms and conditions and those established by CCC's Billing and Payment terms and conditions, these terms and conditions shall control.

14. Revocation: Elsevier or Copyright Clearance Center may deny the permissions described in this License at their sole discretion, for any reason or no reason, with a full refund payable to you. Notice of such denial will be made using the contact information provided by you. Failure to receive such notice will not alter or invalidate the denial. In no event will Elsevier or Copyright Clearance Center be responsible or liable for any costs, expenses or damage incurred by you as a result of a denial of your permission request, other than a refund of the amount(s) paid by you to Elsevier and/or Copyright Clearance Center for denied permissions.

LIMITED LICENSE

The following terms and conditions apply only to specific license types:

15. **Translation**: This permission is granted for non-exclusive world **English** rights only unless your license was granted for translation rights. If you licensed translation rights you may only translate this content into the languages you requested. A professional translator must perform all translations and reproduce the content word for word preserving the integrity of the article. If this license is to re-use 1 or 2 figures then permission is granted for non-exclusive world rights in all languages.

16. **Website**: The following terms and conditions apply to electronic reserve and author websites:
Electronic reserve: If licensed material is to be posted to website, the web site is to be password-protected and made available only to bona fide students registered on a relevant course if:
This license was made in connection with a course,
This permission is granted for 1 year only. You may obtain a license for future website posting,
All content posted to the web site must maintain the copyright information line on the bottom of each image,
A hyper-text must be included to the Homepage of the journal from which you are licensing at http://www.sciencedirect.com/science/journal/xxxxx or the Elsevier homepage for books at http://www.elsevier.com , and
Central Storage: This license does not include permission for a scanned version of the material to be stored in a central repository such as that provided by Heron/XanEdu.

17. **Author website** for journals with the following additional clauses:

All content posted to the web site must maintain the copyright information line on the

bottom of each image, and the permission granted is limited to the personal version of your paper. You are not allowed to download and post the published electronic version of your article (whether PDF or HTML, proof or final version), nor may you scan the printed edition to create an electronic version. A hyper-text must be included to the Homepage of the journal from which you are licensing at http://www.sciencedirect.com/science/journal/xxxxx . As part of our normal production process, you will receive an e-mail notice when your article appears on Elsevier's online service ScienceDirect (www.sciencedirect.com). That e-mail will include the article's Digital Object Identifier (DOI). This number provides the electronic link to the published article and should be included in the posting of your personal version. We ask that you wait until you receive this e-mail and have the DOI to do any posting.

Central Storage: This license does not include permission for a scanned version of the material to be stored in a central repository such as that provided by Heron/XanEdu.

18. **Author website** for books with the following additional clauses:
Authors are permitted to place a brief summary of their work online only.
A hyper-text must be included to the Elsevier homepage at http://www.elsevier.com . All content posted to the web site must maintain the copyright information line on the bottom of each image. You are not allowed to download and post the published electronic version of your chapter, nor may you scan the printed edition to create an electronic version.

Central Storage: This license does not include permission for a scanned version of the material to be stored in a central repository such as that provided by Heron/XanEdu.

19. **Website** (regular and for author): A hyper-text must be included to the Homepage of the journal from which you are licensing at http://www.sciencedirect.com/science/journal/xxxxx. or for books to the Elsevier homepage at http://www.elsevier.com

20. **Thesis/Dissertation**: If your license is for use in a thesis/dissertation your thesis may be submitted to your institution in either print or electronic form. Should your thesis be published commercially, please reapply for permission. These requirements include permission for the Library and Archives of Canada to supply single copies, on demand, of the complete thesis and include permission for UMI to supply single copies, on demand, of the complete thesis. Should your thesis be published commercially, please reapply for permission.

21. **Other Conditions**:

v1.6

If you would like to pay for this license now, please remit this license along with your payment made payable to "COPYRIGHT CLEARANCE CENTER" otherwise you will be invoiced within 48 hours of the license date. Payment should be in the form of a check or money order referencing your account number and this invoice

number RLNK500825729.
Once you receive your invoice for this order, you may pay your invoice by credit card. Please follow instructions provided at that time.

Make Payment To:
Copyright Clearance Center
Dept 001
P.O. Box 843006
Boston, MA 02284-3006

For suggestions or comments regarding this order, contact RightsLink Customer Support: customercare@copyright.com or +1-877-622-5543 (toll free in the US) or +1-978-646-2777.

Gratis licenses (referencing $0 in the Total field) are free. Please retain this printable license for your reference. No payment is required.

RightsLink®

Home | Create Account | Help

Title:	Review of Recent Research into Cellulosic Whiskers, Their Properties and Their Application in Nanocomposite Field
Author:	My Ahmed Said Azizi Samir,†,‡,⊥, Fannie Alloin,‡ and, and Alain Dufresne*,§
Publication:	Biomacromolecules
Publisher:	American Chemical Society
Date:	Mar 1, 2005

PERMISSION/LICENSE IS GRANTED FOR YOUR ORDER AT NO CHARGE

This type of permission/license, instead of the standard Terms & Conditions, is sent to you because no fee is being charged for your order. Please note the following:

- Permission is granted for your request in both print and electronic formats, and translations.
- If figures and/or tables were requested, they may be adapted or used in part.
- Please print this page for your records and send a copy of it to your publisher/graduate school.
- Appropriate credit for the requested material should be given as follows: "Reprinted (adapted) with permission from (COMPLETE REFERENCE CITATION). Copyright (YEAR) American Chemical Society." Insert appropriate information in place of the

capitalized words.

- One-time permission is granted only for the use specified in your request. No additional uses are granted (such as derivative works or other editions). For any other uses, please

Title:	Effect of Reaction Conditions on the Properties and Behavior of Wood Cellulose Nanocrystal Suspensions
Author:	Stephanie Beck-Candanedo,†, Maren Roman,‡ and, and Derek G. Gray*,†
Publication:	Biomacromolecules
Publisher:	American Chemical Society
Date:	Mar 1, 2005

PERMISSION/LICENSE IS GRANTED FOR YOUR ORDER AT NO CHARGE

This type of permission/license, instead of the standard Terms & Conditions, is sent to you because no fee is being charged for your order. Please note the following:

- Permission is granted for your request in both print and electronic formats, and translations.
- If figures and/or tables were requested, they may be adapted or used in part.
- Please print this page for your records and send a copy of it to your publisher/graduate school.
- Appropriate credit for the requested material should be given as follows: "Reprinted (adapted) with permission from (COMPLETE REFERENCE CITATION). Copyright (YEAR) American Chemical Society." Insert appropriate information in place of the capitalized words.

SPRINGER LICENSE
TERMS AND CONDITIONS

Jul 25, 2012

This is a License Agreement between Rajalaxmi Dash ("You") and Springer ("Springer") provided by Copyright Clearance Center ("CCC"). The license consists of your order

details, the terms and conditions provided by Springer, and the payment terms and conditions.

All payments must be made in full to CCC. For payment instructions, please see information listed at the bottom of this form.

License Number	2956230543599
License date	Jul 25, 2012
Licensed content publisher	Springer
Licensed content publication	Cellulose
Licensed content title	Effect of microcrystallite preparation conditions on the formation of colloid crystals of cellulose
Licensed content author	XUE MIN DONG
Licensed content date	Mar 1, 1998
Volume number	5
Issue number	1
Type of Use	Thesis/Dissertation
Portion	Figures
Author of this Springer article	No
Order reference number	
Title of your thesis / dissertation	Synthesis and characterization of novel cellulosics
Expected completion date	Aug 2012
Estimated size(pages)	200
Total	0.00 USD
Terms and Conditions	

Introduction

The publisher for this copyrighted material is Springer Science + Business Media. By clicking "accept" in connection with completing this licensing transaction, you agree that the following terms and conditions apply to this transaction (along with the Billing and Payment terms and conditions established by Copyright Clearance Center, Inc. ("CCC"), at the time that you opened your Rightslink account and that are available at any time at http://myaccount.copyright.com).

Limited License

With reference to your request to reprint in your thesis material on which Springer Science and Business Media control the copyright, permission is granted, free of charge, for the use indicated in your enquiry.

Licenses are for one-time use only with a maximum distribution equal to the number that

you identified in the licensing process.

This License includes use in an electronic form, provided its password protected or on the university's intranet or repository, including UMI (according to the definition at the Sherpa website: http://www.sherpa.ac.uk/romeo/). For any other electronic use, please contact Springer at (permissions.dordrecht@springer.com or permissions.heidelberg@springer.com).

The material can only be used for the purpose of defending your thesis, and with a maximum of 100 extra copies in paper.

Although Springer holds copyright to the material and is entitled to negotiate on rights, this license is only valid, provided permission is also obtained from the (co) author (address is given with the article/chapter) and provided it concerns original material which does not carry references to other sources (if material in question appears with credit to another source, authorization from that source is required as well).

Permission free of charge on this occasion does not prejudice any rights we might have to charge for reproduction of our copyrighted material in the future.

Altering/Modifying Material: Not Permitted
You may not alter or modify the material in any manner. Abbreviations, additions, deletions and/or any other alterations shall be made only with prior written authorization of the author(s) and/or Springer Science + Business Media. (Please contact Springer at (permissions.dordrecht@springer.com or permissions.heidelberg@springer.com)

Reservation of Rights
Springer Science + Business Media reserves all rights not specifically granted in the combination of (i) the license details provided by you and accepted in the course of this licensing transaction, (ii) these terms and conditions and (iii) CCC's Billing and Payment terms and conditions.

Copyright Notice:Disclaimer
You must include the following copyright and permission notice in connection with any reproduction of the licensed material: "Springer and the original publisher /journal title, volume, year of publication, page, chapter/article title, name(s) of author(s), figure number(s), original copyright notice) is given to the publication in which the material was originally published, by adding; with kind permission from Springer Science and Business Media"

Warranties: None

Example 1: Springer Science + Business Media makes no representations or warranties with

respect to the licensed material.

Example 2: Springer Science + Business Media makes no representations or warranties with respect to the licensed material and adopts on its own behalf the limitations and disclaimers established by CCC on its behalf in its Billing and Payment terms and conditions for this licensing transaction.

Indemnity
You hereby indemnify and agree to hold harmless Springer Science + Business Media and CCC, and their respective officers, directors, employees and agents, from and against any and all claims arising out of your use of the licensed material other than as specifically authorized pursuant to this license.

No Transfer of License
This license is personal to you and may not be sublicensed, assigned, or transferred by you to any other person without Springer Science + Business Media's written permission.

No Amendment Except in Writing
This license may not be amended except in a writing signed by both parties (or, in the case of Springer Science + Business Media, by CCC on Springer Science + Business Media's behalf).

Objection to Contrary Terms
Springer Science + Business Media hereby objects to any terms contained in any purchase order, acknowledgment, check endorsement or other writing prepared by you, which terms are inconsistent with these terms and conditions or CCC's Billing and Payment terms and conditions. These terms and conditions, together with CCC's Billing and Payment terms and conditions (which are incorporated herein), comprise the entire agreement between you and Springer Science + Business Media (and CCC) concerning this licensing transaction. In the event of any conflict between your obligations established by these terms and conditions and those established by CCC's Billing and Payment terms and conditions, these terms and conditions shall control.

Jurisdiction
All disputes that may arise in connection with this present License, or the breach thereof, shall be settled exclusively by arbitration, to be held in The Netherlands, in accordance with Dutch law, and to be conducted under the Rules of the 'Netherlands Arbitrage Instituut' (Netherlands Institute of Arbitration).***OR:***

All disputes that may arise in connection with this present License, or the breach thereof, shall be settled exclusively by arbitration, to be held in the Federal Republic of Germany, in accordance with German law.

Order Completed

Thank you very much for your order.

This is a License Agreement between Rajalaxmi Dash ("You") and Springer ("Springer"). The license consists of your order details, the terms and conditions provided by Springer, and the payment terms and conditions.

Get the printable license.

License Number	2977851288740
License date	Aug 28, 2012
Licensed content publisher	Springer
Licensed content publication	Cellulose
Licensed content title	Cellulose: the structure slowly unravels
Licensed content author	ANTOINETTE C. O'SULLIVAN
Licensed content date	Jan 1, 1997
Volume number	4
Issue number	3
Type of Use	Thesis/Dissertation
Portion	Figures
Author of this Springer article	No
Title of your thesis / dissertation	Synthesis and characterization of novel cellulosics
Expected completion date	Aug 2012

Estimated size(pages)	200
Total	0.00 USD

JOHN WILEY AND SONS LICENSE TERMS AND CONDITIONS

Jul 25, 2012

This is a License Agreement between Rajalaxmi Dash ("You") and John Wiley and Sons ("John Wiley and Sons") provided by Copyright Clearance Center ("CCC"). The license consists of your order details, the terms and conditions provided by John Wiley and Sons, and the payment terms and conditions.

All payments must be made in full to CCC. For payment instructions, please see information listed at the bottom of this form.

License Number	2956231082406
License date	Jul 25, 2012
Licensed content publisher	John Wiley and Sons
Licensed content publication	Canadian Journal of Chemical Engineering
Licensed content title	Structure??process??yield interrelations in nanocrystalline cellulose extraction
Licensed content author	Wadood Y. Hamad,Thomas Q. Hu
Licensed content date	May 5, 2010
Start page	392
End page	402
Type of use	Dissertation/Thesis
Requestor type	University/Academic
Format	Electronic
Portion	Figure/table
Number of figures/tables	1
Number of extracts	
Original Wiley figure/table number(s)	1
Will you be translating?	No
Order reference number	
Total	0.00 USD
Terms and Conditions	

TERMS AND CONDITIONS

This copyrighted material is owned by or exclusively licensed to John Wiley & Sons, Inc. or one of its group companies (each a "Wiley Company") or a society for whom a Wiley Company has exclusive publishing rights in relation to a particular journal (collectively WILEY"). By clicking "accept" in connection with completing this licensing transaction, you agree that the following terms and conditions apply to this transaction (along with the

billing and payment terms and conditions established by the Copyright Clearance Center Inc., ("CCC's Billing and Payment terms and conditions"), at the time that you opened your Rightslink account (these are available at any time at http://myaccount.copyright.com)

Terms and Conditions

1. The materials you have requested permission to reproduce (the "Materials") are protected by copyright.

2. You are hereby granted a personal, non-exclusive, non-sublicensable, non-transferable, worldwide, limited license to reproduce the Materials for the purpose specified in the licensing process. This license is for a one-time use only with a maximum distribution equal to the number that you identified in the licensing process. Any form of republication granted by this licence must be completed within two years of the date of the grant of this licence (although copies prepared before may be distributed thereafter). The Materials shall not be used in any other manner or for any other purpose. Permission is granted subject to an appropriate acknowledgement given to the author, title of the material/book/journal and the publisher. You shall also duplicate the copyright notice that appears in the Wiley publication in your use of the Material. Permission is also granted on the understanding that nowhere in the text is a previously published source acknowledged for all or part of this Material. Any third party material is expressly excluded from this permission.

3. With respect to the Materials, all rights are reserved. Except as expressly granted by the terms of the license, no part of the Materials may be copied, modified, adapted (except for minor reformatting required by the new Publication), translated, reproduced, transferred or distributed, in any form or by any means, and no derivative works may be made based on the Materials without the prior permission of the respective copyright owner. You may not alter, remove or suppress in any manner any copyright, trademark or other notices displayed by the Materials. You may not license, rent, sell, loan, lease, pledge, offer as security, transfer or assign the Materials, or any of the rights granted to you hereunder to any other person.

4. The Materials and all of the intellectual property rights therein shall at all times remain the exclusive property of John Wiley & Sons Inc or one of its related companies (WILEY) or their respective licensors, and your interest therein is only that of having possession of and the right to reproduce the Materials pursuant to Section 2 herein during the continuance of this Agreement. You agree that you own no right, title or interest in or to the Materials or any of the intellectual property rights therein. You shall have no rights hereunder other than the license as provided for above in Section 2. No right, license or interest to any trademark, trade name, service mark or other branding ("Marks") of WILEY or its licensors is granted hereunder, and you agree that you shall not assert any such right, license or interest with respect thereto.

5. NEITHER WILEY NOR ITS LICENSORS MAKES ANY WARRANTY OR REPRESENTATION OF ANY KIND TO YOU OR ANY THIRD PARTY, EXPRESS, IMPLIED OR STATUTORY, WITH RESPECT TO THE MATERIALS OR THE ACCURACY OF ANY INFORMATION CONTAINED IN THE MATERIALS, INCLUDING, WITHOUT LIMITATION, ANY IMPLIED WARRANTY OF MERCHANTABILITY, ACCURACY, SATISFACTORY QUALITY, FITNESS FOR A PARTICULAR PURPOSE, USABILITY, INTEGRATION OR NON-INFRINGEMENT AND ALL SUCH WARRANTIES ARE HEREBY EXCLUDED BY WILEY AND ITS LICENSORS AND WAIVED BY YOU.

6. WILEY shall have the right to terminate this Agreement immediately upon breach of this Agreement by you.

7. You shall indemnify, defend and hold harmless WILEY, its Licensors and their respective directors, officers, agents and employees, from and against any actual or threatened claims, demands, causes of action or proceedings arising from any breach of this Agreement by you.

8. IN NO EVENT SHALL WILEY OR ITS LICENSORS BE LIABLE TO YOU OR ANY OTHER PARTY OR ANY OTHER PERSON OR ENTITY FOR ANY SPECIAL, CONSEQUENTIAL, INCIDENTAL, INDIRECT, EXEMPLARY OR PUNITIVE DAMAGES, HOWEVER CAUSED, ARISING OUT OF OR IN CONNECTION WITH THE DOWNLOADING, PROVISIONING, VIEWING OR USE OF THE MATERIALS REGARDLESS OF THE FORM OF ACTION, WHETHER FOR BREACH OF CONTRACT, BREACH OF WARRANTY, TORT, NEGLIGENCE, INFRINGEMENT OR OTHERWISE (INCLUDING, WITHOUT LIMITATION, DAMAGES BASED ON LOSS OF PROFITS, DATA, FILES, USE, BUSINESS OPPORTUNITY OR CLAIMS OF THIRD PARTIES), AND WHETHER OR NOT THE PARTY HAS BEEN ADVISED OF THE POSSIBILITY OF SUCH DAMAGES. THIS LIMITATION SHALL APPLY NOTWITHSTANDING ANY FAILURE OF ESSENTIAL PURPOSE OF ANY LIMITED REMEDY PROVIDED HEREIN.

9. Should any provision of this Agreement be held by a court of competent jurisdiction to be illegal, invalid, or unenforceable, that provision shall be deemed amended to achieve as nearly as possible the same economic effect as the original provision, and the legality, validity and enforceability of the remaining provisions of this Agreement shall not be affected or impaired thereby.

10. The failure of either party to enforce any term or condition of this Agreement shall not constitute a waiver of either party's right to enforce each and every term and condition of this Agreement. No breach under this agreement shall be deemed waived or excused by either party unless such waiver or consent is in writing signed by the party granting such waiver or consent. The waiver by or consent of a party to a breach of any provision of this Agreement shall not operate or be construed as a waiver of or consent to any other or subsequent breach by such other party.

11. This Agreement may not be assigned (including by operation of law or otherwise) by you without WILEY's prior written consent.

12. Any fee required for this permission shall be non-refundable after thirty (30) days from receipt.

13. These terms and conditions together with CCC's Billing and Payment terms and conditions (which are incorporated herein) form the entire agreement between you and WILEY concerning this licensing transaction and (in the absence of fraud) supersedes all prior agreements and representations of the parties, oral or written. This Agreement may not be amended except in writing signed by both parties. This Agreement shall be binding upon and inure to the benefit of the parties' successors, legal representatives, and authorized assigns.

14. In the event of any conflict between your obligations established by these terms and conditions and those established by CCC's Billing and Payment terms and conditions, these terms and conditions shall prevail.

15. WILEY expressly reserves all rights not specifically granted in the combination of (i) the license details provided by you and accepted in the course of this licensing transaction, (ii) these terms and conditions and (iii) CCC's Billing and Payment terms and conditions.

16. This Agreement will be void if the Type of Use, Format, Circulation, or Requestor Type was misrepresented during the licensing process.

17. This Agreement shall be governed by and construed in accordance with the laws of the State of New York, USA, without regards to such state's conflict of law rules. Any legal action, suit or proceeding arising out of or relating to these Terms and Conditions or the breach thereof shall be instituted in a court of competent jurisdiction in New York County in the State of New York in the United States of America and each party hereby consents and submits to the personal jurisdiction of such court, waives any objection to venue in such court and consents to service of process by registered or certified mail, return receipt requested, at the last known address of such party.

Wiley Open Access Terms and Conditions

All research articles published in Wiley Open Access journals are fully open access: immediately freely available to read, download and share. Articles are published under the terms of the Creative Commons Attribution Non Commercial License. which permits use, distribution and reproduction in any medium, provided the original work is properly cited and is not used for commercial purposes. The license is subject to the Wiley Open Access terms and conditions:
Wiley Open Access articles are protected by copyright and are posted to repositories and websites in accordance with the terms of the Creative Commons Attribution Non Commercial License. At the time of deposit, Wiley Open Access articles include all changes made during peer review, copyediting, and publishing. Repositories and websites that host the article are responsible for incorporating any publisher-supplied amendments or retractions issued subsequently. Wiley Open Access articles are also available without charge on Wiley's publishing platform, **Wiley Online Library** or any successor sites.

Use by non-commercial users

For non-commercial and non-promotional purposes individual users may access, download, copy, display and redistribute to colleagues Wiley Open Access articles, as well as adapt, translate, text- and data-mine the content subject to the following conditions:

 The authors' moral rights are not compromised. These rights include the right of "paternity" (also known as "attribution" - the right for the author to be identified as

such) and "integrity" (the right for the author not to have the work altered in such a way that the author's reputation or integrity may be impugned).
 Where content in the article is identified as belonging to a third party, it is the obligation of the user to ensure that any reuse complies with the copyright policies of the owner of that content.
 If article content is copied, downloaded or otherwise reused for non-commercial research and education purposes, a link to the appropriate bibliographic citation (authors, journal, article title, volume, issue, page numbers, DOI and the link to the definitive published version on Wiley Online Library) should be maintained. Copyright notices and disclaimers must not be deleted.
 Any translations, for which a prior translation agreement with Wiley has not been agreed, must prominently display the statement: "This is an unofficial translation of an article that appeared in a Wiley publication. The publisher has not endorsed this translation."

Use by commercial "for-profit" organisations

Use of Wiley Open Access articles for commercial, promotional, or marketing purposes requires further explicit permission from Wiley and will be subject to a fee. Commercial purposes include:

 Copying or downloading of articles, or linking to such articles for further redistribution, sale or licensing;
 Copying, downloading or posting by a site or service that incorporates advertising with such content;
 The inclusion or incorporation of article content in other works or services (other than normal quotations with an appropriate citation) that is then available for sale or licensing, for a fee (for example, a compilation produced for marketing purposes, inclusion in a sales pack)
 Use of article content (other than normal quotations with appropriate citation) by for-profit organisations for promotional purposes
 Linking to article content in e-mails redistributed for promotional, marketing or educational purposes;
 Use for the purposes of monetary reward by means of sale, resale, licence, loan, transfer or other form of commercial exploitation such as marketing products
 Print reprints of Wiley Open Access articles can be purchased from: corporatesales@wiley.com

Other Terms and Conditions:

BY CLICKING ON THE "I AGREE..." BOX, YOU ACKNOWLEDGE THAT YOU HAVE READ AND FULLY UNDERSTAND EACH OF THE SECTIONS OF AND PROVISIONS SET FORTH IN THIS AGREEMENT AND THAT YOU ARE IN AGREEMENT WITH AND ARE WILLING TO ACCEPT ALL OF YOUR OBLIGATIONS AS SET FORTH IN THIS AGREEMENT.

v1.7

If you would like to pay for this license now, please remit this license along with your payment made payable to "COPYRIGHT CLEARANCE CENTER" otherwise you will be invoiced within 48 hours of the license date. Payment should be in the form of a check or money order referencing your account number and this invoice number RLNK500825751.
Once you receive your invoice for this order, you may pay your invoice by credit card. Please follow instructions provided at that time.

Make Payment To:
Copyright Clearance Center
Dept 001
P.O. Box 843006
Boston, MA 02284-3006

For suggestions or comments regarding this order, contact RightsLink Customer Support: customercare@copyright.com or +1-877-622-5543 (toll free in the US) or +1-978-646-2777.

Gratis licenses (referencing $0 in the Total field) are free. Please retain this printable license for your reference. No payment is required.

ELSEVIER LICENSE
TERMS AND CONDITIONS

Jul 26, 2012

This is a License Agreement between Rajalaxmi Dash ("You") and Elsevier ("Elsevier") provided by Copyright Clearance Center ("CCC"). The license consists of your order details, the terms and conditions provided by Elsevier, and the payment terms and conditions.

All payments must be made in full to CCC. For payment instructions, please see information listed at the bottom of this form.

Supplier	Elsevier Limited The Boulevard,Langford Lane Kidlington,Oxford,OX5 1GB,UK
Registered Company Number	1982084
Customer name	Rajalaxmi Dash
Customer address	1012 Center St. NW Atlanta, GA 30318
License number	2956551034124
License date	Jul 26, 2012
Licensed content publisher	Elsevier
Licensed content publication	Carbohydrate Research
Licensed content title	Synthesis of novel water-soluble sulfonated cellulose

Licensed content author	Dash Rajalaxmi,Nan Jiang,Gelbaum Leslie,Arthur J. Ragauskas
Licensed content date	26 January 2010
Licensed content volume number	345
Licensed content issue number	2
Number of pages	7
Start Page	284
End Page	290
Type of Use	reuse in a thesis/dissertation
Portion	full article
Format	electronic
Are you the author of this Elsevier article?	Yes
Will you be translating?	No
Order reference number	
Title of your thesis/dissertation	Synthesis and characterization of novel cellulosics
Expected completion date	Aug 2012
Estimated size (number of pages)	200
Elsevier VAT number	GB 494 6272 12
Permissions price	0.00 USD
VAT/Local Sales Tax	0.0 USD / 0.0 GBP
Total	0.00 USD
Terms and Conditions	

INTRODUCTION

1. The publisher for this copyrighted material is Elsevier. By clicking "accept" in connection with completing this licensing transaction, you agree that the following terms and conditions apply to this transaction (along with the Billing and Payment terms and conditions established by Copyright Clearance Center, Inc. ("CCC"), at the time that you opened your Rightslink account and that are available at any time at http://myaccount.copyright.com).

GENERAL TERMS

2. Elsevier hereby grants you permission to reproduce the aforementioned material subject to the terms and conditions indicated.

3. Acknowledgement: If any part of the material to be used (for example, figures) has appeared in our publication with credit or acknowledgement to another source, permission must also be sought from that source. If such permission is not obtained then that material may not be included in your publication/copies. Suitable acknowledgement to the source

must be made, either as a footnote or in a reference list at the end of your publication, as follows:

"Reprinted from Publication title, Vol /edition number, Author(s), Title of article / title of chapter, Pages No., Copyright (Year), with permission from Elsevier [OR APPLICABLE SOCIETY COPYRIGHT OWNER]." Also Lancet special credit - "Reprinted from The Lancet, Vol. number, Author(s), Title of article, Pages No., Copyright (Year), with permission from Elsevier."

4. Reproduction of this material is confined to the purpose and/or media for which permission is hereby given.

5. Altering/Modifying Material: Not Permitted. However figures and illustrations may be altered/adapted minimally to serve your work. Any other abbreviations, additions, deletions and/or any other alterations shall be made only with prior written authorization of Elsevier Ltd. (Please contact Elsevier at permissions@elsevier.com)

6. If the permission fee for the requested use of our material is waived in this instance, please be advised that your future requests for Elsevier materials may attract a fee.

7. Reservation of Rights: Publisher reserves all rights not specifically granted in the combination of (i) the license details provided by you and accepted in the course of this licensing transaction, (ii) these terms and conditions and (iii) CCC's Billing and Payment terms and conditions.

8. License Contingent Upon Payment: While you may exercise the rights licensed immediately upon issuance of the license at the end of the licensing process for the transaction, provided that you have disclosed complete and accurate details of your proposed use, no license is finally effective unless and until full payment is received from you (either by publisher or by CCC) as provided in CCC's Billing and Payment terms and conditions. If full payment is not received on a timely basis, then any license preliminarily granted shall be deemed automatically revoked and shall be void as if never granted. Further, in the event that you breach any of these terms and conditions or any of CCC's Billing and Payment terms and conditions, the license is automatically revoked and shall be void as if never granted. Use of materials as described in a revoked license, as well as any use of the materials beyond the scope of an unrevoked license, may constitute copyright infringement and publisher reserves the right to take any and all action to protect its copyright in the materials.

9. Warranties: Publisher makes no representations or warranties with respect to the licensed material.

10. Indemnity: You hereby indemnify and agree to hold harmless publisher and CCC, and their respective officers, directors, employees and agents, from and against any and all claims arising out of your use of the licensed material other than as specifically authorized

pursuant to this license.

11. No Transfer of License: This license is personal to you and may not be sublicensed, assigned, or transferred by you to any other person without publisher's written permission.

12. No Amendment Except in Writing: This license may not be amended except in a writing signed by both parties (or, in the case of publisher, by CCC on publisher's behalf).

13. Objection to Contrary Terms: Publisher hereby objects to any terms contained in any purchase order, acknowledgment, check endorsement or other writing prepared by you, which terms are inconsistent with these terms and conditions or CCC's Billing and Payment terms and conditions. These terms and conditions, together with CCC's Billing and Payment terms and conditions (which are incorporated herein), comprise the entire agreement between you and publisher (and CCC) concerning this licensing transaction. In the event of any conflict between your obligations established by these terms and conditions and those established by CCC's Billing and Payment terms and conditions, these terms and conditions shall control.

14. Revocation: Elsevier or Copyright Clearance Center may deny the permissions described in this License at their sole discretion, for any reason or no reason, with a full refund payable to you. Notice of such denial will be made using the contact information provided by you. Failure to receive such notice will not alter or invalidate the denial. In no event will Elsevier or Copyright Clearance Center be responsible or liable for any costs, expenses or damage incurred by you as a result of a denial of your permission request, other than a refund of the amount(s) paid by you to Elsevier and/or Copyright Clearance Center for denied permissions.

LIMITED LICENSE

The following terms and conditions apply only to specific license types:

15. **Translation**: This permission is granted for non-exclusive world **English** rights only unless your license was granted for translation rights. If you licensed translation rights you may only translate this content into the languages you requested. A professional translator must perform all translations and reproduce the content word for word preserving the integrity of the article. If this license is to re-use 1 or 2 figures then permission is granted for non-exclusive world rights in all languages.

16. **Website**: The following terms and conditions apply to electronic reserve and author websites:
Electronic reserve: If licensed material is to be posted to website, the web site is to be password-protected and made available only to bona fide students registered on a relevant course if:
This license was made in connection with a course,
This permission is granted for 1 year only. You may obtain a license for future website posting,

All content posted to the web site must maintain the copyright information line on the bottom of each image,
A hyper-text must be included to the Homepage of the journal from which you are licensing at http://www.sciencedirect.com/science/journal/xxxxx or the Elsevier homepage for books at http://www.elsevier.com , and
Central Storage: This license does not include permission for a scanned version of the material to be stored in a central repository such as that provided by Heron/XanEdu.

17. **Author website** for journals with the following additional clauses:

All content posted to the web site must maintain the copyright information line on the bottom of each image, and the permission granted is limited to the personal version of your paper. You are not allowed to download and post the published electronic version of your article (whether PDF or HTML, proof or final version), nor may you scan the printed edition to create an electronic version. A hyper-text must be included to the Homepage of the journal from which you are licensing at http://www.sciencedirect.com/science/journal/xxxxx . As part of our normal production process, you will receive an e-mail notice when your article appears on Elsevier's online service ScienceDirect (www.sciencedirect.com). That e-mail will include the article's Digital Object Identifier (DOI). This number provides the electronic link to the published article and should be included in the posting of your personal version. We ask that you wait until you receive this e-mail and have the DOI to do any posting.

Central Storage: This license does not include permission for a scanned version of the material to be stored in a central repository such as that provided by Heron/XanEdu.

18. **Author website** for books with the following additional clauses:
Authors are permitted to place a brief summary of their work online only.
A hyper-text must be included to the Elsevier homepage at http://www.elsevier.com . All content posted to the web site must maintain the copyright information line on the bottom of each image. You are not allowed to download and post the published electronic version of your chapter, nor may you scan the printed edition to create an electronic version.

Central Storage: This license does not include permission for a scanned version of the material to be stored in a central repository such as that provided by Heron/XanEdu.

19. **Website** (regular and for author): A hyper-text must be included to the Homepage of the journal from which you are licensing at http://www.sciencedirect.com/science/journal/xxxxx. or for books to the Elsevier homepage at http://www.elsevier.com

20. **Thesis/Dissertation**: If your license is for use in a thesis/dissertation your thesis may be submitted to your institution in either print or electronic form. Should your thesis be published commercially, please reapply for permission. These requirements include permission for the Library and Archives of Canada to supply single copies, on demand, of the complete thesis and include permission for UMI to supply single copies, on demand, of

the complete thesis. Should your thesis be published commercially, please reapply for permission.

21. **Other Conditions**:

v1.6

If you would like to pay for this license now, please remit this license along with your payment made payable to "COPYRIGHT CLEARANCE CENTER" otherwise you will be invoiced within 48 hours of the license date. Payment should be in the form of a check or money order referencing your account number and this invoice number RLNK500826206.
Once you receive your invoice for this order, you may pay your invoice by credit card. Please follow instructions provided at that time.

Make Payment To:
Copyright Clearance Center
Dept 001
P.O. Box 843006
Boston, MA 02284-3006

For suggestions or comments regarding this order, contact RightsLink Customer Support: customercare@copyright.com or +1-877-622-5543 (toll free in the US) or +1-978-646-2777.

Gratis licenses (referencing $0 in the Total field) are free. Please retain this printable license for your reference. No payment is required.

JOHN WILEY AND SONS LICENSE
TERMS AND CONDITIONS

Jul 26, 2012

This is a License Agreement between Rajalaxmi Dash ("You") and John Wiley and Sons ("John Wiley and Sons") provided by Copyright Clearance Center ("CCC"). The license consists of your order details, the terms and conditions provided by John Wiley and Sons, and the payment terms and conditions.

All payments must be made in full to CCC. For payment instructions, please see information listed at the bottom of this form.

License Number	2956790054190
License date	Jul 26, 2012
Licensed content publisher	John Wiley and Sons
Licensed content publication	Journal of Applied Polymer Science
Licensed content title	Mechanical behavior of sheets prepared from sugar beet cellulose microfibrils
Licensed content author	Alain Dufresne,Jean-Yves Cavaillé,Michel R. Vignon
Licensed content date	Dec 7, 1998
Start page	1185
End page	1194
Type of use	Dissertation/Thesis
Requestor type	University/Academic
Format	Electronic
Portion	Figure/table
Number of figures/tables	1
Number of extracts	
Original Wiley figure/table number(s)	1
Will you be translating?	No
Order reference number	
Total	0.00 USD

Terms and Conditions

TERMS AND CONDITIONS

This copyrighted material is owned by or exclusively licensed to John Wiley & Sons, Inc. or one of its group companies (each a "Wiley Company") or a society for whom a Wiley Company has exclusive publishing rights in relation to a particular journal (collectively WILEY"). By clicking "accept" in connection with completing this licensing transaction, you agree that the following terms and conditions apply to this transaction (along with the billing and payment terms and conditions established by the Copyright Clearance Center Inc., ("CCC's Billing and Payment terms and conditions"), at the

time that you opened your Rightslink account (these are available at any time at http://myaccount.copyright.com)

Terms and Conditions

1. The materials you have requested permission to reproduce (the "Materials") are protected by copyright.

2. You are hereby granted a personal, non-exclusive, non-sublicensable, non-transferable, worldwide, limited license to reproduce the Materials for the purpose specified in the licensing process. This license is for a one-time use only with a maximum distribution equal to the number that you identified in the licensing process. Any form of republication granted by this licence must be completed within two years of the date of the grant of this licence (although copies prepared before may be distributed thereafter). The Materials shall not be used in any other manner or for any other purpose. Permission is granted subject to an appropriate acknowledgement given to the author, title of the material/book/journal and the publisher. You shall also duplicate the copyright notice that appears in the Wiley publication in your use of the Material. Permission is also granted on the understanding that nowhere in the text is a previously published source acknowledged for all or part of this Material. Any third party material is expressly excluded from this permission.

3. With respect to the Materials, all rights are reserved. Except as expressly granted by the terms of the license, no part of the Materials may be copied, modified, adapted (except for minor reformatting required by the new Publication), translated, reproduced, transferred or distributed, in any form or by any means, and no derivative works may be made based on the Materials without the prior permission of the respective copyright owner. You may not alter, remove or suppress in any manner any copyright, trademark or other notices displayed by the Materials. You may not license, rent, sell, loan, lease, pledge, offer as security, transfer or assign the Materials, or any of the rights granted to you hereunder to any other person.

4. The Materials and all of the intellectual property rights therein shall at all times remain the exclusive property of John Wiley & Sons Inc or one of its related companies (WILEY) or their respective licensors, and your interest therein is only that of having possession of and the right to reproduce the Materials pursuant to Section 2 herein during the continuance of this Agreement. You agree that you own no right, title or interest in or to the Materials or any of the intellectual property rights therein. You shall have no rights hereunder other than the license as provided for above in Section 2. No right, license or interest to any trademark, trade name, service mark or other branding ("Marks") of WILEY or its licensors is granted hereunder, and you agree that you shall not assert any such right, license or interest with respect thereto.

5. NEITHER WILEY NOR ITS LICENSORS MAKES ANY WARRANTY OR REPRESENTATION OF ANY KIND TO YOU OR ANY THIRD PARTY, EXPRESS, IMPLIED OR STATUTORY, WITH RESPECT TO THE MATERIALS OR THE ACCURACY OF ANY INFORMATION CONTAINED IN THE MATERIALS, INCLUDING, WITHOUT LIMITATION, ANY IMPLIED WARRANTY OF MERCHANTABILITY, ACCURACY, SATISFACTORY QUALITY, FITNESS FOR A PARTICULAR PURPOSE, USABILITY, INTEGRATION OR NON-INFRINGEMENT AND ALL SUCH WARRANTIES ARE HEREBY EXCLUDED BY WILEY AND ITS LICENSORS AND WAIVED BY YOU.

6. WILEY shall have the right to terminate this Agreement immediately upon breach of this Agreement by you.

7. You shall indemnify, defend and hold harmless WILEY, its Licensors and their respective directors, officers, agents and employees, from and against any actual or threatened claims, demands, causes of action or proceedings arising from any breach of this Agreement by you.

8. IN NO EVENT SHALL WILEY OR ITS LICENSORS BE LIABLE TO YOU OR ANY OTHER PARTY OR ANY OTHER PERSON OR ENTITY FOR ANY SPECIAL, CONSEQUENTIAL, INCIDENTAL, INDIRECT, EXEMPLARY OR PUNITIVE DAMAGES, HOWEVER CAUSED, ARISING OUT OF OR IN CONNECTION WITH THE DOWNLOADING, PROVISIONING, VIEWING OR USE OF THE MATERIALS REGARDLESS OF THE FORM OF ACTION, WHETHER FOR BREACH OF CONTRACT, BREACH OF WARRANTY, TORT, NEGLIGENCE, INFRINGEMENT OR OTHERWISE (INCLUDING, WITHOUT LIMITATION, DAMAGES BASED ON LOSS OF PROFITS, DATA, FILES, USE, BUSINESS OPPORTUNITY OR CLAIMS OF THIRD PARTIES), AND WHETHER OR NOT THE PARTY HAS BEEN ADVISED OF THE POSSIBILITY OF SUCH DAMAGES. THIS LIMITATION SHALL APPLY NOTWITHSTANDING ANY FAILURE OF ESSENTIAL PURPOSE OF ANY LIMITED REMEDY PROVIDED HEREIN.

9. Should any provision of this Agreement be held by a court of competent jurisdiction to be illegal, invalid, or unenforceable, that provision shall be deemed amended to achieve as nearly as possible the same economic effect as the original provision, and the legality, validity and enforceability of the remaining provisions of this Agreement shall not be affected or impaired thereby.

10. The failure of either party to enforce any term or condition of this Agreement shall not constitute a waiver of either party's right to enforce each and every term and condition of this Agreement. No breach under this agreement shall be deemed waived or excused by either party unless such waiver or consent is in writing signed by the party granting such waiver or consent. The waiver by or consent of a party to a breach of any provision of this Agreement shall not operate or be construed as a waiver of or consent to any other or subsequent breach by such other party.

11. This Agreement may not be assigned (including by operation of law or otherwise) by you without WILEY's prior written consent.

12. Any fee required for this permission shall be non-refundable after thirty (30) days from receipt.

13. These terms and conditions together with CCC's Billing and Payment terms and conditions (which are incorporated herein) form the entire agreement between you and WILEY concerning this licensing transaction and (in the absence of fraud) supersedes all prior agreements and representations of the parties, oral or written. This Agreement may not be amended except in writing signed by both parties. This Agreement shall be binding upon and inure to the benefit of the parties' successors, legal representatives, and authorized assigns.

14. In the event of any conflict between your obligations established by these terms and conditions and those established by CCC's Billing and Payment terms and conditions, these terms and conditions shall prevail.

15. WILEY expressly reserves all rights not specifically granted in the combination of (i) the license details provided by you and accepted in the course of this licensing transaction, (ii) these terms and conditions and (iii) CCC's Billing and Payment terms and conditions.

16. This Agreement will be void if the Type of Use, Format, Circulation, or Requestor Type was misrepresented during the licensing process.

17. This Agreement shall be governed by and construed in accordance with the laws of the State of New York, USA, without regards to such state's conflict of law rules. Any legal action, suit or proceeding arising out of or relating to these Terms and Conditions or the breach thereof shall be instituted in a court of competent jurisdiction in New York County in the State of New York in the United States of America and each party hereby consents and submits to the personal jurisdiction of such court, waives any objection to venue in such court and consents to service of process by registered or certified mail, return receipt requested, at the last known address of such party.

Wiley Open Access Terms and Conditions

All research articles published in Wiley Open Access journals are fully open access: immediately freely available to read, download and share. Articles are published under the terms of the Creative Commons Attribution Non Commercial License. which permits use, distribution and reproduction in any medium, provided the original work is properly cited and is not used for commercial purposes. The license is subject to the Wiley Open Access terms and conditions:
Wiley Open Access articles are protected by copyright and are posted to repositories and websites in accordance with the terms of the Creative Commons Attribution Non Commercial License. At the time of deposit, Wiley Open Access articles include all changes made during peer review, copyediting, and publishing. Repositories and websites that host the article are responsible for incorporating any publisher-supplied amendments or retractions issued subsequently.
Wiley Open Access articles are also available without charge on Wiley's publishing platform, **Wiley Online Library** or any successor sites.

Use by non-commercial users

For non-commercial and non-promotional purposes individual users may access, download, copy, display and redistribute to colleagues Wiley Open Access articles, as well as adapt, translate, text- and data-mine the content subject to the following conditions:

 The authors' moral rights are not compromised. These rights include the right of "paternity" (also known as "attribution" - the right for the author to be identified as such) and "integrity" (the right for the author not to have the work altered in such a way that the author's reputation or integrity may be impugned).
 Where content in the article is identified as belonging to a third party, it is the obligation of the user to ensure that any reuse complies with the copyright policies of the owner of that

content.
 If article content is copied, downloaded or otherwise reused for non-commercial research and education purposes, a link to the appropriate bibliographic citation (authors, journal, article title, volume, issue, page numbers, DOI and the link to the definitive published version on Wiley Online Library) should be maintained. Copyright notices and disclaimers must not be deleted.
 Any translations, for which a prior translation agreement with Wiley has not been agreed, must prominently display the statement: "This is an unofficial translation of an article that appeared in a Wiley publication. The publisher has not endorsed this translation."

Use by commercial "for-profit" organisations

Use of Wiley Open Access articles for commercial, promotional, or marketing purposes requires further explicit permission from Wiley and will be subject to a fee. Commercial purposes include:

 Copying or downloading of articles, or linking to such articles for further redistribution, sale or licensing;
 Copying, downloading or posting by a site or service that incorporates advertising with such content;
 The inclusion or incorporation of article content in other works or services (other than normal quotations with an appropriate citation) that is then available for sale or licensing, for a fee (for example, a compilation produced for marketing purposes, inclusion in a sales pack)
 Use of article content (other than normal quotations with appropriate citation) by for-profit organisations for promotional purposes
 Linking to article content in e-mails redistributed for promotional, marketing or educational purposes;
 Use for the purposes of monetary reward by means of sale, resale, licence, loan, transfer or other form of commercial exploitation such as marketing products
 Print reprints of Wiley Open Access articles can be purchased from: corporatesales@wiley.com

Other Terms and Conditions:

BY CLICKING ON THE "I AGREE..." BOX, YOU ACKNOWLEDGE THAT YOU HAVE READ AND FULLY UNDERSTAND EACH OF THE SECTIONS OF AND PROVISIONS SET FORTH IN THIS AGREEMENT AND THAT YOU ARE IN AGREEMENT WITH AND ARE WILLING TO ACCEPT ALL OF YOUR OBLIGATIONS AS SET FORTH IN THIS AGREEMENT.

v1.7

If you would like to pay for this license now, please remit this license along with your payment made payable to "COPYRIGHT CLEARANCE CENTER" otherwise you will be invoiced within 48 hours of the license date. Payment should be in the form of a check or money order referencing your account number and this invoice number RLNK500826564.

Once you receive your invoice for this order, you may pay your invoice by credit card. Please follow instructions provided at that time.

Make Payment To:
Copyright Clearance Center
Dept 001
P.O. Box 843006
Boston, MA 02284-3006

For suggestions or comments regarding this order, contact RightsLink Customer Support: customercare@copyright.com or +1-877-622-5543 (toll free in the US) or +1-978-646-2777.

Gratis licenses (referencing $0 in the Total field) are free. Please retain this printable license for your reference. No payment is required.

Copyright Clearance Center RightsLink®

Home | Account Info | Help

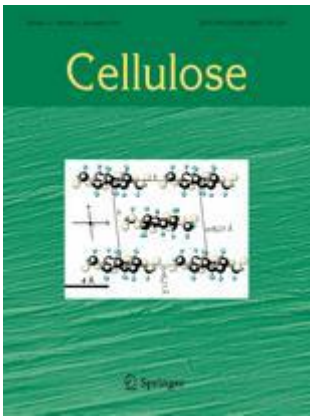

Title: Atomic force microscopy and transmission electron microscopy of cellulose from Micrasterias denticulata; evidence for a chiral helical microfibril twist
Author: SHAUNE J. HANLEY
Publication: Cellulose
Publisher: Springer
Date: Jan 1, 1997

Logged in as:
Rajalaxmi Dash
Account #:
3000555808

LOGOUT

Order Completed

Thank you very much for your order.

This is a License Agreement between Rajalaxmi Dash ("You") and Springer ("Springer"). The license consists of your order details, the terms and conditions provided by Springer, and the payment terms and conditions.

Get the printable license.

License Number	2956800698485
License date	Jul 26, 2012
Licensed content publisher	Springer
Licensed content publication	Cellulose
Licensed content title	Atomic force microscopy and transmission electron microscopy of cellulose from Micrasterias denticulata; evidence for a chiral helical microfibril twist
Licensed content author	SHAUNE J. HANLEY
Licensed content date	Jan 1, 1997
Volume number	4
Issue number	3
Type of Use	Thesis/Dissertation
Portion	Figures
Author of this Springer article	No

Title of your thesis / dissertation	Synthesis and characterization of novel cellulosics
Expected completion date	Aug 2012
Estimated size(pages)	200
Total	0.00 USD

Copyright Clearance Center RightsLink®

Home | Account Info | Help

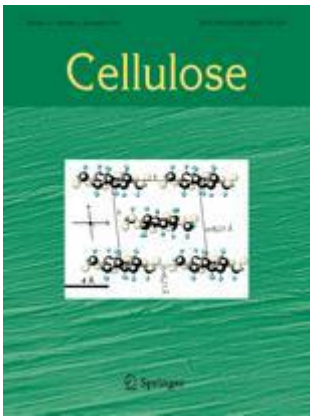

Title: Atomic force microscopy and transmission electron microscopy of cellulose from Micrasterias denticulata; evidence for a chiral helical microfibril twist

Author: SHAUNE J. HANLEY

Publication: Cellulose

Publisher: Springer

Date: Jan 1, 1997

Logged in as:
Rajalaxmi Dash
Account #:
3000555808

LOGOUT

Order Completed

Thank you very much for your order.

This is a License Agreement between Rajalaxmi Dash ("You") and Springer ("Springer"). The license consists of your order details, the terms and conditions provided by Springer, and the payment terms and conditions.

License Number	2956801004534
License date	Jul 26, 2012
Licensed content publisher	Springer
Licensed content publication	Cellulose
Licensed content title	Atomic force microscopy and transmission electron microscopy of cellulose from Micrasterias denticulata; evidence for a chiral helical microfibril twist
Licensed content author	SHAUNE J. HANLEY
Licensed content date	Jan 1, 1997
Volume number	4
Issue number	3
Type of Use	Thesis/Dissertation
Portion	Figures
Author of this Springer article	No
Title of your thesis / dissertation	Synthesis and characterization of novel cellulosics
Expected completion date	Aug 2012
Estimated size(pages)	200

REFERENCES

1. Satyanarayana, K. G.; Arizaga, G. G. C.; Wypych, F., Biodegradable composites based on lignocellulosic fibers-an overview. *Progress in Polymer Science* **2009,** *34* (9), 982-1021.

2. Mohanty, A. K.; Misra, M.; Drzal, L. T., Sustainable bio-composites from renewable resources: Opportunities and challenges in the green materials world. *Journal of Polymers and the Environment* **2002,** *10* (1), 19-26.

3. Rojas J, A., E, Functionalization and crosslinking of microcrystalline cellulose in aqueous media: A safe and economic approach. *Int J Pharm Sci Rev and Res* **2011,** *8*, 28-36.

4. Crini, G., Recent developments in polysaccharide-based materials used as adsorbents in wastewater treatment. *Progress in Polymer Science* **2005,** *30* (1), 38-70.

5. Klemm, D.; Heublein, B.; Fink, H.-P.; Bohn, A., Cellulose: Fascinating biopolymer and sustainable raw material. *Angewandte Chemie International Edition* **2005,** *44* (22), 3358-3393.

6. Klemm D, P. B., Heinze T, Heinze U, Wagenknetch W, Comprehensive cellulose chemistry. Weinheim, Ed. Wiley: 1998.

7. Payne, A., Mémoire sur la composition du tissu propre des plantes et du ligneux. . *C R Hebd Seances Acad Sci* **1838,** *7*, 1052-1056.

8. Dumitriu, S., Polysaccharides: Structural diversity and functional versatility. Dumitriu, S., Ed. CRC press: 2004; p. 1224.

9. Siro, I.; Plackett, D., Microfibrillated cellulose and new nanocomposite materials: A review. *Cellulose* **2010,** *17* (3), 459-494.

10. Parthasarathi, R.; Bellesia, G.; Chundawat, S. P. S.; Dale, B. E.; Langan, P.; Gnanakaran, S., Insights into hydrogen bonding and stacking interactions in cellulose. *Journal of Physical Chemistry A* **2011,** *115* (49), 14191-14202.

11. Nishiyama, Y.; Langan, P.; Wada, M.; Forsyth, V. T., Looking at hydrogen bonds in cellulose. *Acta Crystallographica Section D-Biological Crystallography* **2010,** *66*, 1172-1177.

12. Lima, M. M. D.; Borsali, R., Rodlike cellulose microcrystals: Structure, properties, and applications. *Macromolecular Rapid Communications* **2004,** *25* (7), 771-787.

13. Hon, DNS., Chemical modification of lignocellulosic material. Dekker, M., Ed. New York: 1996.

14. Kamel, S.; Ali, N.; Jahangir, K.; Shah, S. M.; El-Gendy, A. A., Pharmaceutical significance of cellulose: A review. *Express Polymer Letters* **2008,** *2* (11), 758-778.

15. Meyer, K. H.; Misch, L., Positions des atomes dans le nouveau modèle spatial de la cellulose. *Helvetica Chimica Acta* **1937,** *20* (1), 232-244.

16. Langan, P.; Nishiyama, Y.; Wada, M.; Sugiyama, J.; Chanzy, H., Crystal structure and hydrogen-bonding system in cellulose from neutron fiber diffraction. *Abstracts of Papers American Chemical Society* **2000,** *219* (1-2), 34.

17. Kim, N. H.; Imai, T.; Wada, M.; Sugiyama, J., Molecular directionality in cellulose polymorphs. *Biomacromolecules* **2006,** *7* (1), 274-280.

18. KroonBatenburg, L. M. J.; Kroon, J., The crystal and molecular structures of cellulose i and ii. *Glycoconjugate Journal* **1997,** *14* (5), 677-690.

19. Klemm, D.; Philipp, B.; Heinze, T.; Heinze, U.; Wagenknecht, W., Comprehensive cellulose chemistry, volume 1, fundamentals and analytical methods,. Wiley-VCH, Weinheim: 1998; p. 688.

20. Nishiyama, Y.; Langan, P.; Chanzy, H., Crystal structure and hydrogen-bonding system in cellulose 1 beta from synchrotron x-ray and neutron fiber diffraction. *Journal of the American Chemical Society* **2002,** *124* (31), 9074-9082.

21. Nishiyama, Y.; Sugiyama, J.; Chanzy, H.; Langan, P., Crystal structure and hydrogen bonding system in cellulose 1(alpha), from synchrotron x-ray and neutron fiber diffraction. *Journal of the American Chemical Society* **2003,** *125* (47), 14300-14306.

22. Nishiyama, Y.; Johnson, G. P.; French, A. D.; Forsyth, V. T.; Langan, P., Neutron crystallography, molecular dynamics, and quantum mechanics studies of the nature of hydrogen bonding in cellulose i-beta. *Biomacromolecules* **2008,** *9* (11), 3133-3140.

23. Mazeau, K., Structural micro-heterogeneities of crystalline i beta-cellulose. *Cellulose* **2005,** *12* (4), 339-349.

24. Mansikkamaki, P.; Lahtinen, M.; Rissanen, K., Structural changes of cellulose crystallites induced by mercerisation in different solvent systems; determined by powder x-ray diffraction method. *Cellulose* **2005,** *12* (3), 233-242.

25. Ciacco, G. T.; Morgado, D. L.; Frollini, E.; Possidonio, S.; El Seoud, O. A., Some aspects of acetylation of untreated and mercerized sisal cellulose. *Journal of the Brazilian Chemical Society* **2010,** *21* (1), 71-77.

26. Dinand, E.; Vignon, M.; Chanzy, H.; Heux, L., Mercerization of primary wall cellulose and its implication for the conversion of cellulose i -> cellulose ii. *Cellulose* **2002,** *9* (1), 7-18.

27. Langan, P.; Nishiyama, Y.; Chanzy, H., A revised structure and hydrogen-bonding system in cellulose II from a neutron fiber diffraction analysis. *Journal of the American Chemical Society* **1999,** *121* (43), 9940-9946.

28. Klemm, D.; Heinze, T.; Philipp, B.; Wagenknecht, W., New approaches to advanced polymers by selective cellulose functionalization. *Acta Polymerica* **1997,** *48* (8), 277-297.

29. Moon, R. J.; Martini, A.; Nairn, J.; Simonsen, J.; Youngblood, J., Cellulose nanomaterials review: Structure, properties and nanocomposites. *Chemical Society Reviews* **2011,** *40* (7), 3941-3994.

30. Levis, S. R.; Deasy, P. B., Pharmaceutical applications of size reduced grades of surfactant co-processed microcrystalline cellulose. *International Journal of Pharmaceutics* **2001,** *230* (1-2), 25-33.

31. Bondeson, D.; Mathew, A.; Oksman, K., Optimization of the isolation of nanocrystals from microcrystalline cellulose by acid hydrolysis. *Cellulose* **2006,** *13* (2), 171-180.

32. Rondeau-Mouro, C.; Bouchet, B.; Pontoire, B.; Robert, P.; Mazoyer, J.; Buleon, A., Structural features and potential texturising properties of lemon and maize cellulose microfibrils. *Carbohydrate Polymers* **2003,** *53* (3), 241-252.

33. Iwamoto, S.; Abe, K.; Yano, H., The effect of hemicelluloses on wood pulp nanofibrillation and nanofiber network characteristics. *Biomacromolecules* **2008,** *9* (3), 1022-1026.

34. Saito, T.; Hirota, M.; Tamura, N.; Kimura, S.; Fukuzumi, H.; Heux, L.; Isogai, A., Individualization of nano-sized plant cellulose fibrils by direct surface carboxylation using tempo catalyst under neutral conditions. *Biomacromolecules* **2009,** *10* (7), 1992-1996.

35. Saito, T.; Kimura, S.; Nishiyama, Y.; Isogai, A., Cellulose nanofibers prepared by tempo-mediated oxidation of native cellulose. *Biomacromolecules* **2007,** *8* (8), 2485-2491.

36. Fukuzumi, H.; Saito, T.; Wata, T.; Kumamoto, Y.; Isogai, A., Transparent and high gas barrier films of cellulose nanofibers prepared by tempo-mediated oxidation. *Biomacromolecules* **2009,** *10* (1), 162-165.

37. Nogi, M.; Iwamoto, S.; Nakagaito, A. N.; Yano, H., Optically transparent nanofiber paper. *Advanced Materials* **2009,** *21* (16), 1595-1598.

38. Paakko, M.; Ankerfors, M.; Kosonen, H.; Nykanen, A.; Ahola, S.; Osterberg, M.; Ruokolainen, J.; Laine, J.; Larsson, P. T.; Ikkala, O.; Lindstrom, T., Enzymatic hydrolysis combined with mechanical shearing and high-pressure homogenization for nanoscale cellulose fibrils and strong gels. *Biomacromolecules* **2007,** *8* (6), 1934-1941.

39. Elazzouzi-Hafraoui, S.; Nishiyama, Y.; Putaux, J.-L.; Heux, L.; Dubreuil, F.; Rochas, C., The shape and size distribution of crystalline nanoparticles prepared by acid hydrolysis of native cellulose. *Biomacromolecules* **2008,** *9* (1), 57-65.

40. de Rodriguez, N. L. G.; Thielemans, W.; Dufresne, A., Sisal cellulose whiskers reinforced polyvinyl acetate nanocomposites. *Cellulose* **2006,** *13* (3), 261-270.

41. Beck-Candanedo, S.; Roman, M.; Gray, D. G., Effect of reaction conditions on the properties and behavior of wood cellulose nanocrystal suspensions. *Biomacromolecules* **2005,** *6* (2), 1048-1054.

42. Bai, W.; Holbery, J.; Li, K., A technique for production of nanocrystalline cellulose with a narrow size distribution. *Cellulose* **2009,** *16* (3), 455-465.

43. Habibi, Y.; Lucia, L. A.; Rojas, O. J., Cellulose nanocrystals: Chemistry, self-assembly, and applications. *Chemical Reviews* **2010,** *110* (6), 3479-3500.

44. Kim, N. H.; Herth, W.; Vuong, R.; Chanzy, H., The cellulose system in the cell wall of micrasterias. *Journal of Structural Biology* **1996,** *117* (3), 195-203.

45. Sugiyama, J.; Harada, H.; Fujiyoshi, Y.; Uyeda, N., Lattice images from ultrathin sections of cellulose microfibrils in the cell-wall of valonia-macrophysa kutz. *Planta* **1985,** *166* (2), 161-168.

46. Hanley, S. J.; Giasson, J.; Revol, J. F.; Gray, D. G., Atomic force microscopy of cellulose microfibrils - comparison with transmission electron-microscopy. *Polymer* **1992,** *33* (21), 4639-4642.

47. Tokoh, C.; Takabe, K.; Fujita, M.; Saiki, H., Cellulose synthesized by acetobacter xylinum in the presence of acetyl glucomannan. *Cellulose* **1998,** *5* (4), 249-261.

48. Yamanaka, S.; Watanabe, K.; Kitamura, N.; Iguchi, M.; Mitsuhashi, S.; Nishi, Y.; Uryu, M., The structure and mechanical-properties of sheets prepared from bacterial cellulose. *Journal of Materials Science* **1989,** *24* (9), 3141-3145.

49. Grunert, M.; Winter, W. T., Nanocomposites of cellulose acetate butyrate reinforced with cellulose nanocrystals. *Journal of Polymers and the Environment* **2002,** *10* (1-2), 27-30.

50. John, M. J.; Thomas, S., Biofibres and biocomposites. *Carbohydrate Polymers* **2008,** *71* (3), 343-364.

51. Santos, R. B.; Capanema, E. A.; Balakshin, M. Y.; Chang, H. M.; Jameel, H., Effect of hardwoods characteristics on kraft pulping process: Emphasis on lignin structure. *Bioresources* **2011,** *6* (4), 3623-3637.

52. Fengel, D.; Grosser, D., Chemical composition of softwoods and hardwoods - bibliographical review. *Holz Als Roh-Und Werkstoff* **1975,** *33* (1), 32-38.

53. O'Neill JJ, R. E. Cellulose pellets. U.S. 2543928, 1951.

54. Štamberg, J.; Peška, J.; Paul, D.; Philipp, B., Perlcellulose – ein neuer makroporöser träger für ionenaustauscher und analoge systeme. *Acta Polymerica* **1979,** *30* (12), 734-739.

55. Liu, M.; Huang, J.; Deng, Y., Adsorption behaviors of l-arginine from aqueous solutions on a spherical cellulose adsorbent containing the sulfonic group. *Bioresource Technology* **2007,** *98* (5), 1144-1148.

56. Kaster, J. A.; Deoliveira, W.; Glasser, W. G.; Velander, W. H., Optimization of pressure-flow limits, strength, intraparticle transport and dynamic capacity by hydrogel solids content and bead size in cellulose immunosorbents. *Journal of Chromatography* **1993,** *648* (1), 79-90.

57. Luo, X.; Zhang, L., Creation of regenerated cellulose microspheres with diameter ranging from micron to millimeter for chromatography applications. *Journal of Chromatography A* **2010,** *1217* (38), 5922-5929.

58. Yu, H. F.; Fu, G. Q.; Liu, L.; He, B. L., Facile synthesis and adsorption properties of phosphonated cellulose beads for selective removal of low-density lipoprotein. *Chinese Chemical Letters* **2006,** *17* (9), 1193-1196.

59. Chesney, A.; Barnwell, P.; Stonehouse, D. F.; Steel, P. G., Amino-derivatised beaded cellulose gels. Novel accessible and biodegradable scavenger resins for solution phase combinatorial synthesis. *Green Chemistry* **2000,** *2* (2), 57-62.

60. Fan, X.; Liu, Z.-T.; Liu, Z.-W., Preparation and application of cellulose triacetate microspheres. *Journal of Hazardous Materials* **2010,** *177* (1-3), 452-457.

61. Bai, Y. X.; Li, Y. F., Preparation and characterization of crosslinked porous cellulose beads. *Carbohydrate Polymers* **2006,** *64* (3), 402-407.

62. Xia, H.-F.; Lin, D.-Q.; Yao, S.-J., Chromatographic performance of macroporous cellulose-tungsten carbide composite beads as anion-exchanger for expanded bed adsorption at high fluid velocity. *Journal of Chromatography A* **2008,** *1195* (1-2), 60-66.

63. Wang, D.-M.; Sun, Y., Fabrication of superporous cellulose beads with grafted anion-exchange polymer chains for protein chromatography. *Biochemical Engineering Journal* **2007,** *37* (3), 332-337.

64. Gemeiner, P.; Breier, A., Aldehydic derivatives of bead cellulose - relationships between the matrix structure and function in immobilization of enzymes catalyzing hydrolysis of high molecular substrates. *Biotechnology and Bioengineering* **1982,** *24* (11), 2573-2582.

65. Stefuca, V.; Gemeiner, P.; Bales, V., Study of porous cellulose beads as an enzyme carrier via simple mathematical-models for the hydrolysis of saccharose using

immobilized invertase reactors. *Enzyme and Microbial Technology* **1988,** *10* (5), 306-311.

66. Lenfeld, J.; Benes, M. J.; Kucerova, Z., 3,5-diiodo-l-tyrosine immobilized on bead cellulose. *Reactive & Functional Polymers* **1995,** *28* (1), 61-68.

67. Mislovicova, D.; Masarova, J.; Vikartovska, A.; Gemeiner, P.; Michalkova, E., Biospecific immobilization of mannan-penicillin g acylase neoglycoenzyme on concanavalin a-bead cellulose. *Journal of Biotechnology* **2004,** *110* (1), 11-19.

68. Sawayama, S.; Rao, K. K.; Hall, D. O., Immobilization of rhodobacter capsulatus on cellulose beads and water treatment using a photobioreactor. *Journal of Fermentation and Bioengineering* **1998,** *86* (5), 517-520.

69. Wolf, B., Bead cellulose products with film formers and solubilizers for controlled drug release. *International Journal of Pharmaceutics* **1997,** *156* (1), 97-107.

70. Wolf, B.; Finke, I., The use of bead celluloses as carrier for controlled liberation of drugs .3. Investigation of the ion-exchange capacity of bead cellulose and of derivatives of bead cellulose. *Pharmazie* **1991,** *46* (12), 861-863.

71. Wolf, B., The use of bead celluloses as carrier for controlled liberation of drugs .6. Kinetics of liberation of bonded drugs from bead cellulose and bead cellulose derivatives. *Pharmazie* **1992,** *47* (3), 204-207.

72. Boeden, H. F.; Pommerening, K.; Becker, M.; Rupprich, C.; Holtzhauer, M.; Loth, F.; Muller, R.; Bertram, D., Bead cellulose derivatives as supports for immobilization and chromatographic purification of proteins. *Journal of Chromatography* **1991,** *552* (1-2), 389-414.

73. Wang, D.-M.; Hao, G.; Shi, Q.-H.; Sun, Y., Fabrication and characterization of superporous cellulose bead for high-speed protein chromatography. *Journal of Chromatography A* **2007,** *1146* (1), 32-40.

74. Du, K.-F.; Yan, M.; Wang, Q.-Y.; Song, H., Preparation and characterization of novel macroporous cellulose beads regenerated from ionic liquid for fast chromatography. *Journal of Chromatography A* **2010,** *1217* (8), 1298-1304.

75. Zhou, D.; Zhang, L. N.; Zhou, J. P.; Guo, S. L., Cellulose/chitin beads for adsorption of heavy metals in aqueous solution. *Water Research* **2004,** *38* (11), 2643-2650.

76. Weber, V.; Linsberger, I.; Ettenauer, M.; Loth, F.; Hoyhtya, M.; Falkenhagen, D., Development of specific adsorbents for human tumor necrosis factor-alpha: Influence of antibody immobilization on performance and biocompatibility. *Biomacromolecules* **2005,** *6* (4), 1864-1870.

77. Li, N.; Bai, R. B., Copper adsorption on chitosan-cellulose hydrogel beads: Behaviors and mechanisms. *Separation and Purification Technology* **2005,** *42* (3), 237-247.

78. Guo, X.; Du, Y.; Chen, F.; Park, H.-S.; Xie, Y., Mechanism of removal of arsenic by bead cellulose loaded with iron oxyhydroxide (beta-feooh): Exafs study. *Journal of Colloid and Interface Science* **2007,** *314* (2), 427-433.

79. Guo, X. J.; Chen, F. H., Removal of arsenic by bead cellulose loaded with iron oxyhydroxide from groundwater. *Environmental Science & Technology* **2005,** *39* (17), 6808-6818.

80. Mistova, E.; Parschova, H.; Matejka, Z., Selective sorption of metal oxoanions from dilute solution by bead cellulose sorbent. *Separation Science and Technology* **2007,** *42* (6), 1231-1243.

81. Ranby, B. G., Cellulose and muscle - the colloidal properties of cellulose micelles. *Discussions of the Faraday Society* **1951,** (11), 158-164.

82. Mukherjee, S. M.; Woods, H. J., X-ray and electron microscope studies of the degradation of cellulose by sulphuric acid. *Biochimica Et Biophysica Acta* **1953,** *10* (4), 499-511.

83. Eichhorn, S. J., Cellulose nanowhiskers: Promising materials for advanced applications. *Soft Matter* **2011,** *7* (2), 303-315.

84. Revol, J. F.; Godbout, L.; Dong, X. M.; Gray, D. G.; Chanzy, H.; Maret, G., Chiral nematic suspensions of cellulose crystallites - phase-separation and magnetic-field orientation. *Liquid Crystals* **1994,** *16* (1), 127-134.

85. Kontturi, E.; Vuorinen, T., Indirect evidence of supramolecular changes within cellulose microfibrils of chemical pulp fibers upon drying. *Cellulose* **2009,** *16* (1), 65-74.

86. Dong, X. M.; Revol, J. F.; Gray, D. G., Effect of microcrystallite preparation conditions on the formation of colloid crystals of cellulose. *Cellulose* **1998,** *5* (1), 19-32.

87. Hamad, W. Y.; Hu, T. Q., Structure-process-yield interrelations in nanocrystalline cellulose extraction. *Canadian Journal of Chemical Engineering* **2010,** *88* (3), 392-402.

88. Lu, P.; Hsieh, Y.-L., Preparation and properties of cellulose nanocrystals: Rods, spheres, and network. *Carbohydrate Polymers* **2010,** *82* (2), 329-336.

89. Joksimovic, G.; Markovic, Z., Investigation of the mechanism of acidic hydrolysis of cellulose. *Acta Agriculturae Serbica* **2007,** *Vol. XII* (24), 51-57.

90. Araki, J.; Wada, M.; Kuga, S.; Okano, T., Flow properties of microcrystalline cellulose suspension prepared by acid treatment of native cellulose. *Colloids and Surfaces a-Physicochemical and Engineering Aspects* **1998,** *142* (1), 75-82.

91. Araki, J.; Wada, M.; Kuga, S.; Okana, T., Influence of surface charge on viscosity behavior of cellulose microcrystal suspension. *Journal of Wood Science* **1999,** *45*(3), 258-261.

92. Araki, J.; Wada, M.; Kuga, S., Steric stabilization of a cellulose microcrystal suspension by poly(ethylene glycol) grafting. *Langmuir* **2001,** *17* (1), 21-27.

93. Miller, A. F.; Donald, A. M., Imaging of anisotropic cellulose suspensions using environmental scanning electron microscopy. *Biomacromolecules* **2003,** *4* (3), 510-517.

94. Pranger, L.; Tannenbaum, R., Biobased nanocomposites prepared by in situ polymerization of furfuryl alcohol with cellulose whiskers or montmorillonite clay. *Macromolecules* **2008,** *41* (22), 8682-8687.

95. de Menezes, A. J.; Siqueira, G.; Curvelo, A. A. S.; Dufresne, A., Extrusion and characterization of functionalized cellulose whiskers reinforced polyethylene nanocomposites. *Polymer* **2009,** *50* (19), 4552-4563.

96. Lima, A. M. D.; Wong, J. T.; Paillet, M.; Borsali, R.; Pecora, R., Translational and rotational dynamics of rodlike cellulose whiskers. *Langmuir* **2003,** *19* (1), 24-29.

97. Kimura, F.; Kimura, T.; Tamura, M.; Hirai, A.; Ikuno, M.; Horii, F., Magnetic alignment of the chiral nematic phase of a cellulose microfibril suspension. *Langmuir* **2005,** *21* (5), 2034-2037.

98. Revol, J. F.; Gancet, C.; Goring, D. A. I., Orientation of cellulose crystallites in the S2 layer of spruce and birch wood cell-walls. *Wood Science* **1982,** *14* (3), 120-126.

99. Habibi, Y.; Goffin, A.-L.; Schiltz, N.; Duquesne, E.; Dubois, P.; Dufresne, A., Bionanocomposites based on poly(epsilon-caprolactone)-grafted cellulose nanocrystals by ring-opening polymerization. *Journal of Materials Chemistry* **2008,** *18* (41), 5002-5010.

100. Roohani, M.; Habibi, Y.; Belgacem, N. M.; Ebrahim, G.; Karimi, A. N.; Dufresne, A., Cellulose whiskers reinforced polyvinyl alcohol copolymers nanocomposites. *European Polymer Journal* **2008,** *44* (8), 2489-2498.

101. Samir, M.; Alloin, F.; Paillet, M.; Dufresne, A., Tangling effect in fibrillated cellulose reinforced nanocomposites. *Macromolecules* **2004,** *37* (11), 4313-4316.

102. Azizi Samir, M. A. S.; Alloin, F.; Dufresne, A., Review of recent research into cellulosic whiskers, their properties and their application in nanocomposite field. *Biomacromolecules* **2005,** *6* (2), 612-26.

103. Terech, P.; Chazeau, L.; Cavaille, J. Y., A small-angle scattering study of cellulose whiskers in aqueous suspensions. *Macromolecules* **1999,** *32* (6), 1872-1875.

104. Lima, M. M. D.; Borsali, R., Static and dynamic light scattering from polyelectrolyte microcrystal cellulose. *Langmuir* **2002,** *18* (4), 992-996.

105. Lahiji, R. R.; Reifenberger, R.; Raman, A.; Rudie, A.; Moon, R. J., Characterization of cellulose nanocrystal surfaces by SPM. *NSTI-Nanotech* **2008**, *1-3*, 704-707.

106. Onsager, L., The effects of shape on the interaction of colloidal particles. *Annals of the New York Academy of Sciences* **1949,** *51* (4), 627-659.

107. Revol, J. F.; Godbout, L.; Gray, D. G., Solid self-assembled films of cellulose with chiral nematic order and optically variable properties. *Journal of Pulp and Paper Science* **1998,** *24* (5), 146-149.

108. Stroobants, A.; Lekkerkerker, H. N. W.; Odijk, T., Effect of electrostatic interaction on the liquid-crystal phase-transition in solutions of rodlike polyelectrolytes. *Macromolecules* **1986,** *19* (8), 2232-2238.

109. Tahiri, C.; Vignon, M. R., Tempo-oxidation of cellulose: Synthesis and characterisation of polyglucuronans. *Cellulose* **2000,** *7* (2), 177-188.

110. Vold, I. M. N.; Christensen, B. E., Periodate oxidation of chitosans with different chemical compositions. *Carbohydrate Research* **2005,** *340* (4), 679-684.

111. Fan, Q. G.; Lewis, D. M.; Tapley, K. N., Characterization of cellulose aldehyde using fourier transform infrared spectroscopy. *Journal of Applied Polymer Science* **2001,** *82* (5), 1195-1202.

112. Cui, S. W., Structural analysis of polysaccharides. In *Food Carbohydrates Chemistry, Physical Properties, and Applications*, CRC Press: Steve W . Cui 2005.

113. Kristiansen, K. A.; Potthast, A.; Christensen, B. E., Periodate oxidation of polysaccharides for modification of chemical and physical properties. *Carbohydrate Research* **2010,** *345* (10), 1264-1271.

114. Perlin, A. S., Glycol-cleavage oxidation. In *Advances in carbohydrate chemistry and biochemistry, vol 60*, Horton, D., Ed. 2006; Vol. 60, pp 183-250.

115. Criegee, R.; Kraft, L.; Rank, B., The fission of glycol, its mechanism and its application to chemical problems. *Justus Liebigs Annalen Der Chemie* **1933,** *507*, 159-197.

116. Rosenfeld, D. A.; Richtmyer, N. K.; Hudson, C. S., Methyl 2,6-anhydro-alpha-d-altroside and other new derivatives of methyl alpha-d-altroside. *Journal of the American Chemical Society* **1948,** *70* (6), 2201-2206.

117. Angyal, S. J.; Young, R. J., Glycol fission in rigid systems .1. The camphane-2,3-diols. *Journal of the American Chemical Society* **1959,** *81* (20), 5467-5472.

118. Criegee, R.; Buchner, E.; Walther, W., The speed of the glycol fission with lead iv-acetate dependent on the constitution of the glycol. *Berichte Der Deutschen Chemischen Gesellschaft* **1940,** *73*, 571-575.

119. Reeves, R. E., The shape of pyranoside rings. *Journal of the American Chemical Society* **1950,** *72* (4), 1499-1506.

120. Malaprade, L., The oxydation of certain polyhydric alcohol by the application of periodic acid. *Comptes Rendus Hebdomadaires Des Seances De L Academie Des Sciences* **1928,** *186*, 382-385.

121. Criegee, R., An oxidative fission of glycols (ii. Communication. On oxidations with lead(iv)-salts)). *Berichte Der Deutschen Chemischen Gesellschaft* **1931,** *64*, 260-266.

122. Clutterbuck, P. W.; Reuter, F., The reaction of periodic acid with alpha-ketols, alpha-diketones, and alpha-ketonealdehydes. *Journal of the Chemical Society* **1935**, 1467-1469.

123. Baer, E., Oxidative cleavage of alpha-keto acids and alpha-keto alcohols by means of lead tetraacetate. *Journal of the American Chemical Society* **1940,** *62*, 1597-1606.

124. Nicoli, B. H.; Shinn, L. A., The action of periodic acid on alpha-amino alcohols. *Journal of the American Chemical Society* **1939,** *61*, 1615-1615.

125. Browning, B. L., Methods of wood chemistry. Interscience Pub. New York: 1967; p. 538.

126. Maekawa, E.; Kosaki, T.; Koshijima, T., Periodate oxidation of mercerized cellulose and reegenerated cellulose. *Wood research* **1986,** *73*, 44-49.

127. Tang, A. M.; Zhang, H. W.; Chen, G.; Xie, G. H.; Liang, W. Z., Influence of ultrasound treatment on accessibility and regioselective oxidation reactivity of cellulose. *Ultrasonics Sonochemistry* **2005,** *12* (6), 467-472.

128. Sirvio, J.; Hyvakko, U.; Liimatainen, H.; Niinimaki, J.; Hormi, O., Periodate oxidation of cellulose at elevated temperatures using metal salts as cellulose activators. *Carbohydrate Polymers* **2011,** *83* (3), 1293-1297.

129. Sirviö, J.; Liimatainen, H.; Niinimäki, J.; Hormi, O., Dialdehyde cellulose microfibers generated from wood pulp by milling-induced periodate oxidation. *Carbohydrate Polymers* **2011,** *86* (1), 260-265.

130. Varma, A. J.; Chavan, V. B.; Rajmohanan, P. R.; Ganapathy, S., Some observations on the high-resolution solid-state cp-mas c-13-nmr spectra of periodate-oxidised cellulose. *Polymer Degradation and Stability* **1997,** *58* (3), 257-260.

131. Kim, U. J.; Kuga, S.; Wada, M.; Okano, T.; Kondo, T., Periodate oxidation of crystalline cellulose. *Biomacromolecules* **2000,** *1* (3), 488-492.

132. Rohrling, J.; Potthast, A.; Rosenau, T.; Lange, T.; Borgards, A.; Sixta, H.; Kosma, P., A novel method for the determination of carbonyl groups in cellulosics by fluorescence labeling. 2. Validation and applications. *Biomacromolecules* **2002,** *3* (5), 969-975.

133. Potthast, A.; Rosenau, T.; Kosma, P., Analysis of oxidized functionalities in cellulose. In *Polysaccharides ii*, Klemm, D., Ed. 2006; Vol. 205, pp 1-48.

134. Kostic, M.; Potthast, A.; Rosenau, T.; Kosma, P.; Sixta, H., A novel approach to determination of carbonyl groups in dmac/licl-insoluble pulps by fluorescence labeling. *Cellulose* **2006,** *13* (4), 429-435.

135. Potthast, A.; Kostic, M.; Schiehser, S.; Kosma, P.; Rosenau, T., Studies on oxidative modifications of cellulose in the periodate system: Molecular weight distribution and carbonyl group profiles. *Holzforschung* **2007,** *61* (6), 662-667.

136. Hou, Q. X.; Liu, W.; Liu, Z. H.; Bai, L. L., Characteristics of wood cellulose fibers treated with periodate and bisulfite. *Industrial & Engineering Chemistry Research* **2007,** *46* (23), 7830-7837.

137. Feng, Y.; Li, J.; Lin, Q.; Wang, X.; Wu, Z.; Pang, S.; Sun, Z., Crystallinity and thermal decomposition of dialdehyde celluloses from bacterial cellulose. *Key Engineering Materials* **2007,** *330-332*, 1289-1292.

138. Calvini, P.; Gorassini, A.; Luciano, G.; Franceschi, E., Ftir and waxs analysis of periodate oxycellulose: Evidence for a cluster mechanism of oxidation. *Vibrational Spectroscopy* **2006,** *40* (2), 177-183.

139. Rowland, S. P.; Cousins, E. R., Periodate oxidative decrystallization of cotton cellulose. *Journal of Polymer Science Part a-1-Polymer Chemistry* **1966,** *4* (4PA1), 793-&.

140. Bouchard, J.; Methot, M.; Jordan, B., The effects of ionizing radiation on the cellulose of woodfree paper. *Cellulose* **2006,** *13* (5), 601-610.

141. Singh, M.; Ray, A. R.; Vasudevan, P.; Verma, K.; Guha, S. K., Potential biosoluble carriers - biocompatibility and biodegradability of oxidized cellulose. *Biomaterials Medical Devices and Artificial Organs* **1979,** *7* (4), 495-512.

142. Singh, M.; Ray, A. R.; Vasudevan, P., Biodegradation studies on periodate oxidized cellulose. *Biomaterials* **1982,** *3* (1), 16-20.

143. Li, J.; Wan, Y.; Li, L.; Liang, H.; Wang, J., Preparation and characterization of 2,3-dialdehyde bacterial cellulose for potential biodegradable tissue engineering

scaffolds. *Materials Science & Engineering C-Biomimetic and Supramolecular Systems* **2009,** *29* (5), 1635-1642.

144. Devi, K. S.; Sinha, T. J. M.; Vasudevan, P., Biosoluble surgical material from 2,3-dialdehyde cellulose. *Biomaterials* **1986,** *7* (3), 193-196.

145. RoyChowdhury, P.; Kumar, V., Fabrication and evaluation of porous 2,3-dialdehydecellulose membrane as a potential biodegradable tissue-engineering scaffold. *Journal of Biomedical Materials Research Part A* **2006,** *76A* (2), 300-309.

146. RoyChowdhury, P.; Klemuk, S.; Titze, I.; Kumar, V., Effects of fabrication parameters on viscoelastic shear modulus of 2,3-dialdehydecellulose membranes-potential scaffolds for vocal fold lamina propria tissue engineering. *Journal of Biomedical Materials Research Part A* **2009,** *88A* (3), 680-688.

147. Drogat, N.; Granet, R.; Sol, V.; Memmi, A.; Saad, N.; Koerkamp, C. K.; Bressollier, P.; Krausz, P., Antimicrobial silver nanoparticles generated on cellulose nanocrystals. *Journal of Nanoparticle Research* **2011,** *13* (4), 1557-1562.

148. Kim, U. J.; Kuga, S., Polyallylamine-grafted cellulose gel as high-capacity anion-exchanger. *Journal of Chromatography A* **2002,** *946* (1-2), 283-289.

149. Rutherford, H. A.; Minor, F. W.; Martin, A. R.; Harris, M., Oxidation of cellulose: Reaction of cellulose with periodic acid. *Journal of research of the National Bureau of Standards* **1942,** *29*, 131-141.

150. Hofreiter, B. T.; Wolff, I. A.; Mehltretter, C. L., Chlorous acid oxidation of periodate oxidized cornstarch. *Journal of the American Chemical Society* **1957,** *79* (24), 6457-6460.

151. Maekawa, E.; Koshijima, T., Properties of 2,3-dicarboxy cellulose combined with various metallic-ions. *Journal of Applied Polymer Science* **1984,** *29* (7), 2289-2297.

152. Crescenzi, V.; Dentini, M.; Meoli, C.; Casu, B.; Naggi, A.; Torri, G., Dicarboxyamylose and dicarboxycellulose, stereoregular poly-electrolytes - binding of calcium and magnesium-ions. *International Journal of Biological Macromolecules* **1984,** *6* (3), 142-144.

153. Floor, M.; Peters, J. A.; van Bekkum, H.; Kieboom, A. P. G.; Koek, J. H.; Smeets, F. L. M.; Niemantsverdriet, R. E., Structural and conformational effects on the complexation of calcium by 2,3-dicarboxy derivatives of β-cyclodextrin (cyclomaltoheptaose), amylose, and cellulose. *Carbohydrate Research* **1990,** *203* (1), 19-32.

154. Kim, U. J.; Kuga, S., Ion-exchange chromatography by dicarboxyl cellulose gel. *Journal of Chromatography A* **2001,** *919* (1), 29-37.

155. Kumar, V.; Deshpande, G. S., Noncovalent immobilization of bovine serum albumin on oxidized cellulose. *Artificial Cells Blood Substitutes and Immobilization Biotechnology* **2001,** *29* (3), 203-212.

156. Maekawa, E.; Koshijima, T., Preparation and structural consideration of nitrogen-containing derivatives obtained from dialdehyde celluloses. *Journal of Applied Polymer Science* **1991,** *42* (1), 169-178.

157. Maekawa, E.; Koshijima, T., Preparation and characterization of hydroxamic acid derivative and its metal complexes derived from cellulose. *Journal of Applied Polymer Science* **1990,** *40* (9-10), 1601-1613.

158. Wu, M.; Kuga, S., Cationization of cellulose fabrics by polyallylamine binding. *Journal of Applied Polymer Science* **2006,** *100* (2), 1668-1672.

159. Han, S.; Lee, M.; Kim, B. K., Crosslinking reactions of oxidized cellulose fiber. I. Reactions between dialdehyde cellulose and multifunctional amines on lyocell fabric. *Journal of Applied Polymer Science* **2010,** *117* (2), 682-690.

160. Han, S.; Lee, M., Crosslinking reactions of oxidized cellulose fiber. Ii. Reactions between dialdehyde cellulose and chito-oligosaccharides on lyocell fabric. *Journal of Applied Polymer Science* **2009,** *112* (2), 709-714.

161. Janjic, S.; Kostic, M.; Vucinic, V.; Dimitrijevic, S.; Popovic, K.; Ristic, M.; Skundric, P., Biologically active fibers based on chitosan-coated lyocell fibers. *Carbohydrate Polymers* **2009,** *78* (2), 240-246.

162. Liu, X. D.; Nishi, N.; Tokura, S.; Sakairi, N., Chitosan coated cotton fiber: Preparation and physical properties. *Carbohydrate Polymers* **2001,** *44* (3), 233-238.

163. Nikolic, T.; Kostic, M.; Praskalo, J.; Petronijevic, Z.; Skundric, P., Sorption properties of periodate oxidized cotton. *Chemical Industry & Chemical Engineering Quarterly* **2011,** *17* (3), 367-374.

164. Vanleemp.E; Horisber.M, Immobilization of trypsin on partially oxidized cellulose. *Biotechnology and Bioengineering* **1974,** *16* (7), 997-1003.

165. Varavinit, S.; Chaokasem, N.; Shobsngob, S., Covalent immobilization of a glucoamylase to bagasse dialdehyde cellulose. *World Journal of Microbiology & Biotechnology* **2001,** *17* (7), 721-725.

166. Singh, M.; Vasudevan, P.; Sinha, T. J. M.; Ray, A. R.; Misro, M. M.; Guha, K., An insulin delivery system from oxidized cellulose. *Journal of Biomedical Materials Research* **1981,** *15* (5), 655-661.

167. Carneiro-da-Cunha, M. G.; Rocha, J. M. S.; Garcia, F. A. P.; Gil, M. H., Lipase immobilisation on to polymeric membranes. *Biotechnology Techniques* **1999,** *13* (6), 403-409.

168. Singh, M.; Vasudevan, P.; Ray, A. R.; Guha, S. K., Biosoluble polymers for drug delivery. *Macromolecular Chemistry and Physics* **1980,** *181* (12), 2433-2439.

169. Xu, Y.; Du, Z.; Chen, Y., Imine bond characterization and properties for controlled release drugs of collagen protein cross-linked cotton fiber. In *Silk: Inheritance and innovation - modern silk road*, Bai, L. C. G. Q., Ed. 2011; Vol. 175-176, pp 214-219.

170. Dash, R.; Ragauskas, A. J., Synthesis of a novel cellulose nanowhisker-based drug delivery system. *RSC Advances* **2012,** *2* (8), 3403-3409.

171. Hou, Q.; Liu, W.; Liu, Z.; Bai, L., Characteristics of wood cellulose fibers treated with periodate and bisulfite. *Ind. Eng. Chem. Res.* **2007,** *46* (23), 7830-7837.

172. Rahn, K.; Heinze, T., New cellulosic polymers by subsequent modification of 2,3-dialdehyde cellulose. *Cellulose Chemistry and Technology* **1998,** *32* (3-4), 173-183.

173. Shet, R. T. W., P. R. R. Manufacture of sulfonated cellulose with improved absorbent properties. U. S. 57033225, 1997.

174. Peresin, M. S.; Habibi, Y.; Zoppe, J. O.; Pawlak, J. J.; Rojas, O. J., Nanofiber composites of polyvinyl alcohol and cellulose nanocrystals: Manufacture and characterization. *Biomacromolecules* **2010,** *11* (3), 674-681.

175. Dufresne, A., Polysaccharide nano crystal reinforced nanocomposites. *Canadian Journal of Chemistry* **2008,** *86* (6), 484-494.

176. Eichhorn, S. J.; Dufresne, A.; Aranguren, M.; Marcovich, N. E.; Capadona, J. R.; Rowan, S. J.; Weder, C.; Thielemans, W.; Roman, M.; Renneckar, S.; Gindl, W.; Veigel, S.; Keckes, J.; Yano, H.; Abe, K.; Nogi, M.; Nakagaito, A. N.; Mangalam, A.; Simonsen, J.; Benight, A. S.; Bismarck, A.; Berglund, L. A.; Peijs, T., Review: Current international research into cellulose nanofibres and nanocomposites. *Journal of Materials Science* **2010,** *45* (1), 1-33.

177. Sassi, J. F.; Chanzy, H., Ultrastructural aspects of the acetylation of cellulose. *Cellulose* **1995,** *2* (2), 111-127.

178. Cetin, N. S.; Tingaut, P.; Ozmen, N.; Henry, N.; Harper, D.; Dadmun, M.; Sebe, G., Acetylation of cellulose nanowhiskers with vinyl acetate under moderate conditions. *Macromolecular Bioscience* **2009,** *9* (10), 997-1003.

179. Nair, K. G.; Dufresne, A.; Gandini, A.; Belgacem, M. N., Crab shell chitin whiskers reinforced natural rubber nanocomposites. 3. Effect of chemical modification of chitin whiskers. *Biomacromolecules* **2003,** *4* (6), 1835-1842.

180. Angellier, H.; Molina-Boisseau, S.; Belgacem, M. N.; Dufresne, A., Surface chemical modification of waxy maize starch nanocrystals. *Langmuir* **2005,** *21* (6), 2425-2433.

181. Yuan, H. H.; Nishiyama, Y.; Wada, M.; Kuga, S., Surface acylation of cellulose whiskers by drying aqueous emulsion. *Biomacromolecules* **2006,** *7* (3), 696-700.

182. Braun, B.; Dorgan, J. R., Single-step method for the isolation and surface functionalization of cellulosic nanowhiskers. *Biomacromolecules* **2009,** *10* (2), 334-341.

183. Cateto, C. A.; Ragauskas, A., Amino acid modified cellulose whiskers. *RSC Advances* **2011,** *1* (9), 1695-1697.

184. Gousse, C.; Chanzy, H.; Excoffier, G.; Soubeyrand, L.; Fleury, E., Stable suspensions of partially silylated cellulose whiskers dispersed in organic solvents. *Polymer* **2002,** *43* (9), 2645-2651.

185. Siqueira, G.; Bras, J.; Dufresne, A., New process of chemical grafting of cellulose nanoparticles with a long chain isocyanate. *Langmuir* **2010,** *26* (1), 402-411.

186. Follain, N.; Marais, M.-F.; Montanari, S.; Vignon, M. R., Coupling onto surface carboxylated cellulose nanocrystals. *Polymer* **2010,** *51* (23), 5332-5344.

187. Habibi, Y.; Chanzy, H.; Vignon, M. R., Tempo-mediated surface oxidation of cellulose whiskers. *Cellulose* **2006,** *13* (6), 679-687.

188. Johnson, R.; Zink-Sharp, A.; Glasser, W., Preparation and characterization of hydrophobic derivatives of tempo-oxidized nanocelluloses. *Cellulose* **2011,** *18* (6), 1599-1609.

189. Hasani, M.; Cranston, E. D.; Westman, G.; Gray, D. G., Cationic surface functionalization of cellulose nanocrystals. *Soft Matter* **2008,** *4* (11), 2238-2244.

190. Dong, S.; Roman, M., Fluorescently labeled cellulose nanocrystals for bioimaging applications. *Journal of the American Chemical Society* **2007,** *129* (45), 13810-13811.

191. Mahmoud, K. A.; Male, K. B.; Hrapovic, S.; Luong, J. H. T., Cellulose nanocrystal/gold nanoparticle composite as a matrix for enzyme immobilization. *ACS Applied Materials & Interfaces* **2009,** *1* (7), 1383-1386.

192. Mangalam, A. P.; Simonsen, J.; Benight, A. S., Cellulose/DNA hybrid nanomaterials. *Biomacromolecules* **2009,** *10* (3), 497-504.

193. Majoinen, J.; Walther, A.; McKee, J. R.; Kontturi, E.; Aseyev, V.; Malho, J. M.; Ruokolainen, J.; Ikkala, O., Polyelectrolyte brushes grafted from cellulose nanocrystals using cu-mediated surface-initiated controlled radical polymerization. *Biomacromolecules* **2011,** *12* (8), 2997-3006.

194. Harrisson, S.; Drisko, G. L.; Malmstrom, E.; Hult, A.; Wooley, K. L., Hybrid rigid/soft and biologic/synthetic materials: Polymers grafted onto cellulose microcrystals. *Biomacromolecules* **2011,** *12* (4), 1214-1223.

195. Heux, L.; Chauve, G.; Bonini, C., Nonflocculating and chiral-nematic self-ordering of cellulose microcrystals suspensions in nonpolar solvents. *Langmuir* **2000,** *16* (21), 8210-8212.

196. Bondeson, D.; Oksman, K., Dispersion and characteristics of surfactant modified cellulose whiskers nanocomposites. *Composite Interfaces* **2007,** *14* (7-9), 617-630.

197. Kim, J.; Montero, G.; Habibi, Y.; Hinestroza, J. P.; Genzer, J.; Argyropoulos, D. S.; Rojas, O. J., Dispersion of cellulose crystallites by nonionic surfactants in a hydrophobic polymer matrix. *Polymer Engineering and Science* **2009,** *49* (10), 2054-2061.

198. Rojas, O. J.; Montero, G. A.; Habibi, Y., Electrospun nanocomposites from polystyrene loaded with cellulose nanowhiskers. *Journal of Applied Polymer Science* **2009,** *113* (2), 927-935.

199. Katz, S.; Beatson, R. P.; Scallan, A. M., The determination of strong and weak acidic groups in sulfite pulps. *Svensk. Papperstidning* **1984,** *87* (6), 48–53.

200. Bhardwaj, N. K.; Hoang, V.; Nguyen, K. L., A comparative study of the effect of refining on physical and electrokinetic properties of various cellulosic fibres. *Bioresource Technology* **2007,** *98* (8), 1647-1654.

201. Wu, S.-C.; Chang, W.-H.; Dong, G.-C.; Chen, K.-Y.; Chen, Y.-S.; Yao, C.-H., Cell adhesion and proliferation enhancement by gelatin nanofiber scaffolds. *Journal of Bioactive and Compatible Polymers* **2011,** *26* (6), 565-577.

202. Kuijpers, A. J.; Engbers, G. H. M.; Feijen, J.; De Smedt, S. C.; Meyvis, T. K. L.; Demeester, J.; Krijgsveld, J.; Zaat, S. A. J.; Dankert, J., Characterization of the network structure of carbodiimide cross-linked gelatin gels. *Macromolecules* **1999,** *32* (10), 3325-3333.

203. Draye, J. P.; Delaey, B.; Van de Voorde, A.; Van Den Bulcke, A.; Bogdanov, B.; Schacht, E., In vitro release characteristics of bioactive molecules from dextran dialdehyde cross-linked gelatin hydrogel films. *Biomaterials* **1998,** *19* (1-3), 99-107.

204. Fonseca Silva, T. C.; Habibi, Y.; Colodette, J. L.; Lucia, L. A., The influence of the chemical and structural features of xylan on the physical properties of its derived hydrogels. *Soft Matter* **2011,** *7* (3), 1090-1099.

205. Ragauskas, A. J.; Williams, C. K.; Davison, B. H.; Britovsek, G.; Cairney, J.; Eckert, C. A.; Frederick, W. J.; Hallett, J. P.; Leak, D. J.; Liotta, C. L.; Mielenz, J. R.; Murphy, R.; Templer, R.; Tschaplinski, T., The path forward for biofuels and biomaterials. *Science* **2006,** *311* (5760), 484-489.

206. Kulicke, W. M.; Kull, A. H.; Kull, W.; Thielking, H.; Engelhardt, J.; Pannek, J. B., Characterization of aqueous carboxymethylcellulose solutions in terms of their

molecular structure and its influence on rheological behaviour. *Polymer* **1996,** *37* (13), 2723-2731.

207. Gelman, R. A., Characterization of carboxymethylcellulose - distribution of substituent groups along the chain. *Journal of Applied Polymer Science* **1982,** *27* (8), 2957-2964.

208. Koschella, A.; Fenn, D.; Illy, N.; Heinze, T., Regioselectively functionalized cellulose derivatives: A mini review. *Macromolecular Symposia* **2006,** *244*, 59-73.

209. Kim U, K. S., Functionalization of cellulose by periodate oxidation. *Cellulose Communications* **2002,** *9* (2), 69–75.

210. Kim, U. J.; Kuga, S.; Wada, M.; Okano, T., Anomaly in periodate oxidation of crystalline cellulose. *Abstracts of Papers of the American Chemical Society* **1999,** *217*, U259-U259.

211. Guthrie, R. D., The dialdehydes from the periodate oxidation of carbohydrates. *Advances in Carbohydrate Chemistry* **1961,** *16*, 105-158.

212. Vicini, S.; Princi, E.; Luciano, G.; Franceschi, E.; Pedemonte, E.; Oldak, D.; Kaczmarek, H.; Sionkowska, A., Thermal analysis and characterisation of cellulose oxidised with sodium methaperiodate. *Thermochimica Acta* **2004,** *418* (1-2), 123-130.

213. Varma, A. J.; Kulkarni, M. P., Oxidation of cellulose under controlled conditions. *Polymer Degradation and Stability* **2002,** *77* (1), 25-27.

214. Morooka, T.; Norimoto, M.; Yamada, T., Periodate-oxidation of cellulose by homogeneous reaction. *Journal of Applied Polymer Science* **1989,** *38* (5), 849-858.

215. Varma, A. J.; Chavan, V. B., A study of crystallinity changes in oxidized celluloses. *Polymer Degradation and Stability* **1995,** *49* (2), 245-250.

216. Kim, U. J.; Wada, M.; Kuga, S., Solubilization of dialdehyde cellulose by hot water. *Carbohydrate Polymers* **2004,** *56* (1), 7-10.

217. Habibi, Y.; Vignon, M. R., Optimization of cellouronic acid synthesis by tempo-mediated oxidation of cellulose iii from sugar beet pulp. *Cellulose* **2008,** *15* (1), 177-185.

218. Casu, B.; Naggi, A.; Torri, G.; Allegra, G.; Meille, S. V.; Cosani, A.; Terbojevich, M., Stereoregular acyclic polyalcohols and polyacetates from cellulose and amylose. *Macromolecules* **1985,** *18* (12), 2762-2767.

219. Koshijima, T. T., R.; Muraki, E.; Yamada, A.; Yaku, F., Chelating polymers derived from cellulose and chitin. *Cellulose Chemistry and Technology* **1973,** *7*, 197-201.

220. Sarymsakova, A.; Nadzhimutdinov, S.; Tashpulatov, Y., Chemical transformations in the chains of cellulose dialdehydes and cellulose ethers. *Chemistry of Natural Compounds* **1998,** *34* (2), 170-174.

221. Zhang, J.; Jiang, N.; Dang, Z.; Elder, T. J.; Ragauskas, A. J., Oxidation and sulfonation of cellulosics. *Cellulose* **2008,** *15* (3), 489-496.

222. Zhbankov, R. G.; Firsov, S. P.; Buslov, D. K.; Nikonenko, N. A.; Marchewka, M. K.; Ratajczak, H., Structural physico-chemistry of cellulose macromolecules. Vibrational spectra and structure of cellulose. *Journal of Molecular Structure* **2002,** *614* (1-3), 117-125.

223. David N.-S. Hon, N. S., Wood and cellulosic chemistry. 2nd ed.; David N.-S. Hon, N. S., Ed. CRC press: 2000; p. 914.

224. Isogai, A., NMR analysis of cellulose dissolved in aqueous naoh solutions. *Cellulose* **1997,** *4* (2), 99-107.

225. Pu, Y. Q.; Ziemer, C.; Ragauskas, A. J., CP/MASS 13C NMR analysis of cellulase treated bleached softwood kraft pulp. *Carbohydrate Research* **2006,** *341* (5), 591-597.

226. Gagnaire, D.; Mancier, D.; Vincendon, M., Cellulose organic solutions - nuclear magnetic-resonance investigation. *Journal of Polymer Science Part a-Polymer Chemistry* **1980,** *18* (1), 13-25.

227. Kong, D.; Wang, W.; Yu, Y.; Wang, S.; Wang, L.; Ou, L., Phosphate supported chitosan, cellulose or polyvinyl alcohol microsphere absorbent for removing low density lipoprotein by in-vitro whole blood adsorption and preparation method thereof. 2008.

228. Vytrasova, J.; Tylsova, A.; Brozkova, I.; Cervenka, L.; Pejchalova M.; Havelka, P., Antimicrobial effect of oxidized cellulose salts. *Journal of Industrial Microbiology & Biotechnology* **2008,** *35*, 1.

229. Magnani, A.; Consumi, M.; Rossi, C.; Greco, G., Phosphated derivatives of polysaccharides and uses thereof. U.S. Patent WO 2008090583, July 31, 2008..

230. Nagahata, M.; Nakaoka, R.; Teramoto, A.; Abe, K.; Tsuchiya, T., The response of normal human osteoblasts to anionic polysaccharide polyelectrolyte complexes. *Biomaterials* **2005,** *26* (25), 5138-5144.

231. Shaabani, A.; Rahmati, A.; Badri, Z., Sulfonated cellulose and starch: New biodegradable and renewable solid acid catalysts for efficient synthesis of quinolines. *Catalysis Communications* **2008,** *9* (1), 13-16.

232. Zheng, J.; Bragg, W.; Hou, J.; Lin, N.; Chandrasekaran, S.; Shamsi, S. A., Sulfated and sulfonated polysaccharide as chiral stationary phases for capillary

electrochromatography and capillary electrochromatography-mass spectrometry. *Journal of Chromatography A* **2009,** *1216* (5), 857-872.

233. Shenqi, W.; Yaoting, Y.; Tao, C.; Yan, C., Cellulose amphiphilic adsorbent for the removal of low density lipoprotein. *Artificial Cells Blood Substitutes and Immobilization Biotechnology* **2002,** *30* (4), 285-292.

234. Kobayashi, A.; Nakatani, M.; Furuyoshi, S.; Tani, N., In vitro evaluation of dextran sulfate cellulose beads for whole blood infusion low-density lipoprotein-hemoperfusion. *Therapeutic Apheresis* **2002,** *6* (5), 365-371.

235. Toida, T.; Chaidedgumjorn, A.; Linhardt, R. J., Structure and bioactivity of sulfated polysaccharides. *Trends in Glycoscience and Glycotechnology* **2003,** *15* (81), 29-46.

236. Wang, Z. M.; Li, L.; Zheng, B. S.; Normakhamatov, N.; Guo, S. Y., Preparation and anticoagulation activity of sodium cellulose sulfate. *International Journal of Biological Macromolecules* **2007,** *41* (4), 376-382.

237. Christensen, N. D.; Reed, C. A.; Culp, T. D.; Hermonat, P. L.; Howett, M. K.; Anderson, R. A.; Zaneveld, L. J. D., Papillomavirus microbicidal activities of high-molecular-weight cellulose sulfate, dextran sulfate, and polystyrene sulfonate. *Antimicrobial Agents and Chemotherapy* **2001,** *45* (12), 3427-3432.

238. Yamamoto, I.; Takayama, K.; Honma, K.; Gonda, T.; Matsuzaki, K.; Hatanaka, K.; Uryu, T.; Yoshida, O.; Nakashima, H.; Yamamoto, N.; Kaneko, Y.; Mimura, T., Synthesis, structure and antiviral activity of sulfates of cellulose and its branched derivatives. *Carbohydrate Polymers* **1990,** *14* (1), 53-63.

239. Groth, T.; Wagenknecht, W., Anticoagulant potential of regioselective derivatized cellulose. *Biomaterials* **2001,** *22* (20), 2719-2729.

240. Baumann, H.; Richter, A.; Klemm, D.; Faust, V., Concepts for preparation of novel regioselective modified cellulose derivatives sulfated, aminated, carboxylated and acetylated for hemocompatible ultrathin coatings on biomaterials. *Macromolecular Chemistry and Physics* **2000,** *201* (15), 1950-1962.

241. Doczi, J.; Fischman, A.; King, J. A., Direct evidence of the influence of sulfamic acid linkages on the activity of heparin-like anticoagulants. *Journal of the American Chemical Society* **1953,** *75* (6), 1512-1513.

242. Wolfrom, M. L.; Shen, T. M.; Summers, C. G., Sulfated nitrogenous polysaccharides and their anticoagulant activity. *Journal of the American Chemical Society* **1953,** *75* (6), 1519-1519.

243. Bhatt, N.; Gupta, P. K.; Naithani, S., Preparation of cellulose sulfate from alpha-cellulose isolated from lantana camara by the direct esterification method. *Journal of Applied Polymer Science* **2008,** *108* (5), 2895-2901.

244. Zhang, K.; Peschel, D.; Brendler, E.; Groth, T.; Fischer, S., Synthesis and bioactivity of cellulose derivatives. *Macromolecular Symposia* **2009,** *280* (1), 28-35.

245. Volkert, B.; Wolf, B.; Fischer, S.; Li, N.; Lou, C. H., Application of modified bead cellulose as a carrier of active ingredients. *Macromolecular Symposia* **2009,** *280*, 130-135.

246. Rose, T.; Neumann, B.; Thielking, H.; Koch, W.; Vorlop, K. D., Hollow beads of sulfoethyl cellulose (sec) on the basis of polyelectrolyte complexes. *Chemical Engineering & Technology* **2000,** *23* (9), 769-772.

247. Zhou, D.; Zhang, L.; Guo, S. L., Mechanisms of lead biosorption on cellulose/chitin beads. *Water Research* **2005,** *39* (16), 3755-3762.

248. DeOliveira, W.; Glasser, W. G., Hydrogels from polysaccharides .1. Cellulose beads for chromatographic support. *Journal of Applied Polymer Science* **1996,** *60* (1), 63-73.

249. Dash, R.; Jiang, N.; Leslie, G.; Ragauskas, A. J., Synthesis of novel water-soluble sulfonated cellulose. *Carbohydrate Research* **2010,** *345* (2), 284-290.

250. Klemm, D.; Kramer, F.; Moritz, S.; Lindstrom, T.; Ankerfors, M.; Gray, D.; Dorris, A., Nanocelluloses: A new family of nature-based materials. *Angewandte Chemie International Edition* **2011,** *50* (24), 5438-5466.

251. Huang, J. G.; Ichinose, I.; Kunitake, T., Biomolecular modification of hierarchical cellulose fibers through titania nanocoating. *Angewandte Chemie International Edition* **2006,** *45* (18), 2883-2886.

252. Peng, B. L.; Dhar, N.; Liu, H. L.; Tam, K. C., Chemistry and applications of nanocrystalline cellulose and its derivatives: A nanotechnology perspective. *Canadian Journal of Chemical Engineering* **2011,** *89* (5), 1191-1206.

253. Siqueira, G.; Bras, J.; Dufresne, A., Cellulose whiskers versus microfibrils: Influence of the nature of the nanoparticle and its surface functionalization on the thermal and mechanical properties of nanocomposites. *Biomacromolecules* **2009,** *10* (2), 425-432.

254. Montanari, S.; Rountani, M.; Heux, L.; Vignon, M. R., Topochemistry of carboxylated cellulose nanocrystals resulting from tempo-mediated oxidation. *Macromolecules* **2005,** *38* (5), 1665-1671.

255. Alonso, D.; Gimeno, M.; Olayo, R.; Vazquez-Torres, H.; Sepulveda-Sanchez, J. D.; Shirai, K., Cross-linking chitosan into uv-irradiated cellulose fibers for the preparation of antimicrobial-finished textiles. *Carbohydrate Polymers* **2009,** *77* (3), 536-543.

256. Cassano, R.; Trombino, S.; Ferrarelli, T.; Muzzalupo, R.; Tavano, L.; Picci, N., Synthesis and antibacterial activity evaluation of a novel cotton fiber (gossypium barbadense) ampicillin derivative. *Carbohydrate Polymers* **2009,** *78* (3), 639-641.

257. El-Tahlawy, K. F.; El-Bendary, M. A.; Elhendawy, A. G.; Hudson, S. M., The antimicrobial activity of cotton fabrics treated with different crosslinking agents and chitosan. *Carbohydrate Polymers* **2005,** *60* (4), 421-430.

258. Ringot, C.; Sol, V.; Barriere, M.; Saad, N.; Bressollier, P.; Granet, R.; Couleaud, P.; Frochot, C.; Krausz, P., Triazinyl porphyrin-based photoactive cotton fabrics: Preparation, characterization, and antibacterial activity. *Biomacromolecules* **2011,** *12* (5), 1716-1723.

259. Morandi, G.; Heath, L.; Thielemans, W., Cellulose nanocrystals grafted with polystyrene chains through surface-initiated atom transfer radical polymerization (si-atrp). *Langmuir* **2009,** *25* (14), 8280-8286.

260. Park, S.; Baker, J. O.; Himmel, M. E.; Parilla, P. A.; Johnson, D. K., Cellulose crystallinity index: Measurement techniques and their impact on interpreting cellulase performance. *Biotechnology for Biofuels* **2010,** *3*.

261. Larsson, P. T.; Hult, E. L.; Wickholm, K.; Pettersson, E.; Iversen, T., Cp/mas c-13-nmr spectroscopy applied to structure and interaction studies on cellulose i. *Solid State Nuclear Magnetic Resonance* **1999,** *15* (1), 31-40.

262. Liu, Z. H.; Jiao, Y. P.; Wang, Y. F.; Zhou, C. R.; Zhang, Z. Y., Polysaccharides-based nanoparticles as drug delivery systems. *Advanced Drug Delivery Reviews* **2008,** *60* (15), 1650-1662.

263. Zhang, L.; Gu, F. X.; Chan, J. M.; Wang, A. Z.; Langer, R. S.; Farokhzad, O. C., Nanoparticles in medicine: Therapeutic applications and developments. *Clinical Pharmacology & Therapeutics* **2008,** *83* (5), 761-769.

264. Ha, C. S.; Gardella, J. A., Surface chemistry of biodegradable polymers for drug delivery systems. *Chemical Reviews* **2005,** *105* (11), 4205-4232.

265. Zhang, X.; Huang, J.; Chang, P. R.; Li, J.; Chen, Y.; Wang, D.; Yu, J.; Chen, J., Structure and properties of polysaccharide nanocrystal-doped supramolecular hydrogels based on cyclodextrin inclusion. *Polymer* **2010,** *51* (19), 4398-4407.

266. Roman, M., S. P. Dong, H. Anjali, Y. W. Lee, Cellulose nanocrystals for drug delivery in polysaccharide materials: Performance by design. ACS Symposium Series 1017, American *Chemical Society*, Washington DC, 2010; pp 81–91.

267. Kovacs, T.; Naish, V.; O'Connor, B.; Blaise, C.; Gagne, F.; Hall, L.; Trudeau, V.; Martel, P., An ecotoxicological characterization of nanocrystalline cellulose (ncc). *Nanotoxicology* **2010,** *4* (3), 255-270.

268. Dugan, J. M.; Gough, J. E.; Eichhorn, S. J., Directing the morphology and differentiation of skeletal muscle cells using oriented cellulose nanowhiskers. *Biomacromolecules* **2010,** *11* (9), 2498-2504.

269. Aviss, K. J.; Gough, J. E.; Downes, S., Aligned electrospun polymer fibres for skeletal muscle regeneration. *European Cells & Materials* **2010,** *19*, 193-204.

270. Severian, D., Polysaccharides as biomaterials. In *Polymeric biomaterials, revised and expanded*, CRC Press: 2001.

271. Greenwald, R. B.; Choe, Y. H.; McGuire, J.; Conover, C. D., Effective drug delivery by pegylated drug conjugates. *Advanced Drug Delivery Reviews* **2003,** *55* (2), 217-250.

272. Fipula, D.; Zhao, H., Releasable pegylation of proteins with customized linkers. *Advanced Drug Delivery Reviews* **2008,** *60* (1), 29-49.

273. Greenwald, R. B.; Pendri, A.; Conover, C. D.; Zhao, H.; Choe, Y. H.; Martinez, A.; Shum, K.; Guan, S. Y., Drug delivery systems employing 1,4-or 1,6-elimination: Poly(ethylene glycol) prodrugs of amine-containing compounds. *Journal of Medicinal Chemistry* **1999,** *42* (18), 3657-3667.

274. Jiang, N.; Pu, Y. Q.; Samuel, R.; Ragauskas, A. J., Perdeuterated pyridinium molten salt (ionic liquid) for direct dissolution and nmr analysis of plant cell walls. *Green Chemistry* **2009,** *11* (11), 1762-1766.

275. Johnson Jr, C. S., Diffusion ordered nuclear magnetic resonance spectroscopy: Principles and applications. *Progress in Nuclear Magnetic Resonance Spectroscopy* **1999,** *34* (3–4), 203-256.

276. Jerschow, A.; Muller, N., Diffusion-separated nuclear magnetic resonance spectroscopy of polymer mixtures. *Macromolecules* **1998,** *31* (19), 6573-6578.

277. Jagur-Grodzinski, J., Polymeric gels and hydrogels for biomedical and pharmaceutical applications. *Polymers for Advanced Technologies* **2010,** *21* (1), 27-47.

278. Van Vlierberghe, S.; Dubruel, P.; Schacht, E., Biopolymer-based hydrogels as scaffolds for tissue engineering applications: A review. *Biomacromolecules* **2011,** *12* (5), 1387-1408.

279. Chen, J.-P.; Leu, Y.-L.; Fang, C.-L.; Chen, C.-H.; Fang, J.-Y., Thermosensitive hydrogels composed of hyaluronic acid and gelatin as carriers for the intravesical administration of cisplatin. *Journal of Pharmaceutical Sciences* **2011,** *100* (2), 655-666.

280. Dragusin, D. M.; Giol, D. E.; Vasile, E.; Trusca, R.; Teodorescu, M.; Stancu, I.; Vasilescu, D. S.; Iovu, H., Influence of physical interactions on the porosity of gelatin-alginate scaffolds. *Optoelectronics and Advanced Materials-Rapid Communications* **2011,** *5* (3-4), 459-464.

281. Silva, S. S.; Mano, J. F.; Reis, R. L., Potential applications of natural origin polymer-based systems in soft tissue regeneration. *Critical Reviews in Biotechnology* **2010,** *30* (3), 200-221.

282. Huang, S.; Fu, X., Naturally derived materials-based cell and drug delivery systems in skin regeneration. *Journal of Controlled Release* **2010,** *142* (2), 149-159.

283. Bode, F.; da Silva, M. A.; Drake, A. F.; Ross-Murphy, S. B.; Dreiss, C. A., Enzymatically cross-linked tilapia gelatin hydrogels: Physical, chemical, and hybrid networks. *Biomacromolecules* **2011,** *12* (10), 3741-3752.

284. Pena, C.; de la Caba, K.; Eceiza, A.; Ruseckaite, R.; Mondragon, I., Enhancing water repellence and mechanical properties of gelatin films by tannin addition. *Bioresource Technology* **2010,** *101* (17), 6836-6842.

285. Liao, H.; Zhang, H.; Chen, W., Differential physical, rheological, and biological properties of rapid in situ gelable hydrogels composed of oxidized alginate and gelatin derived from marine or porcine sources. *Journal of Materials Science-Materials in Medicine* **2009,** *20* (6), 1263-1271.

286. de Carvalho, R. A.; Grosso, C. R. F., Characterization of gelatin based films modified with transglutaminase, glyoxal and formaldehyde. *Food Hydrocolloids* **2004,** *18* (5), 717-726.

287. Leo, E.; Vandelli, M. A.; Cameroni, R.; Forni, F., Doxorubicin-loaded gelatin nanoparticles stabilized by glutaraldehyde: Involvement of the drug in the cross-linking process. *International Journal of Pharmaceutics* **1997,** *155* (1), 75-82.

288. Liu, W. G.; De Yao, K.; Wang, G. C.; Li, H. X., Intrinsic fluorescence investigation on the change in conformation of cross-linked gelatin gel during volume phase transition. *Polymer* **2000,** *41* (20), 7589-7592.

289. Draye, J. P.; Delaey, B.; Van de Voorde, A.; Van Den Bulcke, A.; De Reu, B.; Schacht, E., In vitro and in vivo biocompatibility of dextran dialdehyde cross-linked gelatin hydrogel films. *Biomaterials* **1998,** *19* (18), 1677-1687.

290. Kuijpers, A. J.; van Wachem, P. B.; van Luyn, M. J. A.; Brouwer, L. A.; Engbers, G. H. M.; Krijgsveld, J.; Zaat, S. A. J.; Dankert, J.; Feijin, J., In vitro and in vivo evaluation of gelatin-chondroitin sulphate hydrogels for controlled release of antibacterial proteins. *Biomaterials* **2000,** *21* (17), 1763-1772.

291. Dawlee, S.; Sugandhi, A.; Balakrishnan, B.; Labarre, D.; Jayakrishnan, A., Oxidized chondroitin sulfate-cross-linked gelatin matrixes: A new class of hydrogels. *Biomacromolecules* **2005,** *6* (4), 2040-2048.

292. Mu, C.; Liu, F.; Cheng, Q.; Li, H.; Wu, B.; Zhang, G.; Lin, W., Collagen cryogel cross-linked by dialdehyde starch. *Macromolecular Materials and Engineering* **2010,** *295* (2), 100-107.

293. Goetz, L.; Mathew, A.; Oksman, K.; Gatenholm, P.; Ragauskas, A. J., A novel nanocomposite film prepared from crosslinked cellulosic whiskers. *Carbohydrate Polymers* **2009,** *75* (1), 85-89.

294. Osorio-Madrazo, A.; Eder, M.; Rueggeberg, M.; Pandey, J. K.; Harrington, M. J.; Nishiyama, Y.; Putaux, J.-L.; Rochas, C.; Burgert, I., Re-orientation of cellulose nanowhiskers in agarose hydrogels under tensile loading. *Biomacromolecules* **2012,** *13*(3) 850-856.

295. Wang, Y.; Chen, L., Impacts of nanowhisker on formation kinetics and properties of all-cellulose composite gels. *Carbohydrate Polymers* **2011,** *83* (4), 1937-1946.

296. Spagnol, C.; Rodrigues, F. H. A.; Neto, A. G. V. C.; Pereira, A. G. B.; Fajardo, A. R.; Radovanovic, E.; Rubira, A. F.; Muniz, E. C., Nanocomposites based on poly(acrylamide-co-acrylate) and cellulose nanowhiskers. *European Polymer Journal* **2012,** *48* (3), 454-463.

297. Karaaslan, M. A.; Tshabalala, M. A.; Yelle, D. J.; Buschle-Diller, G., Nanoreinforced biocompatible hydrogels from wood hemicelluloses and cellulose whiskers. *Carbohydrate Polymers* **2011,** *86* (1), 192-201.

298. Spagnol, C.; Rodrigues, F. H. A.; Pereira, A. G. B.; Fajardo, A. R.; Rubira, A. F.; Muniz, E. C., Superabsorbent hydrogel composite made of cellulose nanofibrils and chitosan-graft-poly(acrylic acid). *Carbohydrate Polymers* **2012,** *87* (3), 2038-2045.

299. Goetz, L.; Foston, M.; Mathew, A. P.; Oksman, K.; Ragauskas, A. J., Poly(methyl vinyl ether-co-maleic acid)-polyethylene glycol nanocomposites cross-linked in situ with cellulose nanowhiskers. *Biomacromolecules* **2010,** *11* (10), 2660-2666.

300. Duer, M. J., Solid state NMR spectroscopy: Principles and applications. Blackwell Science: Malden, MA, 2002.

301. Leisen, J.; Beckham, H. W.; Sharaf, M. A., Evolution of crystallinity, chain mobility, and crystallite size during polymer crystallization. *Macromolecules* **2004,** *37* (21), 8028-8034.

302. Strauss, G.; Gibson, S. A., Plant phenolics as cross-linkers of gelatin gels and gelatin-based coacervates for use as food ingredients. *Food Hydrocolloids* **2004,** *18* (1), 81-89.

303. Lou, X.; Chirila, T. V., Swelling behavior and mechanical properties of chemically cross-linked gelatin gels for biomedical use. *Journal of Biomaterials Applications* **1999,** *14* (2), 184-191.

304. Schacht, E.; Bogdanov, B.; VandenBulcke, A.; DeRooze, N., Hydrogels prepared by crosslinking of gelatin with dextran dialdehyde. *Reactive & Functional Polymers* **1997,** *33* (2-3), 109-116.

305. Su, W.-Y.; Chen, Y.-C.; Lin, F.-H., Injectable oxidized hyaluronic acid/adipic acid dihydrazide hydrogel for nucleus pulposus regeneration. *Acta Biomaterialia* **2010,** *6* (8), 3044-3055.

306. Kim, S. H.; Chu, C. C., Pore structure analysis of swollen dextran-methacrylate hydrogels by SEM and mercury intrusion porosimetry. *Journal of Biomedical Materials Research* **2000,** *53* (3), 258-266.

307. Hoepfner, S.; Ratke, L.; Milow, B., Synthesis and characterisation of nanofibrillar cellulose aerogels. *Cellulose* **2008,** *15* (1), 121-129.

308. Kim, U. J.; Park, J.; Kim, H. J.; Wada, M.; Kaplan, D. L., Three-dimensional aqueous-derived biomaterial scaffolds from silk fibroin. *Biomaterials* **2005,** *26* (15), 2775-2785.

309. Rosenau, T., Liebner, F., Potthast, A., Haimer, E., Wendland, M., Ultralightweight cellulose aerogels from nbnmo-stabilized lyocell dopes. . *Research Letters in Materials Science* **2007,** *2007*, 1-4.

310. Chang, X. H.; Chen, D. R.; Jiao, X. L., Chitosan-based aerogels with high adsorption performance. *Journal of Physical Chemistry B* **2008,** *112* (26), 7721-7725.

311. Barr, S. A.; Luijten, E., Structural properties of materials created through freeze casting. *Acta Materialia* **2010,** *58* (2), 709-715.

312. Deville, S.; Saiz, E.; Tomsia, A. P., Freeze casting of hydroxyapatite scaffolds for bone tissue engineering. *Biomaterials* **2006,** *27* (32), 5480-5489.

313. Deville, S.; Saiz, E.; Tomsia, A. P., Ice-templated porous alumina structures. *Acta Materialia* **2007,** *55* (6), 1965-1974.

314. Zhang, H. F.; Hussain, I.; Brust, M.; Butler, M. F.; Rannard, S. P.; Cooper, A. I., Aligned two- and three-dimensional structures by directional freezing of polymers and nanoparticles. *Nature Materials* **2005,** *4* (10), 787-793.

315. Kawata, M.; Uchida, H.; Itatani, K.; Okada, I.; Koda, S.; Aizawa, M., Development of porous ceramics with well-controlled porosities and pore sizes from apatite fibers and their evaluations. *Journal of Materials Science-Materials in Medicine* **2004,** *15* (7), 817-823.

316. Tsioptsias, C.; Stefopoulos, A.; Kokkinomalis, I.; Papadopoulou, L.; Panayiotou, C., Development of micro- and nano-porous composite materials by processing cellulose with ionic liquids and supercritical co(2). *Green Chemistry* **2008,** *10* (9), 965-971.

317. Mahler, W.; Bechtold, M. F., Freeze-formed silica fibers. *Nature* **1980,** *285* (5759), 27-28.

318. Moon, J. W.; Hwang, H. J.; Awano, M.; Maeda, K., Preparation of nio-ysz tubular support with radially aligned pore channels. *Materials Letters* **2003,** *57* (8), 1428-1434.

319. Mukai, S. R.; Nishihara, H.; Tamon, H., Formation of monolithic silica gel microhoneycombs (smhs) using pseudosteady state growth of microstructural ice crystals. *Chemical Communications* **2004,** *7*, 874-875.

320. Gavillon, R.; Budtova, T., Aerocellulose: New highly porous cellulose prepared from cellulose-naoh aqueous solutions. *Biomacromolecules* **2008,** *9* (1), 269-277.

321. Aaltonen, O.; Jauhiainen, O., The preparation of lignocellulosic aerogels from ionic liquid solutions. *Carbohydrate Polymers* **2009,** *75* (1), 125-129.

322. Heath, L.; Thielemans, W., Cellulose nanowhisker aerogels. *Green Chemistry* **2010,** *12* (8), 1448-1453.

323. Sehaqui, H.; Salajkova, M.; Zhou, Q.; Berglund, L. A., Mechanical performance tailoring of tough ultra-high porosity foams prepared from cellulose i nanofiber suspensions. *Soft Matter* **2010,** *6* (8), 1824-1832.

324. Lee, J.; Deng, Y. L., The morphology and mechanical properties of layer structured cellulose microfibril foams from ice-templating methods. *Soft Matter* **2011,** *7* (13), 6034-6040.

325. Kvien, I.; Oksman, K., Orientation of cellulose nanowhiskers in polyvinyl alcohol. *Applied Physics a-Materials Science & Processing* **2007,** *87* (4), 641-643.

326. Deville, S.; Saiz, E.; Nalla, R. K.; Tomsia, A. P., Freezing as a path to build complex composites. *Science* **2006,** *311* (5760), 515-518.

327. Deville, S., Freeze-casting of porous ceramics: A review of current achievements and issues. *Advanced Engineering Materials* **2008,** *10* (3), 155-169.

328. Fukasawa, T.; Deng, Z. Y.; Ando, M.; Ohji, T.; Kanzaki, S., Synthesis of porous silicon nitride with unidirectionally aligned channels using freeze-drying process. *Journal of the American Ceramic Society* **2002,** *85* (9), 2151-2155.

329. Sekhar, J. A.; Trivedi, R., Solidification microstructure evolution in the presence of inert particles. *Materials Science and Engineering a-Structural Materials Properties Microstructure and Processing* **1991,** *147* (1), 9-21.